Characterization of Stress Responsive Mechanisms in Soybean under Flooding and Drought Stresses using Quantitative Proteomic Approach

July 2017

Xin WANG

Characterization of Stress Responsive Mechanisms in Soybean under Flooding and Drought Stresses using Quantitative Proteomic Approach

A Dissertation Submitted to

the Graduate School of Life and Environmental Sciences,

the University of Tsukuba

in Partial Fulfillment of the Requirements

for the Degree of Doctor of Philosophy in Biotechnology

(Doctoral Program in Life Sciences and Bioengineering)

Xin WANG

Abbreviations

ABA	Abscisic acid
ADH	Alcohol dehydrohenase
BiP	Luminal binding protein
ER	Endoplasmic reticulum
GABA	γ-Aminobutyric acid
HSP	Heat shock protein
KEGG	Kyoto encyclopedia of genes and genomes
LC	Liquid chromatography
MS	Mass spectrometry
P5CS	Pyrroline-5-carboxylate synthase
PDI	Protein disulfide isomerase
qRT-PCR	Quantitative reverse transcription-polymerase chain reaction
ROS	Reactive oxygen species
SAM	*S*-adenosylmethionine
UGGT	UDP glucose: glycoprotein glucosyltransferase
2-APB	2-Aminoethoxydiphenyl borate

TABLE OF CONTENTS

Introduction 1
Tables and figures.....9

Chapter 1. Organ-specific proteomics in soybean under flooding and drought stresses 14
1.1. Introduction.....15
1.2. Materials and methods 16
1.3. Results.....22
1.4. Discussion 28
1.5. Conclusion 37
Tables and figures.....38

Chapter 2. Endoplasmic reticulum proteomics in soybean under flooding and drought stresses 62
2.1. Introduction.....63
2.2. Materials and methods 64
2.3. Results.....69
2.4. Discussion 73
2.5. Conclusion 78
Tables and figures.....79

Chapter 3. Calcium effects on soybean under flooding and drought stresses 98
3.1. Introduction.....99
3.2. Materials and methods 100
3.3. Results.....103
3.4. Discussion 108
3.5. Conclusion 112

Tables and figures.....113

Conclusion and future prospects 126

Tables and figures 132

Summary 140

Acknowledgments 142

References 143

INTRODUCTION

Global climate changes influence the magnitude and frequency of hydrological fluctuations and cause unfavorable environment for plant growth and development (Fukao et al., 2011). Climate changes result in various abiotic stresses such as flooding (Bailey-Serres et al., 2012), drought (Choat et al., 2012), salty (Polle and Chen, 2015), heat (Ozga et al., 2017), and cold (Jha et al., 2017). Growth and productivity of crops are negatively affected by abiotic stresses caused by global climate changes (Hashiguchi et al., 2010). Plants encounter abiotic stresses and modulate adaptive responses through complex signaling pathways to survive the extreme conditions during growth and development (Fukao et al., 2011). Various transcription factors and *cis*-acting elements involve in signal transduction network from perception to response for plant adaption to environmental cues (Yamaguchi-Shinozaki and Shinozaki, 2006). Moreover, novel proteins as well as proteins with different abundance, which are in response to stresses, are associated with plant defense system (Komatsu and Hossain, 2013). The climate changes are potential threat for plants and a serial of processes involving gene expression and protein accumulation are mediated for plant adaption to abiotic stresses.

Crops are mainly intolerant to flooding and such extreme condition affects the patterns of plant distribution and biodiversity (Silvertown et al., 1999). Flooding causes decreased gas diffusion in water (Armstrong, 1979), which is the major problem for plants and limits the entry of oxygen for respiration and carbon dioxide for respiration (Voesenek et al., 2006). In addition, flooding affects the soil chemical characteristics including variations in soil pH (Probert and Keating, 2000), redox potential (Pezeshki, 2001), and microorganism (Kato et al., 2013). Flooding is composed of several underlying changes in substances such as oxygen, carbon dioxide, reactive oxygen species (ROS), phytotoxins, and ethylene inside plants and from environment (Perata et al., 2011). Therefore, flooding threats the environmental conditions as well as inside status for plants.

The detail understanding of morphological, physiological, and molecular mechanisms of flooding tolerance is essential to develop and adopt germplasm to endure the abiotic assaults (Bailey-Serres et al., 2012). Flooding exerted effects on field

bean at both vegetative phase and generative phase, indicating strong reduction in stem elongation, leaf area, and dry matter production (Pociecha et al., 2008). In addition, flooding negatively affected growth of soybean in germination (Wuebker et al., 2001), early vegetative, and early reproductive stages (Linkemer et al., 1998). The root to shoot ratio of flooded plants was higher, the development of adventitious root was increased, and the aerenchyma proliferation in cortex of root was induced compared to unstressed soybeans (Bacanamwo and Purcell, 1999). Root respiration, alcoholic fermentation, stomatal closure, and non-stomatal metabolic alterations were responsible for physiological adaptation for plants exposed to flooding (Liao and Lin, 2001). Moreover, low-oxygen-sensing mechanisms and metabolic adjustments were associated with controlled use of carbohydrate as well as ATP, which were examined through gene regulation and function in model systems (Bailey-Serres and Voesenek, 2008). These findings provide opportunities to uncover the mysterious of flooding and may bring benefits to plant breeding.

Proteomic approaches have been widely used to uncover the flooding responses in plants. In rice, proteins related to stress responses and redox metabolism were differentially changed in response to flooding (Sadiq et al., 2011). In wheat, coordinating methionine assimilation and cell wall hydrolysis were associated with restricting cell growth under flooding (Kong et al., 2010). In maize, proteins related to energy metabolism, photosynthesis, programmed cell death, phytohormones, and polyamines were identified under flooding (Chen et al., 2014). In soybean, a plethora of biological processes underwent flooding including signal transduction, hormone regulation, transcriptional control, glucose degradation, sucrose accumulation, alcoholic fermentation, mitochondrial impairment, proteolysis, and cell wall loosening (Komatsu et al., 2012a). Furthermore, some processes were highlighted involving in flooding-tolerant mechanisms in plants. The ability to maintain glycolysis and to induce fermentation was associated with flooding tolerance in cacao (Bertolde et al., 2014). Protein synthesis and RNA regulation played roles in triggering tolerance at initial stage of flooding, while cell wall integrity and glycolysis balance promoted tolerance during survival stages in soybean (Yin et al., 2016). These findings indicate that proteomic technique is essential to acquire protein profiles in exploring responsive and tolerant

mechanisms in plants under flooding stress.

Drought was evaluated as a meteorological anomaly characterized by a prolonged and abnormal moisture deficiency (Palmer, 1965). The impacts of drought associated with water demand exceeding water supply originated with the usable supplies including soil moisture, ground water, snowpack, streamflow, and reservoir storage (McKee et al., 1993). Because of the growth of population and expansion of agriculture, water demanding increased manifold than ever before and water scarcity occurred in many parts of the world (Mishra and Singh, 2010). Moreover, water was a predominate factor in determining geographic distribution of vegetation on the global scale and the occurrence of drought was a crucial yield factor in agriculture (Boyer, 1982). Drought and salt often integrated and induced similar cellular damage (Wang et al., 2003), while drought was even more pervasive and economically damaging (Boyer, 1982). These results implicate that drought is another major concern factor for agriculture.

Plant growth and productivity are adversely affected under drought, which is limited factor for both elongation and expansion growth (Franco et al., 2011). The meristematic cells were induced to be longer and rates of cell division were reduced due to drought (Sacks et al., 1997). The restriction of stomatal conductance became apparent even with a few changes of water status in soil (Davies and Gowing, 1999). The general positive correlation between stomal conductance and hydraulic conductivity was observed (Küppers, 1984), indicating that changes in hydraulic conductivity from soil and through plants in drying soil affected the stomatal aperture (Schulze, 1986). Cell expansion and cell growth were greatly suppressed under drought because of low turgor pressure (Franco et al., 2011). Plants responded to drought *via* a series of physiological, cellular, and molecular processes culminating in stress tolerance (Shinozaki and Yamaguchi-Shinozaki, 2007). The signal transduction, which consisted of ionic/osmotic homeostasis signaling pathways, detoxification response pathways, and growth regulation pathways, was activated under drought (Zhu, 2002). These reports display that drought causes negative effects on plants and complex pathways are integrated in response to drought stress.

An array of data related to drought responsive and tolerant mechanisms in plants were obtained *via* proteomic approaches. In rice, proteins related to defense, energy,

metabolism, cell structure, and signal transduction were identified under drought (Ali and Komatsu, 2006). In maize, a high abundance of cationic peroxidases with increase in phenylpropanoids led to reduction in lignin biosynthesis in the xylem vessels and induced cell wall stiffening in response to drought (Alvarez et al., 2008). In wheat, comparative proteomic analysis between salinity and drought indicated that ionic stress perception and transduction were differently involved, while toxic by-products elimination and metabolic adaptation processes were shared (Peng et al., 2009). In soybean, proteins related to osmotic adjustment, defense signaling, and programmed cell death played roles for drought adaptation (Alam et al., 2010). Moreover, light harvesting complex chain II and actin depolymerizing factor were accumulated at high levels in drought-tolerant rice (Ali and Komatsu, 2006). Furthermore, a global capacity ranging from intracellular-homeostasis reconstruction, ROS, and toxicant clearance to energy, carbon assimilation as well as growth recovery contributed to drought-tolerant wheat (Peng et al., 2009). These findings exhibit the importance of proteomics in uncovering the relative mechanisms of drought response and tolerance in plants.

Soybean, which is one of the important food crops, is rich in protein, vegetable oil (Sugiyama et al., 2015), and several phytochemicals such as isoflavones and phenolic compounds (Kim et al., 2012). Soybean is the only legume with ample amount of essential ω-3 fatty acid and α-linolenic acid (Messina and Messina, 2010). In addition, biotin, which is recognized as an essential nutrient factor, is included at a higher concentration in soybean compared to vegetables, fruits, and most meat products (Depeint et al., 2006). Notably, soybean and its products provide the most abundant isoflavones (Wang and Murphy, 1994), which contribute to reducing the risk of heart/cardiovascular diseases, osteoporosis, and cancer (Crozier et al., 2009). Besides, soybean seeds contain a variety of phenolic compounds such as chlorogenic acid, caffeic acid, and coumaric acid (Kim et al., 2006), which are beneficial to human health because of the antioxidant activities (Tyug et al., 2010). Such information well documentes the nutritional elements as well as pharmacological values of soybean, suggesting the importance of soybean in providing daily consumption and potential benefits for health promoting.

With the predominate values, soybean is cultivated with a long history, while it is

sensitive to flooding, which suppresses plant growth and grain yield (Li et al., 2017). Flooding responsive mechanisms have been explored in soybean ranging from subcellular organelles, organs, different growth stages of plants, post-flooding recovery, and along with other treatments using proteomic approaches (Table 1, Figure 1A). Subcellular proteomics indicated that flooding altered the regulation of proteins related to ROS scavenging, protein folding, ion flux, energy management, and cell wall synthesis in several subcellular compartments (Wang and Komatsu, 2016). Organ-specific protein profiles were examined under flooding with the demonstration that protein metabolism was increased in root; however, decreased in hypocotyl and leaf (Khatoon et al., 2012). Calcium-related signal transduction was induced at initial stage of flooding (Yin et al., 2014a); an imbalance of metabolic pathways including carbohydrate metabolism was occurred at early stage of flooding (Nanjo et al., 2010); and scavenging of toxic radicals played roles in late stage of flooding as well as post-flooding recovery (Khan et al., 2014). These findings illuminate the flooding responses in soybean from different aspects, and indicate that energy metabolism and ROS scavenging play pivotal roles in response to flooding.

A series of findings were obtained in soybean under flooding along with other treatments such as calcium (Oh et al., 2014a), nanoparticles (Mustafa and Komatsu, 2016), abscisic acid (ABA) (Komatsu et al., 2013a), and gibberellic acid (Oh et al., 2014b). It was reported that calcium affected the proteins related to the metabolisms of cell wall, hormone, protein, and DNA in soybean exposed to flooding (Oh et al., 2014a). Various sizes of aluminum oxide nanoparticles regulated membrane permeability and activity of the tricarboxylic acid cycle under flooding (Mustafa and Komatsu, 2016). In presence of phytohormones, it indicated that ABA enhanced flooding tolerance in soybean through governing energy conservation *via* glycolytic system (Komatsu et al., 2013a), and gibberellic acid induced the proteins related to secondary metabolism, cell cycle, and protein metabolism in flooded soybean (Oh et al., 2014b). These results give insights into the cross-talk between flooding and other treatments, and provide possibility to eliminate the hazards caused by flooding stress.

Drought is another abiotic stress causes deleterious effects on soybean production (Deshmukh et al., 2014). Enormous progress has been made in the area of proteomics of

soybean exposed to drought (Table 2, Figure 1B). In early stage, increased abundance of ferritin effectively sequestered iron and prevented excess free iron in the elongation zone of root under drought (Yamaguchi et al., 2010). Glycerol kinase, arogenate/prephenate dehydratase, and phloem serpin contributed to osmotic adjustment, ROS metabolism, secondary metabolism, and signal transduction in root of drought-stressed seedling (Alam et al., 2010). Carbon metabolism, protein synthesis, amino acid metabolism, and cell growth were the most altered processes in nodule of soybean seedling under drought (Gil-Quintana et al., 2013). Moreover, ROS was increased in response to drought and high amount of carbonic anhydrase aided the cell in becoming tolerant to cytotoxic accumulation of hydrogen peroxide in late stage of soybean leaf (Das et al., 2016). Additionally, organ-specific analysis of soybean seedling indicated that root was the most drought responsive organ compared to hypocotyl and leaf (Mohammadi et al., 2012). These findings indicate that root is more sensitive compared to other organs in response to drought and ROS metabolism might be given priority over other responsive processes for drought adaptation.

Proteomic studies provided valuable information of the mechanisms occurring in soybean recovering from drought (Khan and Komatsu, 2016). Abundance of UDP-glucose pyrophosphorylase and 2,3- bisphosphoglycerate independent phosphoglycerate mutase reverted to control under post-drought recovery, indicating that a shift in carbon partitioning played roles in drought adaptation (Alam et al., 2010). Additionally, peroxidase and aldehyde dehydrogenase were associated with post-drought recovery through scavenging ROS and reducing harmful aldehydes loading (Khan and Komatsu, 2016). Comparative proteomic studies were conducted between drought stress and polyethylene glycol condition, which was a simulation of water withholding, indicating that soybean differently responded to drought stress and polyethylene glycol treatment (Mohammadi et al., 2012). However, caffeoyl-CoA-*O*-methyltransferase and 20S proteasome displayed same changes between drought-stressed seedling and polyethylene glycol-treated plant, indicating common processes of oxidative damage and misfolded proteins increment (Toorchi et al., 2009). These reports enrich the understanding of post-drought recovery and common responses for osmotic adaptation of soybean.

Although flooding and drought negatively affect soybean growth, the morphological characteristics and molecular responses differ in plants under these conditions. In early stage of soybean, root elongation was suppressed under flooding, while root diameter was decreased under drought (Oh and Komatsu, 2015). Different morphological changes were observed in soybean seedling exposed to flooding (Khatoon et al., 2012) and drought (Mohammadi et al., 2012). Morphological differences indicated that independent mechanisms might be applied for stress adaption in soybean. It was demonstrated that activation of plant defense was essential to conquer flooding, while osmotic adjustment, defense signaling, and programmed cell death played roles in drought adaptation (Hossain and Komatsu, 2014). Furthermore, protein abundance and enzyme activity of ascorbate peroxidase were decreased under flooding, whereas they increased under drought, indicating that soybean experienced different levels of intracellular ROS under flooding and drought (Kausar et al., 2012). On the other hand, sufficient information on drought sensing and tolerant mechanisms on the organella proteomic is not available (Hossain et al., 2012). For example, the endoplasmic reticulum (ER) stress occurred due to accumulation of misfolded or unfolded proteins, which were induced by adverse environmental conditions (Howell, 2013). On the basis of these reports, dissecting molecular pathways, which independently or commonly respond to flooding and drought, will facilitate marker-assisted breeding for soybean.

An arsenal of proteomic studies was performed in soybean under flooding ranging from whole organ to in-depth subcellular organelle (Table 1). Compared to flooding, the knowledge of drought responsive and tolerant in soybean is rare (Table 2). Taking these into account, independent responses and cross-talk between flooding and drought need to be explored at the molecular level. In this study, proteomic technique was used to identify the flooding- and drought-responsive proteins in soybean. Firstly, to get insights into the more sensitive organ and growth stage of soybean towards flooding and drought, organ-specific and stage-dependent proteomic analyses were performed. Secondly, to get insights into the protein synthesis/degradation under both stresses, the ER proteomics was conducted. Thirdly, the roles of calcium in ER events as well as in cellular processes were examined using gel-free/label-free proteomic

approach. In the present study, systematic comparisons were conducted in soybean between flooding and drought, and it will facilitate the selection of molecular marker for stress tolerance in soybean.

Table 1. List of publications of proteomics in soybean under flooding stress

Organ	Growth stage/ Flooding duration	Major findings	References
Subcellular			
root including hypocotyl/cell wall	2-day-old/48h	a) Lignification was suppressed through decrease of proteins by downregulation of ROS and JA biosynthesis.	Komatsu et al., 2010
root including hypocotyl/plasma membrane	2-day-old/24h	a) Plasma membrane contributed to cell wall construction. b) Antioxidative system played roles in protecting cell from oxidative damage. c) Heat shock cognate protein protected proteins from degradation. d) Signaling proteins cooperatively worked to maintain ion homeostasis.	Komatsu et al., 2009a
root/nuclei	2-day-old/4h	a) ABA enhanced tolerance through energy conservation *via* glycolytic system and regulation of nuclear proteins including zinc finger proteins, cell division cycle 5 protein, and transducin.	Komatsu et al., 2013a
root tip/nuclei	2-day-old/48h	a) Suppression of RNA metabolism and accumulation of acceleration of poly-ADP-ribosylation were involved.	Oh et al., 2014c
root tip/nuclei	2-day-old/48h	a) RACK 1 in nucleus was accumulated. b) RACK 1 inhibited root growth through ABA action. c) RACK 1 interacted with 14-3-3 protein.	Komatsu et al., 2014
root tip/nuclei	2-day-old/3h	a) Nuclear-localized phosphoproteins were mediated by ABA.	Yin and Komatsu, 2015
root tip/nuclei	2-day-old/3h	a) Protein translation was suppressed through inhibition of pre-ribosome biogenesis- and mRNA processing-related proteins in nuclei.	Yin and Komatsu, 2016
root including hypocotyl/mitochondria	2-day-old/48h	a) Electron transport chains were impaired, although mitochondrial NADH production was increased through the TCA cycle.	Komatsu et al., 2011a
root/mitochondria	2-day-old/48h	a) Oxidative and peroxide scavenging led to biophoton emission and oxidative damage.	Kamal and Komatsu, 2015
root tip/mitochondria	2-day-old/48h	a) Mitochondrial proteins were affected by various sizes of Al_2O_3 NPs by regulating membrane permeability and the TCA cycle activity.	Mustafa and Komatsu, 2016
root tip/ER	2-day-old/48h	a) Protein synthesis and glycosylation were affected.	Komatsu et al., 2012b
Modification			
root tip/phosphorylation	2-day-old/12h	a) Proteins related to energy production were increased, while proteins related to protein folding and cell-structure maintenance were decreased. b) Energy demanding and producing related metabolic pathways were regulated by protein phosphorylation.	Nanjo et al., 2012
root tip/phosphorylation	2-day-old/3h	a) Phosphoproteins were changed with respect to phosphorylation statue after 3 h of stress. b) Ethylene signaling played roles in plant tolerance at initial stage *via* protein phosphorylation.	Yin et al., 2014b
root tip/phosphorylation	2-day-old/3h	a) ABA affected responses *via* the regulation of nuclear-localized phosphoproteins.	Yin and Komatsu, 2015
root/ubiquitination	2-day-old/24h	a) Ubiquitinated proteins were increased after de-submergence. b) Accumulation of COP9 signalosome proteins enhanced degradation of ubiquitinated proteins independent of low oxygen condition.	Yanagawa and Komatsu, 2012

root/glycosylation	2-day-old/48h	a) Accumulation of glycoproteins was decreased. b) *N*-glycosyltaion of proteins related to stress and protein degradation was negatively affected, while glycoproteins in glycolysis were activated.	Mustafa and Komatsu, 2014
root including hypocotyl/ phosphorylation	2-day-old/12h	a) Heat shock proteins and enzymes related to glycolysis and fermentation were key elements in early stress responses. b) Proteins involved in protein folding and synthesis were dephosphorylated.	Nanjo et al., 2010
Post-flooding recovery			
root	2-day-old/24(96), 48(72), 72(48)h*	a) Cell wall metabolism and reorganization of cytoskeleton played roles in recovery process.	Salavati et al., 2012
root	2-day-old/48(48), 48(96), 48(144)h* 2-day-old/96(48), 96(96), 96(144)h*	a) Peroxidase was required for recovery through scavenging toxic radicals.	Khan et al., 2014
root including hypocotyl	2-day-old/96(48), 96(96)h*	a) *S*-adenosyl-*L*-methionine dependent methyltransferases and enolase mediated recovery responses by Al_2O_3 NPs.	Yasmeen et al., 2016
hypocotyl	2-day-old/48(48), 48(96)h*	a) ATP generation and secondary metabolism were regulated in post recovery through pyruvate kinase, nucleotidylyl transferase, and β-ketoacyl reductase.	Khan et al., 2015
Flooding + other treatments			
root tip/ABA	2-day-old/24h	a) Zinc finger/BTB domain-containing protein 47, glycine-rich protein, and rRNA processing protein Rrp5 were phosphorylated after 3 h of stress with ABA.	Yin and Komatsu, 2015
root/ABA	2-day-old/48h	a) Content of ABA was not decreased in stressed root. b) Survival ratio was improved with additional ABA. c) Proteins related to cell organization, vesicle transport, and glycolysis were decreased with additional ABA.	Komatsu et al., 2013a
root/ABA	2-day-old/3, 24, 48, 72, 96h	a) Tolerance of ABA-treated soybean was mediated by nutrient- and growth-related proteins.	Yin et al., 2016
root/GA	2-day-old/48h	a) Protein related to secondary metabolism, cell cycle, and protein metabolism were affected by GA supplementation.	Oh et al., 2014b
root/JA, SA	2-day-old/48h	a) Proteins related to stress, signaling, glycolysis, fermentation, degradation, cell wall, cell organization, as well as metabolisms including secondary, hormone, and amino acid were affected by JA and SA.	Kamal and Komatsu, 2016
root/$CaCl_2$	2-day-old/48h	a) Exogenous calcium enhanced root elongation and suppressed cell death of root tip. b) Calcium affected cell wall, hormone metabolism, protein metabolism, and DNA synthesis.	Oh et al., 2014a
root, cotyledon/AgO NPs	2-day-old/48, 96h	a) AgO NPs with 15 nm and 2 ppm enhanced growth. b) AgO NPs shifted metabolism from fermentation to normal cellular processes and formation of comparatively low cytotoxic by-products.	Mustafa et al., 2015a
root including hypocotyl/AgO NPs	2-day-old/24, 48, 72h	a) AgO NPs with 15 nm promoted growth compared to 2 and 50-80 nm. b) Different sizes of AgO NPs affected growth by regulating proteins related to amino acid synthesis and wax formation.	Mustafa et al., 2016

root including hypocotyl/Al_2O_3 NPs	2-day-old/24, 48, 72h	a) Al_2O_3 NPs with 50 ppm enhanced growth compared to AgO NPs and ZnO NPs. b) Al_2O_3 NPs promoted growth by regulating energy metabolism and cell death.	Mustafa et al., 2015b
root including hypocotyl/Al_2O_3 NPs	2-day-old/24, 48, 72, 96h	a) Length of root including hypocotyl was significantly longer in soybean exposed to Al_2O_3 NPs with 30-60 nm compared to 5 and 135 nm. b) Al_2O_3 NPs with 30-60 nm suppressed glycolysis. c) Reduced activity of ascorbate/glutathione cycle related to reduced ROS scavenging activity on exposure to Al_2O_3 NPs.	Mustafa and Komatsu, 2016
root including hypocotyl/Al_2O_3 NPs	2-day-old/48, 96h	a) Survival ratio and weight/length of root including hypocotyl were improved with 50 ppm Al_2O_3 NPs and led to recovery. b) Al_2O_3 NPs activated enolase and *S*-adenosyl-*L*-methionine dependent methyltransferases to mediate recovery responses.	Yasmeen et al., 2016
No modification			
radicle of seeding	2-day-old/48h	a) Proteins related to RNA binding/processing and flooding indicators were correlated with tolerance.	Nanjo et al., 2014
root, cotyledon	2-day-old/48h	a) 70 kDa heat shock protein was increased in root and cotyledon. b) Calcium played roles through heat shock protein 70 kDa in cotyledon.	Komatsu et al., 2013b
cotyledon	2-day-old/24, 48, 72, 96h	a) Ferritin had an essential role in protecting cell from oxidative damage with stress duration.	Kamal et al., 2015

*, hour of flooding (hour of post-revovery flooding); RACK 1, receptor for activated protein kinase 1; TCA, tricarboxylic acid; GA, gibberellic acid; JA, jasmonic acid; SA, salicylic acid; $CaCl_2$, calcium chloride; AgO NPs, silver nanoparticles; Al_2O_3 NPs, aluminum oxide nanoparticles; ZnO NPs, zinc oxide nanoparticles.

Table 2. List of publications of proteomics in soybean under drought stress

Organ	Growth stage/Drought duration	Major findings	References
nodule	42-day-old/48, 96, 168h	a) Carbon metabolsim, protein synthesis, amino acid metabolism, and cell growth were the most altered processes in nodule.	Gil-Quintana et al., 2013
root	2-day-old/48h	a) Proteins related to protein synthesis and glycolysis were increased. b) Increased SAM synthetase was involved in the regulation.	Oh and Komatsu, 2015
root	14-day-old/120h	a) Proteins associated with osmotic adjustment, defense signaling, and programmed cell death played roles for stress adaptation.	Alam et al., 2010
root, hypocotyl, leaf	3-day-old/96h	a) Decreased methionine synthase impaired seedling growth.	Mohammadi et al., 2012
Post-drought recovery			
root including hypocotyl	2-day-old/96(48), 96(96)h*	a) Peroxidase and aldehyde dehydrogenase played roles in post-stress recovery by scavenging toxic ROS and reducing the load of harmful aldehydes.	Khan and Komatsu, 2016

*, hour of drought (hour of post-revovery drought), SAM, *S*-adenosylmethionine

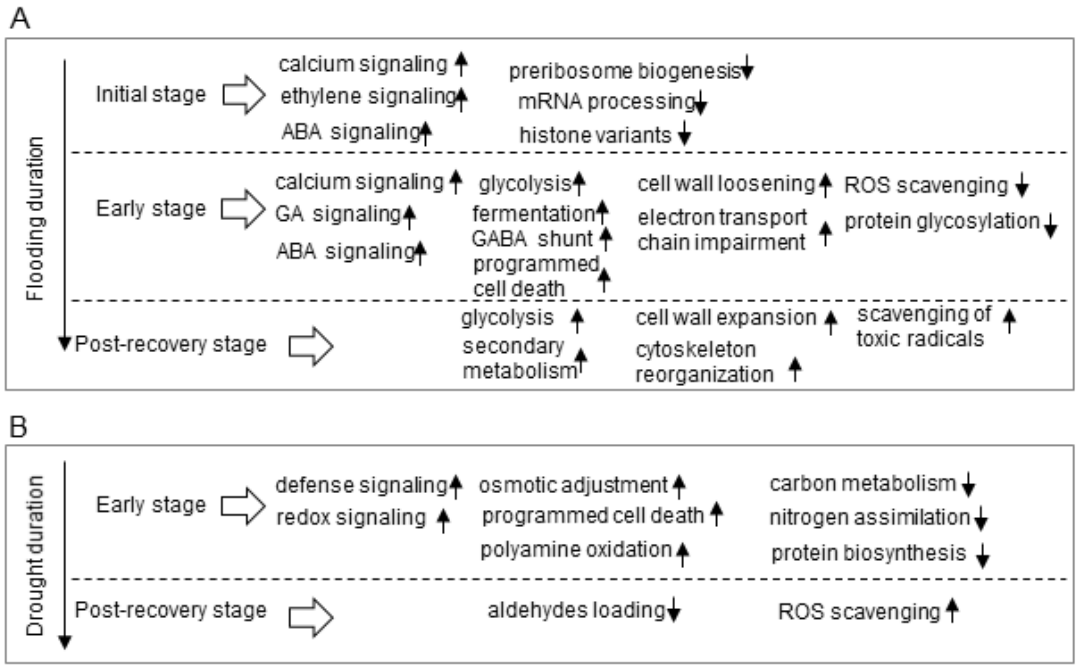

Figure 1. Overview of the cellular events induced by flooding and drought in soybean. The cellular events in soybean exposed to flooding and drought were explored using proteomic techniques. The up- and down-arrows indicated the activated and suppressed metabolisms, respectively, induced by stress. Abbreviations are as follows: GA, gibberellic acid; ROS, reactive oxygen species; GABA, γ-aminobutyric acid.

Chapter 1

Organ-specific proteomics in soybean under flooding and drought stresses

1.1. Introduction

Soybean is sensitive to abiotic stresses, including flooding (Russell et al., 1990) and drought (Korte et al., 1983). Growth rate of soybean was inhibited under both flooding and drought, while there was much difference in morphological responses between these two abiotic stresses, especially in the root compared to hypocotyl and leaf (Kausar et al., 2012). In the early stage of soybean, the length of root tip was markedly suppressed by flooding (Nanjo et al., 2013), whereas the root diameter was reduced by drought (Oh and Komatsu, 2015). In the seedling stage of soybean, weight of root, hypocotyl, and leaf as well as the length of root and hypocotyl were decreased in flooded plants (Khatoon et al., 2012). Similar results of declined weight were shown in soybean seedling exposed to drought (Mohammadi et al., 2012). These findings indicate that flooding and drought exert negative effects on soybean growth at different developmental stages.

Not only morphological parameters, but also biochemical responses were altered by flooding and drought. Following long exposure to flooding, protein abundance and enzyme activity of ascorbate peroxidase decreased, but increased under drought, indicating that intracellular levels of ROS differed in plants under both stresses (Kausar et al., 2012). Oh and Komatsu (2015) reported that fermentation, stress, and cell wall-related proteins were increased in root in response to flooding, whereas cell organization and redox-related proteins increased under drought. In addition, *S*-adenosylmethionine (SAM) synthetases were commonly identified between flooding and drought, while protein abundance differed between these stresses, indicating that redox signaling and polyamine oxidation were differentially controlled in stressed soybean (Oh and Komatsu, 2015). These results highlight the different responses induced by flooding and drought, whereas detail information of affected cellular metabolisms in different organs is warranted.

Because plant responses towards abiotic stresses differ in each organ, organ-specific analyses of protein profiles provide better understanding of cellular processes involved in plant growth and development (Komatsu and Hossain, 2013). For example, organ-specific analysis in flooded-soybean seedling revealed that proteins related to metabolism were increased in root, whereas they decreased in hypocotyl and leaf

(Khatoon et al., 2012). In response to drought stress, more proteins were differentially affected in root compared to leaf and hypocotyl (Mohammadi et al., 2012). Comparative proteomic analysis between root and cotyledon in the early-stage soybean indicated that heat shock protein (HSP) 70 was increased in root and cotyledon of flooded soybean; however, protein abundance of HSP 70 and biophoton emission in the cotyledon was higher than those in the root (Komatsu et al., 2013b). Photosynthetic machinery, carbohydrate metabolism, and ROS metabolism were affected in plants in response to temperature and drought stresses (Johnová et al., 2016). Compared to the studies of soybean seedling in response to flooding and drought, the knowledge of stress responses on organ-specific manner in the early stage is rare. These results indicate that effects induced by flooding and drought appear to be organ-specific dependent; however, the systematic comparisons among organs at different developmental stages are needed.

In this study, to obtain sensitive organ towards flooding and drought at different developmental stages, the organ-specific and stage-dependent proteomic analyses were performed. Enzyme activity was conducted to examine physiological changes induced by flooding and drought. Protein profiles and cluster analysis were examined to determine the most responsive proteins. In addition, bioinformatic analyses such as *in silico* protein-protein interaction and functional visualization were conducted. The quantitative reverse transcription-polymerase chain reaction (qRT-PCR) was carried out to integrate the multiple regulation levels between protein abundance and gene expression.

1.2. Materials and methods

1.2.1. Plant material and treatments

Soybean seeds (*Glycine max* L. cultivar Enrei) were sterilized with 3% sodium hypochlorite solution and rinsed in water. After sowing seeds in 500 mL of silica sand wetted with 150 mL of water in a plastic case (180 mm x 140 mm x 45 mm), soybeans were grown in a growth chamber illuminated with white fluorescent light (160 μmol $m^{-2}s^{-1}$, 16 h light period/day) at 25°C. Stage-dependent experiments included the early stage and seedling stage. For the early stage, 2-day-old soybeans were exposed to flooding or drought for 1 and 2 days. The root tip, root, hypocotyl, and cotyledon were

collected as samples. For the seedling stage, 6-day-old soybeans were exposed to flooding or drought for 4, 6, and 8 days. The root, hypocotyl, and leaf were collected as samples. To expose soybean to stress, excess water was added or withheld for flooding or drought, respectively. Untreated soybeans were collected as controls. Three independent experiments were performed as biological replicates for all experiments. Biological replicate means soybeans sown on different days. Twenty plants were sown in each time point for one replicate (Figure 2).

1.2.2. Extraction of cellular proteins for proteomic analysis

A portion (0.5 g) of samples was ground to powder in liquid nitrogen with a mortar and pestle. The powder was transferred to solution containing 10% trichloroacetic acid and 0.07% β-mercaptoethanol in acetone. The resulting mixture was vortexed, sonicated for 10 min, and incubated for 1 h at -20ºC with vortexing every 15 min. The suspension was centrifuged at 9000 x g for 20 min at 4°C and obtained pellet was washed twice with 0.07% β-mercaptoethanol in acetone. Pellet was dried using a Speed-Vac concentrator (Savant Instruments, Hickville, NY, USA) and resuspended in lysis buffer consisting of 8 M urea, 2 M thiourea, 5% CHAPS, and 2 mM tributylphosphine by vortexing for 1 h. The resulting suspension was centrifuged at 20000 x g for 20 min and supernatant was collected as cellular extract.

1.2.3. Concentration measurement of proteins

The method of Bradford (Bradford, 1976) was used to determine protein concentration.

1.2.4. Clean up and digestion of cellular proteins

Proteins (100 µg) were added to 400 µL of methanol and mixed thoroughly before further adding 100 µL of chloroform and 300 µL of water. After mixing, the samples were centrifuged at 20000 x g for 10 min to achieve phase separation. The upper aqueous phase was discarded and 300 µL of methanol was slowly added to the lower phase. The samples were further centrifuged at 20000 x g for 10 min. The dried pellets were resuspended in 50 mM NH_4HCO_3, reduced with 50 mM dithiothreitol for

30 min at 56ºC, and then alkylated with 50 mM iodoacetamide for 30 min at 37ºC in the dark. Alkylated proteins were digested with trypsin and lysyl endopeptidase (Wako, Osaka, Japan) at 1:100 enzyme/protein concentration at 37ºC for 16 h. The resulting peptides were acidified with formic acid (pH<3) and centrifuged at 20000 x g for 10 min. The supernatant was collected and analyzed by nanoliquid chromatography (LC)-mass spectrometry (MS)/MS.

1.2.5. Mass spectrometry analysis

The peptides in 0.1% formic acid were loaded onto an Ultimate 3000 nanoLC system (Dionex, Germering, Germany) equipped with a C18 PepMap trap column (300 µm ID x 5 mm; Dionex) and were separated by elution from the trap column using 0.1% formic acid in acetonitrile at a flow rate of 200 nL/min on a C18 Tip column (75 µm ID x 120 mm; Nikkyo Technos, Tokyo, Japan) with a spray voltage of 1.8 kV. Peptide ions were analyzed using a nanospray LTQ Orbitrap MS (Thermo Fisher Scientific, San Jose, CA, USA) operated in data-dependent acquisition mode with Xcalibur software (version 2.1; Thermo Fisher Scientific). Full-scan mass spectra were acquired in the MS over 400-1500 *m/z* with a resolution of 30000. A lock mass function was used to obtain high mass accuracy (Olsen et al., 2005). The ions $C_{24}H_{39}O^{+}{}_{4}$ (*m/z* 391.28429), $C_{14}H_{46}NO_{7}Si^{+}{}_{7}$ (*m/z* 536.16536), and $C_{16}H_{52}NO_{8}Si^{+}{}_{8}$ (*m/z* 610.18416) were used as lock mass standards. The top ten most intense precursor ions were selected for collision-induced fragmentation in the linear ion trap at a normalized collision energy of 35%. Dynamic exclusion was employed within 90 sec to prevent the repetitive selection of peptides (Zhang et al., 2009). The MS data have been deposited with the ProteomeXchange Consortium (http://proteomecentral.proteomexchange.org) *via* the PRIDE partner repository (Vizcaíno et al., 2013) with the data set identifiers PXD001687 and PXD005342.

1.2.6. Protein identification using mass spectrometry data

Protein identification was performed using Mascot search engine (version 2.5.1; Matrix Science, London, UK) and Proteome Discoverer software (version 1.4.0.288; Thermo Fisher Scientific) against soybean peptide database (Phytozome, version 9.1;

http://www.phytozome.net/soybean) (Schmutz et al., 2010). For Mascot search, the parameters were as follows: carbamidomethylation of cysteine was fixed modification; oxidation of methionine was variable modification; trypsin was specific proteolytic enzyme; one missed cleavage was allowed; peptide mass tolerance was 10 ppm; fragment mass tolerance was 0.8 Da; and peptide charge was set at +2, +3, and +4. An automatic decoy database search was performed as part of search. The Mascot Percolator was performed to improve accuracy and sensitivity of peptide identification (Brosch et al., 2009). For all searches, false discovery rates (false positive/(false positive+true positive)) for peptide identification were less than 1%. Peptides with more than 13 (p<0.05) percolator ion score were used for protein identification.

1.2.7. Analysis of differentially abundant proteins

The Mascot search results were exported for SIEVE analysis (version 2.2.49; Thermo Fisher Scientific). For analysis, chromatographic peaks detected by MS were aligned and peptide peaks were detected as a frame on all parent ions scanned by MS/MS using 5 min of frame time width and 10 ppm of frame m/z width. Area of chromatographic peak within a frame was compared for each sample and ratios between samples were determined for each frame. The frames with MS/MS scan were matched to the Mascot search results. The ratio of peptides between samples were determined from the variance-weighted average of the ratios in frames, which matched the peptides in the MS/MS spectrum. The ratios of peptides were further integrated to determine the ratios of corresponding proteins. Total ion current was used for normalization of differential analysis of protein abundance. The outliers of ratio were deleted in frame table filter based on the frame area. The minimum requirement for protein identification was two matched peptides. Significance of protein abundance between samples was analyzed (p<0.05). Isoforms were manually deleted based on protein ID.

1.2.8. Analysis of protein function and metabolism pathway

Functional analysis was performed using MapMan bin codes (Usadel et al., 2005). Visualization of protein abundance was performed using MapMan software (version 3.6.0RC1) (Usadel et al., 2009). Pathway mapping of proteins was performed

using Kyoto encyclopedia of genes and genomes (KEGG) database against Gmax (http://www.genome.jp/kegg/) (Kanehisa and Goto, 2000).

1.2.9. Cluster analysis of protein abundance

Ratio of protein abundance calculated by SIEVE software was used for cluster analysis, which was performed with Genesis software (version 17.6, http://genome.tugraz.at) (Sturn et al., 2002).

1.2.10. *In silico* protein-protein interaction analysis

Protein-protein interactions were estimated from temporal profiles of protein abundance utilizing a modified version of the S-system differential equation (Voit, 2000) as a mathematical model: $dx_i/dt = \alpha_i x_j(g_{(ij)}) - \beta_i x_i$, where α_i, $\beta_i \geq 0$. x_j and dx_i/dt denote the expression level of i-th protein and its time-derivative, respectively. Each interaction between proteins was tested based on a goodness-of-fit, which indicates how well the modified S-system differential equation simulates expression of the corresponding target protein. The interactions showing an r^2 value (coefficient of determination) of >0.8 were considered as candidate interactions. Protein abundance was originally obtained at days 2, 3, and 4 using SIEVE software, while it insufficient for the in-house interaction estimation software. Protein abundance was interpolated at days 2.5 and 3.5 by fitting a quadratic function to logarithmic values of the acquired protein abundance at days 2, 3, and 4. The interpolated protein abundance was used to estimate the interactions with protein abundance at days 2, 3, and 4. In the model of protein interaction diagram, a red arrow indicates an inductive interaction and a blue T-bar indicates a suppressive interaction in the S-system differential equation (Tanaka et al., 2005).

1.2.11. Analysis of enzyme activity

A portion (0.2 g) of samples was ground in extraction buffer containing 50 mM HEPES-NaOH (pH 7.5), 5 mM $MgCl_2$, 1 mM EDTA, 2% polyvinylpyrrolidone, 0.1% Triton X-100, 1 mM dithiothreitol, and 1 mM phenylmethylsulfonyl fluoride, with a mortar and pestle on ice. The resulting mixture was centrifuged at 15000 x g for 20 min

at 4°C. The supernatant was collected for enzyme activity assays. Protein concentration was determined using the Bradford as described in 1.2.3 in Chapter 1. Alcohol dehydrogenase (ADH) activity was measured according to Nanjo et al. (2010). The reaction solution of ADH assay was composed of 50 mM MES-NaOH (pH 7.5), 5 mM $MgCl_2$, 1 mM dithiothreitol, 0.1 mM NADH, and 4% acetaldehyde. Pyrroline-5-carboxylate synthase (P5CS) activity was measured according to Wang et al. (2011). The reaction solution of P5CS assay was composed of 100 mM Tris-HCl (pH 7.2), 20 mM $MgCl_2$, 75 mM Glutamate, 0.4 mM NADPH, and 5 mM ATP. Both reactions were measured continuously for 5 min at 25°C at 340 nm (EC_{340} = 6.22 mM^{-1} cm^{-1}). The enzyme activity was calculated using the formula: U/mg protein = [(ΔA340/min x total volume x sample dilution factor)/(6.22 x sample volume)]/protein concentration.

1.2.12. RNA extraction and quantitative reverse transcription-polymerase chain reaction

A portion (0.1 g) of samples was ground to powder in liquid nitrogen using a sterilized mortar and pestle, and total RNA was then extracted using an RNeasy Plant Mini kit (Qiagen, Valencia, CA, USA). Extracted RNA was reverse transcribed to cDNA using iScript Reverse Transcription Supermix (Bio-Rad, Hercules, CA, USA) according to the manufacturer's instructions. qRT-PCR was performed using SsoAdvanced SYBR Green Supermix (Bio-Rad) on a MyiQ Single-Color Real-Time PCR Detection system (Bio-Rad). The PCR conditions were as follows: 95°C for 30 sec, followed by 45 cycles of 95°C for 10 sec, and 60°C for 30 sec. Gene expression was normalized using the 18S rRNA gene (X02623.1) as an internal control. The qRT-PCR primers were designed using the Primer3Plus (http://www.bioinformatics.nl/cgi-bin/primer3plus/primer3plus.cgi) (Table 3). Primer specificity was examined by BLASTN searches against the Phytozome-*Glycine max* database with designed primers as queries and by melt curve analysis. Three biological replicates were performed and each biological replicate was technically duplicated to reduce error rate.

1.2.13. Statistical analysis

Student's *t*-test was performed between two groups using GraphPad Prism (version 6.0; GraphPad software, La Jolla, CA, USA). One-way ANOVA followed by

Tukey's multiple comparison was conducted among multiple groups using SPSS software (version 22.0; IBM, Armonk, NY, USA). A $p<0.05$ was considered as statistical significance.

1.3. Results

1.3.1. Effects of flooding and drought stresses on morphology of the early-stage soybean

To investigate the effects of flooding and drought on soybean morphology, seeds were germinated for 3 days without or with 1-day flooding or drought stress (Figure 3). The fresh/dry weight of plant and fresh weight/length of root including hypocotyl were examined as morphological parameters. Compared to 3-day-old untreated soybean, the fresh weight of plant did not change upon exposure to flooding or drought; however, the dry weight of plant reduced under both stresses. Notably, drought had more serious effects on the fresh weight of plant than flooding. In addition, the fresh weight and length of root including hypocotyl were suppressed under flooding, but the length was increased in response to drought exposure (Figure 3). Because plant morphology was affected by flooding and drought at the early stage of development, the stress responsive mechanisms were explored using proteomic technique.

1.3.2. Organ-specific proteomics and gene expression analysis of the early-stage soybean under flooding and drought stresses

Proteomic technique was used to analyze the organ-specific response to flooding and drought stresses in the early stage of soybean. Two-day-old soybeans were treated without or with flooding and drought stresses for 2 days, and protein samples were analyzed. Proteins identified in the root tip, root, hypocotyl, and cotyledon were classified with organ specificity in response to flooding and drought stresses (Figure 4). In the root tip, there were 504, 1337, and 370 specific proteins among control, flooding, and drought, respectively. In the root, there were 998, 351, and 755 specific proteins among control, flooding, and drought, respectively. In the hypocotyl, a total of 107, 111, and 164 proteins were specific to control, flooding, and drought, respectively. In the cotyledon, a total of 163, 45, and 208 proteins were specific to control, flooding, and

drought, respectively (Figure 4).

The organ-specific proteins were examined to obtain common candidates among control, flooding, and drought, which revealed that 95, 46, 3, and 10 proteins were common in the root tip, root, hypocotyl, and cotyledon, respectively (Table 4). In the root tip, biotin/lipoyl attachment domain containing protein (root tip, number 1) was decreased and increased in response to flooding and drought, respectively (Table 4). In the root, NADH dehydrogenase subunit 7 (root, number 6), TOPLESS RELATED 3 (root, number 24), WUS interacting protein 2 (root, number 26), TOPLESS RELATED 1 (root, number 27), villin 4 (root, number 32), and UDP glucose: glycoprotein glucosyltransferases (UGGT) (root, number 35) were significantly decreased and increased under flooding and drought, respectively (Table 4).

For NADH dehydrogenase subunit 7, gene expression was upregulated during germination, but downregulated under both stresses in the root tip of soybean. For villin 4, in the root tip, it was upregulated during germination, but downregulated under stress conditions. In the root, however, villin 4 was downregulated during germination as well as under stress conditions. For biotin/lipoyl attachment domain containing protein, gene expression was upregulated in the root tip during growth, but downregulated under both stresses. For UGGT, it was significantly changed in the root tip, root, and cotyledon under both stresses, and downregulated in flooded plants. For TOPLESS RELATED 1, it was upregulated in hypocotyl under drought. For WUS interacting protein 2, it was downregulated in the cotyledon of flooded soybean, while there was no significant change under drought (Figure 5).

1.3.3. Time-dependent proteomics, cluster analysis, and *in silico* protein-protein interaction in root tip of the early-stage soybean under flooding and drought stresses

For temporal proteomics, root tip was analyzed because it presented with more stress responsive proteins compared to other organs (Table 4). Two-day-old soybeans were treated without or with flooding and drought stresses for 1 and 2 days, and protein samples were extracted from root tip. Functional analysis of root-tip proteins was performed using MapMan bin codes to determine cellular responses under flooding and

drought over time (Figure 6). Under control, proteins related to the cell wall (13%), cell organization (12%), and protein synthesis/degradation (11%) were the major increased categories. Under flooding, proteins related to fermentation (18%) and cell wall (14%) were induced over time. Under drought, proteins related to protein synthesis/degradation (16%), cell organization (11%), cell wall (10%), and RNA metabolism (10%) were the major increased categories over time (Figure 6).

Cluster analysis of 11 common proteins was performed to investigate protein profiles of root tip among control, flooding, and drought over time (Figure 7). Using this approach, 5 different Clusters (I-V) were recognized. Cluster I consisted of 2 candidates, B-S glucosidase 44 (Figure 7, number 6 and 7), whose abundance were decreased during germination, flooding, and drought. Cluster II consisted of 2 candidates, mitochondrial substrate carrier family protein (Figure 7, number 4 and 5), which were continuously increased during germination and drought, and they decreased after flooding for 1 day. Cluster III consisted of 2 candidates (Figure 7, number 8 and 9) and displayed similar changes under germination and drought. Cluster IV consisted of 3 candidates (Figure 7, number 1-3) and the protein abundance were decreased after 1 day exposure to both stresses. Cluster V consisting of 2 candidates (Figure 7, number 10-11) were increased under both stresses.

In silico protein-protein interaction was conducted to examine potential interactions among 11 common proteins (Figure 8, Table 5). Under control, common proteins were predicted to form a uniform network with both inductive and suppressive connections. Under flooding and drought, coordinated networks were recognized, in which Class II aminoacyl tRNA/biotin synthetases superfamily protein (Figure 8, number 11) was found to be a stress-sensitive candidate for an integral component in the protein interaction network. Notably, protein-protein interaction revealed that B-S glucosidase 44 (Figure 8, number 6) and SAM synthetase family protein (Figure 8, number 3) had inductive interaction under flooding, while they presented with suppressive interaction under drought. In addition, SAM synthetase 1 (Figure 8, number 1), SAM synthetase 2 (Figure 8, number 2), and SAM synthetase family protein (Figure 8, number 3) were predicted to form cross interactions under flooding (Figure 8). The gene expression of SAM synthetases were examined, showing that *SAM synthetase 2*

and *SAM synthetase family protein* were downregulated under flooding compared to control (Figure 9).

1.3.4. Protein abundance and gene expression of biotin/lipoyl attachment domain containing protein and ClassII aminoacyl tRNA/biotin synthetases superfamily protein in the early-stage soybean under flooding and drought stresses

Protein and total RNA were extracted from the root tip during time-dependent stresses. Protein abundance of biotin/lipoyl attachment domain containing protein was continuously increased under drought for 2 days compared to flooding (Figure 10). The gene expression was downregulated in flooded soybean with stress duration (Figure 10). Protein abundance of Class II aminoacyl tRNA/biotin synthetases superfamily protein was increased on time-dependent mananer under both stresses. Meanwhile, gene expression was downregulated in plants exposed to stresses for 1 day (Figure 10).

1.3.5. Physiological responses of soybean seedling under flooding and drought stresses

To investigate the effects of flooding and drought on soybean seedling, the physiological responses were examined in 6-day-old soybeans treated without or with flooding and drought for 4, 6, and 8 days. Under control conditions, ADH and P5CS activities did not change during development. ADH activity was increased in root and leaf of soybean treated with flooding for 4 days, but then decreased in root after 6 days of drought treatment. P5CS activity was increased in root of flooding-stressed soybean after 4 days, and gradually increased in both root and leaf under drought (Figure 11A). In addition, ADH activity was drastically increased in root of flooded soybean compared to control and drought plants with the same age. P5CS activity was increased in leaf of soybean with drought stress compared to control and flooded plants. It was increased in root of soybeans exposed to both stresses compared to control (Figure 11B). Because the activities of ADH and P5CS were increased in soybean seedlings exposed to flooding and drought for 6 days, respectively, proteomic analysis was performed using samples collected after stress treatment for 6 days.

1.3.6. Organ-specific proteomics and functional analysis of identified proteins in

soybean seedling under flooding and drought stresses

Organ-specific protein profiles of flooding- and drought-stressed plants were compared to 6-day-old soybean without treatment (Figure 12). The stress-specific protein profiles of each organ were analyzed among control, flooding, and drought conditions (Figure 12). In root, 200, 362, and 264 proteins were specific to control, flooding, and drought, respectively. In hypocotyl, 40, 223, and 374 proteins were specifically identified in control and flooding- and drought-treated plants, respectively. In leaf, 107, 157, and 220 proteins were specifically identified of plants exposed to control, flooding, and drought, respectively (Figure 12).

To determine the function of flooding- and drought-responsive proteins identified in root, hypocotyl, and leaf of soybean seedling, functional analysis was performed using MapMan bin codes. The number of proteins related to photosynthesis, RNA, DNA, signaling, and the tricarboxylic acid cycle changed (increased or decreased) more than three-fold in root, hypocotyl, and leaf of soybean seedling under control, flooding, and drought (Figure 13). Most of the identified proteins in hypocotyl and leaf under three conditions were involved in photosynthesis. RNA-related proteins were markedly decreased in root and hypocotyl of flooding-stressed plant compared to the control and drought-stressed plants. Proteins related to DNA were decreased in hypocotyl of plants under flooding and drought compared to control plants. In addition, compared to control plants, more proteins related to signaling were increased in hypocotyl of flooding-stressed plant, and in root and hypocotyl of drought-stressed soybean. Proteins related to the tricarboxylic acid cycle were mainly decreased in root and leaf of plant treated with flooding compared to control plants, and more proteins were decreased in root and leaf compared to hypocotyl in soybean under drought (Figure 13).

1.3.7. Effects of flooding and drought on the tricarboxylic acid cycle in soybean seedling

Proteins related to photosynthesis, RNA, DNA, signaling, and the tricarboxylic acid cycle were predominantly affected in soybean seedling exposed to both stresses. Furthermore, abundance of the tricarboxylic acid cycle-related proteins was examined and visualized using MapMan software (Figure 14). In the root, the tricarboxylic acid

cycle-related proteins were markedly decreased under flooding, and only slightly declined in drought-treated plant compared to control. Additionally, in response to both stresses, the tricarboxylic acid cycle-related proteins were decreased in the root and leaf of soybean seedling. In the hypocotyl, more tricarboxylic acid cycle-related proteins responded to both stresses compared to control; however, they did not change in abundance among control, flooding, or drought. In the leaf, the tricarboxylic acid cycle-related proteins were significantly decreased under flooding compared to the control levels, but only slightly declined in response to drought (Figure 14).

To further investigate the effects of flooding and drought on the tricarboxylic acid cycle, the identified stress-responsive proteins were mapped to the KEGG (Figure 14). In the root, pyruvate dehydrogenase, citrate synthase, and malate dehydrogenase were decreased in response to flooding compared to the levels in control plants. Pyruvate dehydrogenase and succinyl-CoA synthetase were decreased, whereas succinate dehydrogenase increased in drought-stressed seedling compared to control. In the hypocotyl, pyruvate dehydrogenase, citrate synthase, isocitrate dehydrogenase, and succinyl-CoA synthetase were increased in seedling treated with flooding and drought compared to control, whereas succinate dehydrogenase decreased. In the leaf, aconitase and succinyl-CoA synthetase were decreased under flooding and drought, compared to control plant. Although malate dehydrogenase was decreased in the leaf in response to flooding, it increased in drought-stressed plant. Additionally, isocitrate dehydrogenase was decreased under flooding, whereas succinate dehydrogenase increased under drought (Figure 14).

1.3.8. Protein abundance and gene expression of β-glucosidase and β-amylase 5 in soybean seedling under flooding and drought stresses

Among flooding- and drought-responsive proteins, 17 proteins were commonly identified in the root, hypocotyl, and leaf (Table 6). Of these proteins, β-glucosidase 31 (Table 6, number 15) was decreased during development in control plants. Although β-glucosidase 31 protein was decreased in the hypocotyl of flooding- and drought-stressed plants compared to the same stage control soybean, it increased in the leaf and root. β-Amylase 5 (Table 5, number 16) was found to be decreased in the hypocotyl and leaf of

control plants during development, but increased in root. The protein abundance of β-amylase 5 was increased in the root, hypocotyl, and leaf in flooding- and drought-treated soybeans compared to the same stage control plant.

As β-glucosidase 31 and β-amylase 5 were increased in the root and leaf of soybean seedling exposed to both stresses, gene expression was further examined (Figure 15). β-Glucosidase 31 was downregulated in the root of flooding- and drought-treated plants as well as in the leaf of soybean exposed to drought, compared to the same stage control plant. In addition, β-amylase 5 was upregulated in the root of flooding-stressed plants and in the leaf of soybean under both stresses compared to controls. The upregulated gene expression of β-amylase 5 was consistent with increased protein abundance in the root under flooding and in the leaf under both stresses (Figure 15).

1.4. Discussion

1.4.1. Root tip and root are sensitive organs of the early-stage soybean in response to flooding and drought

Plants adapt to different stresses by regulating the abundance of responsive proteins in an organ-specific manner (Komatsu and Hossain, 2013). To better understand the effects of flooding and drought stresses on the growth of soybean in the early stage, organ-specific protein profiles of the root tip, root, hypocotyl, and cotyledon exposed to flooding and drought stresses were determined (Figure 4). Previous studies indicated the difference in morphology of stressed soybean even at the same development stage between flooding (Nanjo et al., 2013; Komatsu et al. 2013a; Hashiguchi et al., 2009) and drought (Oh and Komatsu, 2015). Because of this reason, comparisons of protein abundance between control and stress conditions including the starting point were used in the present study. Comparisons of the protein abundance of these four organs indicated that root tip was the most responsive organ to flooding, which diaplayed the largest number of responsive proteins. The different sensitive organs under flooding and drought imply that different mechanisms might be involved for soybeans to struggle against stresses.

1.4.2. Flooding and drought stresses affect TOPLESS RELATED in the early-stage soybean

TOPLESS RELATED 1, TOPLESS RELATED 2, and WUS interacting protein 2 were identified in soybean root under both stresses; and they were reported as corepressors and recruited by transcription factors to regulate the gene expression (Causier et al., 2012a). In *Arabidopsis*, four TOPLESS RELATED candidates were predicated according to similarity of amino acid sequence to TOPLESS (Long et al., 2006), and WUS interacting protein 2 was named as TOPLESS RELATED 4 (Kieffer et al., 2006; Liu and Karmarkar, 2008). TOPLESS/TOPLESS RELATED, general corepressors for plant development (Causier et al., 2012b) were involved in hormone responses such as auxin, ABA, ethylene, and jasmonic acid (Causier et al., 2012a). Although the gene expression was not significantly changed in the root, proteomic results indicated that TOPLESS RELATED candidates were decreased and increased under flooding and drought, respectively. It suggested that decreased TOPLESS RELATED might weaken the repression of hormone-response to struggle against flooding, while increased TOPLESS RELATED might enhance the repression of hormone-response to impair root growth maintenance under drought. Taken together, these results indicate that TOPLESS RELATED corepressors might be involved in hormone responses for root growth in soybean under flooding and drought stresses.

1.4.3. NADH dehydrogenase subunit 7 and villin 4 are involved in tolerance against flooding and drought in the early-stage soybean

NADH dehydrogenase subunit 7, villin 4, and biotin/lipoyl attachment domain containing protein were identified as the organ-specific proteins in soybean under both stresses, which were validated at transcriptional level (Figure 5). NADH dehydrogenase limited the formation of ROS in mitochondria by regulating the mitochondrial electron transport chain (Moller, 2001). Komatsu et al. (2011a) reported that flooding impaired the electron transport chain in soybean. In the present study, NADH dehydrogenase subunit 7 was downregulated in soybean root exposed to flooding, suggesting that flooding negatively affected the function of mitochondria and thereby reduced the supply of ATP for soybean growth. However, it was increased in soybean exposed to

drought, indicating that drought might have opposite manner compared to flooding.

Villins, a member of the villin/gelsolin/fragmin superfamily, were served as major actin filament-binding proteins to modulate actin dynamics (Du et al., 2011; Bao et al., 2012; Huang et al., 2015). Knockout of the villin gene *AtVLN4* inhibited the growth rate of root hairs, eliminated actin cables in root hairs, and disrupted cytoplasmic streaming (Zhang et al., 2011a). Except *AtVLN1*, four other members regulated actin dynamics on the calcium or calcium/calmodulin (Huang et al., 2005; Khurana et al., 2010; Zhang et al., 2010) dependent manner, repressing the length of actin filaments dependent on calcium (Zhang et al., 2011a). Here, villin 4, recognized as a root-specific protein, was increased at higher level under drought compared to flooding. Taken together, these suggest that soybean could adapt itself to drought through villin 4 to ensure cytoskeleton formation and cytoplasmic streaming, which is beneficial to promote growth of root hair to uptake water and nutrients from soil.

1.4.4. Fermentation and protein metabolism are increased in root tip of the early-stage soybean under flooding and drought stresses

Under flooding stress, fermentation was activated in the root tip over the 2-day exposure (Figure 6). Pyruvate dehydrogenase complex catalyzes the decarboxylation of pyruvate to acetaldehyde, and overexpression of *PDC1* or *PDC2* enhanced the survival of *Arabidopsis* under flooding (Ismond et al., 2003). Activity of ADH was reported to be enhanced in the root of flooding-tolerant sorghum during flooding stress (Jain et al., 2010). *ADH2* was a root-specific gene, which was mainly induced in root apical meristem in response to flooding (Komatsu et al., 2009b; Komatsu et al., 2011b), and overexpression of *ADH2* eliminated the growth inhibition caused by flooding in the seedling stage of soybean (Tougou et al., 2012). The results indicate that fermentation metabolism might be enhanced in root tip of soybean to improve survival ability against flooding, but it might not function under drought.

Functional analysis of identified proteins in the root tip under drought indicated that protein synthesis/degradation were significantly activated over time (Figure 6). Under drought, it was reported that an increased abundance of proteins were involved in protein metabolism in the root of *Rangpur lime*, which was the tolerant rootstock for

citrus (Oliveira et al., 2015). Furthermore, there was accumulation of proteins related to protein synthesis in the root of creeping bentgrass, which responded to increased endogenous cytokinins to enhance drought tolerance (Merewitz et al., 2011). Taken together, these findings suggest that enhanced protein metabolism might be essential for drought adaptation.

1.4.5. *S*-adenosylmethionine synthetase family protein and B-S glucosidase 44 are related to soybean growth in the early stage under flooding and drought stresses

Previous studies indicated that ETHYLENE OVERPRODUCER 1-like (Du et al., 2014) and SAM synthetases (Oh and Komatsu, 2015) responded to flooding and drought. In the present study, 11 common proteins were identified under flooding and drought over time (Table 5). *In silico* protein-protein interaction analysis indicated that SAM synthetase family protein and B-S glucosidase 44 had different interaction patterns under control and stress conditions (Figure 8). B-S glucosidase 44 participates in starch and sucrose metabolism, leading to glucose producing (Fayaz et al., 2014), which was increased in the root tip exposed to flooding. Plant submergence increased ethylene production, which was thought to protect plants against low oxygen conditions by either enhancing shoot elongation or promoting fermentation (Pandey et al., 2008; Bailey-Serres and Voesenek, 2010). It was reported that the development of early seedling was regulated through an antagonistic interaction between glucose and ethylene, and ETHYLENE INTENSIVE 3 was involved in the interaction, which mediated protein stability (Rolland et al., 2006). In the present study, SAM synthetase family protein catalyzing formation of SAM synthetase was decreased under both stresses. The suppressive interaction between SAM synthetase family protein and B-S glucosidase 44 under drought may imply an antagonistic interaction between glucose and ethylene, leading to regulating soybean growth. On the other hand, inductive interaction might suggest that ethylene could promote B-S glucosidase 44 to accumulate glucose for carbohydrate consumption in supporting cellular metabolism under flooding.

1.4.6. Early-stage soybean responses to flooding and drought stresses are regulated by

biotin-related proteins

Biotin/lipoyl attachment domain containing protein is multidomain protein, in which biotin or lipoic was attached to the domain for protein biotinylation and lipoylation (Cui et al., 2006). Enzymes such as pyruvate carboxylase and acetyl-CoA carboxylase were biotin-dependent carboxylases that were involved in glucose, amino acid, and fatty acid metabolisms (Tissot et al., 1996; Rodriguez-Melendez and Zempleni, 2003). It was reported that genes responding to glucose were modulated by histone biotinylation (Depeint et al., 2006), and biotin deficiency resulted in cell death and activation of defense signaling for abiotic stress (Li et al., 2012a). Aminoacyl-tRNA synthetases were a family of enzymes which played roles in protein synthesis and transcriptional/translational regulation (Martinis et al., 1999a). These enzymes were grouped into two classes based on sequence motif, active site topology, tRNA binding site, and aminocaylation site (Martinis et al., 1999a; Mucha, 2002). Amino acids were served as precursors for biotin (Asensi-Fabado and Munné-Bosch, 2010). Protein abundance and gene expression of biotin/lipoyl attachment domain containing protein and Class II aminoacyl tRNA/biotin synthetases superfamily protein displayed that they responded to both stresses, and previous studies indicated that biotin and biotinylation were related to stress. Taken together, these findings imply the importance of biotin synthesis and biotinylation, and they could regulate biotin-dependent carboxylases and histone biotinylation to affect glucose metabolism under flooding and drought.

1.4.7. Flooding and drought affect proteins related to photosynthesis, RNA, DNA, and signaling in soybean seedling

Plant organs differentially respond to abiotic stresses, and organ-specific proteins are critical for plant growth and development (Komatsu and Hossain, 2013). Proteins related to RNA, DNA, and signaling were predominantly altered in soybean seedling under both stresses (Figure 13). Photosynthesis converts light energy to chemical energy in integrated photosynthetic-carbon metabolism processes and a systemic approach is needed to coordinately improve plant productivity under environmental stresses (Zhu et al., 2010). Starch granule accumulation and ABA signaling/stomatal conductance were previously found to contribute to reduced photosynthetic activity in soybean under

flooding and drought, respectively (Mutava et al., 2015). Proteins related to photosynthesis, metabolism, and stress/defense were differentially affected in response to flooding stress in tomato (Ahsan et al., 2007) and to drought stress in tobacco (Xie et al., 2016). In rice, drought and heat stresses induced transcriptional activation of several photosynthetic genes, leading to enhanced photosynthesis (Ambavaram et al., 2014). Taken together, the results of present study are not only in consistent with that energy metabolism is associated with flooding and drought stresses in soybean seedling, but also suggest that hormone signaling might contribute to photosynthesis in the hypocotyl and leaf.

Several RNA-related proteins were significantly decreased in the root and hypocotyl of soybean seedling under flooding. Similarly, DNA-related proteins were markedly decreased in the hypocotyl in response to both stresses (Figure 13). Proteomic analysis indicated that RNA regulation-related proteins including glycine-rich RNA-binding protein 3 and eukaryotic aspartyl protease were increased in protein abundance, suggesting that these proteins were required for promoting flooding tolerance in soybean at initial stage (Yin et al., 2016). Previously reported RNA-sequencing analysis demonstrated that genes related to RNA processing were downregulated in soybean during the first 6 h of flooding (Nanjo et al., 2011). Additionally, genes related to DNA metabolism were downregulated in both root and hypocotyl after 12 h of flooding (Nanjo et al., 2011). These results suggest that RNA and DNA metabolisms are sensitive to flooding stress and these processes might be negatively affected in root and hypocotyl with flooding duration.

In addition to RNA- and DNA-related proteins, proteins related to signaling, such as 14-3-3 proteins, responded to both stresses (Figure 13). 14-3-3 proteins affected protein-protein interactions (Roberts et al., 2002) and involved in signal transduction under stresses (Liu et al., 2016). For example, overexpression of *TFT6* and *TFT7*, which are members of the 14-3-3 family, enhanced tomato growth in response to low phosphorus stress (Xu et al., 2012). Additionally, overexpression of *Arabidopsis 14-3-3* in cotton resulted in fewer wilted leaves/higher photosynthetic rates and improved drought tolerance (Yan et al., 2004). Moreover, overexpression of *14-3-3* in potato increased the number and decreased the size of tubers; however, repression of *14-3-3*

reversed these trends (Szopa, 2002). Collectively, these findings indicate that 14-3-3 proteins regulate plant growth and stress responses, and they might be essential proteins in hypocotyl to help soybean seedling cope with flooding and drought.

1.4.8. Proteins related to the tricarboxylic acid cycle are differentially affected in soybean seedling under flooding and drought stresses

In root, pyruvate dehydrogenase was decreased under both stresses compared to control condition. Similarly, citrate synthase/malate dehydrogenase and succinyl-CoA synthetase were decreased under flooding and drought, respectively (Figure 14). In agreement with protein abundance, *pyruvate dehydrogenase* was downregulated under flooding (Nanjo et al., 2011) and drought (Agrawal et al., 2016), indicating that pyruvate dehydrogenase is critical enzyme connecting glycolysis and the tricarboxylic acid cycle for energy regulation. Citrate synthase converts acetyl-CoA to citrate and succinyl-CoA synthetase converts succinyl-CoA to succinate (Bailey-Serres and Voesenek, 2008) in the tricarboxylic acid cycle. Overproduction of citrate conferred aluminum tolerance to transgenic tobacco and papaya (Fuente et al., 1997), and enhancement of citrate synthase activity promoted root elongation in canola exposed to aluminum (Anoop et al., 2003). In addition, activation of γ-aminobutyric acid (GABA) shunt was observed in tomato due to reduction of succinyl-CoA synthetase activity below a certain threshold level (Studart-Guimarães et al., 2007). GABA was previously found to accumulate in soybean under flooding (Nakamura et al., 2012) and drought (Serraj et al., 1998). Taken together, the present and previous findings suggest that citrate synthase and succinyl-CoA synthetase play pivotal roles in the tricarboxylic acid cycle in the root of soybean seedling under flooding and drought, respectively, and that succinyl-CoA synthetase may have decreased involvement in the GABA shunt in drought-stressed plant.

In hypocotyl of examined soybean seedling, more proteins responded to flooding and drought compared to control (Figure 14). Notably, succinate dehydrogenase, which plays a central role in respiratory metabolism as a component of electron transport chain and the tricarboxylic acid cycle (Araújo et al., 2011), was decreased under both stresses (Figure 14). In response to flooding, succinate dehydrogenase was decreased in root

including hypocotyl (Komatsu et al., 2011a; Kamal and Komatsu, 2015). Increased succinate dehydrogenase contributed to tolerance of short-term salt stress (Wang et al., 2014a). Furthermore, upregulated *succinate dehydrogenase* was correlated with its increased activity in absence of mitochondrial damage in the drought-tolerant genotype of *Ilex paraguariensis* (Acevedo et al., 2013). Additionally, succinate dehydrogenase positively regulated the generation of ROS and loss-of-function mutant of *succinate dehydrogenase 1-1* was susceptible to biotic stress (Gleason et al., 2011). The present results in combination with previous findings suggest that succinate dehydrogenase may play roles in modulating the tricarboxylic acid cycle in plant in response to biotic and abiotic stresses, such as flooding and drought.

In leaf, proteins related to the tricarboxylic acid cycle were differentially decreased under flooding and drought (Figure 14). Compared to control plant, pyruvate dehydrogenase, isocitrate dehydrogenase, and malate dehydrogenase were decreased in response to flooding, whereas malate dehydrogenase increased in abundance under drought (Figure 14). Pyruvate dehydrogenase links glycolysis to the tricarboxylic acid cycle (Bailey-Serres and Voesenek, 2008) and pyruvate is oxidatively converted to acetyl-CoA to enable entry into the tricarboxylic acid cycle for energy production (Lakshmanan et al., 2013). In response to flooding, pyruvate was fermented to ethanol in soybean (Nanjo et al., 2010), and a truncated tricarboxylic acid cycle between fumarate and oxaloacetate was observed in rice (Lakshmanan et al., 2013). In addition, *pyruvate dehydrogenase*, *isocitrate dehydrogenase*, and *malate dehydrogenase* were downregulated in the root of cucumber (Qi et al., 2012) and soybean (Nanjo et al., 2011) under flooding. Furthermore, malate dehydrogenase was increased in *Arabidopsis* in response to osmotic stresses (Ndimba et al., 2005). Overexpression of *MdcyMDH* contributed to plant growth and conferred tolerance in apple callus and tomato plants under cold and salt stresses (Yao et al., 2011). Overall, these findings indicate that pyruvate dehydrogenase, isocitrate dehydrogenase, and malate dehydrogenase are negatively affected in soybean under flooding, and that increased malate dehydrogenase may be associated with drought adaptation in the leaf of soybean seedling.

1.4.9. β-Amylase 5 mediates carbohydrate metabolism in soybean seedling under

flooding and drought stresses

β-Glucosidase 31 was differentially affected in the root and leaf of soybean seedling in response to flooding and drought (Table 6, number 16). *β-Glucosidase 31* was downregulated in the root and in the leaf of plants induced by both stresses (Figure 15). β-Glucosidases have various functions in plants, such as cell wall modification, defense, phytohormone signaling, and secondary metabolism (Cairns et al., 2015). β-Glucosidase, which functions in cellulose hydrolysis by converting cellobiose to glucose (Singhania et al., 2013), was decreased in wheat seedling exposed to 2 days of flooding (Kong et al., 2010). *CIBG1*, which is a homologue of *β-Glucosidase 1*, was significantly downregulated in watermelon seedlings under drought (Li et al., 2012b). Loss-of-function of *AtBG1*, a *β-glucosidase* in *Arabidopsis*, resulted in the development of a drought-sensitive phenotype, whereas overexpression of *AtBG1* led to enhanced drought tolerance in *Arabidopsis* (Lee et al., 2006). In the present study, *β-glucosidase 31* was downregulated upon the exposure of seedling to both stresses for 6 days; however, the corresponding protein abundance was increased, likely because of continued protein accumulation during stress exposure. These results suggest that β-glucosidase 31 responds to flooding and drought in soybean seedling, and that the increased abundance of this protein might be associated with the adaptation of abiotic stresses.

β-Amylase 5 was increased in the leaf of soybean seedling under both stresses compared to control condition and the protein level was in accordance with gene expression (Figure 15). Starch, which is hydrolyzed by β-amylase to maltose (Smith et al., 2005), is an abundant storage carbohydrate produced in plants (Orzechowski, 2008). In *Arabidopsis*, *β-amylases* were upregulated in response to drought, cold, and salt stresses (Seki et al., 2002). The induction of β-amylase correlated with the accumulation of maltose in *Arabidopsis* exposed to heat and cold shock on time-dependent manner (Kaplan and Guy, 2004). In addition, elevated β-amylase activity was found to be critical for rice survival during early-germination stage and for subsequent-seedling growth under flooding (Ella et al., 2010). The present results, as well as previous findings, suggest that β-amylase 5 is involved in starch degradation in soybean exposed to flooding and drought, and this enzyme might regulate carbohydrate mobilization to

increase energy provision in leaf of soybean seedling.

1.5. Conclusion

The present proteomic analysis characterized the organ-specific protein profiles of soybean in the early stage and seedling stage under flooding and drought stresses. The major findings are as follows (Figure 16): (i) root tip was the most sensitive organ affected by both stresses in the early-stage soybean; (ii) fermentation and protein metabolism were predominantly affected in root tip of the early-stage soybean under flooding and drought, respectively; (iii) biotin synthetase and biotin attachment domain contain protein were altered in root tip of the early-stage soybean under both stresses; (iv) proteins related to photosynthesis, RNA, DNA, signaling, and the tricarboxylic acid cycle were predominantly affected in seedling exposed to both stresses; (v) the tricarboxylic acid cycle was suppressed in root and leaf of seedling under both stresses; and (vi) increased protein abundance of β-amylase 5 was correlated with upregulated gene expression level in leaf of soybean seedling under both stresses. Taken together, these results suggest that root tip might be more sensitive towards both stresses in the early-stage soybean. Biotin and biotinylation might be involved in energy regulation in root tip of the early-stage soybean under flooding and drought.

Table 3. Primer sequences of genes selected for qRT-PCR in Chapter 1

Protein ID [a)]	Description	Sequence of primers (5'--- 3')
Glyma0776s50.1	NADH dehydrogenase subunit 7	F: TTCGAATTTCGGACCTCAAC
		R: TCTTGGGCCATCGTAGAAAC'
Glyma09g06390.3	villin 4	F: CCACATTGATTGCACAGGAC
		R: TTCTTTCCAATCCACGTTCC
Glyma11g35740.1	biotin/lipoyl attachment domain containing protein	F: AGCATTGGAGGCTTCTGGTA
		R: AGGCTCTCCATCCTCAACAA
Glyma08g20020.1	UGGT	F: CGATTCTCTTGCGTCTTTCC
		R: CAAACAGTTGCGGTCTCTGA
Glyma13g44420.1	TOLESEE RELATED 1	F: GCCAATCCCTTATTTCGTGA
		R: TCCTCCAGCCTTTGGTAATG'
Glyma03g39290.1	TOPLESS RELATED 3	F: TTGTGGATGCTGTCCAATGT
		R: CCAATGCTGTGGAACAACAC
Glyma13g22720.2	WUS interacting protein 2	F: GTCCCAGCGCTCAGATTAAG
		R: TCGTTTGGAGGTGGAGTACC
Glyma15g21890.1	SAM synthetase family	F: GTGCTTCTGGAAGTTAAAATGG
		R: TGATCTCTCCGAAAACCATC
Glyma03g38190.3	SAM synthetase 1	F: GACTGGCAGTATATCCAGTTACAG
		R: GATGCAAAAGAAGGGTGAT
Glyma19g40810.1	SAM synthetase 2	F: CTGCTTCTTCAGCTTGAGAAATG
		R: CAAAGACCATGACCATGTTGG
Glyma17g34070.1	Class II aminoacyl tRNA/biotin synthetases superfamily protein	F: CTGAAGCGGAAAGGAAATTG
		R: ACACGCTGAGCTCCTGAAAT
Glyma08g15960.3	β-glucosidase 31	F: GCATGGCTGAATCAAGGAAT
		R: TGTAACCAGCATCCCATTCA
Glyma06g45700.1	β-amylase 5	F: GGTGTGGACAACGAGCCTAT
		R: GAAATTCGCCAATACCAGGA
X02623.1[b)]	18S rRNA	F: TGATTAACAGGGACAGTCGG
		R: ACGGTATCTGATCGTCTTCG

a, Protein ID according to Phytozome soybean genome database; b, according to Genebank.

Table 4. List of common proteins identified in the root tip, root, hypocotyl, and cotyledon of the early-stage soybean under flooding and drought stresses

			Control	2(0)[a)]	4(0)	Flooding 4(2)		Drought 4(2)		
	Protein ID	Description	M.P.	Ratio	Ratio	M.P.	Ratio	M.P.	Ratio	Function
Root tip										
1	Glyma11g35740.1	biotin/lipoyl attachment domain containing protein	3	1	1.52	2	0.67	4	1.76	lipid metabolism
2	Glyma13g32660.1	pyrophosphorylase 6	6	1	1.41	2	0.35	6	1.40	nucleotide metabolism
3	Glyma13g43430.2	PDI like 16	5	1	0.67	6	0.58	6	0.69	redox
4	Glyma09g37860.1	RAS 5	3	1	0.64	3	0.68	2	0.65	signaling
5	Glyma02g13330.1	reversibly glycosylated polypeptide 3	15	1	0.62	14	0.61	15	0.79	cell wall
6	Glyma01g33220.2	plant VAP homolog 12	4	1	0.62	3	0.39	4	0.62	protein
7	Glyma03g03800.1	plant VAP homolog 12	4	1	0.62	3	0.39	4	0.62	protein
8	Glyma20g01220.1	oxidoreductases acting on the aldehyde	4	1	0.60	4	0.70	4	0.71	amino acid metabolism
9	Glyma03g42150.1	RNA binding family protein	3	1	0.59	4	0.41	5	0.71	RNA
10	Glyma19g44860.1	RNA binding family protein	3	1	0.59	4	0.41	5	0.71	RNA
11	Glyma06g05770.1	nitrilase/cyanide hydratase	3	1	0.58	3	0.62	3	0.60	not assigned
12	Glyma04g40750.2	CTC interacting domain 11	2	1	0.58	2	0.40	2	0.68	RNA
13	Glyma04g40760.1	CTC interacting domain 11	2	1	0.58	2	0.40	2	0.68	RNA
14	Glyma06g14030.1	CTC interacting domain 11	2	1	0.58	2	0.40	2	0.68	RNA
15	Glyma06g14050.3	CTC interacting domain 11	2	1	0.58	2	0.40	2	0.68	RNA
16	Glyma09g02731.1	glycosyl hydrolase family protein	7	1	0.58	6	0.47	6	0.68	misc
17	Glyma15g13620.1	glycosyl hydrolase family protein	7	1	0.58	6	0.47	6	0.68	misc
18	Glyma10g43590.1	Ras related small GTP binding family protein	3	1	0.58	3	0.57	3	0.66	signaling
19	Glyma11g15120.1	Ras related small GTP binding family protein	3	1	0.58	3	0.57	3	0.66	signaling
20	Glyma12g07070.1	Ras related small GTP binding family protein	3	1	0.57	3	0.57	3	0.66	signaling
21	Glyma13g40870.3	RAB GTPase homolog 8A	3	1	0.57	3	0.57	3	0.66	signaling
22	Glyma15g04560.2	Ras related small GTP binding family protein	3	1	0.57	3	0.57	3	0.66	signaling
23	Glyma18g52450.1	Ras related small GTP binding family protein	3	1	0.57	3	0.57	3	0.66	signaling
24	Glyma20g23210.5	Ras related small GTP binding family protein	3	1	0.57	3	0.57	3	0.66	signaling
25	Glyma10g35230.1	Ras related small GTP binding family protein	2	1	0.54	2	0.61	2	0.57	signaling
26	Glyma20g32320.1	Ras related small GTP binding family protein	2	1	0.54	2	0.61	2	0.57	signaling
27	Glyma10g42630.1	GHMP kinase family protein	4	1	0.54	4	0.54	4	0.79	secondary metabolism
28	Glyma18g07030.1	cyclophilin 5	2	1	0.53	2	0.61	3	0.69	cell
29	Glyma02g04980.1	RNA binding family protein	2	1	0.52	2	0.37	2	0.66	RNA
30	Glyma16g23010.1	RNA binding family protein	2	1	0.52	2	0.37	2	0.66	RNA

31	Glyma07g03930.1	dihydrolipoamide acetyltransferase long form protein	11	1	0.52	10	0.61	11	0.72	TCA cycle
32	Glyma16g00590.1	dihydrolipoamide acetyltransferase long form protein	10	1	0.51	10	0.61	10	0.71	TCA cycle
33	Glyma19g39710.1	amino acid dehydrogenase family protein	5	1	0.50	5	0.64	5	0.65	C1-metabolism
34	Glyma16g29450.3	phosphatase related	4	1	0.50	3	0.53	4	0.66	protein
35	Glyma03g37080.4	amino acid dehydrogenase family protein	5	1	0.49	5	0.65	5	0.65	C1-metabolism
36	Glyma19g33140.1	ahal domain containing protein	4	1	0.47	4	0.50	4	0.61	not assigned
37	Glyma03g05135.1	phosphoglucomutase	4	1	0.46	4	0.57	4	0.68	glycolysis
38	Glyma17g08491.1	UDP glucose 6 dehydrogenase family protein	5	1	0.46	5	0.60	5	0.63	cell wall
39	Glyma05g00590.2	UDP glucose 6 dehydrogenase family protein	4	1	0.45	4	0.58	4	0.62	cell wall
40	Glyma10g15910.1	S formylglutathione hydrolase	4	1	0.44	4	0.47	4	0.45	C1-metabolism
41	Glyma17g16850.1	N.D.*	4	1	0.43	3	0.10	4	0.90	not assigned
42	Glyma14g01850.6	20S proteasome β-subunit PBB2	2	1	0.43	2	0.60	2	0.67	protein
43	Glyma11g04650.1	peptidase M20/M25/M40 family protein	6	1	0.43	6	0.62	6	0.58	protein
44	Glyma02g45030.1	putative mitochondrial RNA helicase 2	8	1	0.42	7	0.31	8	0.45	RNA
45	Glyma05g27980.1	Rubber elongation factor protein (REF)	2	1	0.42	2	0.50	2	0.54	not assigned
46	Glyma08g04460.1	ATP dependent caseinolytic protease	5	1	0.41	5	0.33	6	0.68	lipid metabolism
47	Glyma07g00510.2	galactose mutarotase like superfamily protein	2	1	0.41	2	0.47	2	0.59	minor CHO metabolism
48	Glyma08g23910.2	galactose mutarotase like superfamily protein	2	1	0.41	2	0.47	2	0.59	minor CHO metabolism
49	Glyma18g52860.1	O Glycosyl hydrolases family 17 protein	5	1	0.40	5	0.40	5	0.61	misc
50	Glyma07g02470.1	protein phosphatase 2C family protein	2	1	0.39	2	0.29	2	0.77	protein
51	Glyma08g23550.1	protein phosphatase 2C family protein	2	1	0.393	2	0.29	2	0.77	protein
52	Glyma10g35490.1	phosphoglucosamine mutase family protein	6	1	0.38	6	0.46	6	0.49	glycolysis
53	Glyma03g41210.1	rotamase cyclophilin 2	5	1	0.38	4	0.50	5	0.67	cell
54	Glyma13g00780.1	galactose mutarotase like superfamily protein	7	1	0.37	7	0.51	8	0.57	minor CHO metabolism
55	Glyma17g38130.2	ubiquitin like superfamily protein	3	1	0.37	3	0.45	3	0.71	protein
56	Glyma05g03320.1	purple acid phosphatase 27	3	1	0.37	3	0.55	3	0.46	misc
57	Glyma20g32030.1	phosphoglucosamine mutase family protein	7	1	0.36	7	0.45	7	0.50	glycolysis
58	Glyma20g16070.1	heat shock protein 70 (Hsp70) family protein	6	1	0.35	6	0.57	5	0.23	stress
59	Glyma13g42270.1	pyridoxal 5 phosphate dependent enzyme family protein	3	1	0.35	3	0.38	3	0.59	amino acid metabolism
60	Glyma15g03120.1	pyridoxal 5 phosphate dependent enzyme family protein	3	1	0.35	3	0.38	3	0.59	amino acid metabolism
61	Glyma01g44833.1	O acetylserine (thiol) lyase (OAS TL) isoform A1	2	1	0.34	4	0.61	3	0.46	amino acid metabolism
62	Glyma08g42730.1	α/β-Hydrolases superfamily protein	3	1	0.33	4	0.54	2	0.47	protein
63	Glyma12g01291.1	transducin family protein/WD 40 repeat family protein	9	1	0.33	8	0.22	9	0.59	not assigned
64	Glyma01g42120.2	glycine cleavage T protein family	5	1	0.33	5	0.58	5	0.51	not assigned
65	Glyma15g12100.1	fumarylacetoacetase putative	6	1	0.33	6	0.62	6	0.40	amino acid metabolism

66	Glyma18g10460.2	HIS HF	10	1	0.32	10	0.58	10	0.54	amino acid metabolism
67	Glyma18g12920.1	HIS HF	10	1	0.32	10	0.58	10	0.54	amino acid metabolism
68	Glyma13g02870.1	peptidase M20/M25/M40 family protein	3	1	0.32	3	0.66	3	0.53	misc
69	Glyma11g19550.1	UDP D apiose/UDP D xylose synthase 2	5	1	0.31	5	0.44	6	0.62	cell wall
70	Glyma09g06380.2	galactose mutarotase like superfamily protein	6	1	0.31	6	0.49	7	0.52	minor CHO metabolism
71	Glyma15g17630.5	galactose mutarotase like superfamily protein	6	1	0.31	6	0.49	7	0.52	minor CHO metabolism
72	Glyma13g10700.1	heat shock protein 70 (Hsp70) family protein	8	1	0.31	8	0.52	8	0.26	stress
73	Glyma12g08930.1	UDP D apiose/UDP D xylose synthase 2	5	1	0.30	6	0.44	7	0.61	cell wall
74	Glyma05g38120.1	UDP D glucose/UDP D galactose 4 epimerase 1	2	1	0.29	2	0.26	2	0.13	cell wall
75	Glyma08g01480.1	UDP D glucose/UDP D galactose 4 epimerase 1	2	1	0.29	2	0.26	2	0.13	cell wall
76	Glyma04g38590.1	β-galactosidase 10	7	1	0.28	7	0.49	7	0.42	misc
77	Glyma16g27030.1	tubulin α 3	5	1	0.27	5	0.43	5	0.51	cell
78	Glyma06g16420.2	β-galactosidase 10	5	1	0.26	5	0.42	5	0.33	misc
79	Glyma20g19000.1	potassium channel β-subunit 1	4	1	0.25	5	0.61	4	0.41	transport
80	Glyma05g28500.1	subtilisin like serine endopeptidase family protein	2	1	0.22	2	0.54	2	0.28	protein
81	Glyma10g24620.1	potassium channel β subunit 1	4	1	0.22	5	0.60	4	0.39	transport
82	Glyma02g10790.1	protein phosphatase 2A subunit A2	2	1	0.21	2	0.39	2	0.42	protein
83	Glyma11g15010.1	UDP XYL synthase 6	8	1	0.21	8	0.52	8	0.45	cell wall
84	Glyma05g34900.1	arginosuccinate synthase family	5	1	0.20	4	0.46	5	0.32	amino acid metabolism
85	Glyma04g40090.1	nucleic acid binding OB fold like protein	2	1	0.20	2	0.44	2	0.37	protein
86	Glyma06g14760.1	nucleic acid binding OB fold like protein	5	1	0.19	5	0.50	5	0.39	protein
87	Glyma11g11410.1	subtilisin like serine protease 2	2	1	0.15	2	0.26	2	0.34	protein
88	Glyma05g05460.1	glutamate dehydrogenase 2	3	1	0.15	4	0.41	3	0.12	N-metabolism
89	Glyma17g15740.1	glutamate dehydrogenase 2	3	1	0.15	4	0.41	3	0.12	N-metabolism
90	Glyma05g37430.2	monodehydroascorbate reductase 6	2	1	0.14	2	0.54	2	0.38	redox
91	Glyma08g02100.1	monodehydroascorbate reductase 6	2	1	0.14	2	0.54	2	0.38	redox
92	Glyma11g31450.1	regulatory particle triple A ATPase 3	4	1	0.142	3	0.56	3	0.15	protein
93	Glyma11g31470.1	regulatory particle triple A ATPase 3	3	1	0.14	3	0.56	3	0.15	protein
94	Glyma09g08120.1	subtilase family protein	3	1	0.11	3	0.02	3	0.22	protein
95	Glyma12g06970.1	dessication induced 1VOC superfamily protein	3	1	0.09	3	0.61	3	0.12	biodegradation of xenobiotics
Root										
1	Glyma12g09940.2	FAD/NAD(P) binding oxidoreductase family protein	7	1	5.71	5	1.28	6	4.02	not assigned
2	Glyma11g18320.1	FAD/NAD(P) binding oxidoreductase family protein	10	1	5.02	6	1.28	10	4.38	not assigned
3	Glyma01g31750.1	disease resistance responsive family protein	4	1	4.58	4	1.33	4	3.64	stress
4	Glyma09g02670.1	peroxidase 2	2	1	2.83	2	1.38	2	2.48	misc

5	Glyma15g13540.2	peroxidase 2	2	1	2.83	2	1.38	2	2.48	misc
6	Glyma0776s50.1	NADH dehydrogenase subunit 7	4	1	2.11	3	0.64	3	2.73	mito. ETC
7	Glyma10g35381.1	phenylalanine ammonia lyase 2	3	1	2.08	2	0.03	4	1.69	secondary metabolism
8	Glyma20g32135.1	phenylalanine ammonia lyase 2	3	1	2.08	2	0.03	4	1.69	secondary metabolism
9	Glyma04g08070.1	FAD dependent oxidoreductase family protein	4	1	2.06	3	1.04	3	1.52	amino acid metabolism
10	Glyma03g25740.1	nucleotidylyl transferase superfamily protein	5	1	2.05	2	0.52	5	1.76	protein
11	Glyma03g36470.1	eukaryotic translation initiation factor 3C	12	1	2.03	6	0.35	10	1.95	protein
12	Glyma16g27440.1	uridine diphosphate glycosyltransferase 74E2	5	1	1.99	5	1.29	5	1.70	hormone metabolism
13	Glyma06g22050.1	gamma subunit of Mt ATP synthase	4	1	1.94	4	1.23	4	1.83	mito. ETC
14	Glyma03g33880.1	PHE ammonia lyase 1	5	1	1.94	4	0.01	6	1.66	secondary metabolism
15	Glyma03g33890.1	PHE ammonia lyase 1	5	1	1.94	4	0.01	6	1.66	secondary metabolism
16	Glyma19g36620.1	PHE ammonia lyase 1	5	1	1.94	4	0.01	6	1.66	secondary metabolism
17	Glyma07g30090.1	β-ureidopropionase	8	1	1.86	7	1.35	6	1.75	nucleotide metabolism
18	Glyma18g44250.1	PYRIMIDINE 4	8	1	1.60	2	0.72	5	1.35	amino acid metabolism
19	Glyma14g38600.1	eukaryotic translation initiation factor 2 β subunit	3	1	1.58	3	0.64	4	1.37	protein
20	Glyma05g34120.5	translation elongation factor EF1A	6	1	1.57	5	0.49	6	1.52	signaling
21	Glyma08g05570.1	translation elongation factor EF1A	6	1	1.56	4	0.49	5	1.56	signaling
22	Glyma05g30530.1	damaged DNA binding protein 1A	3	1	1.43	2	0.59	2	1.46	stress
23	Glyma08g13680.1	damaged DNA binding protein 1A	3	1	1.43	2	0.59	2	1.46	stress
24	Glyma03g39290.1	TOPLESS RELATED 3	2	1	1.36	2	0.68	2	1.59	development
25	Glyma10g29090.1	TOPLESS RELATED 3	2	1	1.36	2	0.68	2	1.59	development
26	Glyma13g22720.2	WUS interacting protein 2	2	1	1.36	2	0.68	2	1.59	development
27	Glyma13g44420.1	TOPLESS RELATED 1	2	1	1.36	2	0.68	3	1.59	development
28	Glyma17g12110.1	WUS interacting protein 2	2	1	1.36	2	0.68	2	1.59	development
29	Glyma19g41840.1	TOPLESS RELATED 3	2	1	1.36	2	0.68	2	1.59	development
30	Glyma20g38230.1	TOPLESS RELATED 3	2	1	1.36	2	0.68	2	1.59	development
31	Glyma07g03490.3	phospholipase D alpha 1	20	1	1.32	17	0.77	19	1.17	lipid metabolism
32	Glyma09g06390.3	villin 4	2	1	1.31	2	0.65	4	1.75	cell
33	Glyma15g17640.2	villin 4	2	1	1.31	2	0.65	4	1.75	cell
34	Glyma18g12900.1	villin 4	2	1	1.31	2	0.65	2	1.83	cell
35	Glyma08g20020.1	UGGT	4	1	1.26	3	0.32	4	1.60	protein
36	Glyma11g03800.1	acyl CoA oxidase 1	7	1	1.26	8	1.29	7	0.88	lipid metabolism
37	Glyma01g38580.1	clathrin heavy chain	15	1	1.13	12	0.64	15	1.05	cell
38	Glyma07g21100.1	allene oxide synthase	7	1	1.12	2	0.81	7	0.91	hormone metabolism
39	Glyma11g06720.1	clathrin heavy chain	15	1	1.10	11	0.64	14	1.03	cell

40	Glyma14g37510.1	clathrin heavy chain	13	1	1.05	10	0.56	13	1.01	cell
41	Glyma12g02076.1	methionine tRNA ligase putative	8	1	0.66	7	0.54	9	0.44	protein
42	Glyma09g01320.1	N.D.*	2	1	0.47	2	0.30	2	0.53	not assigned
43	Glyma08g22380.1	protein of unknown function DUF642	3	1	0.46	3	0.72	3	0.22	not assigned
44	Glyma19g41660.3	adenine nucleotide alpha hydrolases like superfamily	2	1	0.41	2	1.88	2	0.44	hormone metabolism
45	Glyma18g44300.1	lipid transfer protein 1	2	1	0.19	2	0.53	2	0.29	lipid metabolism
46	Glyma12g01700.1	nucleotide diphospho sugar transferases superfamily	2	1	0.09	2	2.21	2	0.26	not assigned
Hypocotyl										
1	Glyma09g14870.1	temperature induced lipocalin	2	1	0.46	2	0.32	2	0.29	transport
2	Glyma08g46520.1	cytochrome P450 family 93 subfamily D polypeptide 1	2	1	0.25	2	0.28	2	0.08	misc
3	Glyma10g39170.1	cupin family protein	6	1	0.19	6	0.15	6	0.12	development
Cotyledon										
1	Glyma01g41401.1	ribosomal protein L19 family protein	2	1	3.75	2	1.21	2	2.77	protein
2	Glyma11g10040.1	hydroxymethylbilane synthase	2	1	2.91	2	0.66	2	2.11	tetrapyrrole synthesis
3	Glyma12g02385.1	hydroxymethylbilane synthase	2	1	2.91	2	0.66	3	2.28	tetrapyrrole synthesis
4	Glyma11g11900.1	fructose bisphosphate aldolase 2	6	1	2.58	2	0.74	5	2.06	photosynthesis
5	Glyma12g04150.1	fructose bisphosphate aldolase 2	6	1	2.58	2	0.74	5	2.06	photosynthesis
6	Glyma17g20150.1	2 cysteine peroxiredoxin B	2	1	2.26	2	0.68	2	1.59	redox
7	Glyma19g38520.2	2 cysteine peroxiredoxin B	2	1	2.26	2	0.68	2	1.59	redox
8	Glyma03g35860.1	2 cysteine peroxiredoxin B	3	1	2.25	2	0.68	2	1.59	redox
9	Glyma11g06280.1	reticulan like protein B13	3	1	0.54	3	0.80	3	0.62	not assigned
10	Glyma10g33760.1	oleosin 1	3	1	0.32	3	0.61	3	0.44	lipid metabolism

a), day after sowing (day after stress); *, no description in Phytozome database; Protein ID, according to the Phytozome soybean genome database; M.P., number of the matched peptides; Ratio, relative abundance of protein; Function, protein function was categorized using MapMan bin codes; RNA, regulation of transcription/processing/RNA binding; TCA, tricarboxylic acid; mito. ETC, mitochondrial electron transport chain; C1-metabolism, carbon 1-metabolism; minor CHO metabolism, minor carbohydrate metabolism; N-metabolism, nitrogen metabolism; misc, miscellaneous enzyme family.

Table 5. List of common proteins identified in root tip of the early-stage soybean under flooding and drought stresses on time-dependent manner

			Control Ratio			Flooding Ratio			Drought Ratio			
	Protein ID	Description	2(0)[a)]	3(0)	4(0)	2(0)	3(1)	4(2)	2(0)	3(1)	4(2)	Function
1	Glyma03g38190.3	SAM synthetase 1	1	1.32	1.06	1	0.27	0.25	1	0.64	0.97	amino acid metabolism
2	Glyma19g40810.1	SAM synthetase 2	1	1.32	1.06	1	0.27	0.25	1	0.65	0.98	amino acid metabolism
3	Glyma15g21890.1	SAM synthetase family protein	1	1.55	1.18	1	0.29	0.23	1	0.67	1.14	metal handling
4	Glyma05g29050.1	mitochondrial substrate carrier	1	2.43	3.06	1	0.20	3.10	1	4.57	5.84	transport
5	Glyma08g12200.1	mitochondrial substrate	1	2.43	2.67	1	0.20	3.10	1	4.57	5.84	transport
6	Glyma07g11310.1	B-S glucosidase 44	1	0.55	0.23	1	0.75	0.53	1	0.55	0.13	misc
7	Glyma09g30910.1	B-S glucosidase 44	1	0.66	0.44	1	0.82	0.61	1	0.55	0.17	misc
8	Glyma08g47790.1	aldolase type TIM barrel family protein	1	2.06	1.96	1	0.09	2.35	1	1.42	2.50	OPP
9	Glyma18g53700.1	aldolase type TIM barrel family protein	1	2.06	1.96	1	0.09	2.35	1	1.42	2.50	OPP
10	Glyma05g01010.1	malate dehydrogenase	1	2.29	1.57	1	1.19	1.72	1	1.86	1.54	TCA cycle
11	Glyma17g34070.1	Class II aminoacyl tRNA/biotin synthetases superfamily protein	1	1.05	1.10	1	0.84	1.24	1	1.35	1.68	protein

a), day after sowing (day after stress); Protein ID, according to the Phytozome soybean genome database; M.P., number of the matched peptides; Ratio, relative abundance of protein; Function, protein function was categorized using MapMan bin codes; OPP, oxidative pentose phosphate pathways; TCA, tricarboxylic acid; misc, miscellaneous enzyme family.

Table 6. List of common proteins identified in the root, hypocotyl, and leaf of soybean seedling under flooding and drought stresses

			Control 12(0)[a)] Ratio			Flooding 12(6) Ratio			Drought 12(6) Ratio			
	Protein ID	Description	Root	Hypocotyl	Leaf	Root	Hypocotyl	Leaf	Root	Hypocotyl	Leaf	Function
1	Glyma17g04210.1	lipoamide dehydrogenase 2	0.98	2.10	2.10	1.00	1.50	1.99	0.83	1.46	1.41	TCA cycle
2	Glyma07g39380.1	phosphofructokinase	1.87	1.50	1.50	1.18	1.43	1.20	1.00	1.67	2.07	glycolysis
3	Glyma20g25920.1	ATP synthase α/β	0.86	0.81	0.81	1.00	1.45	0.73	1.00	1.41	1.00	mito. ETC
4	Glyma08g11490.1	serine hydroxymethyltransferase 4	0.94	0.81	0.81	0.80	1.43	0.67	0.77	1.72	1.00	C1-metabolism
5	Glyma05g28490.1	serine hydroxymethyltransferase 4	0.94	0.72	0.72	0.79	1.45	0.66	0.77	1.73	1.00	C1-metabolism
6	Glyma04g43540.1	methylenetetrahydrofolate reductase 2	0.73	0.71	0.71	0.71	1.84	0.74	1.00	1.78	0.68	C1-metabolism
7	Glyma06g48360.1	methylenetetrahydrofolate reductase 2	0.73	0.71	0.71	0.71	1.83	0.74	1.00	1.75	0.68	C1-metabolism
8	Glyma11g29460.1	NAD(P) binding Rossmann fold	1.91	0.50	0.50	1.00	2.09	1.53	1.00	1.91	1.00	secondary metabolism
9	Glyma07g03930.1	dihydrolipoamide acetyltransferase	1.54	0.40	0.40	1.00	1.22	0.59	1.59	1.55	0.57	TCA cycle
10	Glyma13g41960.1	pfkB like carbohydrate kinase	1.08	0.40	0.40	0.63	1.60	0.30	1.19	2.42	0.58	major CHO metabolism
11	Glyma16g00590.1	dihydrolipoamide acetyltransferase	1.57	0.39	0.39	1.00	1.30	0.58	1.64	1.62	0.51	TCA cycle
12	Glyma14g04180.1	N.D.*	1.45	0.39	0.39	1.00	1.07	1.00	1.53	1.31	0.70	development
13	Glyma11g13580.1	pfkB like carbohydrate kinase	1.10	0.38	0.38	0.73	2.02	0.29	1.16	2.06	0.53	major CHO metabolism
14	Glyma12g05580.1	pfkB like carbohydrate kinase	1.08	0.38	0.38	0.70	1.97	0.29	1.16	2.16	0.53	major CHO metabolism
15	Glyma08g15960.3	β-glucosidase 31	0.63	0.80	0.33	2.77	0.73	0.42	2.62	0.54	0.41	misc
16	Glyma06g45700.1	β-amylase 5	1.36	0.27	0.27	1.83	1.89	1.22	2.73	1.68	0.41	major CHO metabolism
17	Glyma17g05067.1	sucrose synthase 4	1.39	0.11	0.11	1.00	1.00	0.12	2.83	3.59	0.15	major CHO metabolism

a), day after sowing (day after stress); *, no description in Phytozome database; Protein ID, according to the Phytozome soybean genome database; Ratio, relative abundance of protein was compared to 6-day-old untreated soybean; Function, protein function was categorized using MapMan bin codes; TCA, tricarboxylic acid; mito. ETC, mitochondrial electron transport chain; C1-metabolism, carbon 1-metabolism; major CHO metabolism, major carbohydrate metabolism; misc, miscellaneous enzyme family.

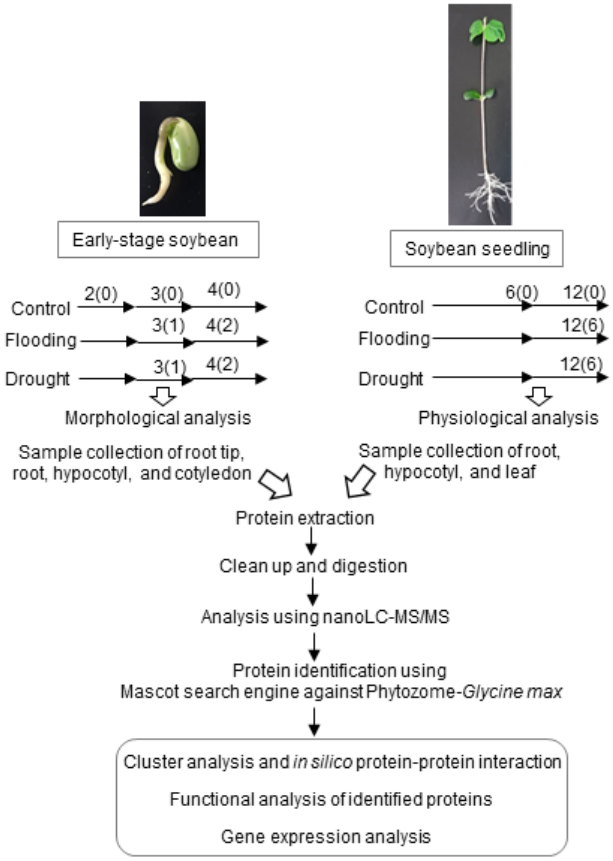

Figure 2. Experimental design of the organ-specific proteomics in the early stage and seedling stage soybean exposed to flooding and drought. For organ-specific experiments in the early-stage soyben, 2-day-old soybeans were treated without or with flooding and drought for 2 days, and the root tip, root, hypocotyl, and cotyledon were collected. For organ-specific experiments in soybean seedling, 6-day-old soybeans were treated without or with flooding and drought for 6 days. Root, hypocotyl, and leaf were collected. Three independent experiments were performed as biological replicates. Three independent experiments were performed as biological replicates.

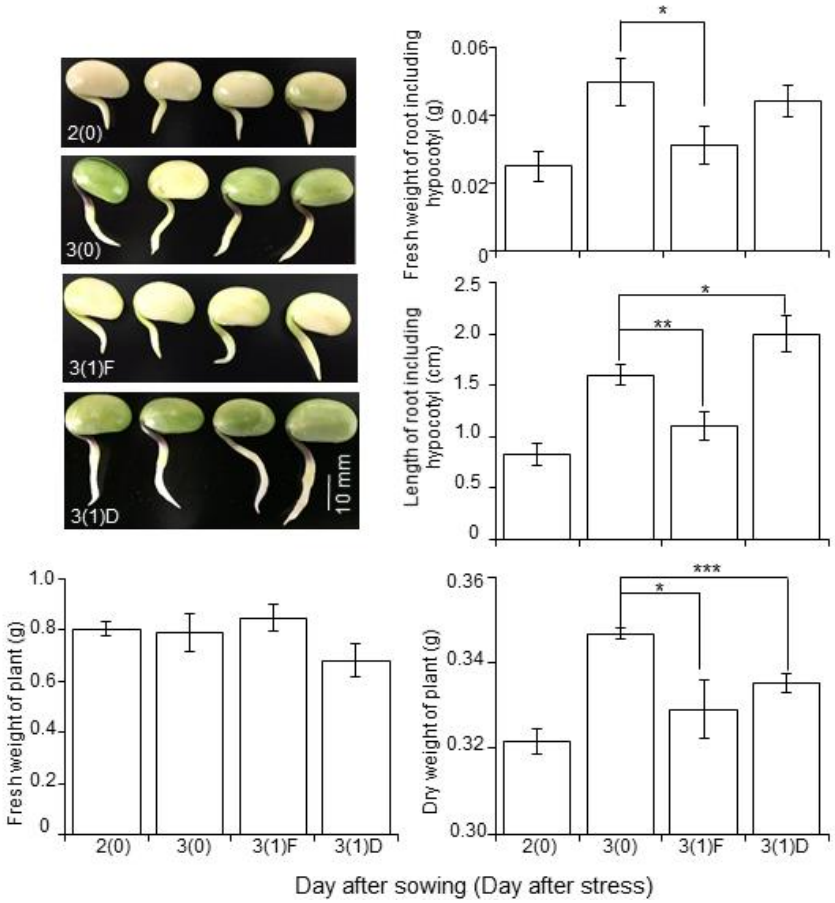

Figure 3. Morphological changes in soybean exposed to flooding and drought. Two-day-old soybeans were exposed to flooding or drought for 1 day. Photographs of soybeans were taken under control, flooding (F), and drought (D). Untreated soybeans were collected as controls. Fresh weight of plant, fresh weight of root including hypocotyl, length of root including hypocotyl, and dry weight of plant were measured at each condition. Data are shown as means ± SD from three independent biological replicates. Student's *t*-test was used for statistical analysis. Asterisks indicate the significance between 3-day-old soybeans without or with flooding or drought (*p<0.05, **p<0.01, ***p<0.001). Scale bar indicates 10 mm.

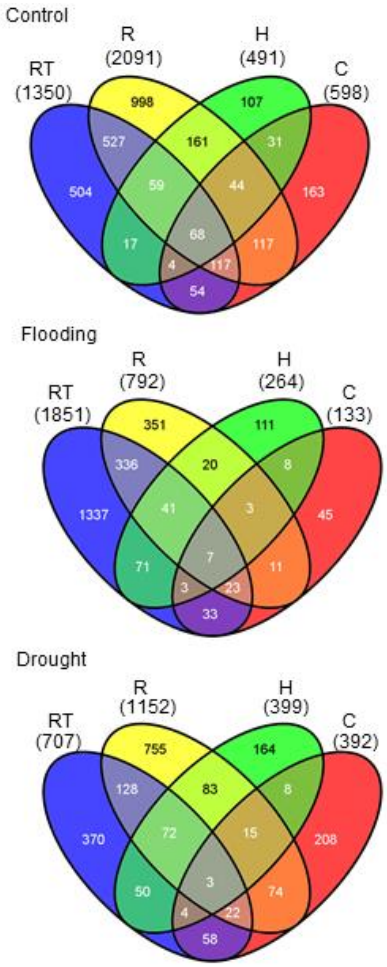

Figure 4. Venn diagrams of significantly changed organ-specific proteins in the early-stage soybean under flooding and drought. Two-day-old soybeans were treated without or with flooding and drought for 2 days. Protein samples were extracted from root tip, root, hypocotyl, and cotyledon and then analyzed by nanoLC-MS/MS. Untreated soybeans were used as controls. The venn diagrams show the number of changed proteins among control, flooding, and drought in root tip (RT, dark blue), root (R, yellow), hypocotyl (H, green), and cotyledon (C, red).

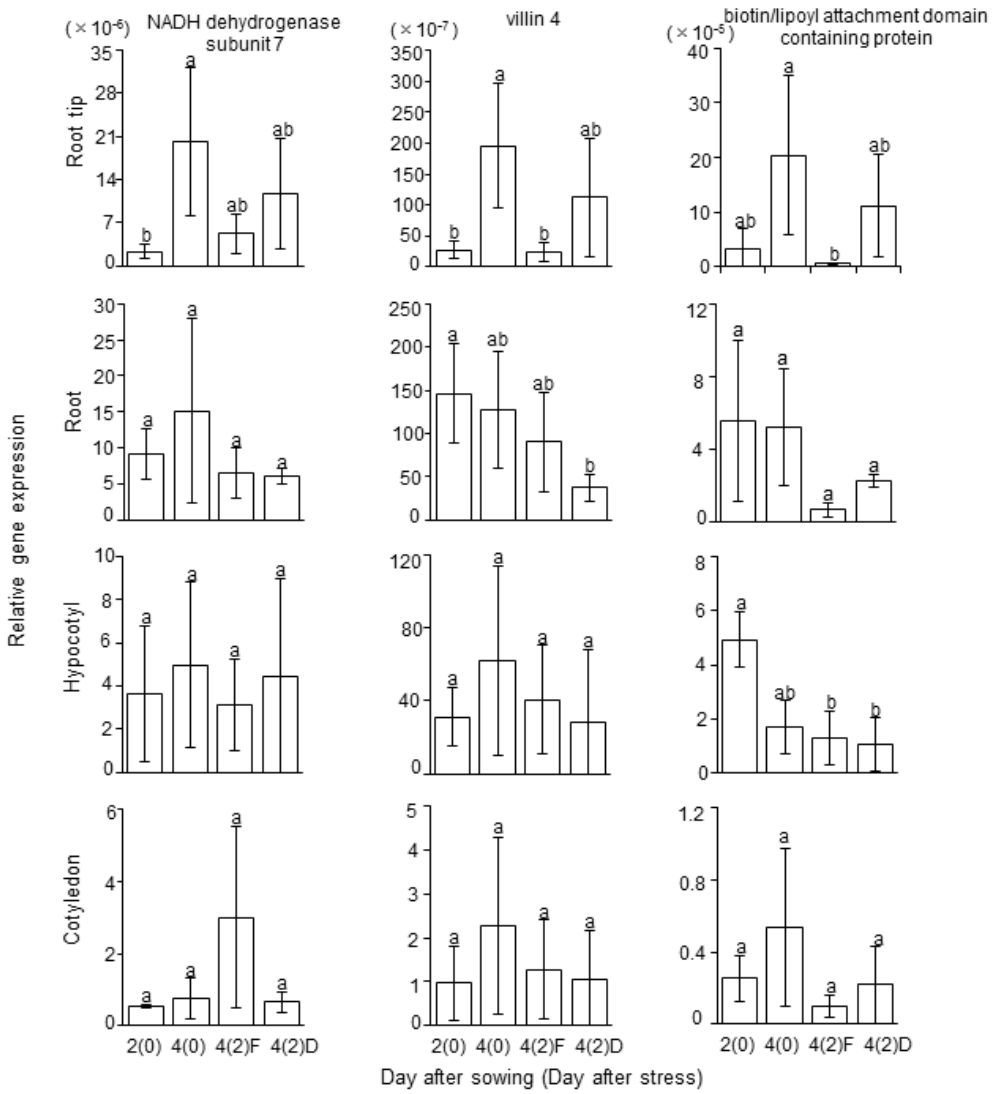
(× 10-6)
NADH dehydrogenase subunit 7
(× 10-7)
villin 4
(× 10-5)
biotin/lipoyl attachment domain containing protein
Root tip
Root
Hypocotyl
Cotyledon
Relative gene expression
2(0) 4(0) 4(2)F 4(2)D
Day after sowing (Day after stress)

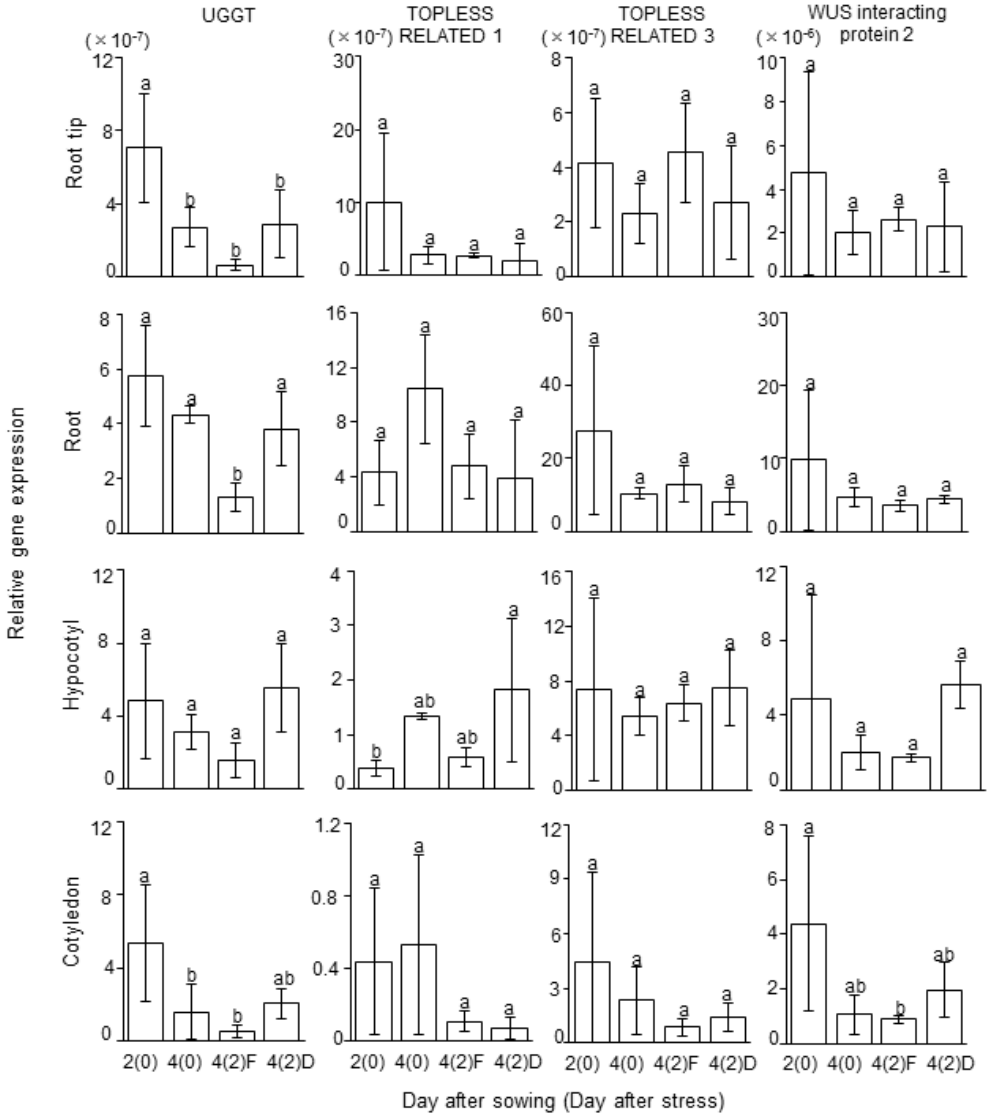

Figure 5. Effects of flooding and drought on gene expression level of the genes encoding organ-specific proteins in the early-stage soybean. Two-day-old soybeans (2(0)) were treated without stress (4(0)), with flooding for 2 days (4(2)F), and with drought for 2 days (4(2)D), and RNA samples were extracted from root tip, root, hypocotyl, and cotyledon. Untreated soybeans were used as control. Gene expression was normalized against that of 18S rRNA. Data are shown as means ± SD from three independent biological replicates. Different letter indicates the change is significant, as determined by one-way ANOVA according to Tukey's Multiple multiple comparison test (p<0.05).

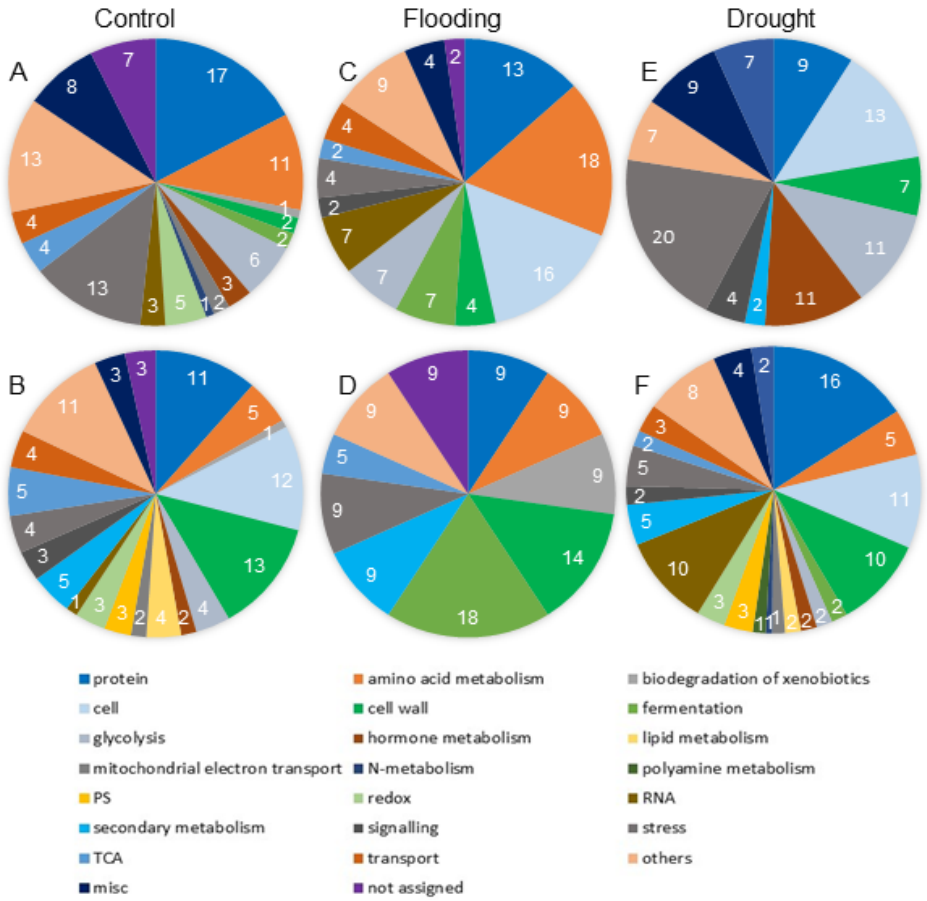

Figure 6. Functional analysis of the identified proteins in root tip of the early-stage soybean exposed to flooding and drought over time. Functional analysis of identified proteins was performed using MapMan bin codes. In control, the functional categories of proteins decreased (A) and increased (B) are shown; under flooding, the functional categories of proteins decreased (C) and increased (D) are shown; under drought, the functional categories of proteins decreased (E) and increased (F) are shown. Abbreviations are as follows: PS, photosynthesis; TCA, tricarboxylic acid; misc, miscellaneous enzyme family. Others included C1-metabolism, development, DNA, major carbohydrate metabolism, minor CHO metabolism, metal handling, nucleotide metabolism, and oxidative pentose phosphate pathway. The numbers in the pie graph indicate the percentage of proteins in each category.

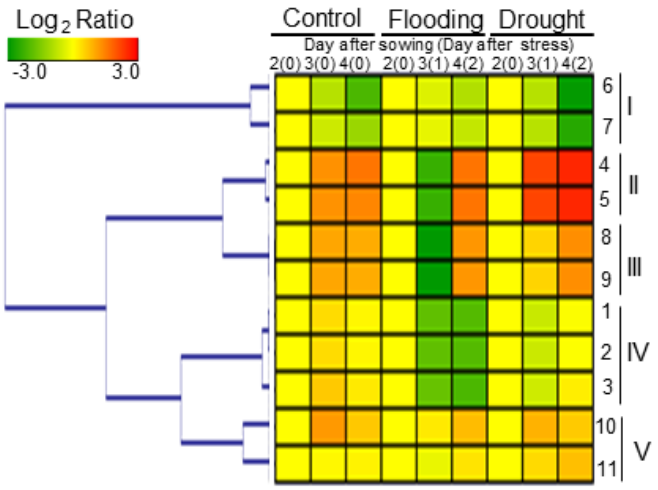

Figure 7. Cluster analysis of commonly changed proteins in root tip of the early-stage soybean under flooding and drought over time. Two-day-old soybeans were treated without or with flooding and drought for 1 and 2 days. Protein samples were extracted from root tip of 2-, 3-, and 4-day-old soybeans without stress (Control); 2-day-old soybeans exposed to flooding for 1 and 2 days (Flooding); and 2-day-old soybeans treated with drought for 1 and 2 days (Drought). In total, 11 common proteins were identified among control, flooding, and drought conditions over time. Black lines denoted the significant clusters based on the logarithmic values of protein abundance. The numbers in the figure show the protein number and correspond to those in Table 5.

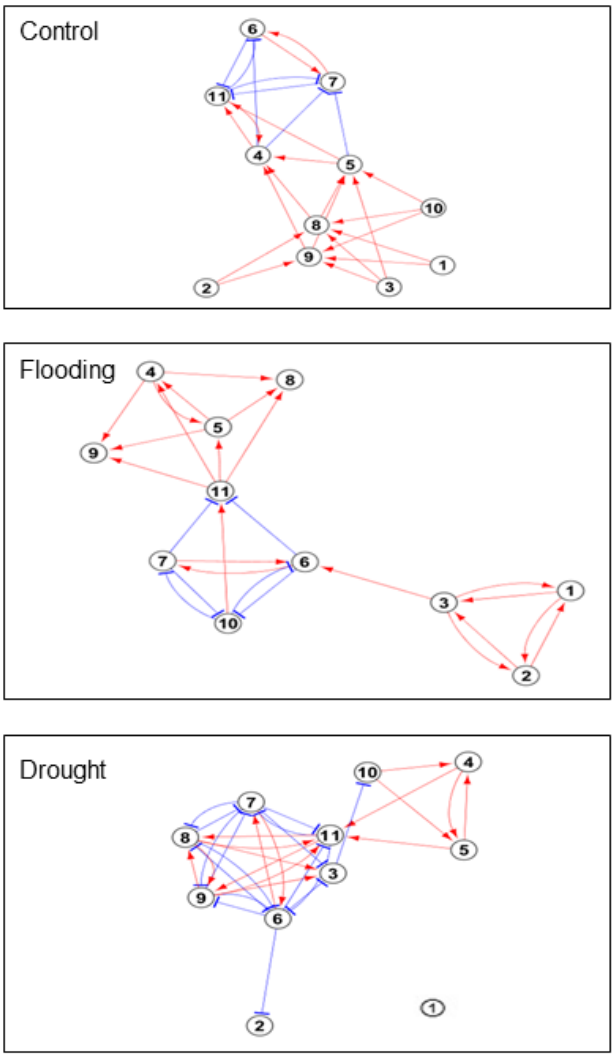

Figure 8. *In silico* protein-protein interaction of commonly identified proteins in root tip of the early-stage soybean under flooding and drought over time. Two-day-old soybeans were treated without or with flooding and drought for 1 and 2 days, and protein samples were extracted from root tip. Eleven common proteins among control, flooding, and drought conditions were analyzed. Protein interactions were estimated based on temporal protein abundance. Interactions showing an r^2 (coefficient of determination) of more than 0.8 were considered as candidate interactions. In the interactions, a red arrow indicates an inductive interaction, and a blue T-bar indicates a suppressive interaction. The numbers in the figure show the protein number and correspond to those in Table 5.

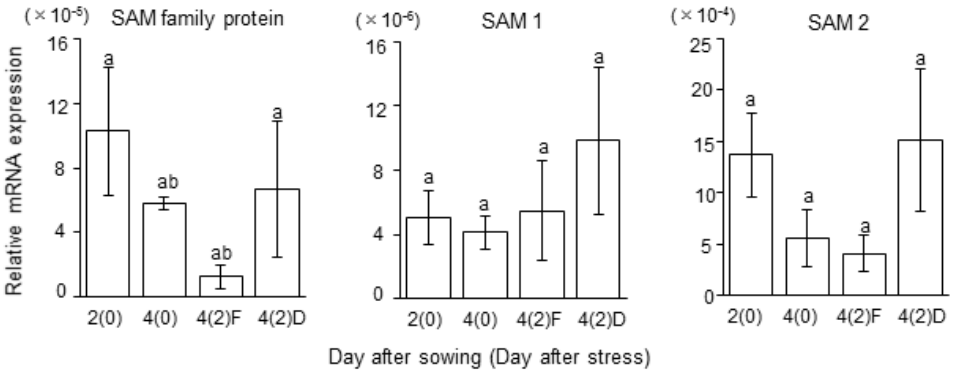

Figure 9. Effects of flooding and drought on gene expression of SAM synthetases in root tip of the early-stage soybean. Two-day-old soybeans were treated without or with flooding (F) and drought (D) for 2 days. RNA samples were extracted from root tip and subjected to gene expression analysis. Untreated soybeans were used as controls. Gene expression was normalized against that of 18S rRNA. Data are shown as means ± SD from three independent biological replicates. Different letter indicates the change is significant, as determined by one-way ANOVA according to Tukey's Multiple multiple comparison test ($p<0.05$).

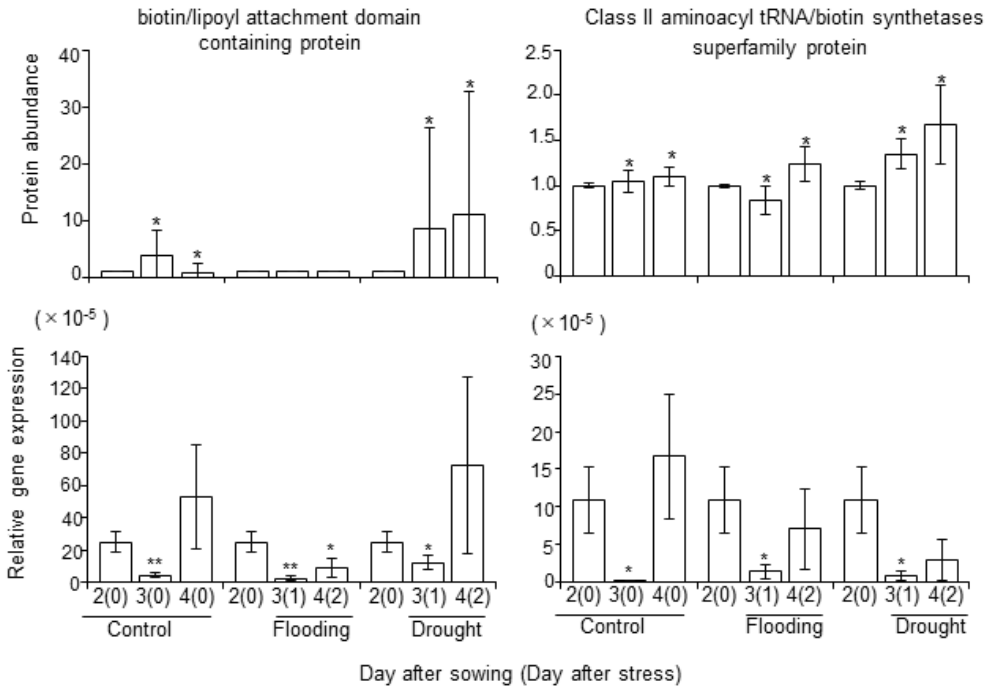

Figure 10. Protein abundance and gene expression of biotin/lipoyl attachment domain containing protein and Class II aminoacyl tRNA/biotin synthetases superfamily protein in root tip of the early-stage soybean. Two-day-old soybeans were treated without or with flooding and drought for 1 and 2 days. Protein samples were extracted from root tip and analyzed by nanoLC-MS/MS. RNA samples were extracted from the root tip and subjected to qRT-PCR analysis. Untreated soybeans were used as controls. The protein abundance was acquired by comparison to untreated soybeans using SIEVE software (p<0.05). Gene expression was normalized against that of 18S rRNA. Data are shown as means ± SD from three independent biological replicates. Student's t-test analysis was used to evaluate protein abundance and gene expression. Two-day-old untreated soybean was used as the comparison point among control, flooding, and drought. The asterisks indicate significance between different time points (*p<0.05, **p <0.01).

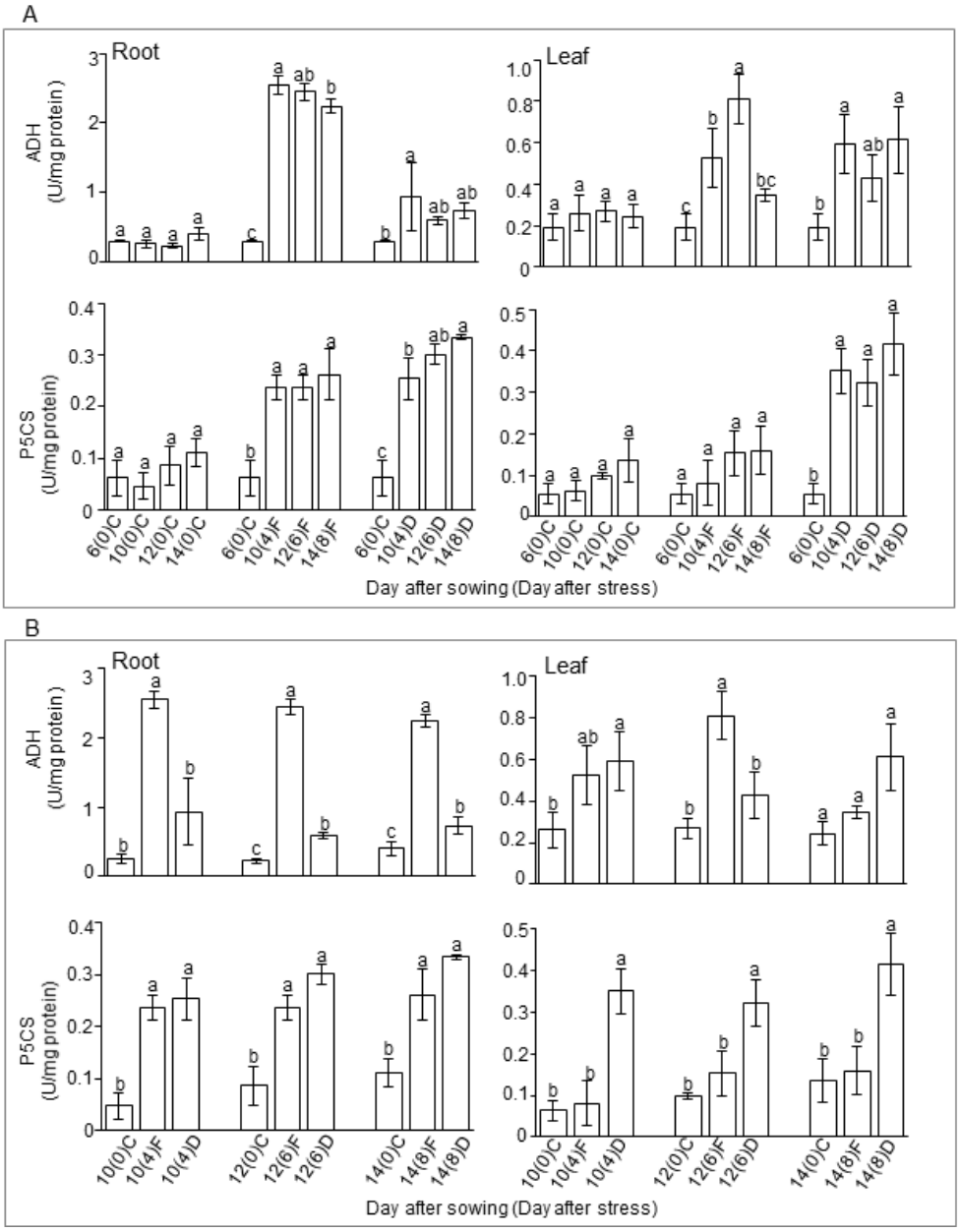

Figure 11. Organ-specific enzyme assay of alcohol dehydrogenase and pyrroline-5-carboxylate synthase in soybean seedling under flooding and drought. Six-day-old soybeans were treated without or with flooding and drought for 4, 6, and 8 days. Enzyme activities of ADH and P5CS were examined in root and leaf of soybean under control (C), flooding (F), and drought (D) on time-dependent manner (A). Enzyme activities of ADH and P5CS were examined in root and leaf of soybean at indicated points among different conditions (B). Data are shown as means ± SD from three independent biological replicates. Different letter indicates the change is significant, as determined by one-way ANOVA according to Tukey's multiple comparison test (p<0.05). Abbreviations are as follows: ADH, alcohol dehydrogenase; P5CS, pyrroline-5-carboxylate synthase.

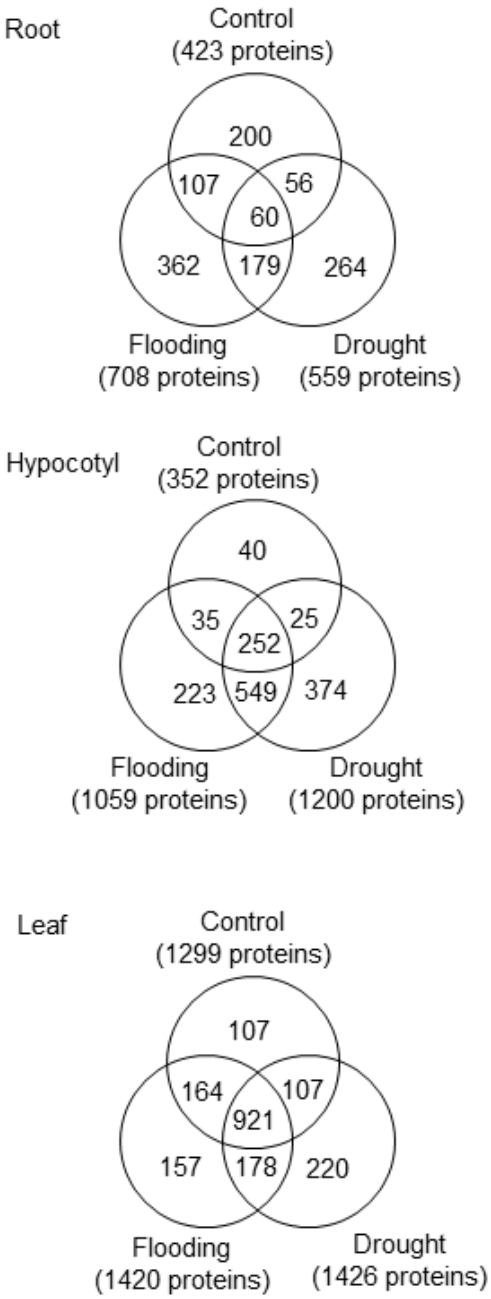

Figure 12. Venn diagrams of flooding- and drought-responsive proteins in soybean seedling. Six-day-old soybeans were treated without or with flooding and drought for 6 days. Root, hypocotyl, and leaf were collected for protein extraction. Extracted proteins were analyzed by nanoLC-MS/MS. Untreated soybeans were used as controls. Venn diagrams show stress-specific proteins in root, hypocotyl, and leaf of soybean seedling among control, flooding, and drought.

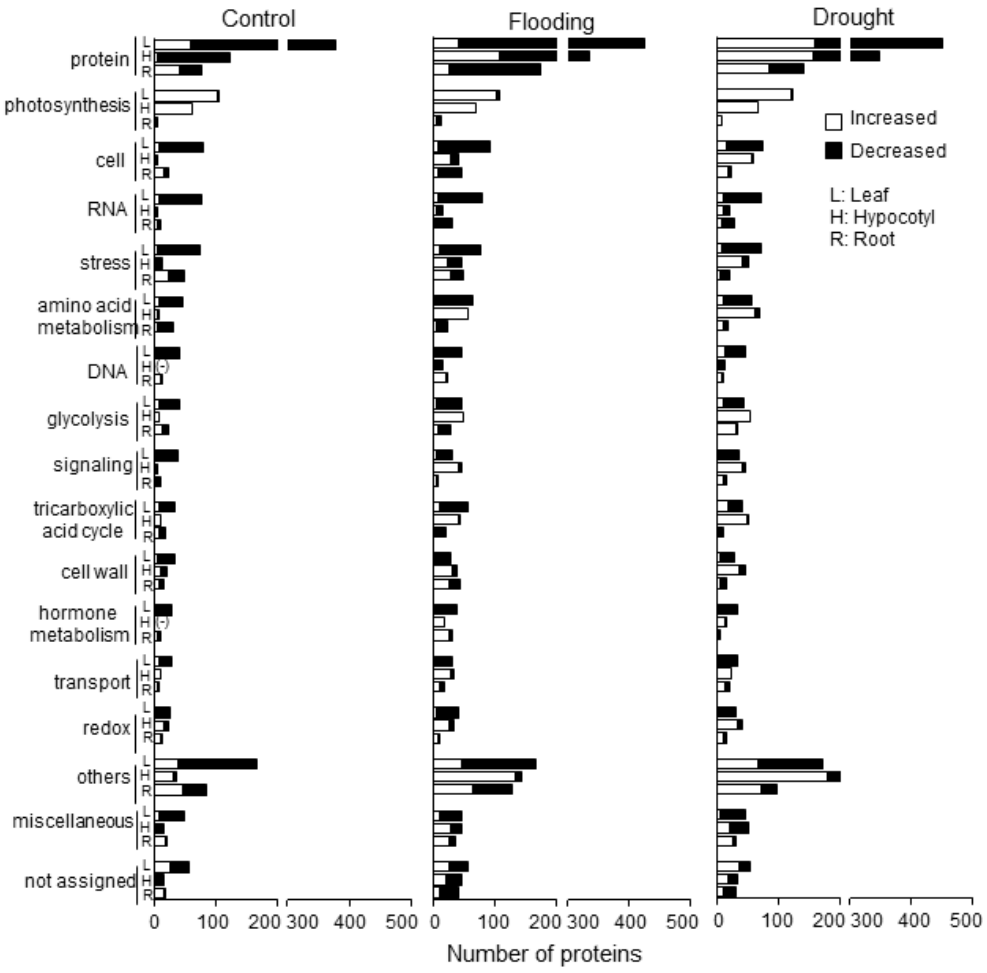

Figure 13. Functional analysis of flooding- and drought-responsive proteins in soybean seedling. Six-day-old soybeans were treated without or with flooding and drought for 6 days. Root (R), hypocotyl (H), and leaf (L) were collected. Functional analysis of identified proteins was performed using MapMan bin codes. Untreated soybeans were used as controls. Others included major/minor carbohydrate metabolism, secondary metabolism, lipid metabolism, polyamine metabolism, vitamin metabolism, C1/N metabolism, nucleotide metabolism, tetrapyrrole synthesis, metal handing, mitochondrial electron transport, fermentation, biodegradation of xenobiotics, oxidative pentose phosphate, development, and gluconeogenesis. Abbreviations are as follows: protein, protein synthesis/degradation; cell, cell division/organization; RNA, RNA metabolsim. The number of categorized proteins are shown in the graph. Open and filled bars indicate increased and decreased proteins, respectively.

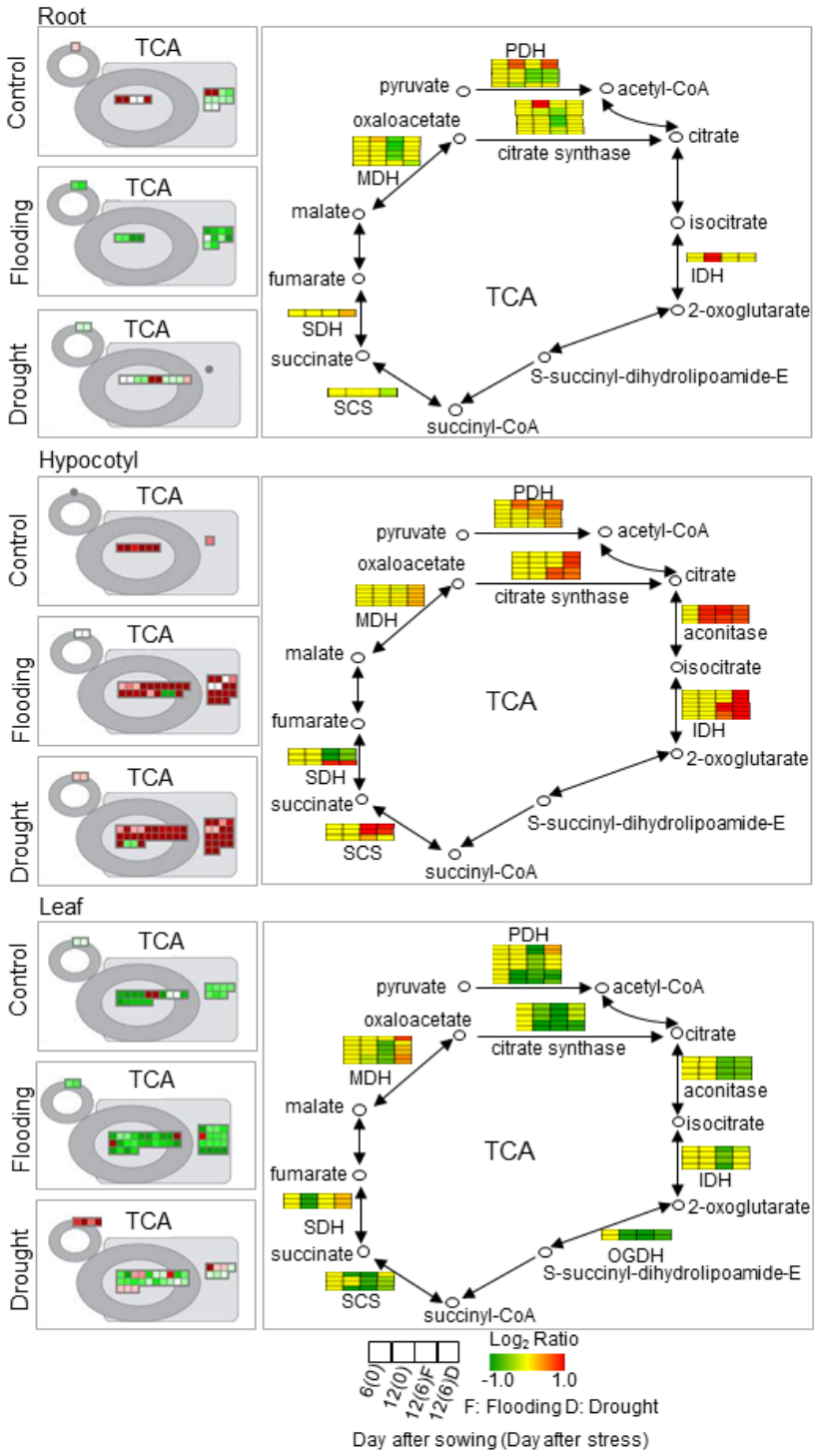

Figure 14. Mapping of identified proteins to the tricarboxylic acid cycle in soybean seedling under flooding and drought. The abundance of identified proteins was compared to 6-day-old untreated soybean. Each square and color indicate Log_2 Ratio of identified protein. Green and red colors indicate decrease and increase, respectively, in the Log_2 Ratio values. Abbreviations are as follows: PDH, pyruvate dehydrogenase; IDH, isocitrate dehydrogenase; OGDH, 2-oxoglutarate dehydrogenase; SCS, succinyl-CoA synthetase; SDH, succinate dehydrogenase; MDH, malate dehydrogenase.

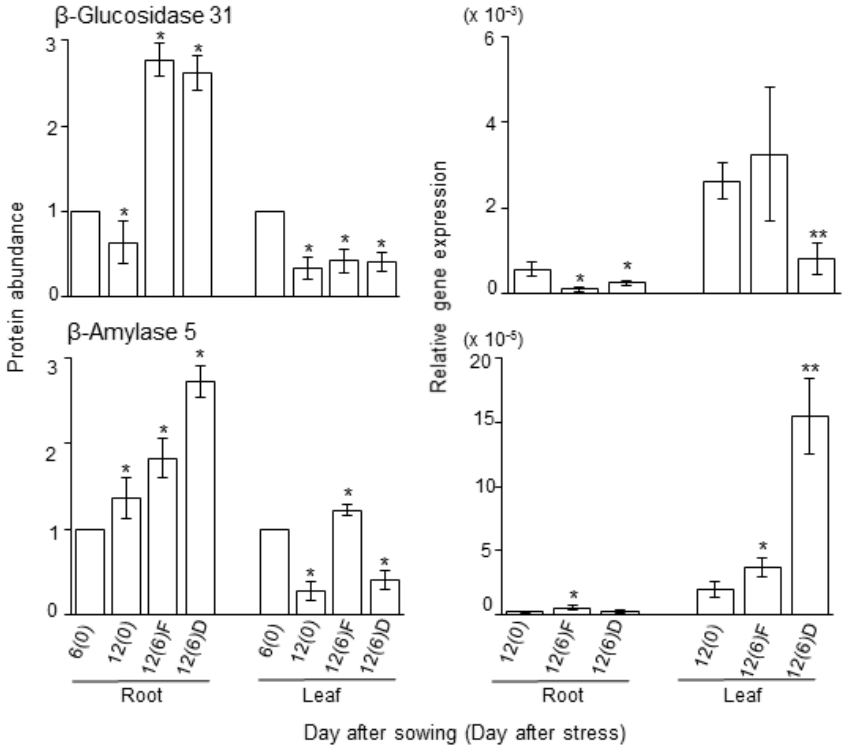

Figure 15. Protein abundance and gene expression of β-glucosidase 31 and β-amylase 5 in soybean seedling under flooding and drought stresses. Six-day-old soybeans were treated without or with flooding and drought for 6 days. Protein samples were extracted and analyzed by nanoLC-MS/MS. RNA samples were extracted and analyzed by qRT-PCR. Untreated soybeans were collected as controls. The protein abundance was acquired by comparison to 6-day-old untreated soybean using SIEVE software (p<0.05). Gene expression was normalized against that of 18S rRNA and significance was examined using the Student's t-test. Data are shown as means ± SD from three independent biological replicates. The asterisks indicate the significance between 12-day-old soybeans without or with flooding and drought (*p< 0.05, **p< 0.01).

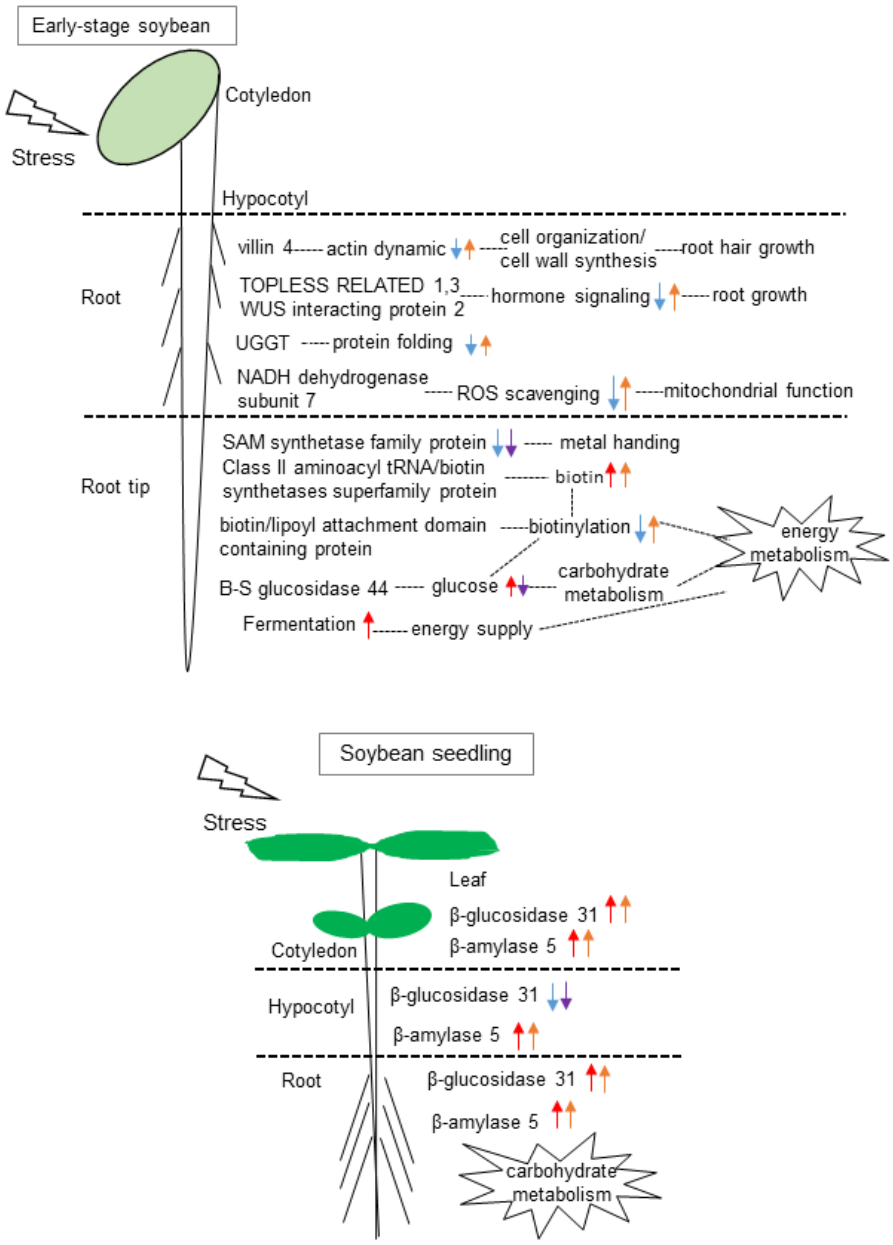

Figure 16. Schematic representation of flooding and drought responsive mechanisms in different organs of soybean in the early stage and seedling stage. The red and blue arrows indicate changes of protein abundance under flooding; orange and purple arrows indicate changes of protein abundance under drought; and upward and downward arrows indicate increased and decreased changes of protein abundance, respectively.

Chapter 2
Endoplasmic reticulum proteomics in soybean under flooding and drought stresses

2.1. Introduction

The cellular processes for sensing environmental changes and responsive mechanisms are highly organized (Heino and Palva, 2003). Subcellular proteomics elucidates the functions of spatially organized proteins in specific organelle (Lilley and Dupree, 2006). Proteomic analyses of cell wall (Mithöfer et al., 2002; Komatsu et al., 2010), plasma membrane (Komatsu et al., 2009a; Nouri and Komatsu, 2010), nucleus (Wu et al., 2009; Yin and Komatsu, 2015), and mitochondria (Yin et al., 2009; Komatsu et al., 2011a) have been conducted to investigate the role of proteins in plant development and stress responses of soybean. Under flooding, signal-related proteins in plasma membrane cooperatively regulated H^+-ATPase activity (Komatsu et al., 2009a), which also increased in response to drought to accelerate ion efflux (Nouri and Komatsu, 2010). In soybean nucleus, variants and modifications of histone were observed during development (Wu et al., 2009), and ABA treatment altered the levels of several phosphoproteins in flooded soybean (Yin and Komatsu, 2015). Flooding disrupted electron transport chains in soybean mitochondria (Komatsu et al., 2011a), which displayed changes in ultrastructure and metabolic activity in response to cold (Yin et al., 2009). Based on these reports, investigating the functions of subcellular organelles under various stress conditions is expected to provide insights into the mechanisms by which plants attempt to cope with unfavorable growth conditions.

The ER is a continuous membrane system, which consists of a nuclear envelope and flattened peripheral sheets containing ribosomes and interconnected tubules that extend throughout most of cytoplasm (Healy et al., 2012). The ER functions as a protein factory and calcium reservoir (Papp et al., 2003), and serves as the cabinet for protein quality, which is monitored by various signaling pathways mediated by protein folding assistants (Sitia and Braakman, 2003; Tu and Weissman, 2004). Accumulation of misfolded or unfolded proteins causes ER stress and it ultimately leads to cell death under adverse environmental conditions (Vitale and Boston, 2008; Howell, 2013). Proteomic analysis of the ER revealed that protein synthesis and glycosylation were affected in soybean exposed to flooding (Komatsu et al., 2012b). Although these findings indicated that ER function was altered under flooding (Komatsu et al., 2012b), ER proteins induced by abiotic stresses have not been fully resolved.

Root tip is essential for root growth and development (Mathesius et al., 2011), and it undergoes morphological and physiological changes in response to various stresses (Feldman, 1984). For example, in root tip of *Arabidopsis*, primordia formation of lateral root was inhibited under high salt condition and elongation of existing lateral root increased due to auxin accumulation (Wang et al., 2009). In root tip of soybean, exposure to flooding induced protein phosphorylation, which altered the regulation of metabolic pathways and led to decreased cellular ATP content (Nanjo et al., 2012). Exposure to sudden flooding induced accumulation of ROS and programmed cell death in root tip of pea, allowing for rapid diversion of resources to lateral root for stimulating growth (Gladish et al., 2006; Cheng et al., 2013). Under drought, elongation was maintained at normal rates in the apical zone of maize root; however, progressive inhibition of elongation occurred at greater distances from the root tip (Sharp et al., 2004). Taken together, these properties demonstrate that root tip is associated with plant growth and stress responses.

Stage-dependent proteomics was conducted in soybean under flooding and drought stresses, indicating that early-stage soybean was more sensitive compared to seedling stage. Especially, root tip presented with more responsive proteins compared to other organs in the early-stage soybean (Chapter 1). To uncover the response mechanisms triggered in the ER by flooding and drought stresses, proteomic analysis was performed. The rough ER fraction was enriched from soybean-root tip and proteins were analyzed using gel-free/label-free proteomic technique. Based on ER proteomic results, analyses of gene expression, glycoproteomics, and endogenous calcium content were further conducted.

2.2. Materials and methods

2.2.1. Plant material and treatments

Soybean was used as plant material in this study. Plant growth conditions were the same as described in 1.2.1 in Chapter 1. For treatment, 2-day-old soybeans were exposed to flooding or drought by adding 700 mL of excess water or withholding water for 2 days, respectively. For all experiments, untreated soybeans were collected as controls. Three independent experiments were performed as the biological replicates for

all experiments. Biological replicate means soybeans sown on different days. One hundred and fifty plants were collected as material for one replicate (Figure 17).

2.2.2. Enrichment of rough endoplasmic reticulum

Rough ER was enriched according to the instructions supplied by the Endoplasmic Reticulum Enrichment Kit (Novus, Littleton, CO, USA) with some modifications (Figure 18). All the procedures were performed at 4ºC. For enrichment, a portion (1.0 g) of root tips was ground with a mortar and pestle in grinding buffer containing 4 mL of 1 x Isosmotic Homogenization Buffer and 40 µL of 100 x Protease Inhibitor Cocktail (Novus). Homogenates were centrifuged at 1000 x g for 10 min and pellet was collected as Fraction 1. The supernatant was centrifuged at 10000 x g for 15 min and the pellet was collected as Fraction 2. The transferred supernatant was centrifuged at 12000 x g for 15 min. After centrifugation, the supernatant was collected and 8 mM $CaCl_2$ was added drop by drop with stirring for 15 min. The precipitated sample was centrifuged at 8000 x g for 10 min. The obtained pellet was collected as rough ER fraction.

2.2.3. Enrichment of glycoproteins

A portion (0.5 g) of root tips was ground with a mortar and pestle in extraction buffer consisting of 20 mM HEPES-NaOH (pH 7.5), 150 mM NaCl, 10% glycerol, 1% Nonidet P-40, and 0.25% sodium deoxycholate. The homogenates were centrifuged at 20000 x g for 10 min at 4ºC. The obtained supernatant was subjected to glycoprotein enrichment using the Glycoprotein Isolation Kit, ConA (Thermo Scientific, Rockford, IL, USA). All the procedures were carried out at 25ºC. The extracts were equilibrated with the binding buffer supplied in the kit. ConA resin was placed into the spin column and centrifuged at 1000 x g for 1 min. ConA resin was washed three times using the binding buffer. The equilibrated extracts were added to the ConA resin, mixed for 10 min, and centrifuged at 1000 x g for 1 min. The flow-through was discarded and resin was washed four times using the binding buffer. SDS-sample buffer consisting of 60 mM Tris-HCl (pH 6.8), 2% SDS, 10% glycerol, and 5% β-mercaptoethanol (Laemmli, 1970) was added to the resin and kept rotating for 30 min. The resin was centrifuged at

1000 x g for 1 min. The flow-through was determined as enriched glycoproteins.

2.2.4. Extraction of cellular proteins for immunoblot and enzyme activity analyses

For immunoblot analysis, a portion (0.1 g) of root tips was ground with a mortar and pestle in the SDS-sample buffer. The homogenates were centrifuged at 20000 x g for 20 min at 25°C. The supernatant was collected as cellular protein extracts. For enzyme assay, a portion (0.1 g) of root tips was ground with a mortar and pestle in the enzyme extraction buffer containing 50 mM HEPES-NaOH (pH 7.5), 1 mM phenylmethylsulfonyl fluoride, 0.1% Triton X-100, 5 mM $MgCl_2$, 1 mM dithiothreitol, 2% polyvinylpyrrolidone-40, and 1 mM EDTA. The homogenates were centrifuged at 20000 x g for 20 min at 4°C. The supernatant was collected as cellular protein extracts.

2.2.5. Concentration measurement of proteins and peptides

The method of Braford (Braford, 1976) as described in 1.2.3 in Chapter 1 was used to determine protein concentration of the samples for proteomic, enzyme activity, and clalium quantification analyses. The method of Pierce 660 nm Protein Assay Kit with Ionic Detergent Compatibility Reagent (Thermo Scientific) was used to determine protein concentration of the samples, which were dissolved in SDS-sample buffer. The Direct Detect Spectrometer (Millipore, Billerica, MA, USA) with the Direct Detect software (version 3.0.25.0) was used to determine peptide concentration.

2.2.6. Immunoblot analysis for purity assessment of the endoplasmic reticulum

Histone H3 was used as marker protein for nucleus. Each fraction collected in rough ER isolation procedure was added SDS-sample buffer. Cellular protein extracts and each collected fraction in SDS-sample buffer were sonicated for 20 min followed by centrifuged at 20000 x g for 20 min at 25°C. Proteins (10 µg) of each sample were separated using 17% SDS-polyacrylamide gel electrophoresis and transferred onto the polyvinylidene difluoride membrane using a semidry transfer blotter. The blotted membrane was blocked overnight at 4°C in the buffer containing 500 mM NaCl, 20 mM Tris-HCl (pH 7.5), 0.1% Tween-20, and 5% skim milk (Difco, Sparks, MD, USA). After blocking, the membrane was incubated with a 1: 9000 diluted anti-histone H3

antibody (Santa Cruz Biotechnology, Santa Cruz, CA, USA) for 1 h at 25ºC. Subsequently, the membrane was washed three times using the buffer containing 500 mM NaCl, 20 mM Tris-HCl (pH 7.5), and 0.1% Tween-20. The anti-rabbit IgG conjugated with horseradish peroxidase (Bio-Rad) was used as the secondary antibody and incubated for 1 h at 25ºC. Signals were detected using the Chem-Lumi One Super kit (Nacalai tesque, Kyoto, Japan) and visualized by LAS-3000 luminescent image analyzer (Fujifilm, Tokyo, Japan). The relative intensities of bands were calculated using ImageJ software (version 1.46). Coomassie brilliant blue staining was used as loading control.

2.2.7. Enzyme activity analysis for purity assessment of the endoplasmic reticulum

ADH, fumarase, and NADH cytochrome *c* reductase were used as marker proteins for cytosol, mitochondria, and the ER, respectively. Each fraction collected in the rough ER isolation procedure was added enzyme extraction buffer. Cellular protein extracts and each collected fraction in enzyme extraction buffer were sonicated in cold water for 40 min followed by centrifuged at 20000 x g for 20 min at 4ºC. The supernatant was collected for enzyme assay analysis.

ADH: the activity of ADH was performed as described in 1.2.11 in Chapter 1.

Fumarase: the reaction solution contained 70 mM KH_2PO_4-NaOH (pH 7.7), 50 mM *L*-malic acid, and 0.05% Triton X-100. The reaction was measured continuously for 5 min at 25ºC at 340 nm (EC_{340} = 2.55 mM^{-1} cm^{-1}). The activity of fumarase was calculated using formula: U/mg protein = [(ΔA340/min x total volume x sample dilution factor)/(2.55 x sample volume)]/protein concentration (Huang et al., 2014).

NADH cytochrome *c* reductase: the reaction solution contained 20 mM potassium phosphate buffer (pH 7.2), 0.2 mM NADH, 0.02 mM cytochrome *c*, and 6 mM NaN_3. The reaction was measured continuously for 5 min at 25ºC at 550 nm (EC_{550} = 21.1 mM^{-1} cm^{-1}). The activity of NADH cytochrome *c* reductase was calculated using formula: U/mg protein = [(ΔA550/min x total volume x sample dilution factor)/(21.1 x sample volume)]/protein concentration (Hasinoff, 1990; Gomez and Chrispeels, 1994).

2.2.8. Clean up and digestion of cellular proteins

Rough ER fraction was added lysis buffer containing 7 M urea, 2 M thiourea, 5% CHAPS, and 2 mM tributylphosphine. The homogenates were centrifuged at 20000 x g for 20 min at 25°C. The supernatant was collected as rough ER proteins. Rough ER proteins (100 µg) and enriched glycoproteins (100 µg) were cleaned up and digested as described in 1.2.4 in Chapter 1. For glycoproteomics, the Pierce Detergent Removal Spin Columns (Thermo Scientific) was further used to remove detergent in the peptides following manufacturer's instruction.

2.2.9. Mass spectrometry analysis

Mass spectrometry analysis was performed as described in 1.2.5 in Chapter 1. The MS data have been deposited with the ProteomeXchange Consortium (http://proteomecentral.proteomexchange.org) *via* the PRIDE partner repository (Vizcaíno et al., 2013) with the data set identifier PXD003397.

2.2.10. Protein identification using mass spectrometry data

Protein identification was carried out as described in 1.2.6 in Chapter 1.

2.2.11. Analysis of differentially abundant proteins

The acquired Mascot results were exported into SIEVE for the ER proteomic analysis as described in 1.2.7 in Chapter 1. Additionally, exported XML files from Mascot were used for protein abundance through emPAI values for glycoproteomic analysis. The protein abundance was determined by molar percentage (mol%) (Ishihama et al., 2005).

2.2.12. Analyses of protein localization and function

Protein localization was predicated using intracellular targeting prediction programs of SUBA3 (http://suba3.plantenergy.uwa.edu.au/) (Tanz et al., 2013), MultiLoc2 (http://abi.inf.uni-tuebingen.de/Services/MultiLoc2) (Blum et al., 2009), and WoLF PSORT (http://www.genscript.com/wolf-psort.html) (Horton et al., 2007). For predication of the ER proteins, the minimum requirement was that the identified protein was predicated by one software. The *N*-glycosylation consensus of identified

glycoproteins was predicated using NetNGlyc 1.0 Server (http://www.cbs.dtu.dk/services/NetNGlyc/) (Gupta and Brunak, 2002). Funational analysis was performed using MapMan bin codes (Usadel et al., 2005).

2.2.13. Quantification of endogenous calcium content

A portion (0.1 g) of root tips was ground with a mortar and pestle in calcium extraction buffer containing 50 mM phosphate buffered saline (pH 7.5), and the homogenates were centrifuged at 12000 x g for 15 min at 4°C. The supernatant was collected for calcium quantification using the Calcium Colorimetric Assay Kit (Sigma-Aldrich, St. Louis, MO, USA) according to manufacturer's instructions. The absorbance of complex was measured at 575 nm and quantified based on known concentration of calcium solution. The calcium content was determined as mmol/g protein to minimize the effect of sample variance during extraction process.

2.2.14. RNA extraction and quantitative reverse transcription-polymerase chain reaction

RNA extraction and qRT-PCR analysis were performed as described in 1.2.12 in Chapter 1. The qRT-PCR primers were designed using the Primer3Plus web interface (http://www.bioinformatics.nl/cgi-bin/primer3plus/primer3plus.cgi/) (Table 7).

2.2.15 Statistical analysis

Statistical analysis was performed as described in 1.2.13 in Chapter 1.

2.3. Results

2.3.1. Purity of the endoplasmic reticulum in soybean-root tip

The proteomic technique was performed to investigate roles of the ER in soybean-root tip under flooding and drought stresses (Figure 17). Two-day-old soybeans were treated without or with flooding or drought for 2 days, and rough ER was isolated (Figure 18). The purity of the ER isolated from root tips of 2-day-old soybeans was assessed by immunoblot analysis (Figure 19) and enzyme activity (Figure 20). For immunoblot analysis, anti-histone H3 antibody was used as a positive marker of nuclear proteins, indicating that it cross-reacted with a 17-kDa protein in cellular-protein

fraction, Fraction 1, Fraction 2, and rough ER fraction (Figure 19). However, relative intensity of corresponding signal band was nine-fold less in the ER fraction than in the Fraction 1 (Figure 19). In addition, the immunoblot analysis of 4-day-old soybeans without or with flooding and drought indicated that corresponding band was higher in the Fraction 1 than in other fractions (Figure 21).

The purity of the ER fraction was also assessed using enzyme activity analyses for ADH and fumarase, which were used as markers of contamination from cytosolic and mitochondrial proteins, respectively; and for NADH cytochrome *c* reductase, which was used as positive marker of the ER proteins (Figures 20 and 21). In the 2-day-old soybeans, the highest activity of ADH was detected in the cellular-protein fraction; the highest activity of fumarase was detected in Fraction 2; and the highest activity of NADH cytochrome *c* reductase was detected in the rough ER fraction, which was two-fold higher than in other fractions (Figure 20). In addition, enzyme activity analysis of 4-day-old soybeans without or with flooding or drought indicated that the activity of NADH cytochrome *c* reductase was higher in the rough ER fraction than in other fractions (Figure 21). Based on the results of immunoblot and enzyme activity analyses, it indicated that the ER was isolated with high purity from root tip of soybean under control, flooding, and drought conditions using current method.

2.3.2. Effects of flooding and drought stresses on ribosomal proteins

Rough ER fraction was isolated from the root tips of 2-day-old soybeans without or with flooding or drought for 2 days. Extracted rough ER proteins were analyzed using gel-free/label-free proteomic technique. In the rough ER fraction, 1511, 1770, and 770 proteins were identified from control, and flooding- and drought-stressed plants, respectively (Figure 22). Among the identified proteins, 63, 74, and 40 ribosomal proteins were detected in the control, and flooding- and drought-stressed plants, respectively (Figures 22 and 23). Comparison of the relative protein levels revealed that 73% (46/63) of the identified ribosomal proteins were increased during development, whereas 65% (48/74) and 80% (32/40) of them were decreased in response to flooding and drought, respectively (Figure 23).

To improve identification accuracy of the ER proteins, localization of 1448, 1696,

and 730 proteins in the control, and flooding- and drought-stressed plants, respectively, was predicated using several subcellular prediction programs including SUBA3, MultiLoc2, and WoLF PSORT. Using this approach, 255, 368, and 103 proteins in the control, and flooding- and drought-stressed samples, respectively, were predicted to be ER proteins (Figure 22). Functional analysis of the predicted ER proteins was performed using MapMan bin codes. Functional category of protein was separated into several subcategories including glycosylation, degradation, and targeting (Figure 24). The ER proteins related to protein glycosylation and signaling were changed in abundance by more than three-fold in the control, and flooding- and drought-stressed plants. Redox homeostasis was the major functional category in control plants during development, whereas several transport-related proteins were increased under flooding and drought. Additionally, proteins related to stress, development, and protein degradation were markedly decreased in response to drought (Figure 24).

2.3.3. Effects of flooding and drought stresses on protein glycosylation and signaling

Functional analysis of predicated ER proteins indicated that proteins related to protein glycosylation and signaling were significantly altered under flooding and drought (Figure 24). To further explore the effects of stresses on protein glycosylation and signaling in the ER, proteins related to protein glycosylation, redox homeostasis, signaling, and transport were examined at gene expression level (Table 8, Figures 25 and 26). Among the genes related to protein glycosylation, *dolichyl-diphospho-oligosaccharide protein glycosyltransferase* (Table 8, number 4) was downregulated after 1-day flooding and 2-day drought (Figure 25). *β-Xylosyltransferase* (Table 8, number 9) was upregulated at the early stage of development and after 1 day of flooding exposure, but downregulated after 3 days of flooding and 2 days of drought (Figure 25). *α-Mannosyl glycoprotein N-acetylglucosaminyl transferase* (Table 8, number 10) was downregulated after 1 day of both stresses (Figure 25).

Expression level of genes related to protein folding was also altered in response to flooding and drought (Figure 25). *Calnexin 1* (Table 8, number 15) was upregulated at the early stage of development, but downregulated under both stresses (Figure 25). Similarly, *calreticulin 3* (Table 8, number 28) and *protein disulfide isomerase (PDI)-like*

proteins 1,2; 1,1; and *1,6* (Table 8, number 47, 48, and 69) were downregulated after 1-day flooding and 3-day drought (Figure 25). In contrast, *UGGT* (Table 8, number 12) was upregulated during development and downregulated after 3 days of drought, but unaltered in response to flooding (Figure 25). *Ribophorin I* (Table 8, number 3 and 8) was downregulated after 1 day of both stresses (Figure 25). *Chaperone regulator-like protein* (Table 8, number 37) was downregulated after 2 days of flooding and 3 days of drought (Figure 25).

Gene expression of proteins related to signaling and transport was analyzed (Figure 26). *Calmodulin-binding proteins* (Table 8, number 18 and 30) were downregulated at the early stage of flooding and after 3 days of drought (Figure 26). *RAB homolog 1* (Table 8, number 33), but not *GTPase homolog B1C* (Table 8, number 26), was downregulated after 2 days of both stresses (Figure 26). *Ca^{2+}-transporting ATPase* (Table 8, number 98) was downregulated after 2-day flooding and 1-day drought (Figure 26). In addition, several genes had different expression levels between flooding and drought. For example, *leucine-rich repeat receptor-like protein kinase* (Table 8, number 36) and *inorganic H^+ pyrophosphatase family protein* (Table 8, number 96) were upregulated under flooding, but downregulated or unaltered in response to drought (Figure 26).

2.3.4. Effects of flooding and drought stresses on glycoproteins

Functional analysis and gene expression indicated that protein glycosylation and folding responded to both stresses (Figures 24 and 25). To further examine the effects of flooding and drought on protein glycosylation, glycoproteomic analysis was conducted using enriched glycoproteins from cellular protein extracts in root tips of 2-day-old soybeans exposed to flooding or drought for 2 days (Figure 27). A total of 162 (118+44) and 293 (199+94) proteins were identified in the root tip of 2- and 4-day-old soybeans under control condition, and of these proteins, 118 and 199 proteins were predicted with *N*-glycosylation sites, respectively. In addition, 286 (187+99) and 251 (177+74) proteins were identified including 187 and 177 predicted as *N*-glycoproteins exposed to flooding and drought, respectively. Furthermore, the ratio of *N*-glycoproteins was 64% (18.47/29.08), 65% (39.39/60.68), 57% (39.86/70.03), and 61% (33.85/55.42) under

each condition (Figure 27). These results indicated that *N*-glycoproteins accumulated in the root tip of soybean during development; however, the number and accumulation of *N*-glycoproteins were reduced exposed to both stresses.

2.3.5. Effects of flooding and drought stresses on endogenous calcium level

Functional analysis and gene expression of the predicted ER proteins indicated that proteins related to calcium signaling and transport were triggered under both stresses (Figures 24 and 26). To further examine the effects of flooding and drought on calcium, the endogenous calcium contents were quantified in the root tips of 2-day-old soybeans treated without or with flooding or drought for 2 days (Figure 28). Compared to 2-day-old soybeans, calcium level was increased during development and it responsed to both stresses. Furthermore, compared to 4-day-old soybeans, calcium levels were increased exposed to both stresses (Figure 28).

2.4. Discussions

2.4.1. Protein synthesis is suppressed in soybean-root tip under flooding and drought stresses

The rough ER tends to form large flattened sheets studded with ribosomes (Healy et al., 2012), which are composed of ribosomal RNAs and ribosomal proteins (Wilson and Doudna Cate, 2012). Ribosomal proteins are critical for protein synthesis and play regulatory roles in plant development (Byrne, 2009), as well as sensing environmental stimuli (Falcone Ferreyra et al., 2010; Wang et al., 2013). The abnormal-development traits of embryo-lethal and pointed/narrow leaf mutants were attributable to ribosomal protein mutations that disturbed the capacity of cells to maintain normal levels of protein synthesis (Byrne, 2009). Furthermore, post-translational modifications of ribosomal proteins have been shown to be responsive for environmental conditions (Pérez et al., 1990; Weis et al., 2015). In *Arabidopsis*, a knockdown mutant of ribosomal protein *RPL23aA*, which was involved in ribosome biogenesis, displayed retarded growth and irregular root morphology (Degenhardt et al., 2008). The present analysis revealed that ribosomal proteins were mainly decreased under both stresses (Figure 23). Protein synthesis was previously shown to be altered in the root tip of flooded soybean

(Komatsu et al., 2012b). In addition, upregulated gene expression of ribosomal protein mediated translational process and ribosome functioned to enhance cold tolerance in soybean (Kim et al., 2004). The present results combined with previous findings, indicate that protein synthesis is impaired in soybean under flooding and drought stresses, which might be due to the decreased abundance of ribosomal proteins.

2.4.2. Cytochrome *b5* isoform E and inorganic H^+ pyrophosphate family protein are associated with flooding and drought stresses

Functional analysis of redox homeostasis and transport indicated that cytochrome *b5* isoform E and inorganic H^+-pyrophosphate family protein were the most responsive proteins during development and under both stresses (Table 8). Cytochrome *b5* was presented in the Golgi apparatus; however, specific membrane shuttled between the ER and the Golgi through a recycling process (Collot et al., 1982). In *Arabidopsis*, four ER-localized cytochrome *b5* isoforms interacted with REVERSION TO ETHYLENE SENSITIVITY 1, and overexpression of *cytochrome b5D* reduced ethylene sensitivity (Chang et al., 2014). In soybean, ethylene signaling played roles in flooding tolerance through protein phosphorylation (Yin et al., 2014b). In the present study, cytochrome *b5* isoform E was decreased under flooding, suggesting that cytochrome *b5* isoform E might be associated with ethylene signaling in soybean-root tip under flooding. Inorganic H^+ pyrophosphate was involved in generating proton electrochemical gradients and acidified vacuolar lumen, as well as other endomembrane compartments in plants (Sze et al., 1999). Overexpression of *H^+- pyrophosphates* from wheat promoted tobacco growth under normal conditions and enhanced tolerance against unfavorable environments including salt and drought stresses (Li et al., 2014). In the present study, inorganic H^+ pyrophosphatase family protein was increased under drought, while decreased under flooding, suggesting that vacuolar H^+-pyrophosphate might play roles in acidifying the ER lumen and is required for enhancing drought tolerance in soybean.

2.4.3. *N*-glycan synthesis is enhanced under flooding, but not under drought

In the ER, nascent polypeptides bearing glycosylated sites are folded in an *N*-

glycan-dependent manner (Howell, 2013). In the present study, the ER proteins related to protein glycosylation responded to both stresses (Figures 22 and 24). Dolichyl-diphospho-oligosaccharide protein glycosyltransferase is the subunit of an oligosaccharyltransferase, which transfers oligosaccharides to proteins after the synthesis of lipid-linked oligosaccharide (Pattison and Amtmann, 2009). β-Xylosyltransferase (Kajiura et al., 2012) and α-mannosyl glycoprotein *N*-acetylglucosaminyl transferase (Bakker et al., 1999) are involved in *N*-linked glycan synthesis. In *Arabidopsis*, enhancement of oligosaccharyltransferase anchoring protected cells from DNA fragmentation induced by ultraviolet C irradiation (Gallois et al., 1997; Danon et al., 2004), and maturation of *N*-glycan complexes was essential for adaptation to high-salt condition (Kang et al., 2008). In the present study, dolichyl-diphospho-oligosaccharide protein glycosyltransferase, β-xylosyltransferase, and α-mannosyl glycoprotein *N*-acetylglucosaminyl transferase were increased under flooding, but unaltered under drought. These results indicate that *N*-glycan synthesis is activated under flooding and *N*-glycan complexes might be associated with flooding adaptation in soybean.

2.4.4. Calnexin cycle is suppressed under flooding and drought stresses

N-glycosylation has critical roles in proper folding for glycoproteins. After addition of oligosaccharide, the two outermost glucosyl residues are removed by glucosidases I and II, resulting in a monoglucosylated oligosaccharide, which is specifically recognized by ER lectins, such as calnexin and calreticulin (Healy et al., 2012; Howell, 2013). Protein folding is regulated with the help of recruited foldases, which are associated with oxidative environment of the ER (Williams, 2006). In the present study, calnexin, calreticulin, PDI-like proteins, chaperones, UGGT, and ribophorin I were identified with different abundance in the root tip of soybean under flooding and drought, indicating that calnexin cycle of protein folding might be affected by both stresses. Calnexin and calreticulin create the cabinet for protein folding, and calnexin expression contributed to the regulation of ER-mediated cell death (Delom et al., 2007). Previous reports in soybean indicated that calnexin level was affected by flooding (Nanjo et al., 2010) and osmotic stresses (Nouri et al., 2012). Consistent with

these findings, calnexin was decreased in soybean-root tip under both stresses (Table 8). Taken together, these results suggest that decreased accumulation of calnexin might suppress protein folding under flooding and drought.

2.4.5. Folding-assistant proteins are affected under flooding and drought stresses

To fully investigate the roles of calnexin cycle under both stresses, folding-assistant proteins were further examined. As many as 17 members in the PDI family serve as folding enzymes, which form and interchange disulfide bonds (Williams, 2006). The ER provides an optimized environment for oxidative protein folding (Tu and Weissman, 2004). The major-stress factor associated with flooding is decreased oxygen (Nanjo et al., 2013). In the present study, identified PDI-like proteins were mainly decreased under flooding; however, unaltered under drought. These results imply that protein folding in the ER might be suppressed due to dysfunction of PDI-like proteins under hypoxic condition. In addition to foldases, several chaperone proteins assist with protein folding in the ER. For example, DnaJ proteins functioned as co-chaperones with HSP70 (Ohta and Takaiwa, 2014) and enhanced drought tolerance when they were overexpressed (Wang et al., 2014b). In the present study, DnaJ proteins and HSP70 were decreased under drought (Table 8). These results indicate that protein folding might be impaired in response to drought due to reduced accumulation of HSPs. Taken together, these findings suggest that PDI-like proteins or HSPs might serve as the major-folding assistants under flooding or drought, respectively.

2.4.6. Fewer glycoproteins are accumulated in soybean-root tip under flooding and drought stresses

Protein folding proceeds with the assistance of foldases and chaperones; however, misfolded or unfolded proteins accumulate due to ER stress causing by adverse environmental conditions (Vitale and Boston, 2008). UGGT recognizes and modifies unfolded proteins, and the reglycosylated proteins undergo protein folding (Healy et al., 2012). Ribophorins are transmembrane glycoproteins, which bind ribosomes in rough ER (Rosenfeld et al., 1984), and ribophorin I functions as a chaperone that interacts with misfolded proteins (Qin et al., 2012). In the present study, UGGT and ribophorin I were

increased under flooding, but unaltered under drought (Table 8). These results indicate that refolding might be activated under flooding condition to eliminate ER stress.

In respect to glycoprotein synthesis under both stresses, the subunits of oligosaccharyltransferase were increased under flooding; calnexin was decreased under both stresses; and PDI-like proteins or HSPs were decreased by flooding or drought, respectively (Table 8). To examine the effects of flooding and drought on glycoprotein accumulation, glycoproteomics was further conducted in soybean-root tip (Figure 27). ConA is applicable to isolate most *N*-linked glycan, which has the consensus sequence (Fitchette et al., 2007; Ruiz-May et al., 2012), and it is suitable to evaluate glycoprotein accumulation in stressed soybean (Mustafa and Komatsu, 2014). The results of glycoproteomics indicated that glycoproteins were accumulated during development and comparatively fewer glycoproteins accumulated under both stresses than control (Figure 27). Similarly, fewer glycoproteins were identified in soybean root exposed to flooding (Mustafa and Komatsu, 2014). The present results suggest that decreased calnexin and PDI-like proteins or HSPs under flooding or drought, respectively, might impair protein folding, leading to reduced glycoprotein accumulation.

2.4.7. Cytosolic calcium is increased under flooding and drought stresses

Calcium is an essential nutrient for plant development and serves as the second messenger in plant-signal transduction (Hepler, 2005; Huda et al., 2013). In *Cynodon dactylon*, exogenous calcium improved cold tolerance by reducing ROS (Shi et al., 2014). In flooded soybean, calcium-related signaling responded to stress (Yin et al., 2014a), and exogenous calcium enhanced root elongation and suppressed cell death in root tip (Oh et al., 2014a). In addition, calcium involved in drought tolerance (Shao et al., 2008) and enhanced antioxidative activity when applied exogenously, leading to improved drought recovery in *Camellia sinensis* (Upadhyaya et al., 2011). Taken together, these reports indicate that calcium is associated with various stresses, and exogenous calcium has the capacity to activate cellular metabolism and enhance stress tolerance. In the present study, under both stresses, several signaling-related proteins were changed (Figure 24) and gene expression of proteins related to calcium signaling/transport was downregulated (Figure 26). These results indicate that calcium

levels might fluctuate under flooding and drought stresses. The cytosolic calcium content was further examined, showing that it was increased under both stresses (Figure 28).

The ER is a subcellular organelle that is involved in protein folding and serves as calcium reservoir (Healy et al., 2012; Burgoyne et al., 2015) with the aid of calcium-binding proteins, calcium ATPase, and calcium-release channels (Papp et al., 2003). In the present study, under both stresses, calmodulin-binding proteins were decreased in soybean-root tip, whereas calcium-transporting ATPases increased (Table 8). Furthermore, endogenous calcium levels were increased in cytosol under both stresses (Figure 28). It was reported that cytosolic calcium levels were elevated during development and under various environmental conditions to trigger downstream responses (Kudla et al., 2010; Zhu et al., 2013). Taken together, these results suggest that calcium might be released from the ER into cytosol under flooding and drought, and increased cytosolic calcium functions as the secondary messenger to mediate stress responses in soybean.

2.5. Conclusion

The present proteomic analysis examined protein profiles of the ER in soybean-root tip under flooding and drought stresses. The main findings are as follows (Figure 29): (i) ribosomal proteins were decreased under both stresses; (ii) proteins related to protein glycosylation and signaling responded to both stresses; (iii) calnexin was decreased under both stresses, and PDI-like proteins or HSPs declined under flooding or drought, respectively; (iv) cytosolic calcium was increased under both stresses; and (v) fewer glycoproteins were accumulated under both stresses. Taken together, these findings indicate that calnexin in combination with PDI-like proteins or HSPs plays roles in protein folding under flooding or drought, respectively, and suggest that the reduced accumulation of glycoproteins under both stresses might be due to dysfunction of protein folding. Furthermore, increased cytosolic calcium induced by flooding and drought might alter calcium homeostasis in the ER, leading to suppressed protein folding.

Table 7. Primer sequences of genes selected for qRT-PCR in Chapter 2

Protein ID [a)]	Description	Sequence of primers (5'--- 3')
Glyma04g42690.1	PDI like 1,2	F: TCAACACAATGACGGGAAAA
		R: CTGTTTGCAATGACCACACC
Glyma14g24090.1	PDI like 1,1	F: CACCTTGGATGCCAAATACC
		R: ACAAAAGGGTGATTGCTTGG
Glyma13g40130.1	PDI like 1,4	F: TTTGAGGACTTCGAGGAGGA
		R: TACGTCTTCGCCCTTGAGTT
Glyma15g01880.1	PDI like 1,6	F: TGGAGGTATTTACGCCTTGG
		R: AGCGTGGGGTAGTCATTCAC
Glyma09g38410.2	calreticulin 3	F: ACATCCAGTGATGCCAAACA
		R: CCCCACCAAACTTCTTTTGA
Glyma07g35090.1	calmodulin binding protein	F: TCATTGCTCTGCTTCTGGTG
		R: TGTCCTGCATTCCGACAATA
Glyma15g12880.1	RAB GTPase homolog B1C	F: CATCGGTGTTGAATTTGGTG
		R: CTTCCAACCAGCTAGCCAAG
Glyma11g13460.1	calreticulin 3	F: CATGGATTGGGACATCCTTC
		R: TCAACAGGCTTCTTGGCTTT
Glyma20g02951.1	calmodulin binding protein	F: GATTTCTGCGATTGTGCTGA
		R: CCATCGTATTCATCGGTTCC
Glyma09g40980.1	receptor like protein kinase family protein	F: GGGGTTCCAGTGCATAAAGA
		R: CTAGCCGTTGATGGGTCAAT
Glyma20g23490.1	calcium binding EF hand family protein	F: ATGGTTGTGCAAGGAGGAAG
		R: GTTTGCCAATTATGGGCTGT
Glyma11g33100.1	RAB homolog 1	F: CAGACGCTGGCAGTAAATGA
		R: TGAAGCTCTTGGACCCACTT
Glyma11g34490.1	leucine-rich repeat receptor like protein kinase	F: AGTATGTGGGGTTGGAGCTG
		R: CTAGAAGCCGGTCACTGGAG
Glyma09g36560.1	chaperone regulator like protein	F: TCGAGAATGAGTTGCGTTTG
		R: CTCCGCAACCCACTTGTACT
Glyma13g23170.1	inorganic H^+ pyrophosphatase family protein	F: GACTGGGGTGGTCTTTTTGA
		R: CTTCGGGGATGTTTCTTTCA
Glyma04g04810.1	Ca^{2+}-transporting ATPase	F: AGACGCTCCAATCAGGAGAA
		R: TCAAATCACGTCCCTCAACA
Glyma10g28880.1	inorganic H^+ pyrophosphatase family protein	F: GGCCGGAATGAGACATAAGA
		R: AGAGCTGCACTCCCAACACT
Glyma10g35450.1	ribophorin I	F: CGGGCCATATGAAAATCATC
		R: CTTTATGTCGAGCACCAGCA
Glyma11g12800.1	dolichyl diphospho oligosaccharide protein glycosyltransferase	F: AACCGATTTTTCACGTCAGG
		R: CCAACTTTGTGGTGTTGCAC
Glyma20g32070.2	ribophorin I	F: CGGGCCATATGAAAATCATC

		R: CTTTATGTCGAGCACCAGCA
Glyma08g43680.1	β-xylosyltransferase	F: ACTGCACGCCTTTCTGAGTT
		R: GCCCAGCTCTTCAATGAGTC
Glyma04g00200.1	α-mannosyl glycoprotein *N*-acetylglucosaminyl transferase	F: TCACCAAAATGGCCTAAAGC
		R: CATTCAGCTTGATTGGCTCA
Glyma05g30230.2	UGGT	F: GGCTCTGTTGAGCTGGTAGG
		R: GCACCAACAGAACCACAATG
Glyma04g38000.1	calnexin 1	F: GGATCCTGTTTTTAACGCAGATTAG
		R: AAATTATCATTATTCTATTGCATTAGTAGG

a, Protein ID according to Phytozome soybean genome database.

Table 8. List of predicted ER proteins related to protein glycosylation, signaling, redox, transport, and stress in the root tip of soybean under flooding and drought stresses

			Ratio				
	Protein ID	Description	Control 2(0) [a)]	Control 4(0)	Flooding 4(2)	Drought 4(2)	Function
Protein glycosylation							
1	Glyma04g01690.1	ribophorin I	1	1.41	1.36	-	protein glycosylation
2	Glyma06g01790.1	ribophorin I	1	1.41	1.43	-	protein glycosylation
3	Glyma10g35450.1	ribophorin I	1	0.15	1.12	-	protein glycosylation
4	Glyma11g12800.1	dolichyl diphospho oligosaccharide protein glycosyltransferase 48kDa subunit	1	0.05	1.45	-	protein glycosylation
5	Glyma12g04950.1	dolichyl diphospho oligosaccharide protein glycosyltransferase 48kDa subunit	1	0.06	1.49	-	protein glycosylation
6	Glyma08g13400.1	UGGT	1	1.17	-	-	protein glycosylation
7	Glyma08g20020.1	UGGT	1	0.80	-	-	protein glycosylation
8	Glyma20g32070.2	ribophorin I	1	-	2.87	-	protein glycosylation
9	Glyma08g43680.1	β-1,2 xylosyltransferase	1	-	2.73	-	protein glycosylation
10	Glyma04g00200.1	α-1,3 mannosyl glycoprotein β 1,2 *N*-acetylglucosaminyl transferase putative	1	-	1.91	-	protein glycosylation
11	Glyma06g00230.1	α-1,3 mannosyl glycoprotein β 1,2 *N*-acetylglucosaminyl transferase putative	1	-	1.81	-	protein glycosylation
12	Glyma05g30230.2	UGGT	1	-	1.81	-	protein glycosylation
13	Glyma18g09480.1	β-1,2 xylosyltransferase	1	-	1.10	-	protein glycosylation
14	Glyma08g43670.1	β-1,2 xylosyltransferase	1	-	0.90	-	protein glycosylation
Signaling							
15	Glyma04g38000.1	calnexin 1	1	1.54	0.36	0.34	signaling
16	Glyma06g17060.1	calnexin 1	1	1.46	0.35	0.37	signaling
17	Glyma09g38410.2	calreticulin 3	1	2.97	1.88	-	signaling
18	Glyma07g35090.1	calmodulin binding protein	1	1.89	0.07	-	signaling
19	Glyma09g37860.1	RAS 5	1	1.09	1.37	-	signaling
20	Glyma18g48610.2	RAS 5	1	1.07	1.69	-	signaling
21	Glyma05g33700.1	receptor like kinase 1	1	0.95	0.82	-	signaling
22	Glyma03g26090.1	RAS 5	1	0.93	1.11	-	signaling
23	Glyma05g33330.1	calnexin 1	1	0.92	0.98	-	signaling
24	Glyma08g00920.1	calnexin 1	1	0.89	1.00	-	signaling
25	Glyma08g06020.1	receptor like kinase 1	1	0.73	0.71	-	signaling
26	Glyma15g12880.1	RAB GTPase homolog B1C	1	0.38	2.30	-	signaling
27	Glyma09g01950.2	RAB GTPase homolog B1C	1	0.38	2.28	-	signaling
28	Glyma11g13460.1	calreticulin 3	1	0.19	2.96	-	signaling
29	Glyma20g23080.1	calreticulin 1b	1	0.00	0.25	-	signaling
30	Glyma20g02951.1	calmodulin binding protein	1	0.04	-	0.26	signaling
31	Glyma09g40980.1	receptor like protein kinase family protein	1	3.32	-	-	signaling
32	Glyma20g23490.1	calcium binding EF hand family protein	1	2.46	-	-	signaling
33	Glyma11g33100.1	RAB homolog 1	1	2.17	-	-	signaling
34	Glyma10g43360.1	calcium binding EF hand family protein	1	2.11	-	-	signaling
35	Glyma10g28890.1	calreticulin 1b	1	0.05	-	-	signaling

36	Glyma11g34490.1	leucine-rich repeat receptor like protein kinase family protein	1	-	7.73	-	signaling
37	Glyma09g36560.1	chaperone regulator like protein	1	-	2.38	-	signaling
38	Glyma07g10695.1	protein kinase superfamily protein	1	-	2.06	-	signaling
39	Glyma09g31333.1	protein kinase superfamily protein	1	-	2.04	-	signaling
40	Glyma02g16130.2	guanylate binding family protein	1	-	1.82	-	signaling
41	Glyma10g35230.1	Ras related small GTP binding family protein	1	-	1.47	-	signaling
42	Glyma07g13890.2	RAS 5	1	-	1.23	-	signaling
43	Glyma12g05460.4	calreticulin 3	1	-	0.89	-	signaling
Redox							
44	Glyma03g42070.3	cytochrome *b5* isoform E	1	3.54	1.81	3.70	redox
45	Glyma19g44780.1	cytochrome *b5* isoform E	1	2.63	1.51	4.04	redox
46	Glyma13g03650.1	plant L ascorbate oxidase	1	0.51	0.60	1.70	redox
47	Glyma04g42690.1	PDI like 1,2	1	0.15	0.22	0.31	redox
48	Glyma14g24090.1	PDI like 1,1	1	2.41	1.16	-	redox
49	Glyma04g41010.1	cytochrome *b5* isoform E	1	1.84	1.59	-	redox
50	Glyma15g18310.1	glutaredoxin family protein	1	1.61	1.20	-	redox
51	Glyma09g07040.1	glutaredoxin family protein	1	1.61	1.21	-	redox
52	Glyma13g40350.1	PDI like 5,1	1	1.56	0.30	-	redox
53	Glyma13g40130.1	PDI like 1,4	1	1.55	0.02	-	redox
54	Glyma07g05830.1	cytochrome *b5* isoform E	1	1.49	1.51	-	redox
55	Glyma16g02410.3	cytochrome *b5* isoform E	1	1.45	1.08	-	redox
56	Glyma19g41690.1	thioredoxin family protein	1	1.27	1.35	-	redox
57	Glyma03g00920.1	NADH: cytochrome *b5* reductase 1	1	1.26	0.95	-	redox
58	Glyma03g39130.1	thioredoxin family protein	1	1.14	1.40	-	redox
59	Glyma10g36170.1	PDI like 5,2	1	1.13	1.78	-	redox
60	Glyma19g29720.1	NADH: cytochrome *b5* reductase 1	1	1.01	1.06	-	redox
61	Glyma13g03600.2	PDI like 1,1	1	1.01	0.65	-	redox
62	Glyma12g07260.1	PDI like 1,4	1	0.91	0.32	-	redox
63	Glyma11g20630.1	PDI like 1,4	1	0.86	0.09	-	redox
64	Glyma20g29660.1	membrane steroid binding protein1	1	0.73	1.20	-	redox
65	Glyma06g12090.1	PDI like 1,2	1	0.66	1.09	-	redox
66	Glyma13g43430.2	PDI like 1,6	1	0.65	0.33	-	redox
67	Glyma16g31873.1	membrane associated progesterone binding protein 3	1	0.63	1.32	-	redox
68	Glyma09g25940.1	membrane associated progesterone binding protein 3	1	0.58	1.44	-	redox
69	Glyma15g01880.1	PDI like 1,6	1	0.47	1.46	-	redox
70	Glyma12g29550.1	PDI like 1,4	1	0.28	0.02	-	redox
71	Glyma14g05520.1	PDI like 2,2	1	0.14	0.13	-	redox
72	Glyma02g01750.2	thioredoxin family protein	1	0.10	1.38	-	redox
73	Glyma10g01820.1	thioredoxin family protein	1	0.09	1.36	-	redox
74	Glyma02g43460.1	PDI like 2,2	1	0.08	0.12	-	redox
75	Glyma13g09130.1	thioredoxin family protein	1	0.04	1.27	-	redox
76	Glyma11g11460.1	ascorbate peroxidase 3	1	1.13	-	0.09	redox

77	Glyma20g26050.1	sulfhydryl oxidase 1	1	2.61	-	-	redox
78	Glyma06g42130.1	PDI like 5,4	1	1.49	-	-	redox
79	Glyma10g38150.1	membrane steroid binding protein 1	1	0.50	-	-	redox
80	Glyma06g13840.5	cytochrome *b5* isoform E	1	0.14	-	-	redox
81	Glyma06g24520.2	thioredoxin family protein	1	0.10	-	-	redox
82	Glyma14g20360.1	thioredoxin family protein	1	-	1.37	-	redox
83	Glyma18g45500.1	PDI like 1,2	1	-	0.63	-	redox
84	Glyma20g12150.1	plant *L* ascorbate oxidase	1	-	0.52	1.80	redox
85	Glyma20g12230.2	plant *L* ascorbate oxidase	1	-	-	1.67	redox
Transport							
86	Glyma13g23170.1	inorganic H^+ pyrophosphatase family protein	1	1.99	0.73	2.66	transport
87	Glyma19g35960.1	Ca^{2+}-transporting ATPase	1	0.02	1.17	1.37	transport
88	Glyma03g33240.1	Ca^{2+}-transporting ATPase	1	0.02	1.16	1.37	transport
89	Glyma04g04810.1	Ca^{2+}-transporting ATPase	1	2.97	2.78	-	transport
90	Glyma04g38190.1	phosphate deficiency response 2	1	1.78	1.56	-	transport
91	Glyma05g30330.1	emp24/gp25L/p24 family/GOLD family protein	1	1.43	0.65	-	transport
92	Glyma07g03220.1	inorganic H^+ pyrophosphatase family protein	1	1.12	0.60	-	transport
93	Glyma10g02370.1	ABC transporter C family member 4-like	1	0.37	0.12	-	transport
94	Glyma06g07290.3	nucleotide sugar transporter family protein	1	5.00	-	-	transport
95	Glyma13g20810.3	ethylene-insensitive protein 2-like	1	3.20	-	-	transport
96	Glyma10g28880.1	inorganic H^+ pyrophosphatase family protein	1	-	7.50	-	transport
97	Glyma20g27980.1	oligosaccharyltransferase complex	1	-	2.69	-	transport
98	Glyma06g04900.1	Ca^{2+}-transporting ATPase	1	-	2.30	-	transport
99	Glyma20g03930.1	emp24/gp25L/p24 family/GOLD family protein	1	-	2.26	-	transport
100	Glyma07g35490.1	emp24/gp25L/p24 family/GOLD family protein	1	-	1.94	-	transport
101	Glyma06g16860.1	phosphate deficiency response 2	1	-	1.47	-	transport
102	Glyma10g39750.1	oligosaccharyltransferase complex	1	-	1.09	-	transport
103	Glyma09g04980.1	ABC transporter C family member 14-like	1	-	0.80	-	transport
104	Glyma15g15870.1	ABC transporter C family member 14-like	1	-	0.71	-	transport
105	Glyma07g12680.2	ABC transporter C family member 15-like	1	-	0.17	-	transport
Stress							
106	Glyma01g35220.2	early responsive dehydration stress protein	1	0.22	0.14	0.19	stress
107	Glyma03g37650.1	DnaJ heat shock family protein	1	0.20	0.18	0.32	stress
108	Glyma05g36600.1	HSP 70 protein 5	1	0.20	0.14	0.71	stress
109	Glyma05g36620.1	HSP 70 family protein	1	0.04	1.38	0.05	stress
110	Glyma16g08105.1	early responsive dehydration stress protein	1	0.00	0.14	0.33	stress
111	Glyma18g15080.2	methyltransferase	1	0.00	0.14	0.73	stress
112	Glyma02g11890.1	methyltransferase	1	1.62	1.23	-	stress
113	Glyma01g05580.1	*S* adenosyl *L* methionine dependent methyltransferases superfamily protein	1	1.61	0.05	-	stress
114	Glyma20g35120.5	*S* adenosyl *L* methionine dependent methyltransferases superfamily protein	1	1.33	1.48	-	stress
115	Glyma20g16070.1	HSP 70 family protein	1	1.32	1.70	-	stress
116	Glyma02g00550.1	*S* adenosyl *L* methionine dependent methyltransferases superfamily protein	1	1.27	2.10	-	stress

117	Glyma03g33710.1	DnaJ homolog subfamily	1	1.07	0.69	-	stress
118	Glyma13g10700.1	HSP 70 family protein	1	0.82	1.32	-	stress
119	Glyma08g41220.4	*S* adenosyl *L* methionine dependent methyltransferases superfamily protein	1	0.23	0.19	-	stress
120	Glyma11g14970.1	pathogenesis related thaumatin superfamily protein	1	0.15	1.45	-	stress
121	Glyma14g40320.1	HSP 90	1	1.14	-	-	stress
122	Glyma17g37820.1	HSP 90	1	1.14	-	-	stress
123	Glyma10g32000.1	HSP 20 family protein	1	0.09	-	-	stress
124	Glyma16g08410.1	staurosporin and temperature sensitive 3 like A	1	-	4.40	-	stress
125	Glyma15g20400.1	DnaJ/Sec 63 Brl domains containing protein	1	-	3.73	-	stress
126	Glyma19g34890.1	*S* adenosyl *L* methionine dependent methyltransferases superfamily protein	1	-	2.82	-	stress
127	Glyma09g29470.1	staurosporin and temperature sensitive 3 like b	1	-	2.59	-	stress
128	Glyma16g33881.1	staurosporin and temperature sensitive 3 like b	1	-	2.57	-	stress
129	Glyma09g08830.1	DnaJ/Sec63 Brl domains containing protein	1	-	2.45	-	stress
130	Glyma10g04370.1	*S* adenosyl *L* methionine dependent methyltransferases superfamily protein	1	-	2.40	-	stress
131	Glyma10g00880.2	*S* adenosyl *L* methionine dependent methyltransferases superfamily protein	1	-	2.11	-	stress
132	Glyma06g21060.2	DnaJ heat shock N terminal domain containing protein	1	-	1.60	-	stress
133	Glyma13g18630.1	*S* adenosyl *L* methionine dependent methyltransferases superfamily protein	1	-	1.58	-	stress
134	Glyma02g43110.1	*S* adenosyl *L* methionine dependent methyltransferases superfamily protein	1	-	1.58	-	stress
135	Glyma04g33740.1	*S* adenosyl *L* methionine dependent methyltransferases superfamily protein	1	-	1.39	-	stress
136	Glyma09g16690.1	chaperone protein htpG family protein	1	-	0.21	-	stress
137	Glyma16g17500.1	*S* adenosyl *L* methionine dependent methyltransferases superfamily protein	1	-	0.14	-	stress
138	Glyma08g02940.1	HSP 70 family protein	1	-	0.71	-	stress
139	Glyma08g41220.3	*S* adenosyl *L* methionine dependent methyltransferases superfamily protein	1	-	0.29	-	stress

a), day after sowing (day after stress); Protein ID, according to the Phytozome soybean genome database; Ratio, relative abundance of protein was compared to 2-day-old untreated soybean; Function, protein function was categorized using MapMan bin codes; "-", proteins with the same relative ratio as 2-day-old untreated soybeans.

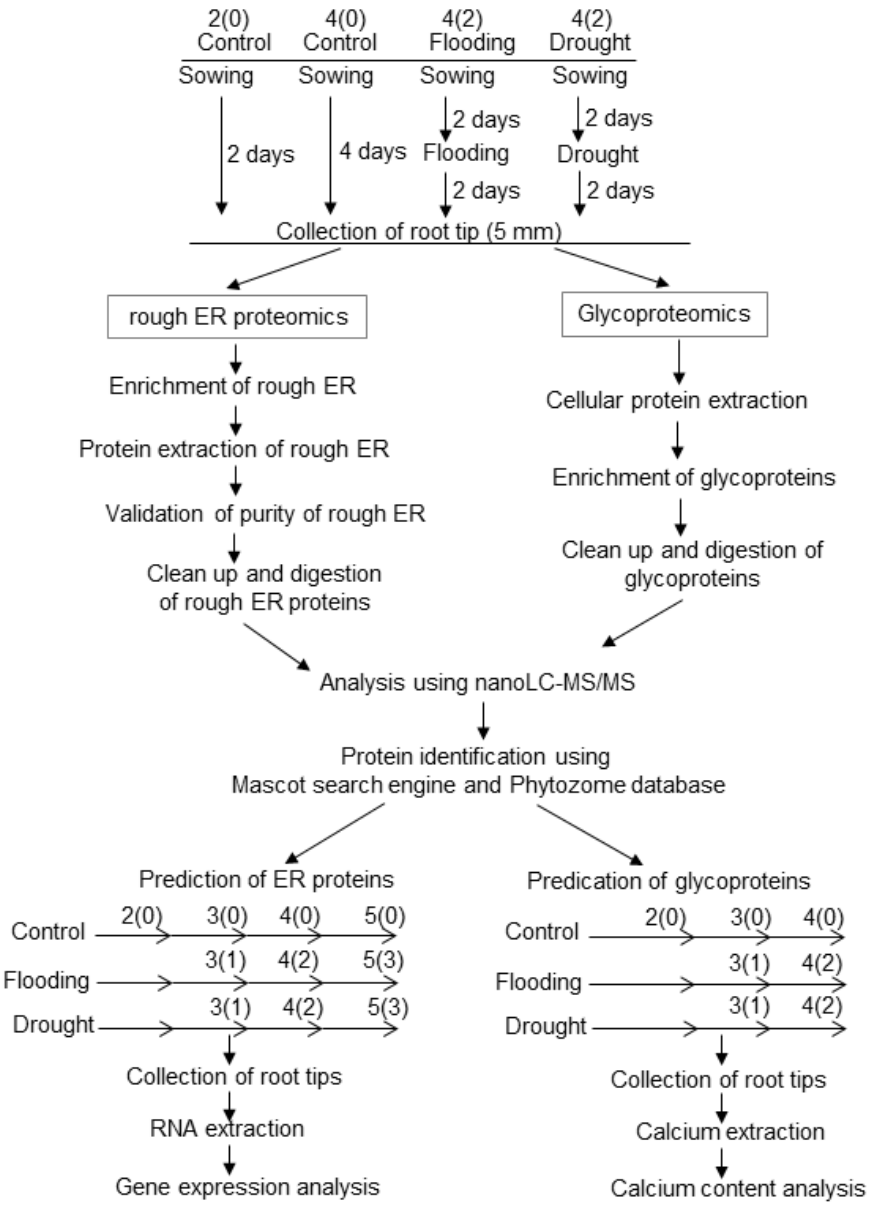

Figure 17. Experimental design for the endoplasmic reticulum proteomics in soybean. Two-day-old (2(0)) soybeans were treated without or with flooding and drought for 2 days (4(2)). Soybeans without treatments were collected as controls. Root tips were collected 5 mm from the end of roots for rough ER enrichment. Proteins were extracted and analyzed using nanoLC-MS/MS. Glycoproteomics, gene expression, and endogenous calcium content were further analyzed. Three independent experiments were conducted as biological replicates.

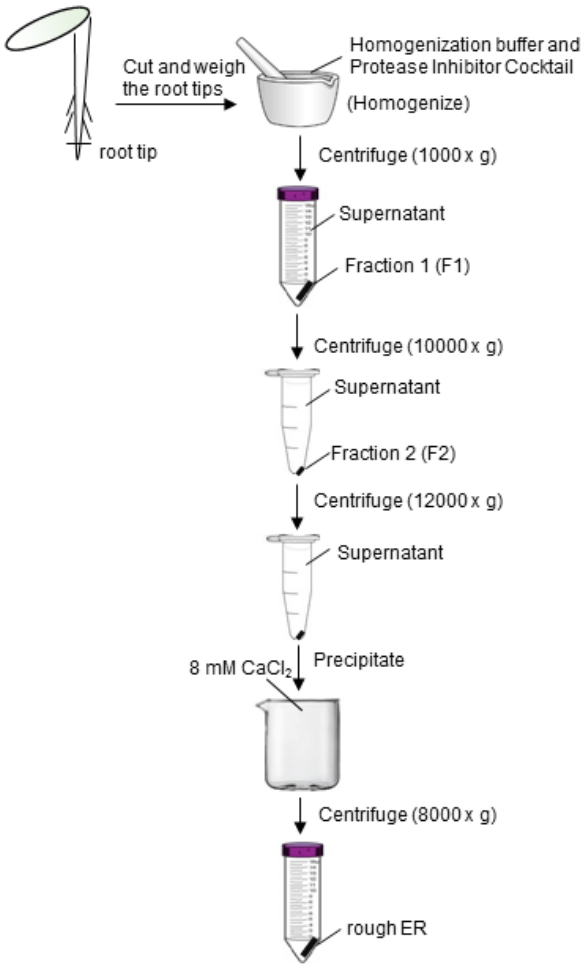

Figure 18. Enrichment of rough endoplasmic reticulum in soybean. Two-day-old soybeans were treated without or with flooding or drought for 2 days, and root tips were collected. All the procedures were performed at 4ºC. Rough ER was enriched according to the instructions supplied by the Endoplasmic Reticulum Enrichment Kit with some modifications. A portion (1.0 g) of fresh root tips was ground with the homogenization buffer and protease inhibitor cocktail. The resulting homogenates were centrifuged at 1000 x g for 10 min and pellet was collected as Fraction 1 (F1). The supernatant was transferred and centrifuged at 10000 x g for 15 min. The pellet was collected as Fraction 2 (F2) and supernatant was centrifuged at 12000 x g for 15 min. The supernatant was precipitated using 8 mM $CaCl_2$ and centrifuged at 8000 x g for 10 min. The pellet was collected as rough ER.

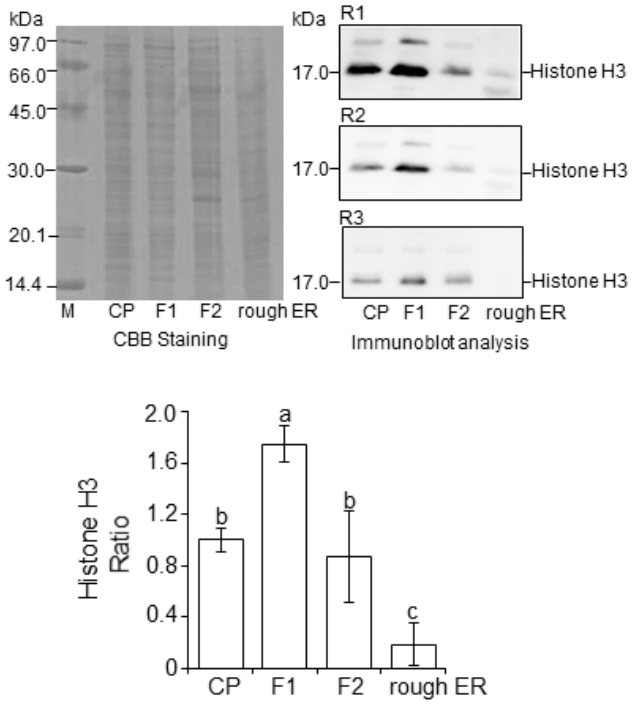

Figure 19. Immunoblot analysis to evaluate purity of endoplasmic reticulum in soybean. Rough ER was enriched from root tips of 2-day-old soybeans and purity of obtained fraction was assessed by immunoblot analysis. The cellular proteins (CP), proteins in Faction 1 (F1), Fraction 2 (F2), and rough ER were extracted and separate by SDS-polyacrylamide gel electrophoresis, transferred to the polyvinylidine disfluoride membrane, reacted with anti-histone H3 (nucleus) antibody, and then signals were detected using the Chem-Lumi One Super kit. The relative intensities of bands were calculated using ImageJ software. Coomassie brilliant blue (CBB) staining pattern was used as loading control. Data are shown as means ± SD from three independent biological replicates. Different letter indicates the change is significant, as determined by one-way ANOVA according to Tukey's multiple comparison test (p<0.05).

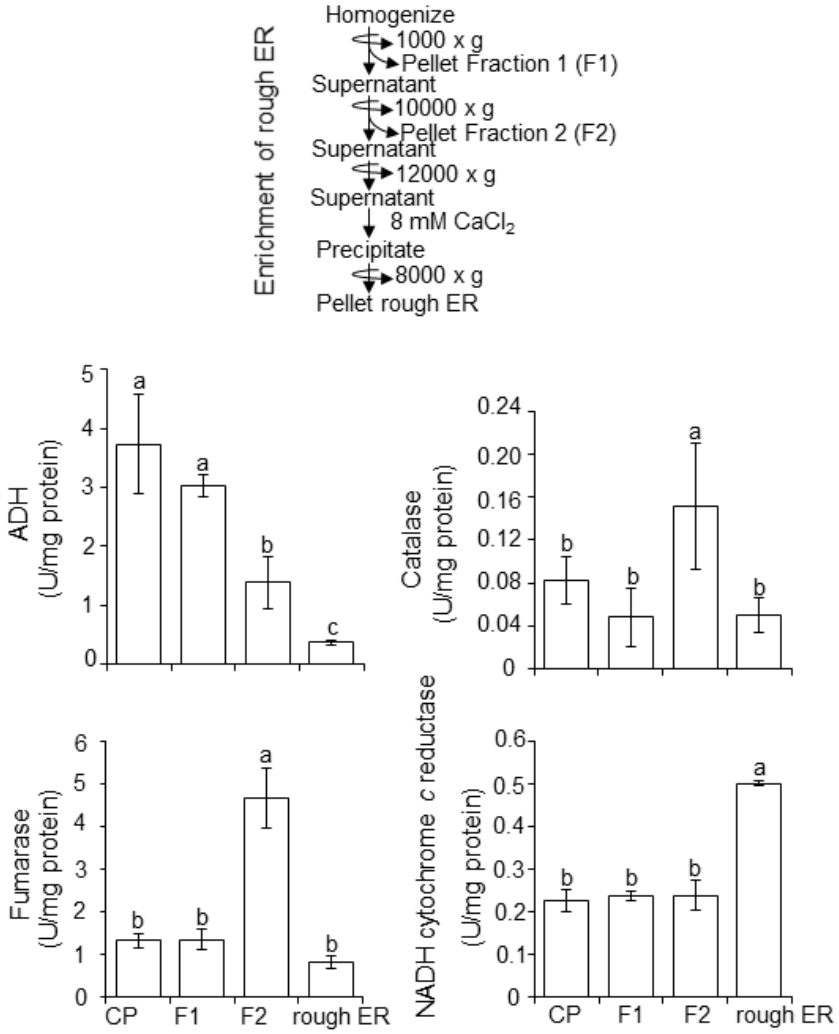

Figure 20. Enzyme assay to evaluate purity of endoplasmic reticulum in soybean. Rough ER was enriched from the root tips of 2-day-old soybeans and purity of obtained fraction was assessed by enzyme assays. The cellular proteins (CP), proteins in Fraction 1 (F1), Fraction 2 (F2), and rough ER were used. For enzyme activity analyses, CP, F1, F2, and rough ER were examined by ADH (cytosol), fumarase (mitochondria), and NADH cytochrome *c* reductase activities (ER). Data are shown as means ± SD from three independent biological replicates. Different letter indicates the change is significant, as determined by one-way ANOVA according to Tukey's multiple comparison test ($p<0.05$).

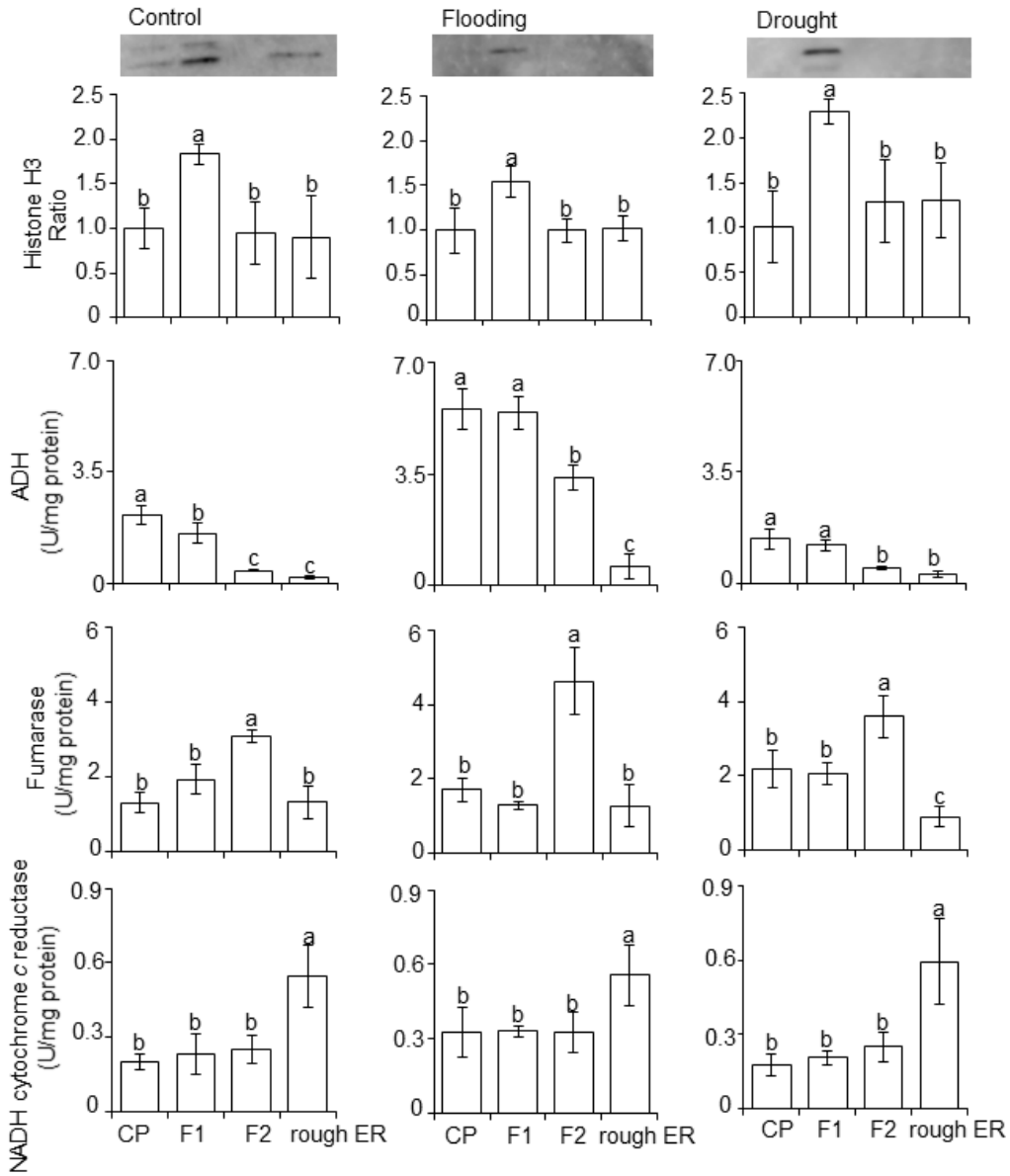

Figure 21. Immunoblot analysis and enzyme assay to evaluate purity of endoplasmic reticulum in soybean under flooding and drought. Two-day-old soybeans were treated without or with flooding and drought for 2 days. Rough ER was enriched from root tips under control, flooding, and drought. The cellular proteins (CP), proteins in Fraction 1 (F1), Fraction 2 (F2), and rough ER were used. Each sample was separated by SDS-polyacrylamide gel electrophoresis and transferred to polyvinylidene difluoride membrane for reaction with anti-histone H3 (nucleus) antibody. CP, F1, F2, and rough ER were assayed by ADH (cytosol), fumarase (mitochondria), and NADH cytochrome *c* reductase activities (ER). Data are shown as means ± SD from three independent biological replicates. Different letter indicates the significant change, as determined by one-way ANOVA according to Tukey's multiple comparison test ($p<0.05$).

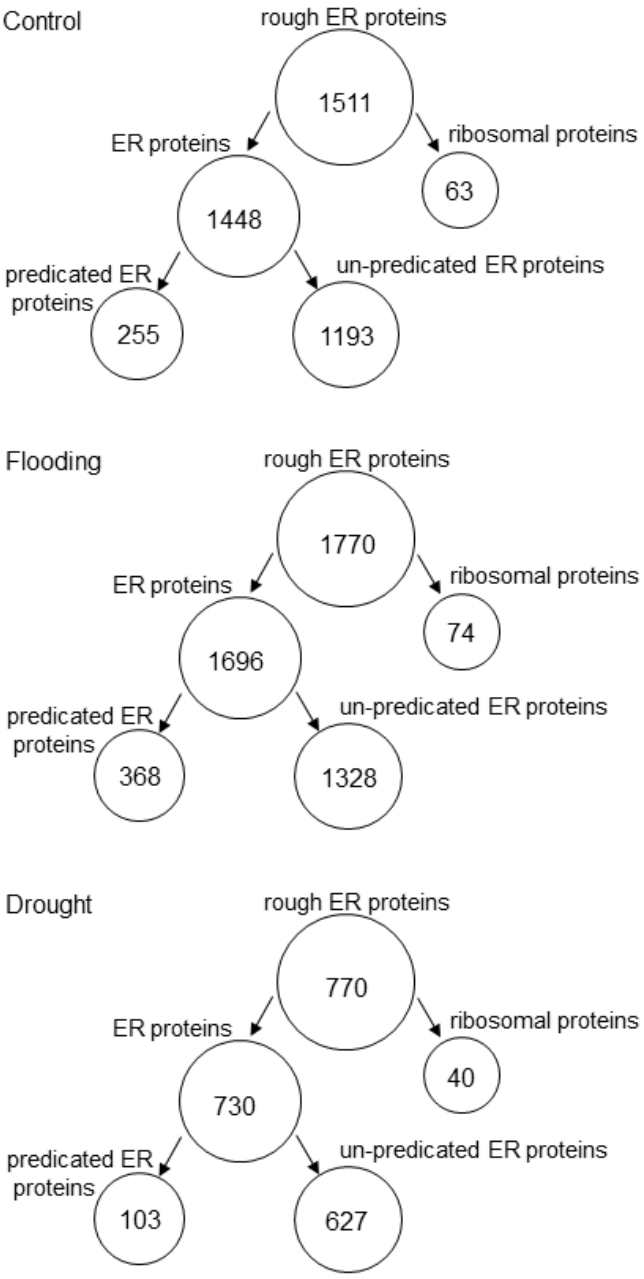

Figure 22. Diagrams of identified proteins in rough endoplasmic reticulum in soybean under flooding and drought. Two-day-old soybeans were treated without or with flooding and drought for 2 days, and rough ER was enriched from the root tips. The proteins were extracted and analyzed using nanoLC-MS/MS. The diagrams show that 1511, 1770, and 770 proteins were identified in rough ER from control, and flooding- and drought-stressed seedlings, respectively, and included 63, 74, and 40 ribosomal proteins, respectively. A total of 255, 368, and 103 proteins were predicted to be ER proteins under control, flooding, and drought conditions, respectively.

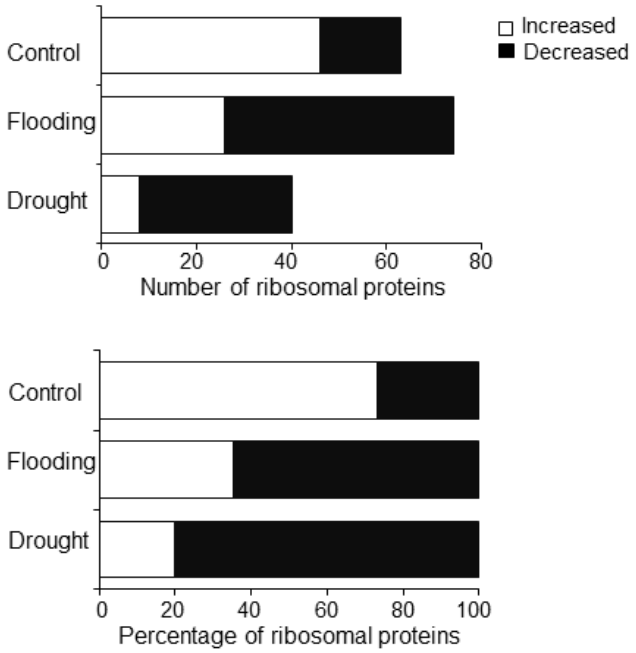

Figure 23. Ribosomal proteins in soybean affected by flooding and drought. Two-day-old soybeans were treated without or with flooding and drought for 2 days. The number and percentage of identified ribosomal proteins with increased and decreased abundance were shown for control, flooded, and drought-stressed soybean. Open and filled bars indicate increased and decreased protein abundance, respectively.

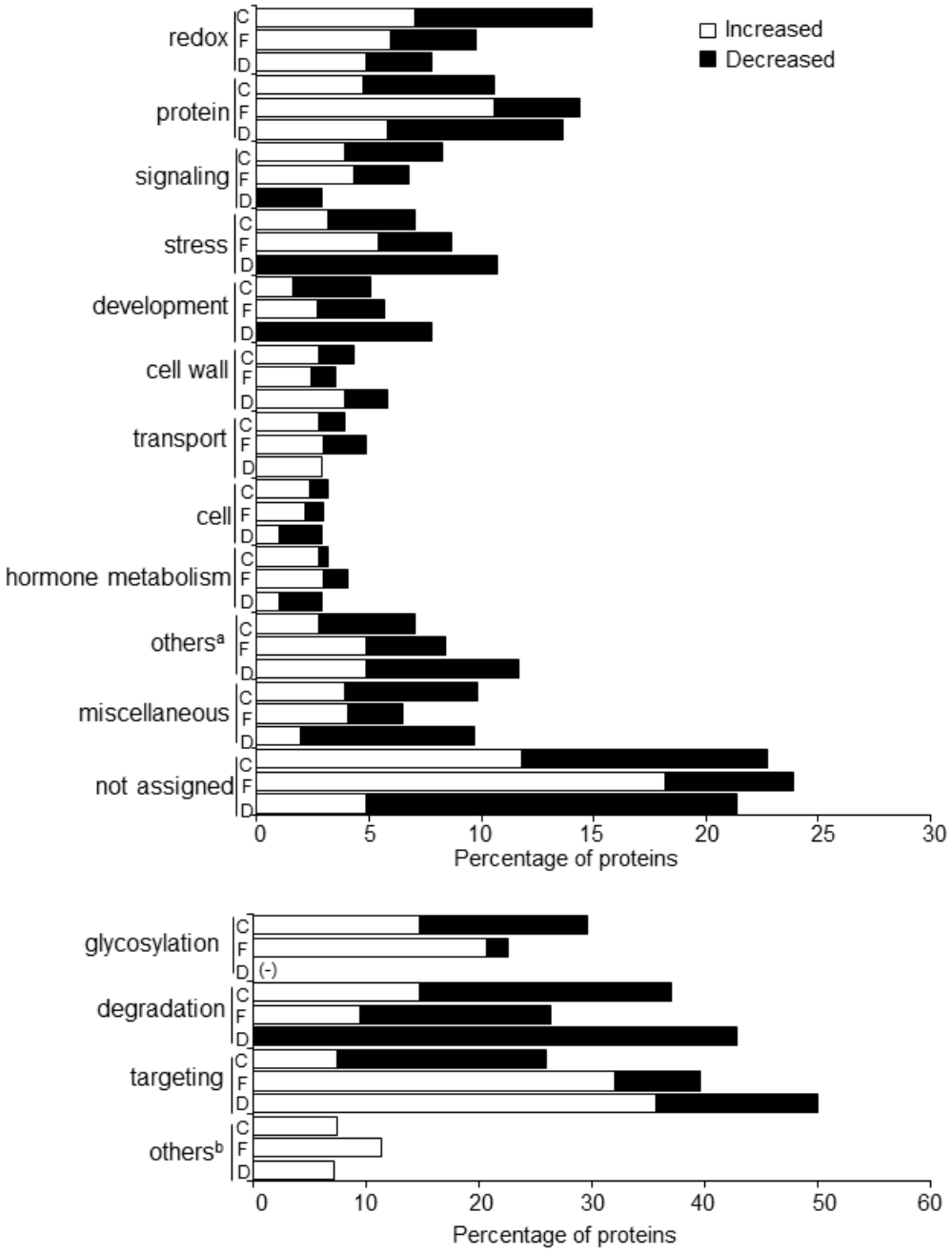

Figure 24. Functional analysis of predicted endoplasmic reticulum proteins in soybean under flooding and drought. Functional analysis of predicated ER proteins under control (C), flooding (F), and drought (D) was performed using MapMan bin codes. The functional category of protein was further classified into several subcategories. [a]Others included lipid metabolism, secondary metabolism, nucleotide metabolism, amino acid metabolism, major CHO metabolism, minor CHO metabolism, RNA metabolism, fermentation, and the tricarboxylic acid cycle. [b]Others included amino acid activation, post modification, and folding.

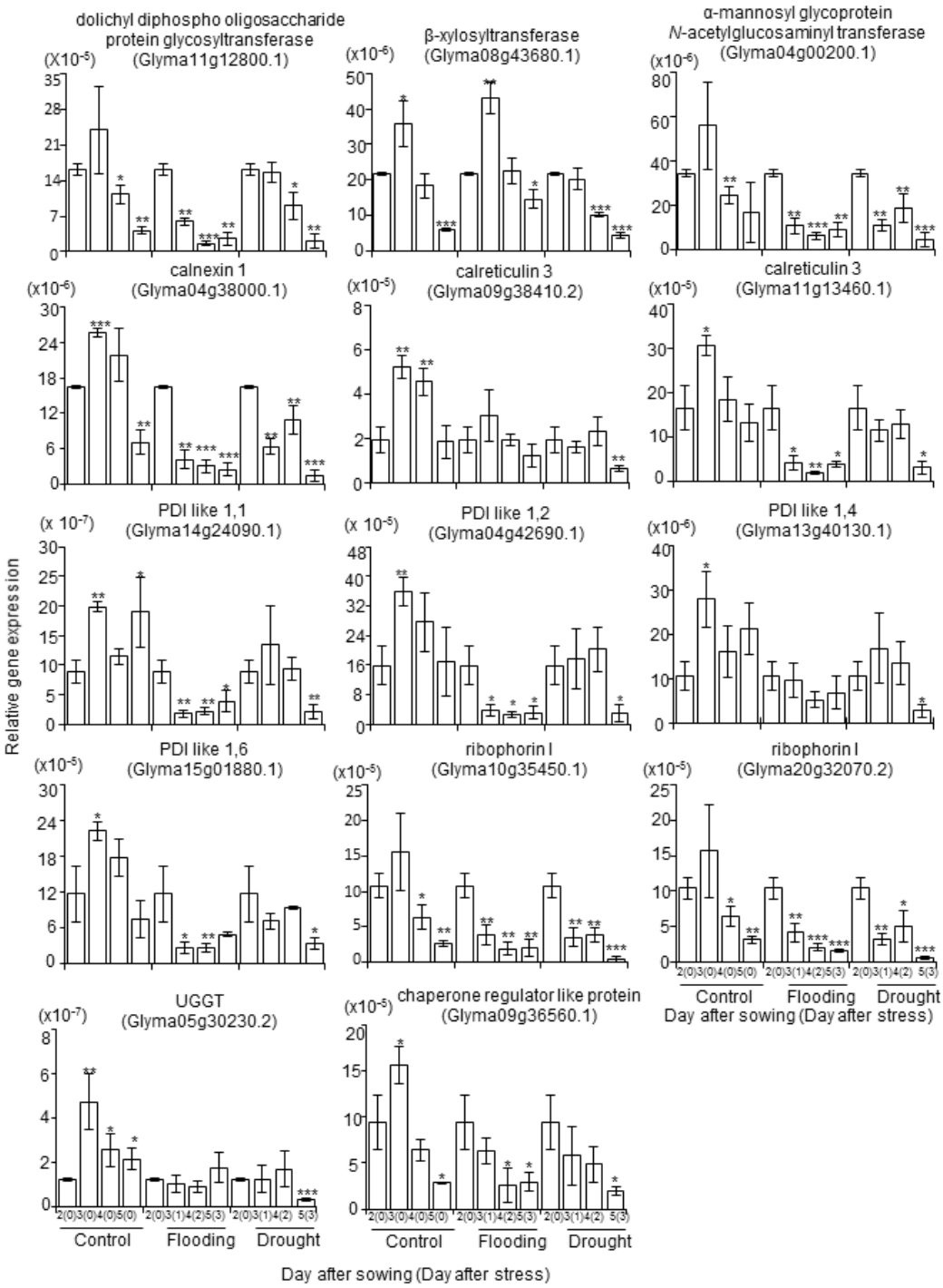

Figure 25. Gene expression of the endoplasmic reticulum proteins related to protein glycosylation and redox homeostasis. Two-day-old soybeans were treated without or with flooding and drought for 1, 2, and 3 days. RNA samples were extracted from the root tips. Gene expression was normalized against that of 18S rRNA. Data are shown as means ± SD from three independent biological replicates. Student's *t*-test was used for statistical analysis. Two-day-old untreated soybeans were used for comparison point. The asterisks indicate the significance between different time points (*p<0.05, **p<0.01, ***p<0.001).

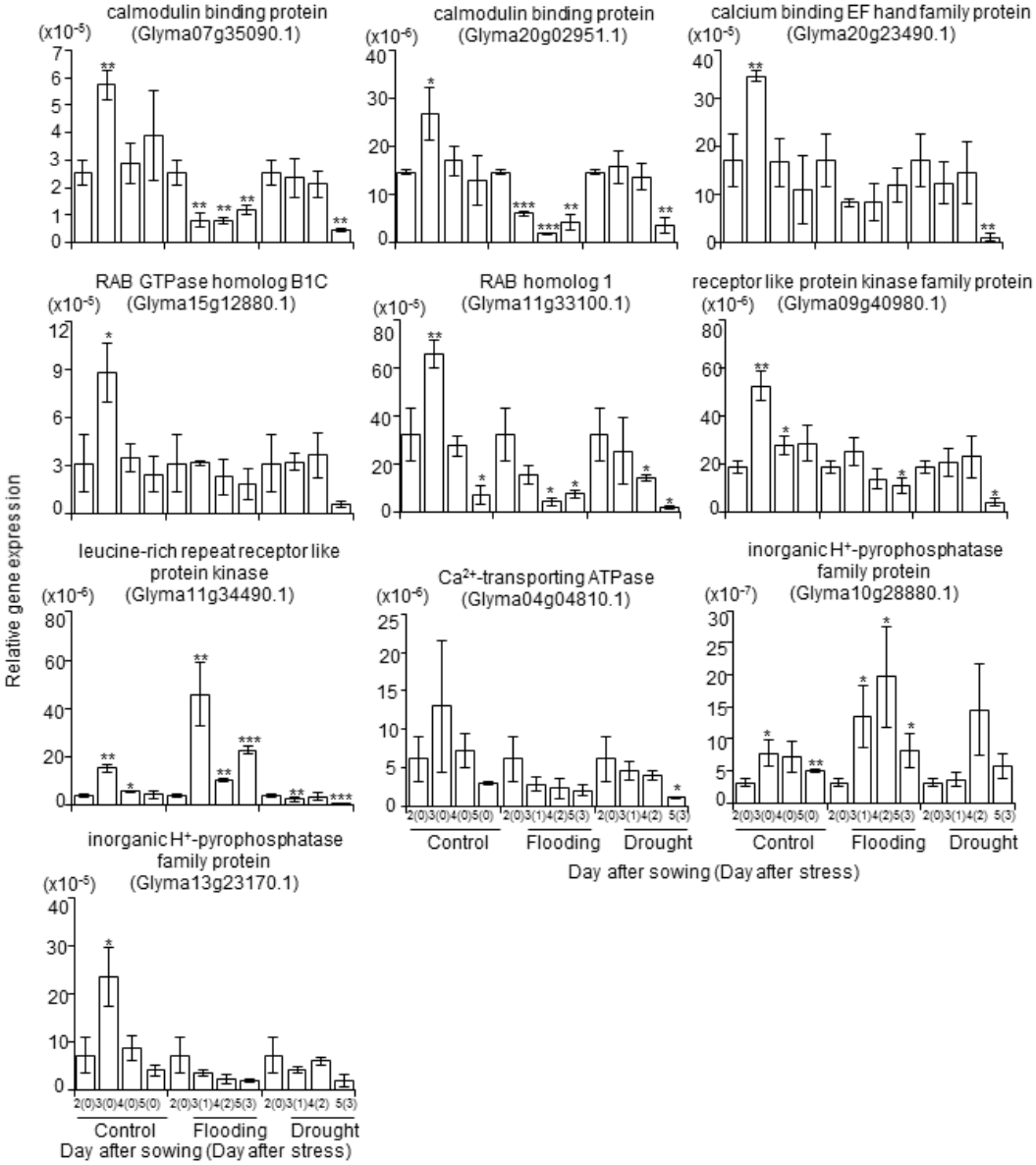

Figure 26. Gene expression of the endoplasmic reticulum proteins related to signaling and transport. RNA samples were extracted from the root tips. Gene expression was normalized against that of 18S rRNA. Data are shown as means ± SD from three independent biological replicates. Student's *t*-test was used for statistical analysis. Two-day-old untreated soybeans were used for comparison point. The asterisks indicate the significance between different time points (*p<0.05, **p<0.01, ***p<0.001).

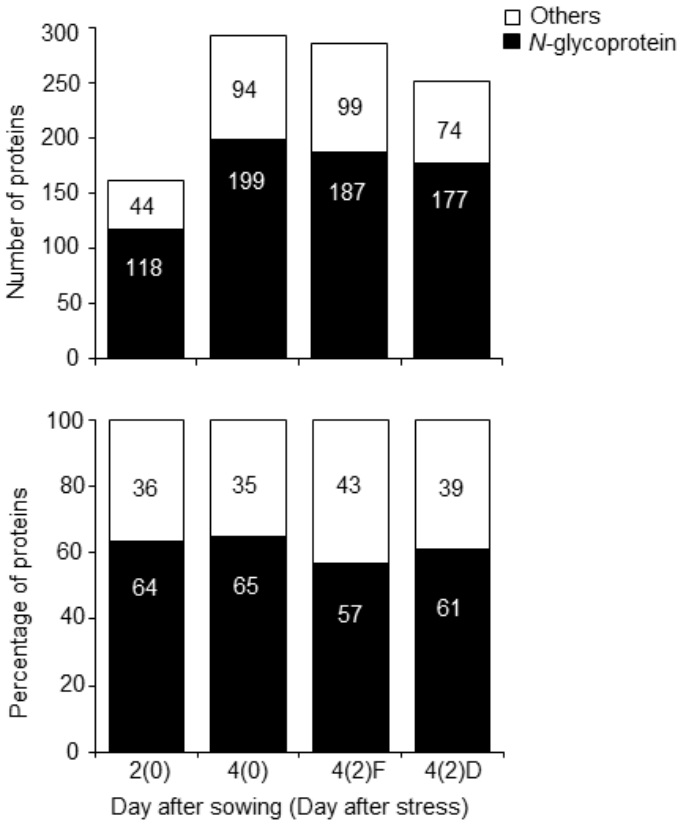

Figure 27. Glycoproteins affected by flooding and drought in soybean. Two-day-old soybeans (2(0)) were treated without stresses for 2 days (4(0)) or with flooding (F) or drought (D) for 2 days (4(2)), and root tips were collected. Glycoproteins were enriched in root tips using the Glycoprotein Isolation Kit, ConA; and peptides were analyzed using nanoLC-MS/MS. *N*-glycosylation sites were predicted using NetNGlyc 1.0 Server. The number of identified proteins, predicted *N*-glycoproteins, and percentage of *N*-glycoprotein abundance were presented for each condition. The filled and opened bars indicate proteins with or without *N*-glycosylation sites, respectively.

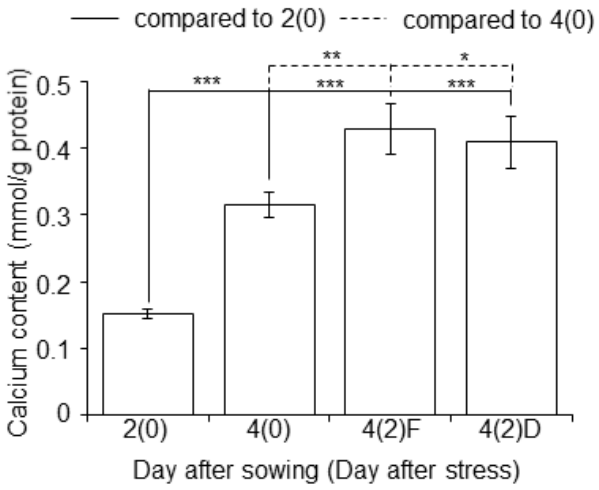

Figure 28. Effect of flooding and drought on endogenous calcium content in soybean. Two-day-old (2(0)) soybeans were treated without or with flooding (F) or drought (D) for 2 days and root tips were collected for endogenous calcium content analysis, using the Calcium Colorimetric Assay Kit. Data are shown as means ± SD from three independent biological replicates. Student's *t*-test was used for statistical analysis. The solid and dotted lines indicate the comparisons using 2(0) and 4-day-old (4(0)) soybeans as control, respectively. The asterisks indicate the significant change (*p<0.05, **p<0.01, ***p<0.001).

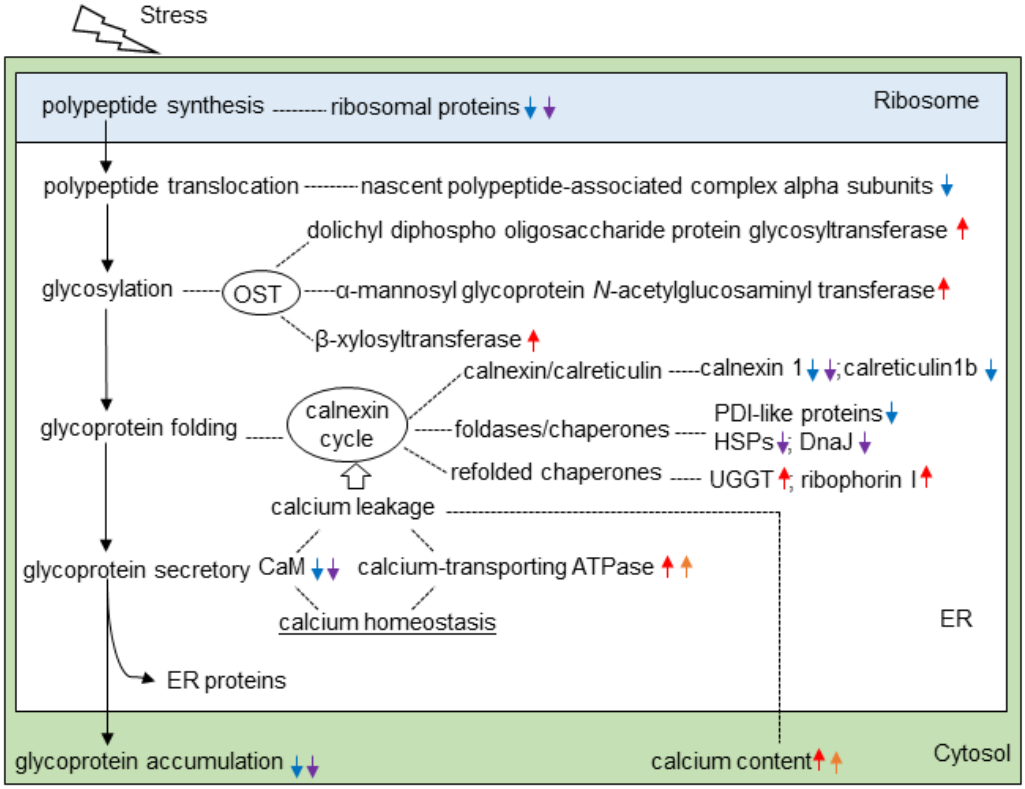

Figure 29. Proposed model for glycoprotein synthetic pathways affected by flooding and drought in the endoplasmic reticulum of soybean. The red and blue arrows indicate changes of protein abundance under flooding; orange and purple arrows indicate changes of protein abundance under drought; and upward and downward arrows indicate increased and decreased changes of protein abundance, respectively, compared to untreated soybean. Abbreviations are as follows: OST, oligosaccharyltransferase; PDI, protein disulfide isomerase; HSP, heat shock protein; UGGT, UDP glucose: glycoprotein glucosyltransferase; CaM, calmodulin-binding protein.

Chapter 3
Calcium effects on soybean under flooding and drought stresses

3.1. Introduction

Calcium is an important secondary messenger playing vital roles in stress signaling and increased cytosolic calcium caused by adverse environmental conditions triggers downstream responses to cope with the stresses (Huda et al., 2013, Zhu et al. 2013). Calcium signaling pathways involve calcium sensors and several downstream factors, such as calmodulin (Harmon et al., 2000), calcineurin B-like proteins (Luan et al., 2002), and calcium-dependent protein kinases (Zhu et al., 2007). In soybean, exogenous calcium enhanced root elongation and suppressed cell death in root tip under flooding (Oh et al., 2014a). In addition, calcium pretreatment increased biomass and improved drought tolerance of zoysiagrass through regulation of photosynthesis and antioxidant responses (Xu et al., 2013). Based on these findings, further studies are necessary to examine the effects of calcium on soybean under flooding and drought stresses.

Plants have developed complex strategies to maintain balance between protein folding demand and folding capacity in the ER (Deng et al., 2013). Misfolded or unfolded proteins accumulate under adverse environmental conditions due to dysfunction of the ER (Vitale and Boston, 2008). Calcium homeostasis is maintained through distribution of calcium-binding proteins, calcium pumps, and calcium-release channels in the ER (Papp et al., 2003). Overexpression of *luminal binding protein (BiP)*, which is a calcium-handling protein in the ER, mediated the capacity of calcium homeostasis under drought (Valente et al., 2009). Additionally, protein abundance of BiP was decreased upon exposure to flooding (Mustafa and Komatsu, 2014). Although these findings indicate cross-talk between calcium and the ER, the mechanisms by which calcium modulates ER-associated degradation/unfolded protein response in soybean to cope with ER stress induced by flooding and drought is not well understood.

Metabolic regulation was activated in plants under stress conditions. Energy sensor Snf1-related protein kinase 1, which is metabolic master regulator in eukaryotic cells, played modulatory role in plant hypoxia adaptation and salt tolerance (Im et al., 2014). Calcium was not only associated with ER function in plants under stress conditions (Liu et al., 2011), but also participated in metabolic regulation in plants. For example, calcium was involved in the regulation of aquaporins, which played key roles

in hydraulic mediation in response to flooding and drought stresses (Maurel et al., 2015). Calcium-dependent mitochondrial carriers functioned as mitochondrial-ATP importers to balance the loss of mitochondrial-oxidative phosphorylation during hypoxia condition (Stael et al., 2011). Calcium-transporter systems including calcium/proton exchanger 11 mediated calcium homeostasis under hypoxia in *Arabidopsis* (Wang et al., 2016). Exogenous calcium improved metabolism and ion transport to increase tolerance in cucumber under hypoxia (He et al., 2015). These findings indicate versatile roles of calcium in flooded plants, while metabolic regulation induced by drought is limited.

It was demonstrated that disruption of calcium homeostasis in the ER affected protein folding in calnexin cycle and declined accumulation of glycoproteins in soybean exposed to flooding and drought (Chapter 2). To better understand the responsive mechanisms in soybean related to calcium effects in the ER and the systems plant used to alleviate ER stress under flooding and drought, gel-free/label-free proteomic technique was used. To regulate calcium content, 2-aminoethoxydiphenyl borate (2-APB) was used to inhibit inositol-trisphosphate receptor, which is a gated-calcium channel in the ER (Parre et al., 2007; Healy et al., 2012), and $LaCl_3$ was used to block Ca^{2+}-ATPase in the plasma membrane (Xu and Heath 1998; Chung et al., 2000). Bioinformatic, transcriptional, and biochemical analyses were further conducted to determine the function of flooding- and drought-responsive proteins.

3.2. Materials and methods

3.2.1. Plant material and treatments

Soybean was used as plant material in this study. 2-APB (Sigma-Aldrich) and $LaCl_3$ (Wako) were separately dissolved in ethanol to prepare 100 mM stock solutions. EGTA (Sigma-Aldrich) and $CaCl_2$ (Wako) were separately dissolved in water to prepare 500 mM stock solutions. Working solutions of 0.1 mM 2-APB (Liu et al., 2011), 0.1 mM $LaCl_3$ (Maintz et al., 2014), 1 mM EGTA (Li et al., 2011), and 1 mM $CaCl_2$ (Li et al., 2011) were used in the experiments. The silica sand was wetted with 150 mL of 0.1 mM 2-APB, 0.1 mM $LaCl_3$, 1 mM EGTA, 1 mM $CaCl_2$, or water (untreated). Plant growth conditions were the same as described in 1.2.1 in Chapter 1. For treatment, 2-

day-old soybeans were exposed to flooding or drought by adding 700 mL of excess water or withholding water for 1 day, respectively. Non-stressed soybeans were collected as controls. In time-dependent experiment, 2-day-old soybeans were exposed to flooding or drought for 1, 2, 3, and 4 days, and root tips were collected. Three independent experiments were performed as the biological replicates for all experiments. Biological replicate means soybeans sown on different days. Twenty plants were sown in each time point for one replicate (Figure 30).

3.2.2. Quantification of endogenous calcium content

Quantification of endogenous calcium content was performed as described in 2.2.13 in Chapter 2.

3.2.3. Protein extraction for proteomic, enzymatic, and immunoblot analyses

For proteomic analysis, protein extraction was performed as described in 1.2.2 in Chapter 1. For enzyme activity analysis, a portion (0.1 g) of root tips was ground with a mortar and pestle in enzyme extraction buffer consisting of 50 mM HEPES-NaOH (pH 7.5), 1 mM phenylmethylsulfonyl fluoride, 0.1% Triton X-100, 5 mM $MgCl_2$, 1 mM dithiothreitol, 2% polyvinylpyrrolidone-40, and 1 mM EDTA. The homogenates were sonicated for 20 min in cold water and centrifuged at 15000 x g for 20 min at 4°C. The supernatant was collected as protein extracts. For immunoblot analysis, protein extraction was performed as described in 2.2.6 in Chapter 2.

3.2.4 Concentration measurement of proteins

Concentration measurement of proteins was performed as described in 1.2.3 in Chapter 1.

3.2.5 Clean up and digestion of cellular proteins

Clean up and digestion of cellular proteins was performed as described in 1.2.4 in Chapter 1.

3.2.6 Mass spectrometry analysis

Mass spectrometry analysis was performed as described in 1.2.5 in Chapter 1. The MS data have been deposited with the ProteomeXchange Consortium (http://proteomecentral.proteomexchange.org) *via* the PRIDE partner repository (Vizcaíno et al., 2013) with the data set identifier PXD005281.

3.2.7 Protein identification using mass spectrometry data

Protein identification was performed as described in 1.2.6 in Chapter 1.

3.2.8 Analysis of differentially abundant proteins

The acquired Mascot results were exported into SIEVE for proteomic analysis as described in 1.2.7 in Chapter 1.

3.2.9 Analyses of protein localization, protein function, and metabolism pathway

Protein localization was predicted using SUBA3 intracellular targeting prediction program (http://suba3.plantenergy.uwa.edu.au/) (Tanz et al. 2013). Functional analysis and metabolism pathway were performed as described in 1.2.8 in Chapter 1.

3.2.10 Cluster analysis of protein abundance

Cluster analysis of protein abundance was performed as described in 1.2.9 in Chapter 1.

3.2.11 Enzyme activity analysis of pyruvate decarboxylase

Proteins in enzyme extraction buffer were used to examine the activity of pyruvate decarboxylase as described by Gounaris et al. (1971) with some modifications. The reaction solution contained 400 mM Tris-HCl (pH 6.0), 30 mM sodium pyruvate, 75 μM NADH, and 3 U/mL ADH. The reaction was measured continuously for 5 min at 25°C at 340 nm (EC_{340} = 6.22 mM^{-1} cm^{-1}) and enzyme activity was calculated using formula: U/mg protein = [(ΔA340/min x total volume x sample dilution factor)/(6.22 x sample volume)]/protein concentration.

3.2.12 Immunoblot analysis

Immunoblot analysis was performed as described in 2.2.6 in Chapter 2 using anti-calnexin antibody with the ratio of 1: 3000 (Nouri and Komatsu, 2010).

3.2.13 RNA extraction and quantitative reverse transcription-polymerase chain reaction

RNA extraction and qRT-PCR were performed as described in 1.2.12 in Chapter 1. The qRT-PCR primers were designed using the Primer3Plus web interface (http://www.bioinformatics.nl/cgi-bin/primer3plus/primer3plus.cgi/) (Table 9).

3.2.14 Statistical analysis

Statistical analysis was performed as described in 1.2.13 in Chapter 1.

3.3. Results

3.3.1. Effects of 2-APB and $LaCl_3$ on calcium content under flooding and drought stresses

As cytosolic calcium content was increased in root tip of soybean under flooding and drought (Chapter 2), the source of increased calcium under these abiotic stresses was examined using 2-APB and $LaCl_3$. Soybean seeds were germinated for 2 days without or with treatment of 2-APB and $LaCl_3$, and 2-day-old soybeans were exposed to flooding or drought for 1 day before the root tips were collected. In absence of chemical treatment, calcium content was increased in soybeans under both stresses compared to non-stressed plants. Calcium content was not increased in soybeans treated by 2-APB under flooding compared to non-treated soybeans without stresses. Moreover, calcium level did not change by $LaCl_3$ under flooding and drought compared to non-stressed plants (Figure 31). Because calcium content was not increased by chemical treatment under both stresses, 2-APB and $LaCl_3$ were used to regulate cellular calcium level in the following experiments.

3.3.2. Effects of chemical treatment on gene expression of calcium-related proteins under flooding and drought stresses

Inositol trisphosphate, which was phosphorylated by inositol 1,3,4-trisphosphate 5/6 kinase, mediated calcium release from the ER (Du et al., 2011). Ca^{2+}-transporting

ATPase in the plasma membrane was decomposed by $LaCl_3$ (Carafoli, 1991). Gene expression of inositol 1,3,4-trisphosphate 5/6 kinase and Ca^{2+}-transporting ATPase was examined to determine the effects of 2-APB and $LaCl_3$ on calcium mediation. Soybean seeds were germinated for 2 days without or with treatment of 2-APB, $LaCl_3$, or EGTA, and 2-day-old soybeans were exposed to flooding or drought for 1 day before the root tips were collected. *Inositol 1,3,4-trisphosphate 5/6-kinase family protein* was upregulated and downregulated without chemical treatment under flooding and drought, respectively, compared to non-stressed soybeans. It was downregulated by chemical treatment compared to untreated soybeans under flooding condition. *Ca^{2+}-transporting ATPase* was upregulated without chemical treatment under drought (Figure 32).

3.3.3. Effects of chemical treatment on gene expression and protein abundance of calnexin under flooding and drought stresses

The ER is involved in protein folding through calnexin cycle (Healy et al., 2012) and calnexin was decreased in root tip of soybean exposed to flooding and drought for 2 days (Chapter 2). To examine the effects of calcium on calnexin under flooding and drought, gene expression and protein abundance of calnexin were examined. Soybean seeds were germinated for 2 days without or with treatment of 2-APB, $LaCl_3$, or EGTA, and were exposed to flooding or drought for 1 day before the root tips were collected. *Calnexin* was downregulated without chemical treatment under both stresses compared to non-stressed soybeans and downregulated by 2-APB and $LaCl_3$ compared to untreated soybeans under both stresses (Figure 33A). Calcium effects on calnexin abundance were also examined, but the abundance was unaltered without or with chemical treatment in control or flooding- or drought-stressed plants (Figure 33B).

3.3.4. Effects of chemical treatment and stress duration on gene expression of ER-stress related proteins under flooding and drought stresses

To determine the effects of calcium on ER stress, gene expression of HCP-like superfamily protein and GRP78/BiP, which are involved in ER-associated degradation and unfolded protein response, was analyzed. Soybean seeds were germinated for 2 days without or with treatment of 2-APB, $LaCl_3$, or EGTA, and 2-day-old soybeans

were exposed to flooding or drought for 1 day before the root tips were collected. *HCP-like superfamily protein* was upregulated without chemical treatment under flooding compared to non-stressed soybeans, but downregulated by 2-APB compared to untreated soybeans under both stresses (Figure 34A). *GRP78/BiP* was downregulated without chemical treatment under both stresses compared to non-stressed plants (Figure 34A). Because gene expression of these ER stress-related proteins was affected under both stresses, it was analyzed in detail on time-dependent manner. *HCP-like superfamily protein* was upregulated in the first day of exposure to both stresses (Figure 34B). *GRP78/BiP* was downregulated after 1 day of flooding and after 3 days of drought (Figure 34B).

3.3.5. Calcium effects on the abundance of ER proteins under flooding and drought stresses

To explore the effects of calcium on soybean under flooding and drought stresses, proteomic analysis was conducted. Soybean seeds were germinated for 2 days without or with treatment of 2-APB, $LaCl_3$, EGTA, or $CaCl_2$, and 2-day-old soybeans were exposed to flooding or drought for 1 day before the root tips were collected. To examine the effects of 2-APB and $LaCl_3$ on ER function, the abundance of predicted ER proteins was analyzed. Among the predicted ER proteins, calnexin, PDI-like proteins, HSPs, and thioredoxin family proteins were the most abundant. Cluster analysis of these abundant ER proteins was further performed to examine the protein abundance induced by 2-APB and $LaCl_3$ under both stresses (Figure 35). Under flooding, increased calnexin and PDI-like proteins were identified in absence of chemical treatment. Calnexin and HSPs were decreased; however, PDI-like proteins unaltered or increased in soybeans with 2-APB treatment under flooding compared to untreated plants. Thioredoxin family proteins were decreased in flooded soybeans and it further declined with 2-APB or $LaCl_3$ treatment compared to untreated plants. Under drought, calnexin was increased in absence of chemical treatment. Calnexin was increased and decreased by 2-APB and $LaCl_3$, respectively, compared to untreatment. PDI-like proteins were decreased by 2-APB treatment under drought compared to untreated soybeans. HSPs were slightly increased by 2-APB compared to untreated soybeans under drought. In addition, more

proteins were decreased in plants treated with $LaCl_3$ under both stresses compared to untreated soybeans (Figure 35).

3.3.6. Primary metabolic pathways related to calcium under flooding and drought stresses

To determine the function of responsive proteins induced by chemical treatment, functional analysis was performed using MapMan bin codes under control, flooding, and drought. The fold change of protein abundance was visualized using MapMan software to examine the affected metabolism. Out of all the primary metabolism, glycolysis, fermentation, the tricarboxylic acid cycle, and amino acid metabolism were significantly altered by calcium (Figure 36).

Effects of calcium on the ER and plasma membrane were examined using 2-APB and $LaCl_3$. Under control, 2-APB treatment suppressed the tricarboxylic acid cycle (Figure 36C), whereas $LaCl_3$ enhanced amino acid metabolism (Figure 36D). Under flooding, 2-APB treatment suppressed the tricarboxylic acid cycle (Figure 36A, G) and $LaCl_3$ suppressed fermentation compared to untreated soybeans (Figure 36A, H). Under drought, 2-APB and $LaCl_3$ inhibited glycolysis and amino acid metabolism (Figure 36B, K, L). Under control, EGTA suppressed glycolysis, fermentation, the tricarboxylic acid cycle, and amino acid metabolism (Figure 36E), whereas $CaCl_2$ enhanced fermentation (Figure 36F). Under flooding, EGTA suppressed fermentation (Figure 36A, I) compared to $CaCl_2$ (Figure 36A, J) or untreatment. Under drought, EGTA suppressed glycolysis, the tricarboxylic acid cycle, and amino acid metabolism (Figure 36B, M), whereas $CaCl_2$ enhanced the tricarboxylic acid cycle, compared to untreated soybeans (Figure 36B, N).

Abundance of the most affected proteins in response to calcium under flooding and drought stresses was examined. Under flooding, pyruvate decarboxylase 2 (Table 10, number 25) and NADP malic enzyme 4 (Table 10, number 38) displayed the highest and the lowest protein abundance, respectively. Under drought, ATP citrate lyase subunit B2 (Table 10, number 42) and pyruvate decarboxylase 2 (Table 10, number 41) were determined with the highest and the lowest protein abundance, respectively.

3.3.7. Calcium effects on the abundance of proteins related to glycolysis, fermentation, the tricarboxylic acid cycle, and amino acid metabolism under flooding and drought stresses

Because glycolysis, fermentation, the tricarboxylic acid cycle, and amino acid metabolism were altered in response to chemical treatment under both stresses (Figure 36), the effects of calcium on protein abundance of these categories were further analyzed. A total of 47 proteins were determined to be calcium responsive under both stresses (Table 10). Of these 47 proteins, 36 were mapped to glycolysis, fermentation, the tricarboxylic acid cycle, and amino acid metabolism against KEGG (Figure 37).

Among the identified proteins, pyruvate decarboxylase, ATP citrate lyase, isocitrate dehydrogenase, and 2-oxoglutarate dehydrogenase were changed in response to calcium under both stresses. Pyruvate decarboxylase was the most changed protein and found increased and decreased in untreated plants under flooding and drought, respectively, compared to non-stressed plants. Under both stresses, pyruvate decarboxylase was decreased in plants treated with 2-APB and $LaCl_3$, but increased by $CaCl_2$, compared to untreated soybeans. ATP citrate lyase was decreased and increased in untreated plants under flooding and drought, respectively, compared to non-stressed plants. The same change tendency of ATP citrate lyase was further induced by 2-APB treatment under both stresses compared to untreatment. Isocitrate dehydrogenase was decreased without chemical treatment under both stresses compared to non-stressed soybeans. 2-Oxoglutarate dehydrogenase was increased without chemical treatment under both stresses compared to non-stressed soybeans, but decreased and increased in response to 2-APB treatment under flooding and drought, respectively, compared to untreated soybeans (Figure 37).

Furthermore, the abundance of several other proteins including aconitase, succinate dehydrogenase, and asparate aminotransferases, was altered in soybeans under flooding or drought. Under flooding, succinate dehydrogenase was decreased without chemical treatment compared to non-stressed soybeans, but increased by 2-APB and EGTA compared to untreated soybeans. Aspartate aminotransferases were slightly increased without chemical treatment, but increased by 2-APB and EGTA treatment compared to untreated soybeans under flooding. Under drought, aconitase was slightly

decreased without chemical treatment compared to non-stressed soybeans (Figure 37).

The abundance of proteins related to glycolysis was significantly altered in soybean exposed to flooding. Under flooding, phosphofructokinase was decreased, whereas enolase and pyruvate kinase increased in absence of chemical treatment compared to non-stressed soybeans. In contrast, phosphofructokinase was increased by 2-APB, whereas enolase decreased by 2-APB and $LaCl_3$ compared to untreated soybeans under flooding. Pyruvate kinase was slightly decreased by 2-APB, $LaCl_3$, and EGTA, but increased by $CaCl_2$ compared to untreated soybeans under flooding. Furthermore, proteins related to amino acid metabolism were decreased without chemical treatment compared to non-stressed soybeans, but they exhibited variable changes in response to chemical treatment compared to untreated soybeans under flooding (Figure 37).

3.3.8. Effects of flooding and drought on pyruvate decarboxylase activity

Protein abundance of pyruvate decarboxylase was increased and decreased under flooding and drought, respectively, and markedly affected by calcium (Figures 37 and 38A, Table 10). To further characterize the properties of pyruvate decarboxylase in soybean under flooding and drought, temporal changes in enzyme activity were examined (Figure 38B). Two-day-old soybeans were exposed to flooding or drought for 1, 2, 3, and 4 days, and the root tips were collected for pyruvate decarboxylase activity analysis. Pyruvate decarboxylase activity was decreased in 5-day-old soybeans under control, but gradually increased during the 4 days of flooding. In contrast, pyruvate decarboxylase activity was continuously decreased under drought (Figure 38B).

3.4. Discussion

3.4.1. Calcium is involved in the ER function in soybean-root tip under flooding and drought stresses

Because cytosolic calcium content was reportedly increased in root tip of soybean under flooding and drought, source of increased cytosolic calcium was examined using 2-APB and $LaCl_3$. 2-APB functions as a non-competitive antagonist of inositol-trisphosphate receptor in the ER (Prakriya and Lewis 2001; Healy et al., 2012) and

$LaCl_3$ is a blocker of Ca^{2+}-ATPase activity in the plasma membrane (Xu and Heath 1998; Chung et al., 2000). Treatment of 2-APB and $LaCl_3$ did not induce calcium elevation in cytosol under both stresses in soybean (Figure 31), suggesting that calcium might be released from the ER or from the outside of plasma membrane, under flooding or drought.

In response to ER stress, ER-associated degradation and unfolded protein response are activated (Howell, 2013). *HCP-like superfamily protein* was upregulated and downregulated, respectively, under flooding and drought, whereas *GRP78/BiP* downregulated under both stresses (Figure 34). *HCP-like superfamily protein* is a homologue of *Arabidopsis HRD3A*, which was a component of ER-associated degradation complex (Liu et al., 2011). In *Arabidopsis*, ER-associated degradation was involved in stress response (Chen et al., 2016), and impairment of HRD3A altered unfolded protein response and increased plant sensitivity to salt stress (Liu et al., 2011). *GRP78/BiP*, which is an *HSP* homologue, has multiple roles in the ER, including ER-associated folding, ER-associated degradation, and unfolded protein response (Healy et al., 2012). Taken together, these findings indicate that HCP-like superfamily protein is a component of ER-associated degradation complex in soybean and might alleviate ER stress in root tip at initial stage of soybean exposed to flooding and drought, as well as salt stress.

Calnexin was increased in root tip of soybean exposed to flooding and drought for 1 day (Figure 35). Calnexin, which is an ER-localized protein involved in protein folding and quality control (Bergeron et al., 1994), was increased in root including hypocotyl of the early-stage soybean in the first day of flooding (Nanjo et al., 2010). Exposed to flooding for 2 days, decreased calnexin was reported in soybean (Komatsu et al., 2012b); however, it increased in flooding-tolerant mutant (Yin et al., 2016). Calnexin was decreased in soybean exposed to drought for 2 days (Chapter 2) and heterogenous expression of *OsCNX* in tobacco enhanced germination under mannitol stress (Sarwat and Naqvi, 2013). Taken together, these results suggest that increased calnexin might maintain protein folding in root tip of the early-stage soybean under flooding and drought.

The ER regulates protein folding and assembly of multimeric proteins through an

array of chaperones including calnexin, PDI, and HSPs (Healy et al., 2012). The accumulation of misfolded or unfolded proteins under adverse environmental conditions leads to ER stress (Vitale and Boston, 2008). In the present study, the treatment of 2-APB resulted in decreased and increased levels of calnexin/HSPs under flooding and drought, respectively, and slightly increased the abundance of PDI-like proteins under flooding (Figure 35). 2-APB inhibited calcium release induced by inositol trisphosphate in animals (Maruyama et al., 1997) and mediated ER calcium in fungi (Silverman-Gavrila and Lew, 2001), as well as in plants (Liu et al., 2011). Calnexin, together with PDI-like proteins or HSPs, was involved in protein folding under flooding and drought, respectively (Chapter 2). The present results combined with previous findings suggest that calcium in the ER is associated with protein folding and reduction of cytosolic calcium might weaken ER stress under drought.

3.4.2. Calcium is associated with energy supply in soybean-root tip exposed to flooding and drought stresses

In response to calcium, several proteins involved in primary metabolic pathways including glycolysis, fermentation, the tricarboxylic acid cycle, and amino acid metabolism were differentially affected under flooding and drought (Figures 36 and 37). Proteins involved in glycolysis were increased and responded to calcium level under flooding (Figure 37). Genes associated with glycolysis were downregulated or unaltered in potato exposed to drought (Watkinson et al., 2008), but upregulated in flooded soybean (Nanjo et al., 2011). Various glycolysis-related proteins were increased in flooded soybean exposed to aluminum oxide nanoparticles (Mustafa et al., 2015b) and enhanced-glycolytic activity was required for mediating waterlogging tolerance in mung bean (Sairam et al., 2009). Additionally, disruption of calcium homeostasis in the ER reduced the accumulation of glycoproteins under flooding and drought (Chapter 2), whereas glycoproteins involved in glycolysis were activated in response to flooding (Mustafa and Komatsu, 2014). Taken together, these findings suggest that calcium in the ER is involved in glycolysis and increased-glycolytic activity might be required to meet energy demand during the early stage of flooding.

The present finding that proteins involved in the tricarboxylic acid cycle were

modulated in response to calcium in the ER was not unexpected, because 2-APB reduced the extent of mitochondrial-calcium uptake (Peppiatt et al., 2003). Notably, isocitrate dehydrogenase and 2-oxoglutarate dehydrogenase were decreased and increased in soybean-root tip under flooding and drought, respectively (Figure 37). In the tricarboxylic acid cycle, isocitrate dehydrogenase catalyzes the conversion of 2-oxyglutarate to isocitrate (Bailey-Serres and Voesenek, 2008) and 2-oxoglutarate dehydrogenase is involved in the conversion of 2-oxoglutarate to succinate (Hassel et al., 1998). γ-Aminobutyrate metabolism was functional bypass of 2-oxyglutarate to succinate of the tricarboxylic acid cycle in plants (Studart-Guimarães et al., 2007). GABA was accumulated in soybean under flooding (Komatsu et al., 2011a) and drought (Serraj et al., 1998). In addition, succinate accumulated in soybean under flooding (Komatsu et al., 2011a) and in tobacco under salt (Zhang et al., 2011b). These findings indicate that the balance between succinate and GABA might play roles in energy replenishment in response to depleted-energy production induced by flooding and drought in soybean.

Protein abundance and enzyme activity of pyruvate decarboxylase were increased under flooding or decreased under drought, in absence of chemical treatment (Figures 37 and 38). The protein abundance was decreased and increased following treatment with 2-APB and $CaCl_2$, respectively, under both stresses (Figures 37 and 38). Pyruvate decarboxylase was key fermentative enzyme under flooding (Komatsu et al., 2011b) and involved in drought adaptation (Ranjan et al., 2012). Energy sensor Snf1-related protein kinase 1 underwent activation under hypoxia-inducible energy deprivation (Fragoso et al., 2009). Faster consuming of pyruvate was reported in plants under control than under extended darkness conditions, which was validated with significant alterations in the activity of pyruvate dehydrogenase complex (Nägele et al., 2014). Calcium transients were required for alterations in gene expression enhancing fermentation and ATP management under stress (Bailey-Serres and Voesenek, 2008). In root of flooded cucumber, upregulated gene expression and increased protein abundance of pyruvate decarboxylase were further induced by exogenous calcium application (He et al., 2012). Taken together, these findings suggest that pyruvate decarboxylase responds to calcium and might be a key enzyme to switch energy metabolism in root tip of soybean under

flooding and drought.

3.5. Conclusion

The present study investigated calcium effects on ER function and cellular metabolisms of soybean under flooding and drought stresses. The main findings are as follows (Figure 39): (i) 2-APB and $LaCl_3$ inhibited the elevation of cytosolic calcium in soybean under both stresses; (ii) calnexin, PDI-like proteins, HSPs, and thioredoxin family proteins were affected as abundant ER proteins in response to calcium under both stresses; (iii) HCP-like superfamily protein responded to calcium and its gene expression was upregulated upon 1-day exposure to both stresses; (iv) glycolysis, fermentation, the tricarboxylic acid cycle, and amino acid metabolism were altered as main cellular metabolisms in response to calcium under both stresses; (v) protein abundance of pyruvate decarboxylase was increased under flooding and decreased under drought, respectively, in absence of chemical treatment; and it presented with increased abundance in response to elevated cytosolic calcium; and (vi) enzyme activity of pyruvate decarboxylase was increased and decreased under flooding and drought, respectively. Collectively, these findings indicate that calcium is involved in ER function and ER-associated degradation might eliminate ER stress during the early stage of both stresses. In addition, calcium might play roles in energy production in soybean-root tip exposed to flooding and drought, and pyruvate decarboxylase may be a key enzyme for modifying energy metabolism in response to these abiotic stresses.

Table 9. Primer sequences of genes selected for qRT-PCR in Chapter 3

Protein ID [a)]	Description	Sequence of primers (5'--- 3')
Glyma04g09290.2	inositol 1,3,4-trisphosphate 5/6-kinase family protein	F: GCTGTTGCGGATATGAACCT R: ACTCCTGGAGCACAAGAGGA
Glyma19g35960.1	Ca^{2+}-transporting ATPase	F: GGGAGTATGTGGATGGATGG R: GGCCATCTTTCGAGTACCAA
Glyma04g38000.1	calnexin	F: GGATCCTGTTTTTAACGCAGATTAG R: AAATTATCATTATTCTATTGCATTAGTAGG
Glyma11g13460.1	calreticulin 3	F: CATGGATTGGGACATCCTTC R: TCAACAGGCTTCTTGGCTTT
Glyma14g24090.1	PDI like 1,1	F: CACCTTGGATGCCAAATACC R: ACAAAAGGGTGATTGCTTGG
Glyma05g33770.1	HCP-like superfamily protein	F: TCCAGGCACCACCTCTATTC R: GGTTAGCAGCGAGGACAAAG
Glyma05g36600.1	GRP78/BiP	F: AGCTCGGTTTGAGGAGTTGA R: TTGTTTGGCTCCTTTCCATC

a, Protein ID according to Phytozome soybean genome database.

Table 10. List of proteins related to glycolysis, fermentation, the tricarboxylic acid cycle, and amino acid metabolism in response to calcium in the root tip of soybean under flooding and drought stresses

			Ratio						
	Protein ID	Description	3(0)[a)]	3(1)	2-APB 3(1)	$LaCl_3$ 3(1)	EGTA 3(1)	$CaCl_2$ 3(1)	Function
Flooding									
1	Glyma10g34490.1	pyruvate kinase family protein	1	1.72	1.51	1.57	1.70	1.89	glycolysis
2	Glyma09g28100.1	enolase	1	1.28	1.03	0.60	1.14	1.35	glycolysis
3	Glyma10g25683.1	phosphofructokinase family protein	1	0.68	0.71	0.61	1.00	0.67	glycolysis
4	Glyma16g09020.1	glyceraldehyde 3 phosphate dehydrogenase of plastid 2	1	0.66	0.64	0.83	0.58	1.00	glycolysis
5	Glyma03g22790.1	glyceraldehyde 3 phosphate dehydrogenase of plastid 2	1	0.62	0.56	0.27	0.54	0.62	glycolysis
6	Glyma09g01270.1	fumarylacetoacetase putative	1	1.56	1.81	1.56	1.67	1.52	amino acid metabolism
7	Glyma05g27840.1	urease	1	1.19	1.37	0.87	2.06	0.74	amino acid metabolism
8	Glyma06g08670.1	aspartate aminotransferase 3	1	1.06	1.22	0.94	1.17	1.06	amino acid metabolism
9	Glyma04g08560.1	aspartate aminotransferase 3	1	1.05	1.20	0.94	1.17	1.05	amino acid metabolism
10	Glyma19g29180.3	cobalamin independent synthase family protein	1	0.36	1.00	0.02	0.50	0.17	amino acid metabolism
11	Glyma02g04760.1	phosphoserine aminotransferase	1	0.71	1.00	0.09	1.00	0.67	amino acid metabolism
12	Glyma14g35370.2	class II DAHP synthetase family protein	1	0.14	1.00	0.02	1.00	0.09	amino acid metabolism
13	Glyma05g03190.1	arginosuccinate synthase family	1	0.82	0.92	0.85	1.00	0.75	amino acid metabolism
14	Glyma19g36580.1	pyridoxal dependent decarboxylase family protein	1	0.73	0.85	0.67	1.00	0.72	amino acid metabolism
15	Glyma20g31980.1	chorismate synthase putative	1	0.75	0.76	0.63	1.00	0.68	amino acid metabolism
16	Glyma13g15140.1	cobalamin independent synthase family protein	1	0.76	0.71	0.13	0.73	0.92	amino acid metabolism
17	Glyma04g30350.1	cobalamin independent synthase family protein	1	0.78	0.69	0.16	0.68	0.90	amino acid metabolism
18	Glyma17g23730.1	cobalamin independent synthase family protein	1	0.68	0.54	0.07	0.62	0.72	amino acid metabolism
19	Glyma17g24366.1	cobalamin independent synthase family protein	1	0.68	0.54	0.07	0.61	0.68	amino acid metabolism
20	Glyma13g21230.1	threonine dehydratase	1	0.45	0.51	0.37	1.00	0.45	amino acid metabolism
21	Glyma20g01180.2	peroxisomal 3 ketoacyl CoA thiolase 3	1	0.61	0.49	0.58	0.58	0.65	amino acid metabolism
22	Glyma08g17760.1	mercaptopyruvate sulfurtransferase 1	1	0.56	0.43	1.31	0.38	1.00	amino acid metabolism
23	Glyma14g39170.1	glutamate decarboxylase	1	0.51	0.37	0.42	0.50	0.62	amino acid metabolism
24	Glyma05g10840.2	cobalamin independent synthase family protein	1	0.20	0.25	0.01	0.58	0.14	amino acid metabolism
25	Glyma13g30490.1	pyruvate decarboxylase 2	1	2.03	1.51	0.20	1.32	2.63	fermentation
26	Glyma08g17450.1	aldehyde dehydrogenase 5F1	1	1.51	2.33	1.00	2.02	1.00	TCA cycle
27	Glyma15g41690.1	aldehyde dehydrogenase 5F1	1	1.55	2.01	1.44	1.58	1.10	TCA cycle
28	Glyma02g10470.1	2-oxoglutarate dehydrogenase E1 component	1	1.28	1.00	0.64	1.19	1.34	TCA cycle
29	Glyma16g00590.1	dihydrolipoamide acetyltransferase long form protein	1	0.83	1.00	0.89	1.00	0.75	TCA cycle
30	Glyma18g52430.2	2-oxoglutarate dehydrogenase E1 component	1	1.25	1.00	1.00	1.17	1.28	TCA cycle

31	Glyma14g39160.2	cytosolic NADP dependent isocitrate dehydrogenase	1	0.54	1.00	1.00	1.00	0.41	TCA cycle
32	Glyma01g38200.1	succinate dehydrogenase	1	0.79	0.90	0.66	1.00	0.77	TCA cycle
33	Glyma05g08770.1	isocitrate/isopropylmalate dehydrogenase family protein	1	0.70	0.58	0.83	0.63	1.00	TCA cycle
34	Glyma09g04000.2	ATP citrate lyase B1	1	0.78	0.57	1.00	0.70	1.00	TCA cycle
35	Glyma08g17080.1	cytosolic NADP dependent isocitrate dehydrogenase	1	0.66	0.49	0.80	0.47	1.00	TCA cycle
36	Glyma02g04120.1	ATP citrate lyase A1	1	0.65	0.49	0.69	0.60	0.70	TCA cycle
37	Glyma07g37050.1	lipoamide dehydrogenase 1	1	0.67	0.44	0.45	0.63	0.70	TCA cycle
38	Glyma15g02230.1	NADP malic enzyme 4	1	0.10	0.18	0.08	0.11	0.09	TCA cycle
Drought									
39	Glyma04g36860.1	glyceraldehyde 3 phosphate dehydrogenase C2	1	0.93	0.86	0.68	0.90	1.00	glycolysis
40	Glyma12g02510.1	pyridoxal phosphate dependent transferases superfamily	1	0.89	0.80	0.73	0.77	1.00	amino acid metabolism
41	Glyma13g30490.1	pyruvate decarboxylase 2	1	0.67	0.58	0.28	0.54	0.71	fermentation
42	Glyma15g15010.1	ATP citrate lyase subunit B2	1	1.34	1.42	1.57	1.40	1.27	TCA cycle
43	Glyma18g52430.2	2-oxoglutarate dehydrogenase E1 component	1	1.16	1.34	1.13	1.16	1.00	TCA cycle
44	Glyma15g02230.1	NADP malic enzyme 4	1	0.97	1.00	0.23	0.99	0.89	TCA cycle
45	Glyma02g40820.1	cytosolic NADP dependent isocitrate dehydrogenase	1	0.76	1.00	1.02	1.00	0.63	TCA cycle
46	Glyma03g24630.1	NAD dependent malic enzyme 1	1	1.19	1.00	0.98	1.00	1.20	TCA cycle
47	Glyma12g32000.1	aconitase 3	1	0.92	0.92	0.92	0.89	1.01	TCA cycle

a), day after sowing (day after stress); Protein ID, according to Phytozome soybean genome database; Ratio, relative abundance of protein was compared to 3-day-old untreated soybeans without stresses; Function, functional analysis was performed using MapMan bin codes. Proteins related to glycolysis, fermentation, the tricarboxylic acid (TCA) cycle, and amino acid metabolism affected by chemical treatment were selected. The following criteria were used: change tendency of stress-response protein was opposite between 2-APB/$CaCl_2$ and EGTA/$CaCl_2$, but it similar between 2-APB and EGTA.

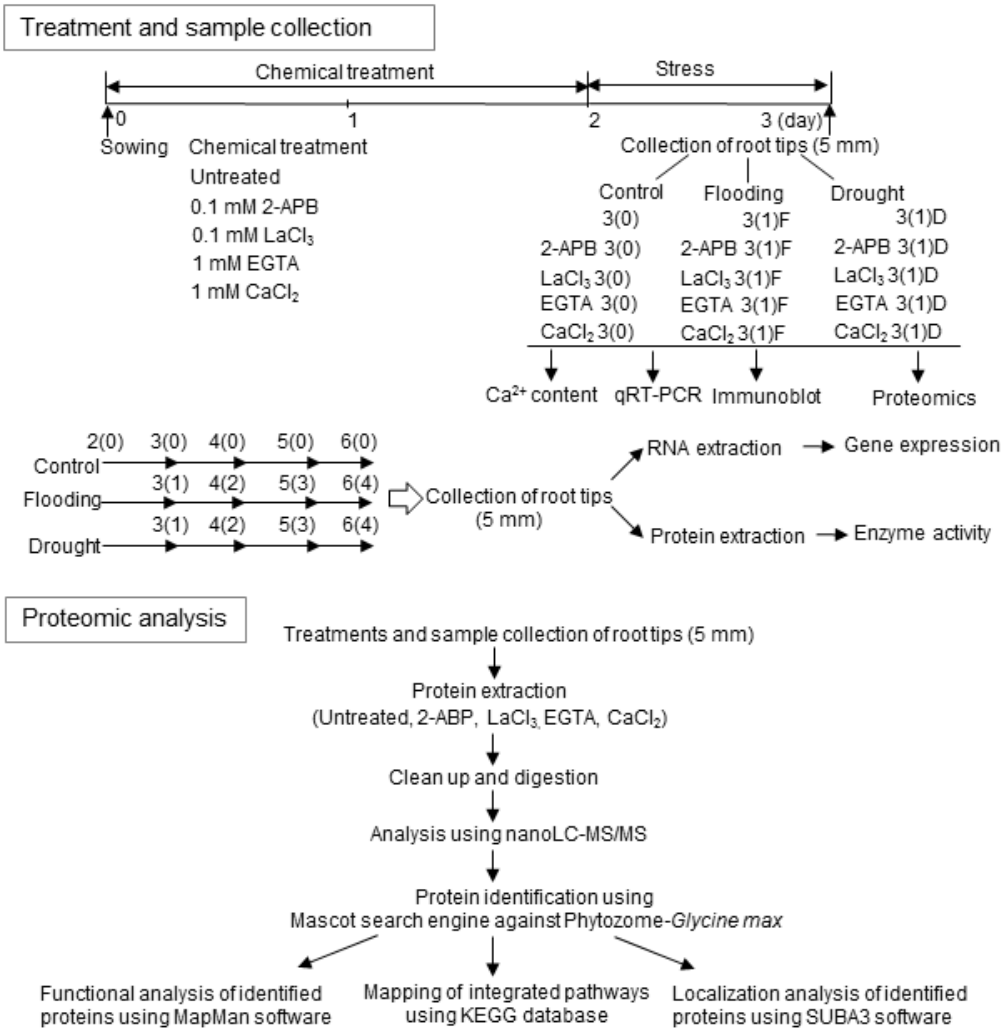

Figure 30. Experimental design to examine calcium effects in soybean under flooding and drought. Two-day-old soybeans were exposed to flooding or drought for 1 day. Soybean seeds were germinated for 2 days without or with treatment of 2-APB, $LaCl_3$, EGTA, or $CaCl_2$. Root tips of 3-day-old soybeans without or with chemical treatment were collected for calcium content, gene expression, immunoblot, and proteomic analyses. Two-day-old soybeans without chemical treatment were exposed to flooding or drought for 1, 2, 3, and 4 days and root tips were collected for gene expression and enzyme activity analyses.

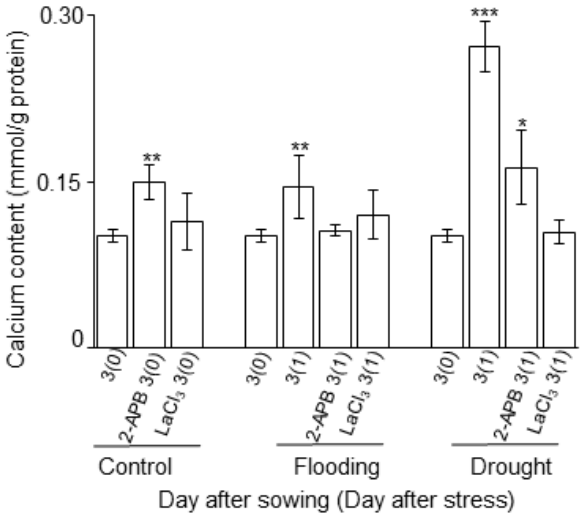

Figure 31. Effects of 2-APB and $LaCl_3$ on calcium content in soybean under flooding and drought. Soybean seeds were germinated for 2 days without or with treatment of 2-APB or $LaCl_3$. Two-day-old soybeans were exposed to flooding or drought for 1 day and root tips were collected for the measurement of calcium content. Data are shown as means ± SD from three independent biological replicates. Student's *t*-test was used for statistical analysis. Asterisks indicate the significance between 3-day-old soybeans treated without or with 2-APB or $LaCl_3$ and non-stressed soybeans without treatment under control, flooding, and drought conditions (*p<0.05, **p<0.01, ***p< 0.001).

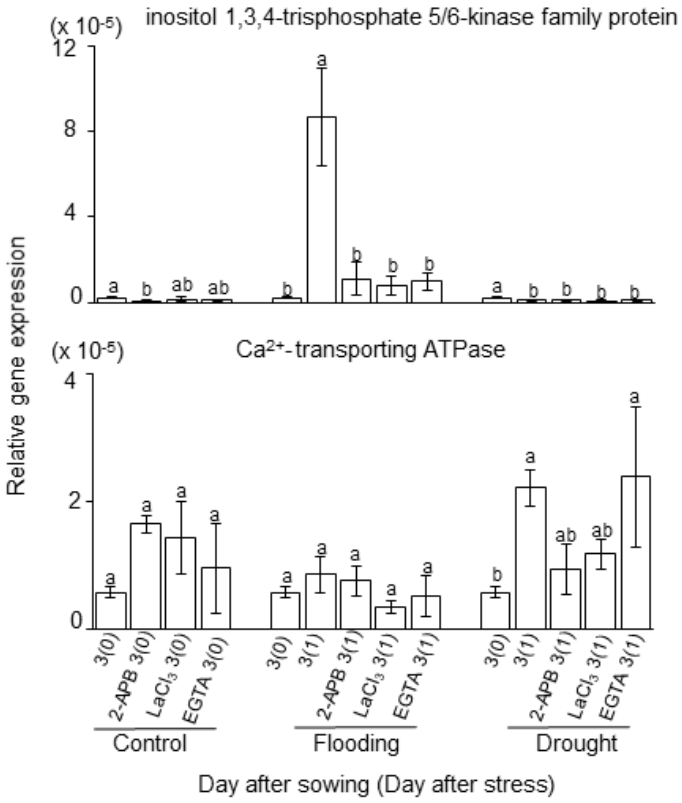

Figure 32. Effects of chemical treatment on gene expression of calcium-related proteins in soybean under flooding and drought. Soybean seeds were germinated for 2 days without or with treatment of 2-APB, $LaCl_3$, or EGTA. Two-day-old soybeans were exposed to flooding or drought for 1 day and root tips were collected for RNA extraction. Gene expression was normalized against that of 18S rRNA. Data are shown as means ± SD from three independent biological replicates. Different letter indicates the change is significant, as determined by one-way ANOVA according to Tukey's multiple comparison test ($p<0.05$).

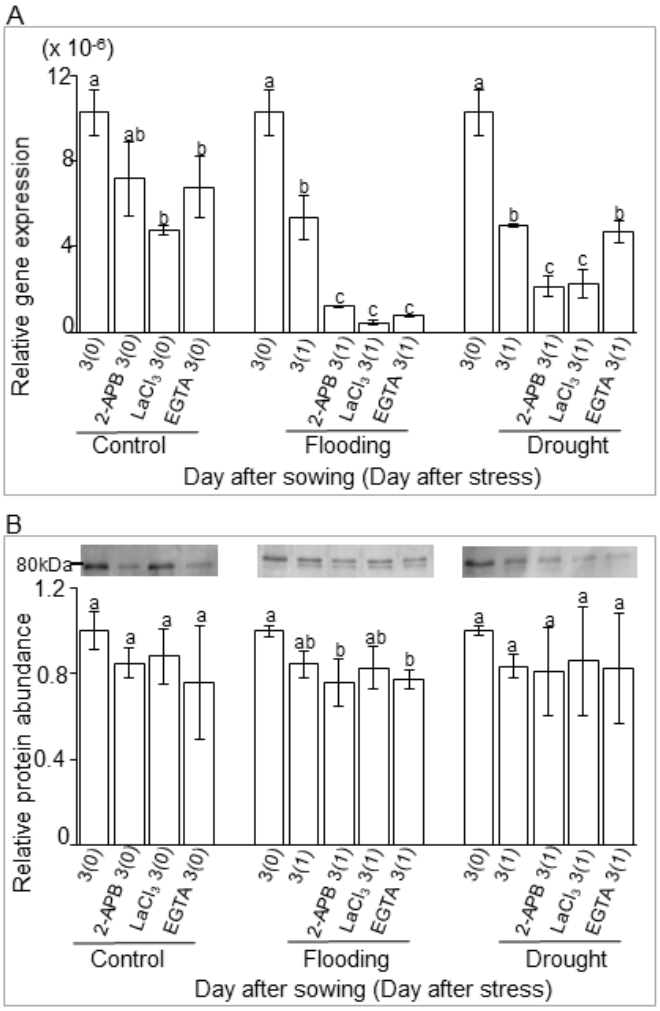

Figure 33. Gene expression and protein abundance of calnexin in soybean treated with 2-APB, $LaCl_3$, or EGTA under flooding and drought. Soybean seeds were germinated for 2 days without or with 2-APB, $LaCl_3$, or EGTA treatment, and 2-day-old soybeans were exposed to flooding or drought for 1 day before the collection of root tips. Gene expression was normalized against that of 18S rRNA (A). Immunoblot analysis was performed for calnexin using anti-calnexin antibody and relative protein abundance was compared to untreated soybeans without stresses (B). Data are shown as means ± SD from three independent biological replicates. Different letter indicates the change is significant, as determined by one-way ANOVA according to Tukey's multiple comparison test ($p<0.05$).

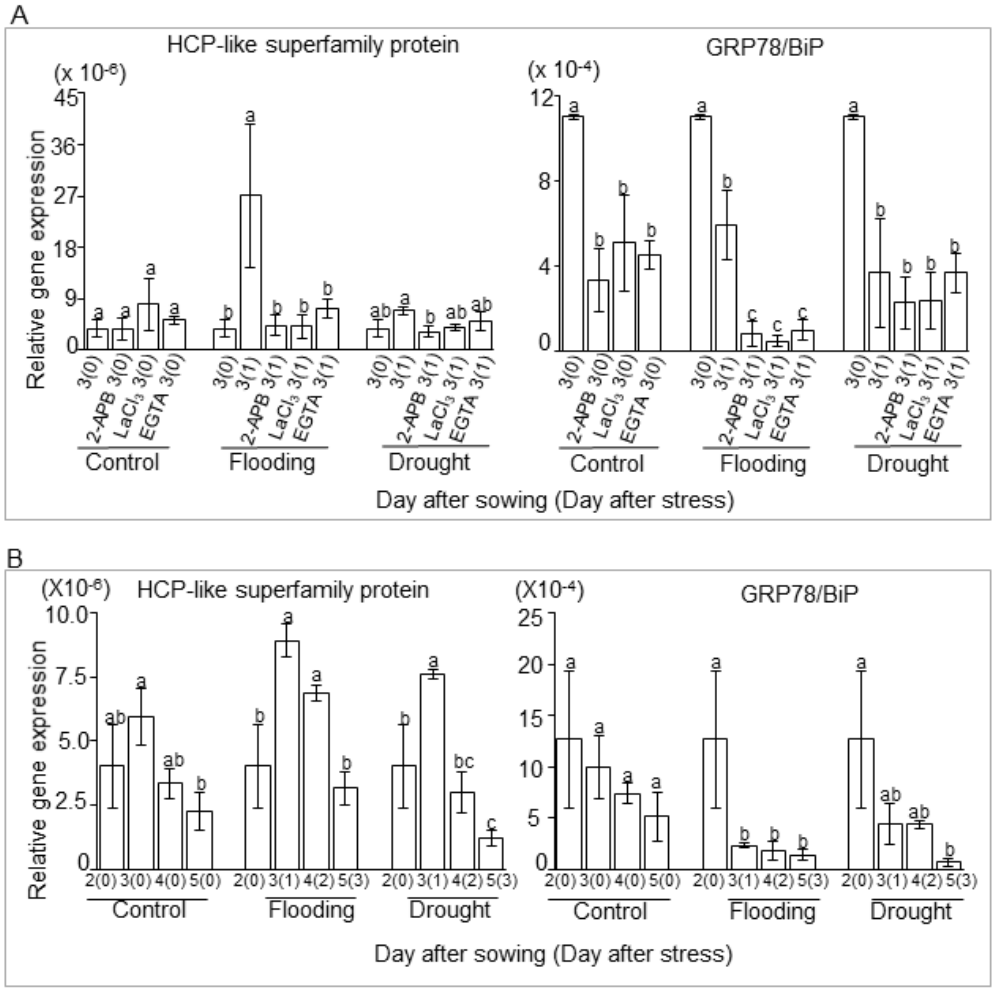

Figure 34. Gene expression of the endoplasmic reticulum stress-related proteins in soybean under flooding and drought. Soybean seeds were germinated for 2 days without or with treatment of 2-APB, $LaCl_3$, or EGTA, and 2-day-old soybeans were exposed to flooding or drought for 1 day before the collection of root tips (A). Two-day-old soybeans were exposed to flooding or drought for 1, 2, 3, and 4 days, and root tips were collected (B). Gene expression was normalized against that of 18S rRNA. Data are shown as means ± SD from three independent biological replicates. Different letter indicates the change is significant, as determined by one-way ANOVA according to Tukey's multiple comparison test ($p<0.05$).

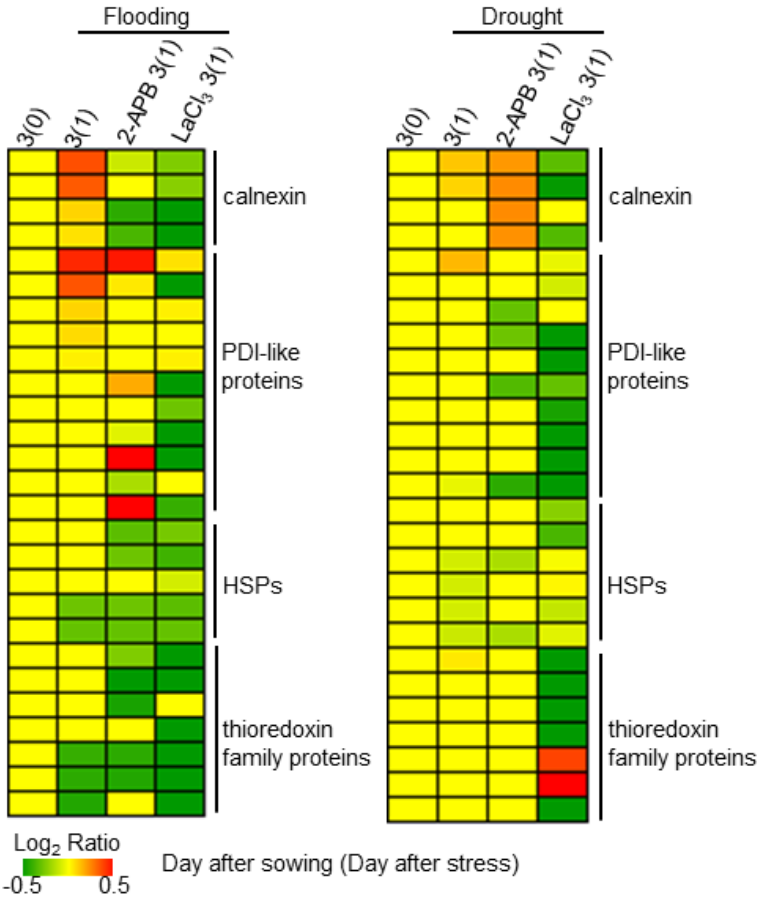

Figure 35. Cluster analysis of the endoplasmic reticulum proteins in soybean treated with 2-APB and $LaCl_3$ under flooding and drought. Soybeans seeds were germinated for 2 days without or with treatment of 2-APB or $LaCl_3$, and 2-day-old soybeans were exposed to flooding or drought for 1 day before the collection of root tips. Proteins were extracted from the root tips and analyzed using nanoLC-MS/MS. Localization of the identified proteins was performed using SUBA3 intracellular targeting prediction program. Out of all the ER proteins, the abundant proteins including calnexin, PDI-like proteins, HSPs, and thioredoxin family proteins were subjected to cluster analysis. Black lines indicate these abundant ER proteins based on the logarithmic values of protein abundance. Green and red colors indicate decrease and increase, respectively, in Log_2 Ratio compared to 3-day-old untreated soybeans without stresses.

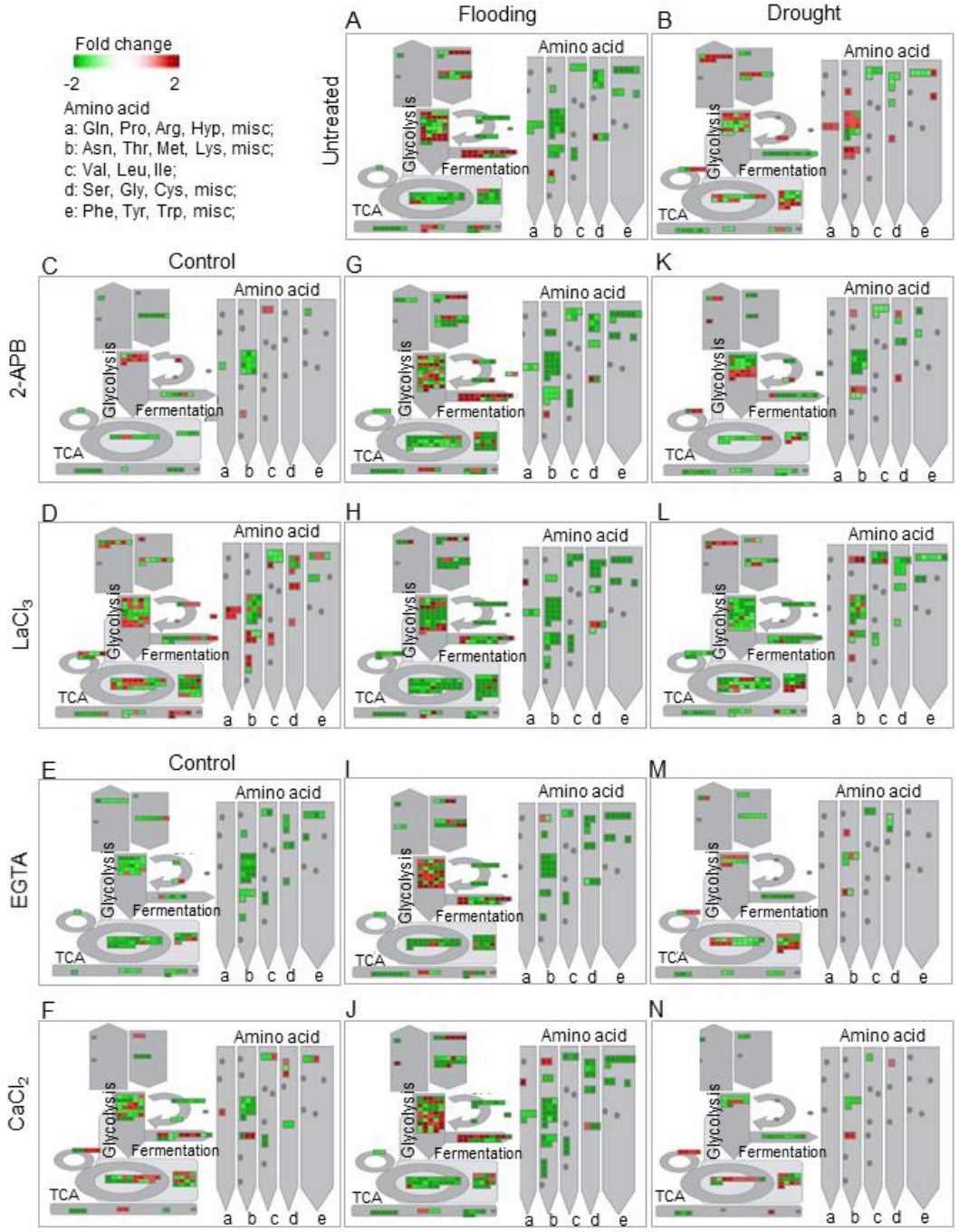

Figure 36. Abundance of proteins identified in soybean with chemical treatment under flooding and drought. Soybean seeds were germinated for 2 days without or with chemical treatment, and 2-day-old soybeans were exposed to flooding or drought for 1 day before root tips were collected for protein extraction. The fold change of proteins grouped into primary metabolism was visualized using MapMan software. The functional categories of the primary metabolic pathways of glycolysis, fermentation, the tricarboxylic acid (TCA) cycle, and amino acid metabolism are shown. Each square and color indicate the fold change value of a differentially changed protein. Green and red colors indicate decrease and increase, respectively, in fold change values compared to 3-day-old untreated soybeans without stresses.

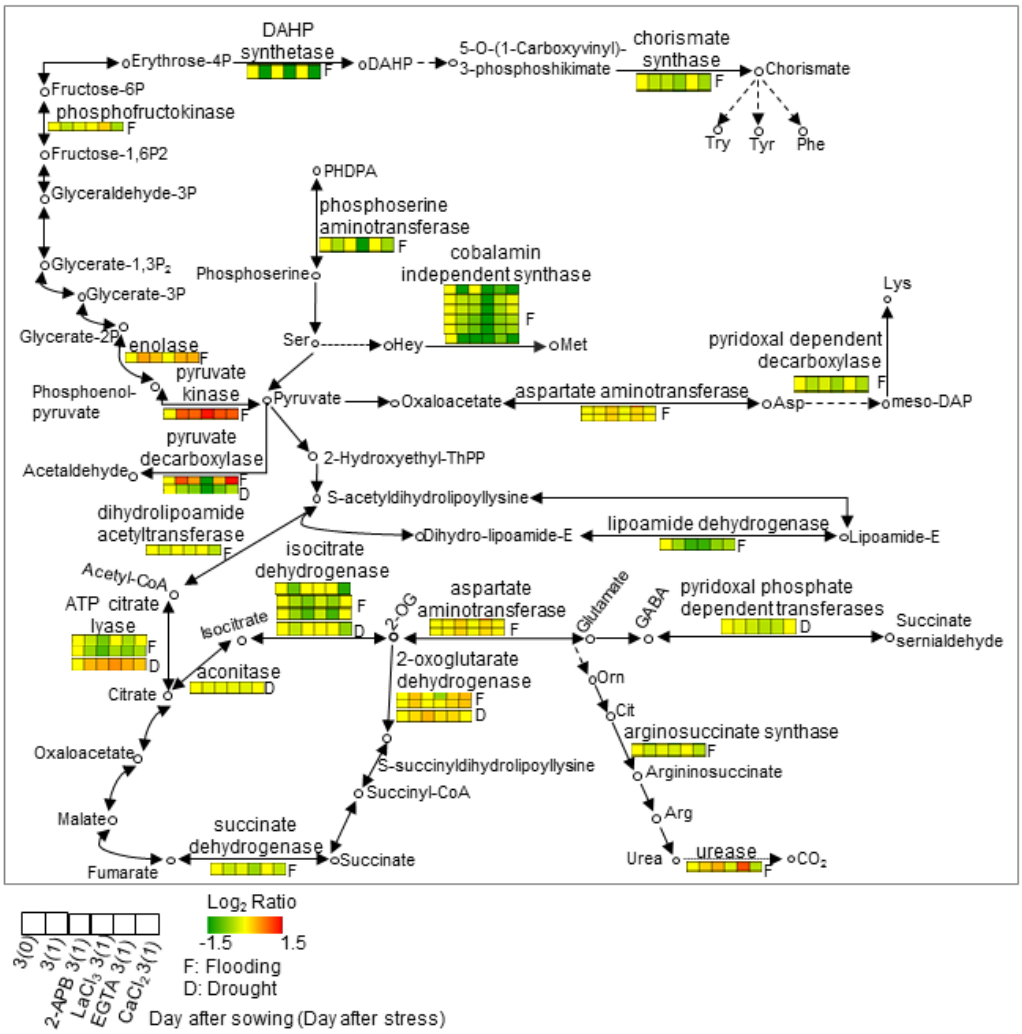

Figure 37. Integrated pathways affected by calcium in soybean exposed to flooding and drought. Pathways of glycolysis, fermentation, the tricarboxylic acid cycle, and amino acid metabolism were integrated based on the responsive proteins. Each square and color indicate the Log_2 Ratio of a differentially changed protein. Green and red colors indicate Log_2 Ratio values of identified enzymes compared to untreated plants without stresses. Full and dash lines indicate single and multiple steps, respectively. Abbreviations are as follows: DAHP, 3-deoxy-D-arabino-heptulosonic acid 7-phosphate; PHDPA, 3-phosphohydroxypyruvic acid; meso-DAP, meso-2, 6-diaminopimelate; 2-hydroxyethyl-ThPP, 2-(alpha-hydroxyethyl) thiamine pyrophosphate; 2-OG, 2-oxoglutarate.

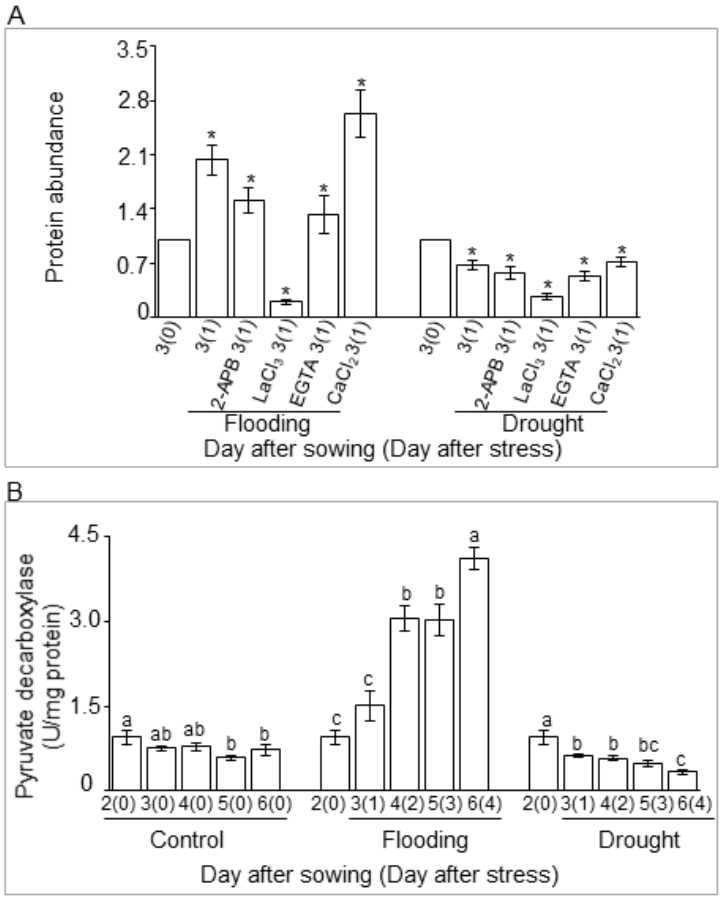

Figure 38. Protein abundance and enzyme activity of pyruvate decarboxylase in response to calcium in soybean under flooding and drought. Soybean seeds were germinated for 2 days without or with treatment of 2-APB, $LaCl_3$, EGTA, or $CaCl_2$, and 2-day-old soybeans were exposed to flooding or drought for 1 day before the collection of root tips to examine protein abundance of pyruvate decarboxylase (A). The protein abundance was compared to untreated plants without stresses using SIEVE software (p<0.05). Two-day-old soybeans were exposed to flooding or drought for 1, 2, 3, and 4 days, and root tips were collected to examine enzyme activity of pyruvate decarboxylase (B). Significance of enzyme activity was determined by one-way ANOVA according to Tukey's multiple comparison test (p<0.05) and different letter indicates the change is significant. Data are shown as means ± SD from three independent biological replicates.

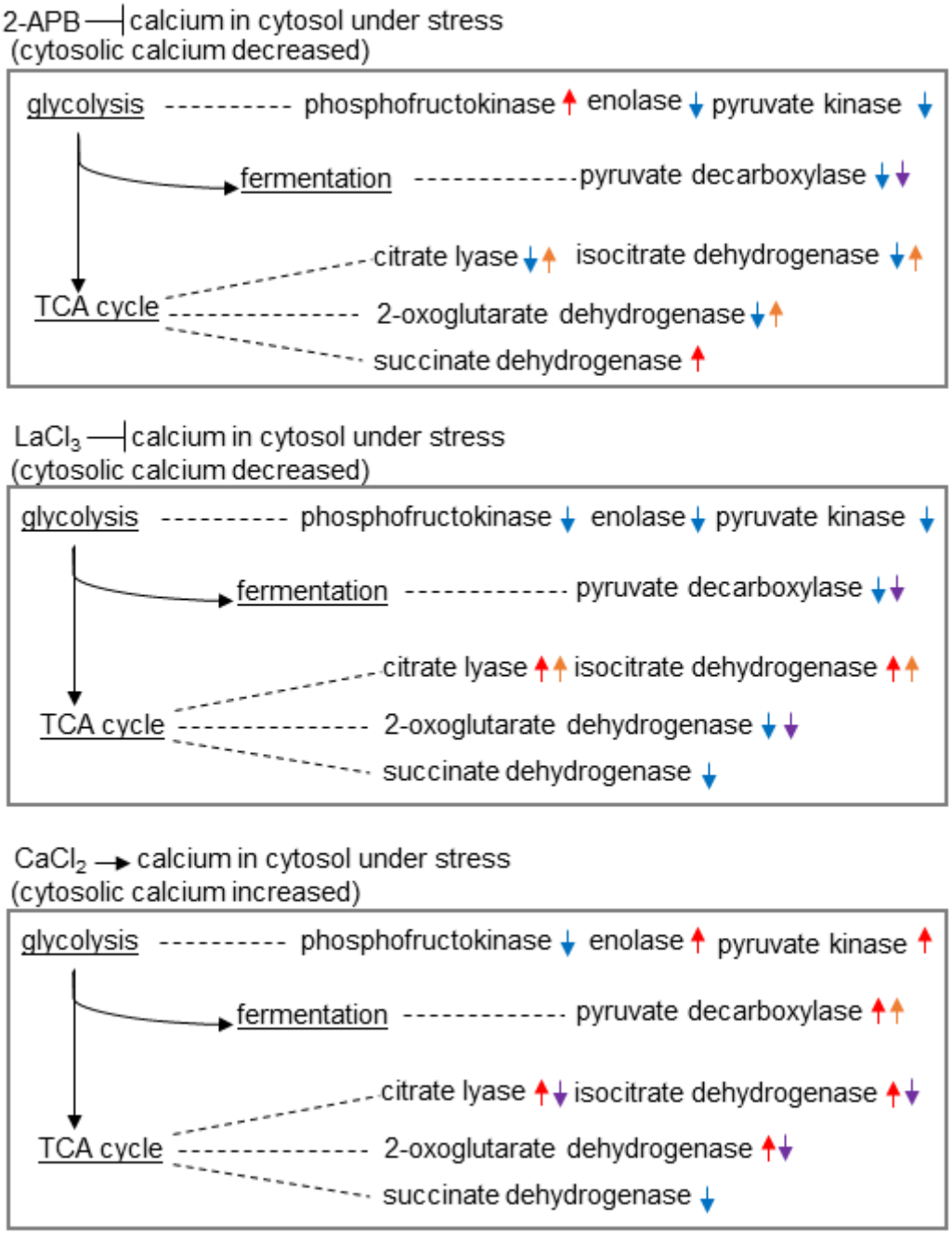

Figure 39. Schematic representation of responsive mechanisms induced by calcium under flooding and drought. 2-APB, $LaCl_3$, and $CaCl_2$ were used to change cytosolic calcium in soybean under flooding and drought. Based on the proteomic data, highlighted proteins were explained. Untreated soybean without stresses was used as comparison point. The red and blue arrows indicate changes of protein abundance under flooding; orange and purple arrows indicate changes of protein abundance under drought; and upward and downward arrows indicate increased and decreased changes of protein abundance, respectively. Abbreviations are as follows: TCA, tricarboxylic acid; 2-APB, 2-aminoethoxydiphenyl borate.

CONCLUSION AND FUTURE PROSPECTS

Global climate changes influence the magnitude and frequency of hydrological fluctuations and cause unfavorable environment for plant growth and development (Fukao et al., 2011). Abiotic stresses are potential threat to biodiversity (Eigenbrod et al., 2015) and cause extensive losses to agricultural production (Mittler and Blumwald, 2010). Soybean, which is one of the important food crops, is rich in protein, vegetable oil (Sugiyama et al., 2015), and several phytochemicals, such as isoflavones and phenolic compounds (Kim et al., 2012). Because of the nutritional and pharmacological values, soybean and its products are considered with the benefits for health promoting. However, soybean growth was significantly suppressed under flooding (Khatoon et al., 2012) and drought (Mohammadi et al., 2012). Root elongation was inhibited under flooding and root diameter was reduced under drought in the early-stage soybean (Oh and Komatsu, 2015). In flooded soybean, proteomics has been utilized to uncover the stress responsive proteins, which were involved in hormonal signaling, transcriptional regulation, glycolysis, fermentation, GABA shunt, mitochondrial impairment, proteolysis, cell-wall loosening, and ROS suppression (Komatsu et al., 2015). Osmotic adaptation, ROS metabolism, secondary metabolism, and signal transduction were induced by drought in soybean (Alam et al., 2010). The current study not only enriches the knowledge of flooding and drought mechanisms, but also points out the feature between both stresses in soybean.

Stage-dependent proteomic analysis indicated that early-stage soybean is more sensitive to flooding and drought than seedling-stage plant (Chapter 1). Class II aminoacyl tRNA/biotin synthetases superfamily protein, biotin/lipoyl attachment domain containing protein, SAM synthetase family protein, B-S glucosidase 44 were in response to both stresses in root tip (Figure 40). In cytosol, Class II aminoacyl tRNA/biotin synthetases superfamily protein was increased under flooding and drought; however, biotin/lipoyl attachment domain containing protein decreased and increased under flooding and drought, respectively (Figure 40). Aminoacyl-tRNA synthetases are a family of enzymes known for their roles in protein synthesis and a variety of critical cellular activities including cellular fidelity, tRNA processing, RNA splicing, RNA

trafficking, apoptosis, and transcriptional/translational regulation (Martinis et al., 1999b). With specific interactions with amino acids, tRNAs, and universal cellular energy source of ATP, they represented the bridge between RNA and contemporary cellular milieu (Francklyn et al., 1997). Class II aminoacyl tRNA/biotin synthetases superfamily protein was also described as aspartate-tRNA ligase and mediated plant perception of β-aminobutyric acid, which provided broad-spectrum disease protection in *Arabidopsis* (Luna et al., 2014). Biotin/lipoyl attachment domain containing protein harbors multidomain, in which biotin or lipoic was attached for protein biotinylation or lipoylation (Cui et al., 2006). Biotin deficiency resulted in cell death and activation of defense signaling for abiotic stresses (Li et al., 2012a). These findings suggest that biotin synthesis might be enhanced under both stresses; however, biotinylation is likely to be suppressed or activated in flooded or drought-stressed soybean.

SAM synthetase is the key enzyme catalyzing the formation of SAM, which is the precursor of polyamines and ethylene (Guo et al., 2014). In flooded rice, ethylene accumulated and induced the gene expression of *SNORKEL1* and *SNORKEL2* to trigger internode elongation *via* gibberellin (Hattori et al., 2009). In flooded soybean, ethylene signaling played roles in plant tolerance *via* protein phosphorylation at initial-flooding stress (Yin et al., 2014b). Besides, polyamines played pivotal roles in plant defense to various types of environmental stresses (Bouchereau et al., 1999) and polyamine oxidation was related to stress response of soybean exposed to early-stage flooding and drought (Oh and Komatsu, 2015). In the present study, SAM synthetase family protein was decreased under both stresses (Figure 40). Taken together, these results indicate that decreased SAM synthetase family protein might cause soybean sensitivity to both stresses through decline in polyamine metabolism.

B-S glucosidase 44 displayed converted protein abundance in response to flooding and drought (Figure 40). Flooding is a compound stress in which the decline in molecular oxygen and thus the restriction of ATP synthesis and carbohydrate resources have major consequences for growth and survival of plants (Bailey-Serres and Voesenek, 2008). B-S glucosidase 44 is β-glucosidase-related protein, which played roles in cellulose hydrolysis by converting cellobiose to glucose (Singhania et al., 2013). On the other hand, the tricarboxylic acid cycle provided energy for plant under

drought (Bian et al., 2017). These findings suggest that B-S glucosidase 44 might play roles in glucose production to sustain energy from glycolysis in flooded soybean. However, the tricarboxylic acid cycle might be major process for energy metabolism in drought-stressed soybean.

In respect to rough ER, peptide glycosylation related proteins and folding assistants were differentially affected by flooding and drought (Figure 40). Overexpression of *At-DAD1*, which locates in the ER membrane and is the anchorage protein in the oligosaccharyltransferase complex, affected induction of DNA fragmentation by limiting or preventing ER stress (Danon et al., 2004). In *Arabidopsis*, mutant defective in *N*-glycan maturation was more sensitive to salt stress than wild-type plant; and ER oligosaccharyltransferase mutant led to growth inhibition, aberrant morphology of root tip, and callose accumulation (Kang et al., 2008). In the present study, oligosaccharyltransferases were increased under flooding, suggesting that ER might be more sensitive to flooding than drought. In addition, PDI-like proteins form and interchange disulfide bonds (Freedman et al., 1994), and HSPs/chaperones are responsible for protein refolding under stress conditions (Wang et al., 2004). In the present study, PDI-like proteins or HSPs were decreased in response to flooding or drought, suggesting the stress specific of folding assistants in the ER. These findings indicate that different response of *N*-glycan synthesis and folding assistants might be induced by flooding and drought.

In addition, ribosomal proteins, calnexin, and calmodulin-binding protein were decreased, while Ca^{2+}-transporting ATPase increased, exposed to both stresses (Figure 40). Protein synthesis and RNA regulation were associated with flooding tolerance in soybean (Yin et al., 2016). It was further reported that protein synthesis was suppressed through the decreased mRNA export/pre-ribosome biogenesis-related proteins (Yin and Komatsu, 2016). Protein synthesis was inhibited during osmotic stress (Irsigler et al., 2007), which was found in polyethylene glycol-treated and drought-stressed soybean (Mohammadi et al., 2012). Calnexin provides the cabinet for protein folding (Ou et al., 1993) and maintains calcium homeostasis, which is mediated by calmodulin-binding proteins (Harmon et al., 2000), calcineurin B-like proteins (Luan et al., 2002), and calcium-dependent protein kinases (Zhu et al., 2007), is responsible for the ER

environment. In addition, Ca^{2+}-transporting ATPase, which locates in the ER or in the plasma membrane (Thomson et al., 1993), is associated with calcium content (Bush, 1995). These findings represent the interaction between protein folding and calcium homeostasis, suggesting that maintain calcium level in the ER might facilitate protein folding in soybean under flooding and drought.

Pyruvate decarboxylase was increased and decreased under flooding and drought, respectively, in absence of chemical treatment. In addition, it responded to calcium level and its abundance was accumulated with elevated cytosolic calcium under flooding and drought (Figure 40). Proteins related to glycolysis and fermentation were induced in plant exposed to anaerobic conditions; and *pyruvate decarboxylase* was dramatically upregulated (Umeda and Uchimiya, 1994). Overexpression of *pyruvate decarboxylase* showed high enzyme activity and ethanol production, which was positively correlated with survival after flooding (Quimio et al., 2000). Although pyruvate decarboxylase was critical fermentative enzyme under flooding (Komatsu et al., 2011b), it also involved in stress signal and adaptation of plants under drought (Ranjan et al., 2012). Fast consuming of pyruvate was examined in dark-stressed plant, which was validated with enzyme activity of pyruvate decarboxylase (Nägele et al., 2014). In addition, pyruvate decarboxylase was indicated to switch energy metabolism in response to flooding and drought stresses in soybean (Chapter 3). These findings suggest that increased cytosolic calcium induces the accumulation of pyruvate decarboxylase for stress adaptation under flooding and drought. Additionally, direction of pyruvate flux to fermentation or to the tricarboxylic acid cycle might dependent on stress specificity of flooding or drought.

Genetic dissection of quantitative traits controlling abiotic-stress adaptation is effective application of genomic-based approaches to improve sustainability and stability of yield under adverse conditions (Collins et al., 2008). Single quantitative trait loci, which linked to marker Sat_064, was associated with growth improvement and grain yield for flooded soybean (vanToai et al., 2001). Molecular markers including Satt226, Sat_044, Satt205-satt489, A489H, and B031-1 were linked to quantitative trait loci for drought tolerance in soybean (Manavalan et al., 2009). These reports demonstrate the importance of application of quantitative trait loci on plant growth under different conditions. In the present study, the location of genes encoding

responsive proteins was analyzed using DAIZUbase (Tables 11 and 12; Figures 41 and 42). The location of genes forms the basis of genetic analysis for plant breeding under environmental stimuli. Under flooding, more genes located in the chromosomes 5, 10, 11, and 13. Under drought, more genes located in the chromosomes 5 and 13. These findings suggest that chromosomes 5 and 13 might harbor many quantitative trait loci for stress responses in soybean under flooding and drought.

Chromosomes 5 and 13 presented with abundant responsive genes under flooding and drought (Figures 41 and 42) such as calnexin, PDI-like proteins, HSPs, and pyruvate decarboxylase (Figure 41, number 124; Figure 42, number 68). Exposed to flooding and drought, calnexin, PDI-like proteins, and HSPs were associated with protein folding (Chapter 2); and pyruvate decarboxylase was reported as switch enzyme in energy (Chapter 3). Pyruvate decarboxylase responded to calcium level and its protein abundance was accumulated in flooded and drought-stressed soybean in presence of additional calcium (Chapter 3). Overexpression of *pyruvate decarboxylase* enhanced the survival of flooded plant (Ismond et al., 2003). Longer-root length, which is obvious effect of drought on root morphology (Oh and Komatsu, 2015), was observed in the loss-of-function mutation of *pyruvate decarboxylase 1* (Kürsteiner et al., 2003). Furthermore, cytosolic calcium was elevated in plants induced by oxygen deprivation (Subbaiah et al., 1994) and osmotic condition (Knight et al., 1997). Taken together, these findings suggest that elevating cytosolic calcium over certain threshold is potential for pyruvate carboxylase to govern the pyruvate flux into energy metabolism to confer flooding and drought in soybean.

Soybean is intolerant to flooding (Githiri et al., 2006) and drought (Deshmukh et al., 2014), which cause adverse effects to its plant growth and grain yield. However, morphological characteristics (Oh and Komatsu, 2015; Khatoon et al., 2012; Mohammadi et al., 2012) and molecular responses (Kausar et al., 2012; Hossain and Komatsu, 2014; Oh and Komatsu, 2015) differ in soybean exposed to both stresses. Energy regulation was affected by both stresses and biotin/lipoyl attachment domain containing protein displayed opposite changes in the early-stage soybean exposed to flooding and drought. Protein folding was suppressed under both stresses, while PDI-like proteins and HSPs might serve as folding assistants, respectively, with calnexin

under floodind and drought. Pyruvate decarboxylase was increased and decreased under flooding and drouhgt, respectively; and its abundance correlated with elevated cytosolic calcium. This study will be helpful to understand molecular basis of flooding and drought; and gives rise to possible-interacted mechanisms between calcium homeostasis and stress responses in soybean. Proteomic study in combination with quantitative trait loci approach will facilitate the selection of molecular marker for stress tolerance in soybean.

Table 11. List of genes encoding flooding-responsive proteins in soybean

No.	Ratio	Protein ID	Location	Description
1	De[a)]	Glyma01g05580.1	Gm01 : 5372500 - 5376619 (strand : -)	*S* adenosyl *L* methionine dependent methyltransferases superfamily protein
2	De	Glyma01g35220.2	Gm01 : 47744169 - 47746902 (strand : -)	plant VAP homolog 12
3	In	Glyma02g00550.1	Gm02 : 328488 - 333545 (strand : -)	*S* adenosyl *L* methionine dependent methyltransferases superfamily protein
4	In	Glyma02g01750.2	Gm02 : 1271084 - 1276344 (strand : +)	thioredoxin family protein
5	De	Glyma02g04980.1	Gm02 : 4030951 - 4034105 (strand : +)	RNA binding family protein
6	De	Glyma02g10790.1	Gm02 : 8679102 - 8686798 (strand : +)	protein phosphatase 2A subunit A2
7	In	Glyma02g11890.1	Gm02 : 10096333 - 10101410 (strand : -)	methyltransferase
8	De	Glyma02g13330.1	Gm02 : 11601786 - 11605281 (strand : +)	reversibly glycosylated polypeptide 3
9	In	Glyma02g43110.1	Gm02 : 47984584 - 47988358 (strand : -)	*S* adenosyl *L* methionine dependent methyltransferases superfamily protein
10	De	Glyma02g43460.1	Gm02 : 48222057 - 48226061 (strand : -)	PDI like 2,2
11	De	Glyma02g45030.1	Gm02 : 49443006 - 49447931 (strand : +)	putative mitochondrial RNA helicase 2
12	De	Glyma03g00920.1	Gm03 : 626722 - 631477 (strand : -)	NADH: cytochrome *b5* reductase 1
13	De	Glyma03g03800.1	Gm03 : 3633770 - 3638147 (strand : -)	plant VAP homolog 12
14	In	Glyma03g26090.1	Gm03 : 33434531 - 33438525 (strand : +)	RAS 5
15	In	Glyma03g33240.1	Gm03 : 40885587 - 40891963 (strand : +)	Ca^{2+}-transporting ATPase
16	De	Glyma03g33710.1	Gm03 : 41215500 - 41220643 (strand : +)	DnaJ homolog subfamily
17	De	Glyma03g37650.1	Gm03 : 44190430 - 44194864 (strand : +)	DnaJ heat shock family protein
18	In	Glyma03g39130.1	Gm03 : 45329036 - 45332552 (strand : +)	thioredoxin family protein
19	De	Glyma03g41210.1	Gm03 : 46735997 - 46737827 (strand : -)	rotamase cyclophilin 2
20	In	Glyma03g42070.3	Gm03 : 47374627 - 47378345 (strand : +)	cytochrome *b5* isoform E
21	De	Glyma03g42150.1	Gm03 : 47428796 - 47435494 (strand : -)	RNA binding family protein
22	In	Glyma04g00200.1	Gm04 : 7268 - 22892 (strand : -)	α-1,3 mannosyl glycoprotein β 1,2 *N*-acetylglucosaminyl transferase putative
23	In	Glyma04g01690.1	Gm04 : 1128740 - 1133407 (strand : -)	ribophorin I
24	In	Glyma04g04810.1	Gm04 : 3567380 - 3577561 (strand : +)	Ca^{2+}-transporting ATPase
25	In	Glyma04g33740.1	Gm04 : 39489463 - 39495115 (strand : +)	*S* adenosyl *L* methionine dependent methyltransferases superfamily protein
26	De	Glyma04g38000.1	Gm04 : 44418156 - 44421941 (strand : +)	calnexin 1
27	In	Glyma04g38190.1	Gm04 : 44589289 - 44604291 (strand : -)	phosphate deficiency response 2
28	De	Glyma04g38590.1	Gm04 : 44957860 - 44971142 (strand : +)	β-galactosidase 10
29	De	Glyma04g40090.1	Gm04 : 46218142 - 46227070 (strand : +)	nucleic acid binding OB fold like protein
30	De	Glyma04g40750.2	Gm04 : 46699533 - 46705586 (strand : +)	CTC interacting domain 11
31	De	Glyma04g40760.1	Gm04 : 46724021 - 46729598 (strand : +)	CTC interacting domain 11
32	In	Glyma04g41010.1	Gm04 : 46901418 - 46904354 (strand : -)	cytochrome *b5* isoform E
33	De	Glyma04g42690.1	Gm04 : 48376626 - 48381064 (strand : -)	PDI like 1,2
34	In	Glyma05g01010.1	Gm05 : 609594 - 611534 (strand : +)	malate dehydrogenase
35	De	Glyma05g03320.1	Gm05 : 2547518 - 2552812 (strand : -)	purple acid phosphatase 27
36	De	Glyma05g05460.1	Gm05 : 4767337 - 4771477 (strand : -)	glutamate dehydrogenase 2
37	De	Glyma05g27980.1	Gm05 : 33852909 - 33854869 (strand : +)	Rubber elongation factor protein (REF)
38	De	Glyma05g28500.1	Gm05 : 34296431 - 34303454 (strand : -)	subtilisin like serine endopeptidase family protein
39	In	Glyma05g29050.1	Gm05 : 34730528 - 34735631 (strand : +)	mitochondrial substrate carrier
40	De	Glyma05g30330.1	Gm05 : 35722786 - 35726536 (strand : +)	emp24/gp25L/p24 family/GOLD family protein
41	De	Glyma05g33330.1	Gm05 : 38028921 - 38032577 (strand : -)	calnexin 1
42	De	Glyma05g33700.1	Gm05 : 38278126 - 38280829 (strand : +)	receptor like kinase 1
43	De	Glyma05g34900.1	Gm05 : 39094615 - 39098883 (strand : +)	arginosuccinate synthase family
44	De	Glyma05g36600.1	Gm05 : 40426908 - 40430703 (strand : -)	HSP 70 protein 5
45	In	Glyma05g36620.1	Gm05 : 40443124 - 40447225 (strand : -)	HSP 70 family protein
46	De	Glyma05g38120.1	Gm05 : 41530564 - 41533554 (strand : +)	UDP D glucose/UDP D galactose 4 epimerase 1
47	In	Glyma06g00230.1	Gm06 : 24815 - 43462 (strand : +)	α-1,3 mannosyl glycoprotein β 1,2 *N*-acetylglucosaminyl transferase putative
48	In	Glyma06g01790.1	Gm06 : 1129858 - 1134208 (strand : -)	ribophorin I
49	In	Glyma06g04900.1	Gm06 : 3460618 - 3467695 (strand : +)	Ca^{2+}-transporting ATPase
50	De	Glyma06g05770.1	Gm06 : 4127859 - 4132398 (strand : +)	nitrilase/cyanide hydratase
51	In	Glyma06g12090.1	Gm06 : 9308451 - 9312386 (strand : +)	PDI like 1,2
52	De	Glyma06g14030.1	Gm06 : 11079494 - 11084221 (strand : -)	CTC interacting domain 11
53	De	Glyma06g14760.1	Gm06 : 11565183 - 11572316 (strand : -)	nucleic acid binding OB fold like protein
54	In	Glyma06g16860.1	Gm06 : 13253251 - 13268511 (strand : +)	phosphate deficiency response 2
55	De	Glyma06g17060.1	Gm06 : 13418027 - 13421764 (strand : -)	calnexin 1
56	De	Glyma07g02470.1	Gm07 : 1682404 - 1690170 (strand : +)	protein phosphatase 2C family protein
57	De	Glyma07g03220.1	Gm07 : 2263708 - 2268409 (strand : -)	inorganic H^+ pyrophosphatase family protein
58	De	Glyma07g03930.1	Gm07 : 2782652 - 2789177 (strand : +)	dihydrolipoamide acetyltransferase long form protein
59	In	Glyma07g05830.1	Gm07 : 4519394 - 4525700 (strand : -)	cytochrome *b5* isoform E
60	De	Glyma07g11310.1	Gm07 : 9498808 - 9503366 (strand : +)	B-S glucosidase 44
61	De	Glyma07g35090.1	Gm07 : 40210582 - 40221957 (strand : +)	calmodulin binding protein
62	In	Glyma07g35490.1	Gm07 : 40668330 - 40671317 (strand : -)	emp24/gp25L/p24 family/GOLD family protein
63	De	Glyma08g01480.1	Gm08 : 939512 - 942346 (strand : -)	UDP D glucose/UDP D galactose 4 epimerase 1
64	De	Glyma08g02100.1	Gm08 : 1432092 - 1438807 (strand : +)	monodehydroascorbate reductase 6

65	De	Glyma08g02940.1	Gm08 : 2029928 - 2033740 (strand : +)	HSP 70 family protein
66	De	Glyma08g04460.1	Gm08 : 3149759 - 3155385 (strand : +)	ATP dependent caseinolytic protease
67	De	Glyma08g06020.1	Gm08 : 4278474 - 4281591 (strand : -)	receptor like kinase 1
68	In	Glyma08g12200.1	Gm08 : 8865640 - 8870375 (strand : +)	mitochondrial substrate
69	De	Glyma08g23550.1	Gm08 : 17944940 - 17951613 (strand : -)	protein phosphatase 2C family protein
70	De	Glyma08g41220.3	Gm08 : 41236106 - 41240034 (strand : -)	*S* adenosyl *L* methionine dependent methyltransferases superfamily protein
71	De	Glyma08g42730.1	Gm08 : 42711059 - 42724363 (strand : +)	α/β-Hydrolases superfamily protein
72	De	Glyma08g43670.1	Gm08 : 43456275 - 43459631 (strand : +)	β-1,2 xylosyltransferase
73	In	Glyma08g43680.1	Gm08 : 43461710 - 43464771 (strand : +)	β-1,2 xylosyltransferase
74	In	Glyma08g47790.1	Gm08 : 46591084 - 46595539 (strand : -)	aldolase type TIM barrel family protein
75	De	Glyma09g04980.1	Gm09 : 3758897 - 3769175 (strand : -)	ABC transporter C family member 14-like
76	In	Glyma09g07040.1	Gm09 : 5857812 - 5860477 (strand : +)	glutaredoxin family protein
77	De	Glyma09g08120.1	Gm09 : 7185807 - 7188643 (strand : +)	subtilase family protein
78	In	Glyma09g08830.1	Gm09 : 8241631 - 8249457 (strand : +)	DnaJ/Sec63 Brl domains containing protein
79	De	Glyma09g16690.1	Gm09 : 20098535 - 20099611 (strand : +)	chaperone protein htpG family protein
80	In	Glyma09g25940.1	Gm09 : 32168675 - 32172540 (strand : +)	membrane associated progesterone binding protein 3
81	In	Glyma09g29470.1	Gm09 : 36349061 - 36355214 (strand : +)	staurosporin and temperature sensitive 3 like b
82	De	Glyma09g30910.1	Gm09 : 37693814 - 37698798 (strand : -)	B-S glucosidase 44
83	In	Glyma09g36560.1	Gm09 : 42263808 - 42266564 (strand : +)	chaperone regulator like protein
84	In	Glyma09g38410.2	Gm09 : 43780130 - 43785822 (strand : +)	calreticulin 3
85	In	Glyma10g00880.2	Gm10 : 610809 - 617509 (strand : +)	*S* adenosyl *L* methionine dependent methyltransferases superfamily protein
86	In	Glyma10g01820.1	Gm10 : 1317528 - 1323204 (strand : +)	thioredoxin family protein
87	De	Glyma10g02370.1	Gm10 : 1629329 - 1637165 (strand : -)	ABC transporter C family member 4-like
88	In	Glyma10g04370.1	Gm10 : 3364599 - 3368253 (strand : +)	*S* adenosyl *L* methionine dependent methyltransferases superfamily protein
89	De	Glyma10g15910.1	Gm10 : 18699198 - 18719524 (strand : +)	S formylglutathione hydrolase
90	De	Glyma10g24620.1	Gm10 : 32175274 - 32180564 (strand : -)	potassium channel β subunit 1
91	In	Glyma10g28880.1	Gm10 : 37780349 - 37784273 (strand : +)	inorganic H^+ pyrophosphatase family protein
92	In	Glyma10g35450.1	Gm10 : 43648036 - 43656146 (strand : +)	ribophorin I
93	De	Glyma10g35490.1	Gm10 : 43714944 - 43722164 (strand : +)	phosphoglucosamine mutase family protein
94	In	Glyma10g36170.1	Gm10 : 44352238 - 44357180 (strand : -)	PDI like 5,2
95	In	Glyma10g39750.1	Gm10 : 47377444 - 47378739 (strand : +)	oligosaccharyltransferase complex
96	De	Glyma10g42630.1	Gm10 : 49524298 - 49528280 (strand : -)	GHMP kinase family protein
97	De	Glyma10g43590.1	Gm10 : 50228552 - 50231641 (strand : +)	Ras related small GTP binding family protein
98	De	Glyma11g04650.1	Gm11 : 3182802 - 3186273 (strand : +)	peptidase M20/M25/M40 family protein
99	De	Glyma11g11410.1	Gm11 : 8132034 - 8134710 (strand : +)	subtilisin like serine protease 2
100	In	Glyma11g12800.1	Gm11 : 9149894 - 9154262 (strand : +)	dolichyl diphospho oligosaccharide protein glycosyltransferase 48kDa subunit
101	In	Glyma11g13460.1	Gm11 : 9552340 - 9559012 (strand : +)	calreticulin 3
102	In	Glyma11g14970.1	Gm11 : 10720268 - 10721423 (strand : +)	pathogenesis related thaumatin superfamily protein
103	De	Glyma11g15010.1	Gm11 : 10752370 - 10757000 (strand : +)	UDP XYL synthase 6
104	De	Glyma11g15120.1	Gm11 : 10824406 - 10828605 (strand : +)	Ras related small GTP binding family protein
105	De	Glyma11g19550.1	Gm11 : 16310166 - 16313231 (strand : -)	UDP D apiose/UDP D xylose synthase 2
106	De	Glyma11g20630.1	Gm11 : 17418671 - 17423245 (strand : +)	PDI like 1,4
107	De	Glyma11g31450.1	Gm11 : 32629475 - 32634601 (strand : -)	regulatory particle triple A ATPase 3
108	De	Glyma11g31470.1	Gm11 : 32684322 - 32688565 (strand : -)	regulatory particle triple A ATPase 3
109	In	Glyma11g34490.1	Gm11 : 36309028 - 36312310 (strand : +)	leucine-rich repeat receptor like protein kinase family protein
110	De	Glyma11g35740.1	Gm11 : 37351501 - 37358128 (strand : +)	biotin/lipoyl attachment domain containing protein
111	In	Glyma12g04950.1	Gm12 : 3287891 - 3292128 (strand : +)	dolichyl diphospho oligosaccharide protein glycosyltransferase 48kDa subunit
112	De	Glyma12g05460.4	Gm12 : 3635192 - 3641756 (strand : +)	calreticulin 3
113	De	Glyma12g06970.1	Gm12 : 4751921 - 4752781 (strand : -)	dessication induced 1VOC superfamily protein
114	De	Glyma12g07070.1	Gm12 : 4818042 - 4822153 (strand : +)	Ras related small GTP binding family protein
115	De	Glyma12g07260.1	Gm12 : 4957660 - 4961664 (strand : +)	PDI like 1,4
116	De	Glyma12g08930.1	Gm12 : 6693116 - 6695951 (strand : +)	UDP D apiose/UDP D xylose synthase 2
117	De	Glyma12g29550.1	Gm12 : 32985108 - 32989483 (strand : +)	PDI like 1,4
118	De	Glyma13g00780.1	Gm13 : 493912 - 501516 (strand : +)	galactose mutarotase like superfamily protein
119	De	Glyma13g02870.1	Gm13 : 2823368 - 2830952 (strand : -)	peptidase M20/M25/M40 family protein
120	De	Glyma13g03650.1	Gm13 : 3663883 - 3672157 (strand : +)	plant L ascorbate oxidase
121	In	Glyma13g09130.1	Gm13 : 10116237 - 10116628 (strand : +)	thioredoxin family protein
122	In	Glyma13g18630.1	Gm13 : 22300713 - 22304473 (strand : +)	*S* adenosyl *L* methionine dependent methyltransferases superfamily protein
123	De	Glyma13g23170.1	Gm13 : 26624092 - 26628887 (strand : +)	inorganic H^+ pyrophosphatase family protein
124	In	Glyma13g30490.1	Gm13 : 33109988 - 33114029 (strand : -)	pyruvate decarboxylase 2
125	De	Glyma13g32660.1	Gm13 : 34763980 - 34767201 (strand : +)	pyrophosphorylase 6
126	De	Glyma13g40130.1	Gm13 : 40681809 - 40686147 (strand : +)	PDI like 1,4
127	De	Glyma13g40350.1	Gm13 : 40852483 - 40855002 (strand : -)	PDI like 5,1
128	De	Glyma13g40870.3	Gm13 : 41317042 - 41320023 (strand : -)	RAB GTPase homolog 8A
129	De	Glyma13g42270.1	Gm13 : 42303058 - 42305143 (strand : +)	pyridoxal 5 phosphate dependent enzyme family protein
130	De	Glyma13g43430.2	Gm13 : 43121828 - 43126858 (strand : +)	PDI like 16
131	De	Glyma14g05520.1	Gm14 : 3948810 - 3952784 (strand : +)	PDI like 2,2

132	In	Glyma14g20360.1	Gm14 : 23336396 - 23337161 (strand : +)	thioredoxin family protein
133	In	Glyma14g24090.1	Gm14 : 28767127 - 28771904 (strand : -)	PDI like 1,1
134	In	Glyma15g01880.1	Gm15 : 1245193 - 1250273 (strand : -)	PDI like 1,6
135	De	Glyma15g03120.1	Gm15 : 2171866 - 2174277 (strand : -)	pyridoxal 5 phosphate dependent enzyme family protein
136	De	Glyma15g04560.2	Gm15 : 3179074 - 3182655 (strand : +)	Ras related small GTP binding family protein
137	De	Glyma15g12100.1	Gm15 : 8968913 - 8975996 (strand : +)	fumarylacetoacetase putative
138	In	Glyma15g12880.1	Gm15 : 9554380 - 9557776 (strand : +)	RAB GTPase homolog B1C
139	De	Glyma15g13620.1	Gm15 : 10209940 - 10216791 (strand : -)	glycosyl hydrolase family protein
140	De	Glyma15g15870.1	Gm15 : 12196351 - 12206082 (strand : +)	ABC transporter C family member 14-like
141	In	Glyma15g18310.1	Gm15 : 15003048 - 15005641 (strand : +)	glutaredoxin family protein
142	In	Glyma15g20400.1	Gm15 : 18260654 - 18267258 (strand : +)	DnaJ/Sec 63 Brl domains containing protein
143	De	Glyma15g21890.1	Gm15 : 20279967 - 20282605 (strand : -)	*S*-adenosylmethionine synthetase family protein
144	De	Glyma16g00590.1	Gm16 : 247496 - 254683 (strand : +)	dihydrolipoamide acetyltransferase long form protein
145	In	Glyma16g08410.1	Gm16 : 7765711 - 7774194 (strand : -)	staurosporin and temperature sensitive 3 like A
146	De	Glyma16g17500.1	Gm16 : 19007669 - 19013835 (strand : +)	*S* adenosyl *L* methionine dependent methyltransferases superfamily protein
147	De	Glyma16g23010.1	Gm16 : 26638616 - 26641814 (strand : +)	RNA binding family protein
148	De	Glyma16g27030.1	Gm16 : 31081828 - 31086763 (strand : +)	tubulin α 3
149	De	Glyma17g15740.1	Gm17 : 12459363 - 12463520 (strand : -)	glutamate dehydrogenase 2
150	De	Glyma17g16850.1	Gm17 : 13635703 - 13638881 (strand : -)	N. D.*
151	In	Glyma17g34070.1	Gm17 : 37961077 - 37965016 (strand : -)	Class II aminoacyl tRNA/biotin synthetases superfamily protein
152	De	Glyma18g07030.1	Gm18 : 5730116 - 5732839 (strand : +)	cyclophilin 5
153	In	Glyma18g09480.1	Gm18 : 8374020 - 8378571 (strand : -)	β-1,2 xylosyltransferase
154	De	Glyma18g12920.1	Gm18 : 12333170 - 12343800 (strand : +)	HIS HF
155	De	Glyma18g45500.1	Gm18 : 55246255 - 55246808 (strand : -)	PDI like 1,2
156	De	Glyma18g52450.1	Gm18 : 61052857 - 61057770 (strand : -)	Ras related small GTP binding family protein
157	De	Glyma18g52860.1	Gm18 : 61306195 - 61309857 (strand : -)	O Glycosyl hydrolases family 17 protein
158	In	Glyma18g53700.1	Gm18 : 61964545 - 61968719 (strand : +)	aldolase type TIM barrel family protein
159	In	Glyma19g29720.1	Gm19 : 37451136 - 37455763 (strand : +)	NADH: cytochrome *b5* reductase 1
160	De	Glyma19g33140.1	Gm19 : 40772865 - 40774370 (strand : -)	ahal domain containing protein
161	In	Glyma19g34890.1	Gm19 : 42485179 - 42490482 (strand : +)	*S* adenosyl *L* methionine dependent methyltransferases superfamily protein
162	In	Glyma19g35960.1	Gm19 : 43384216 - 43390334 (strand : +)	Ca^{2+} transporting ATPase
163	De	Glyma19g39710.1	Gm19 : 46301684 - 46304736 (strand : +)	amino acid dehydrogenase family protein
164	De	Glyma19g40810.1	Gm19 : 47126385 - 47129171 (strand : +)	*S*-adenosylmethionine synthetase 2
165	In	Glyma19g41690.1	Gm19 : 47898502 - 47902440 (strand : +)	thioredoxin family protein
166	In	Glyma19g44780.1	Gm19 : 50096715 - 50101693 (strand : +)	cytochrome *b5* isoform E
167	De	Glyma19g44860.1	Gm19 : 50167251 - 50174260 (strand : -)	RNA binding family protein
168	De	Glyma20g01220.1	Gm20 : 833962 - 839151 (strand : +)	oxidoreductases acting on the aldehyde
169	In	Glyma20g03930.1	Gm20 : 3862190 - 3865257 (strand : -)	emp24/gp25L/p24 family/GOLD family protein
170	De	Glyma20g12150.1	Gm20 : 17069690 - 17077611 (strand : +)	plant *L* ascorbate oxidase
171	De	Glyma20g19000.1	Gm20 : 26702308 - 26707310 (strand : -)	potassium channel β-subunit 1
172	De	Glyma20g23080.1	Gm20 : 33012502 - 33015990 (strand : +)	calreticulin 1b
173	In	Glyma20g27980.1	Gm20 : 36953778 - 36956758 (strand : -)	oligosaccharyltransferase complex
174	In	Glyma20g29660.1	Gm20 : 38514463 - 38517385 (strand : -)	membrane steroid binding protein1
175	De	Glyma20g32030.1	Gm20 : 40646909 - 40654749 (strand : -)	phosphoglucosamine mutase family protein
176	De	Glyma20g32320.1	Gm20 : 40930276 - 40936570 (strand : +)	Ras related small GTP binding family protein

a), Increased (In) and decreased (De) protein abundance in flooded plant was compared to 2-day-old untreated soybean; Protein ID, according to Phytozome soybean genome database; Location, location was analyzed using DAIZUbase.

Table 12. List of genes encoding drought-responsive proteins in soybean

No.	Ratio	Protein ID[a)]	Location	Description
1	De[b)]	Glyma01g35220.2	Gm01 : 47744169 - 47746902 (strand : -)	early responsive dehydration stress protein
2	De	Glyma02g04980.1	Gm02 : 4030951 - 4034105 (strand : +)	RNA binding family protein
3	De	Glyma02g10790.1	Gm02 : 8679102 - 8686798 (strand : +)	protein phosphatase 2A subunit A2
4	De	Glyma02g13330.1	Gm02 : 11601786 - 11605281 (strand : +)	reversibly glycosylated polypeptide 3
5	De	Glyma02g45030.1	Gm02 : 49443006 - 49447931 (strand : +)	putative mitochondrial RNA helicase 2
6	De	Glyma03g03800.1	Gm03 : 3633770 - 3638147 (strand : -)	plant VAP homolog 12
7	In	Glyma03g33240.1	Gm03 : 40885587 - 40891963 (strand : +)	Ca^{2+}-transporting ATPase
8	De	Glyma03g37650.1	Gm03 : 44190430 - 44194864 (strand : +)	DnaJ heat shock family protein
9	De	Glyma03g41210.1	Gm03 : 46735997 - 46737827 (strand : -)	rotamase cyclophilin 2
10	In	Glyma03g42070.3	Gm03 : 47374627 - 47378345 (strand : +)	cytochrome *b5* isoform E
11	De	Glyma03g42150.1	Gm03 : 47428796 - 47435494 (strand : -)	RNA binding family protein
12	De	Glyma04g38000.1	Gm04 : 44418156 - 44421941 (strand : +)	calnexin 1
13	De	Glyma04g38590.1	Gm04 : 44957860 - 44971142 (strand : +)	β-galactosidase 10
14	De	Glyma04g40090.1	Gm04 : 46218142 - 46227070 (strand : +)	nucleic acid binding OB fold like protein
15	De	Glyma04g40750.2	Gm04 : 46699533 - 46705586 (strand : +)	CTC interacting domain 11
16	De	Glyma04g40760.1	Gm04 : 46724021 - 46729598 (strand : +)	CTC interacting domain 11
17	De	Glyma04g42690.1	Gm04 : 48376626 - 48381064 (strand : -)	PDI like 1,2
18	In	Glyma05g01010.1	Gm05 : 609594 - 611534 (strand : +)	malate dehydrogenase
19	De	Glyma05g03320.1	Gm05 : 2547518 - 2552812 (strand : -)	purple acid phosphatase 27
20	De	Glyma05g05460.1	Gm05 : 4767337 - 4771477 (strand : -)	glutamate dehydrogenase 2
21	De	Glyma05g27980.1	Gm05 : 33852909 - 33854869 (strand : +)	Rubber elongation factor protein (REF)
22	De	Glyma05g28500.1	Gm05 : 34296431 - 34303454 (strand : -)	subtilisin like serine endopeptidase family protein
23	In	Glyma05g29050.1	Gm05 : 34730528 - 34735631 (strand : +)	mitochondrial substrate carrier
24	De	Glyma05g34900.1	Gm05 : 39094615 - 39098883 (strand : +)	arginosuccinate synthase family
25	De	Glyma05g36600.1	Gm05 : 40426908 - 40430703 (strand : -)	HSP 70 protein 5
26	De	Glyma05g36620.1	Gm05 : 40443124 - 40447225 (strand : -)	HSP 70 family protein
27	De	Glyma05g38120.1	Gm05 : 41530564 - 41533554 (strand : +)	UDP D glucose/UDP D galactose 4 epimerase 1
28	De	Glyma06g05770.1	Gm06 : 4127859 - 4132398 (strand : +)	nitrilase/cyanide hydratase
29	De	Glyma06g14030.1	Gm06 : 11079494 - 11084221 (strand : -)	CTC interacting domain 11
30	De	Glyma06g14760.1	Gm06 : 11565183 - 11572316 (strand : -)	nucleic acid binding OB fold like protein
31	De	Glyma06g17060.1	Gm06 : 13418027 - 13421764 (strand : -)	calnexin 1
32	De	Glyma07g02470.1	Gm07 : 1682404 - 1690170 (strand : +)	protein phosphatase 2C family protein
33	De	Glyma07g03930.1	Gm07 : 2782652 - 2789177 (strand : +)	dihydrolipoamide acetyltransferase long form protein
34	De	Glyma07g11310.1	Gm07 : 9498808 - 9503366 (strand : +)	B-S glucosidase 44
35	De	Glyma08g01480.1	Gm08 : 939512 - 942346 (strand : -)	UDP D glucose/UDP D galactose 4 epimerase 1
36	De	Glyma08g02100.1	Gm08 : 1432092 - 1438807 (strand : +)	monodehydroascorbate reductase 6
37	De	Glyma08g04460.1	Gm08 : 3149759 - 3155385 (strand : +)	ATP dependent caseinolytic protease
38	In	Glyma08g12200.1	Gm08 : 8865640 - 8870375 (strand : +)	mitochondrial substrate
39	De	Glyma08g23550.1	Gm08 : 17944940 - 17951613 (strand : -)	protein phosphatase 2C family protein
40	De	Glyma08g42730.1	Gm08 : 42711059 - 42724363 (strand : +)	α/β-Hydrolases superfamily protein
41	In	Glyma08g47790.1	Gm08 : 46591084 - 46595539 (strand : -)	aldolase type TIM barrel family protein
42	De	Glyma09g08120.1	Gm09 : 7185807 - 7188643 (strand : +)	subtilase family protein
43	De	Glyma09g30910.1	Gm09 : 37693814 - 37698798 (strand : -)	B-S glucosidase 44
44	De	Glyma09g37860.1	Gm09 : 43388629 - 43392321 (strand : -)	RAS 5
45	De	Glyma10g15910.1	Gm10 : 18699198 - 18719524 (strand : +)	S formylglutathione hydrolase
46	De	Glyma10g24620.1	Gm10 : 32175274 - 32180564 (strand : -)	potassium channel β subunit 1
47	De	Glyma10g35230.1	Gm10 : 43422479 - 43430194 (strand : -)	Ras related small GTP binding family protein
48	De	Glyma10g35490.1	Gm10 : 43714944 - 43722164 (strand : +)	phosphoglucosamine mutase family protein
49	De	Glyma10g42630.1	Gm10 : 49524298 - 49528280 (strand : -)	GHMP kinase family protein
50	De	Glyma10g43590.1	Gm10 : 50228552 - 50231641 (strand : +)	Ras related small GTP binding family protein
51	De	Glyma11g04650.1	Gm11 : 3182802 - 3186273 (strand : +)	peptidase M20/M25/M40 family protein
52	De	Glyma11g11410.1	Gm11 : 8132034 - 8134710 (strand : +)	subtilisin like serine protease 2
53	De	Glyma11g11460.1	Gm11 : 8165996 - 8170401 (strand : -)	ascorbate peroxidase 3
54	De	Glyma11g15010.1	Gm11 : 10752370 - 10757000 (strand : +)	UDP XYL synthase 6
55	De	Glyma11g15120.1	Gm11 : 10824406 - 10828605 (strand : +)	Ras related small GTP binding family protein
56	De	Glyma11g19550.1	Gm11 : 16310166 - 16313231 (strand : -)	UDP D apiose/UDP D xylose synthase 2
57	De	Glyma11g31450.1	Gm11 : 32629475 - 32634601 (strand : -)	regulatory particle triple A ATPase 3
58	De	Glyma11g31470.1	Gm11 : 32684322 - 32688565 (strand : -)	regulatory particle triple A ATPase 3
59	In	Glyma11g35740.1	Gm11 : 37351501 - 37358128 (strand : +)	biotin/lipoyl attachment domain containing protein
60	De	Glyma12g06970.1	Gm12 : 4751921 - 4752781 (strand : -)	dessication induced 1VOC superfamily protein
61	De	Glyma12g07070.1	Gm12 : 4818042 - 4822153 (strand : +)	Ras related small GTP binding family protein
62	De	Glyma12g08930.1	Gm12 : 6693116 - 6695951 (strand : +)	UDP D apiose/UDP D xylose synthase 2
63	De	Glyma13g00780.1	Gm13 : 493912 - 501516 (strand : +)	galactose mutarotase like superfamily protein
64	De	Glyma13g02870.1	Gm13 : 2823368 - 2830952 (strand : -)	peptidase M20/M25/M40 family protein
65	In	Glyma13g03650.1	Gm13 : 3663883 - 3672157 (strand : +)	plant L ascorbate oxidase
66	De	Glyma13g10700.1	Gm13 : 12773297 - 12782079 (strand : +)	heat shock protein 70 (Hsp70) family protein
67	In	Glyma13g23170.1	Gm13 : 26624092 - 26628887 (strand : +)	inorganic H^+ pyrophosphatase family protein
68	De	Glyma13g30490.1	Gm13 : 33109988 - 33114029 (strand : -)	pyruvate decarboxylase 2
69	In	Glyma13g32660.1	Gm13 : 34763980 - 34767201 (strand : +)	pyrophosphorylase 6
70	De	Glyma13g40870.3	Gm13 : 41317042 - 41320023 (strand : -)	RAB GTPase homolog 8A

71	De	Glyma13g42270.1	Gm13 : 42303058 - 42305143 (strand : +)	pyridoxal 5 phosphate dependent enzyme family protein
72	De	Glyma13g43430.2	Gm13 : 43121828 - 43126858 (strand : +)	PDI like 16
73	De	Glyma15g03120.1	Gm15 : 2171866 - 2174277 (strand : -)	pyridoxal 5 phosphate dependent enzyme family protein
74	De	Glyma15g04560.2	Gm15 : 3179074 - 3182655 (strand : +)	Ras related small GTP binding family protein
75	De	Glyma15g12100.1	Gm15 : 8968913 - 8975996 (strand : +)	fumarylacetoacetase putative
76	De	Glyma15g13620.1	Gm15 : 10209940 - 10216791 (strand : -)	glycosyl hydrolase family protein
77	In	Glyma15g21890.1	Gm15 : 20279967 - 20282605 (strand : -)	*S*-adenosylmethionine synthetase family protein
78	De	Glyma16g00590.1	Gm16 : 247496 - 254683 (strand : +)	dihydrolipoamide acetyltransferase long form protein
79	De	Glyma16g23010.1	Gm16 : 26638616 - 26641814 (strand : +)	RNA binding family protein
80	De	Glyma16g27030.1	Gm16 : 31081828 - 31086763 (strand : +)	tubulin α 3
81	De	Glyma17g15740.1	Gm17 : 12459363 - 12463520 (strand : -)	glutamate dehydrogenase 2
82	De	Glyma17g16850.1	Gm17 : 13635703 - 13638881 (strand : -)	N. D.*
83	In	Glyma17g34070.1	Gm17 : 37961077 - 37965016 (strand : -)	Class II aminoacyl tRNA/biotin synthetases superfamily protein
84	De	Glyma18g07030.1	Gm18 : 5730116 - 5732839 (strand : +)	cyclophilin 5
85	De	Glyma18g12920.1	Gm18 : 12333170 - 12343800 (strand : +)	HIS HF
86	De	Glyma18g52450.1	Gm18 : 61052857 - 61057770 (strand : -)	Ras related small GTP binding family protein
87	De	Glyma18g52860.1	Gm18 : 61306195 - 61309857 (strand : -)	O Glycosyl hydrolases family 17 protein
88	In	Glyma18g53700.1	Gm18 : 61964545 - 61968719 (strand : +)	aldolase type TIM barrel family protein
89	De	Glyma19g33140.1	Gm19 : 40772865 - 40774370 (strand : -)	ahal domain containing protein
90	In	Glyma19g35960.1	Gm19 : 43384216 - 43390334 (strand : +)	Ca^{2+} transporting ATPase
91	De	Glyma19g39710.1	Gm19 : 46301684 - 46304736 (strand : +)	amino acid dehydrogenase family protein
92	De	Glyma19g40810.1	Gm19 : 47126385 - 47129171 (strand : +)	*S*-adenosylmethionine synthetase 2
93	In	Glyma19g44780.1	Gm19 : 50096715 - 50101693 (strand : +)	cytochrome *b5* isoform E
94	De	Glyma19g44860.1	Gm19 : 50167251 - 50174260 (strand : -)	RNA binding family protein
95	De	Glyma20g01220.1	Gm20 : 833962 - 839151 (strand : +)	oxidoreductases acting on the aldehyde
96	In	Glyma20g12150.1	Gm20 : 17069690 - 17077611 (strand : +)	plant *L* ascorbate oxidase
97	De	Glyma20g16070.1	Gm20 : 22168983 - 22178286 (strand : -)	heat shock protein 70 (Hsp70) family protein
98	De	Glyma20g19000.1	Gm20 : 26702308 - 26707310 (strand : -)	potassium channel β-subunit 1
99	De	Glyma20g32030.1	Gm20 : 40646909 - 40654749 (strand : -)	phosphoglucosamine mutase family protein
100	De	Glyma20g32320.1	Gm20 : 40930276 - 40936570 (strand : +)	Ras related small GTP binding family protein

a), Increased (In) and decreased (De) protein abundance in drought-stressed plant was compared to 2-day-old untreated soybean; Protein ID, according to Phytozome soybean genome database; Location, location was analyzed using DAIZUbase.

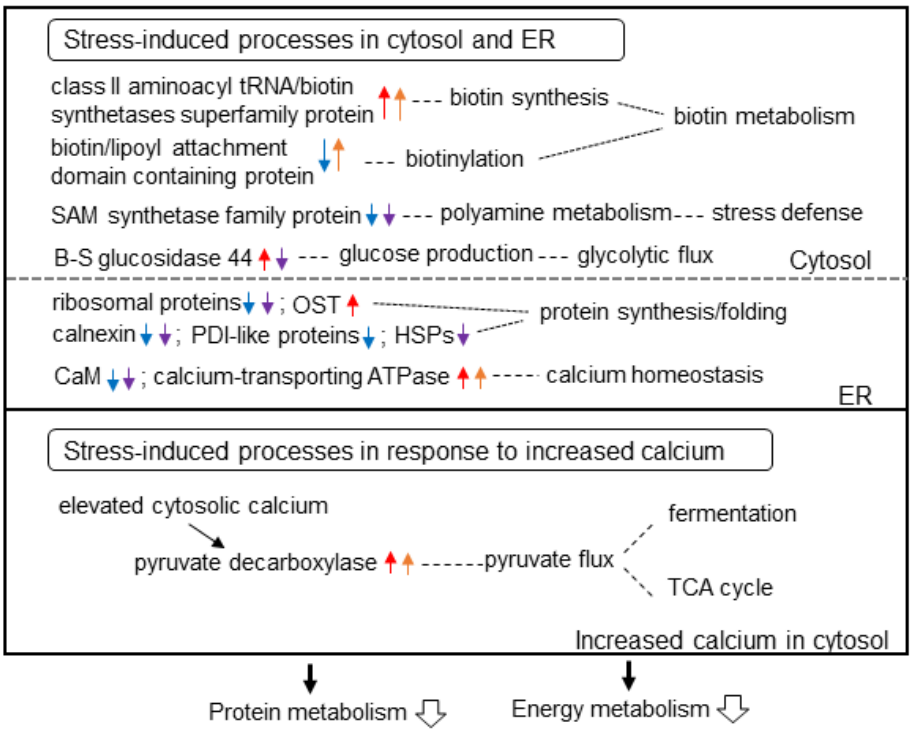

Figure 40. Schematic representation of stress-induced processes and events in response to calcium in soybean under flooding and drought. The red and blue arrows indicate changes of protein abundance under flooding; orange and purple arrows indicate changes of protein abundance under drought; and upward and downward arrows indicate increased and decreased changes of protein abundance, respectively. The abundance of protein induced by stresses in cytosol and the ER was compared to untreated soybean without stresses. The abundance of protein in response to additional calcium was compared to stressed plant without reagent application. Abbreviations are as follows: OST, oligosaccharyltransferase; CaM, calmodulin-binding protein; TCA, tricarboxylic acid.

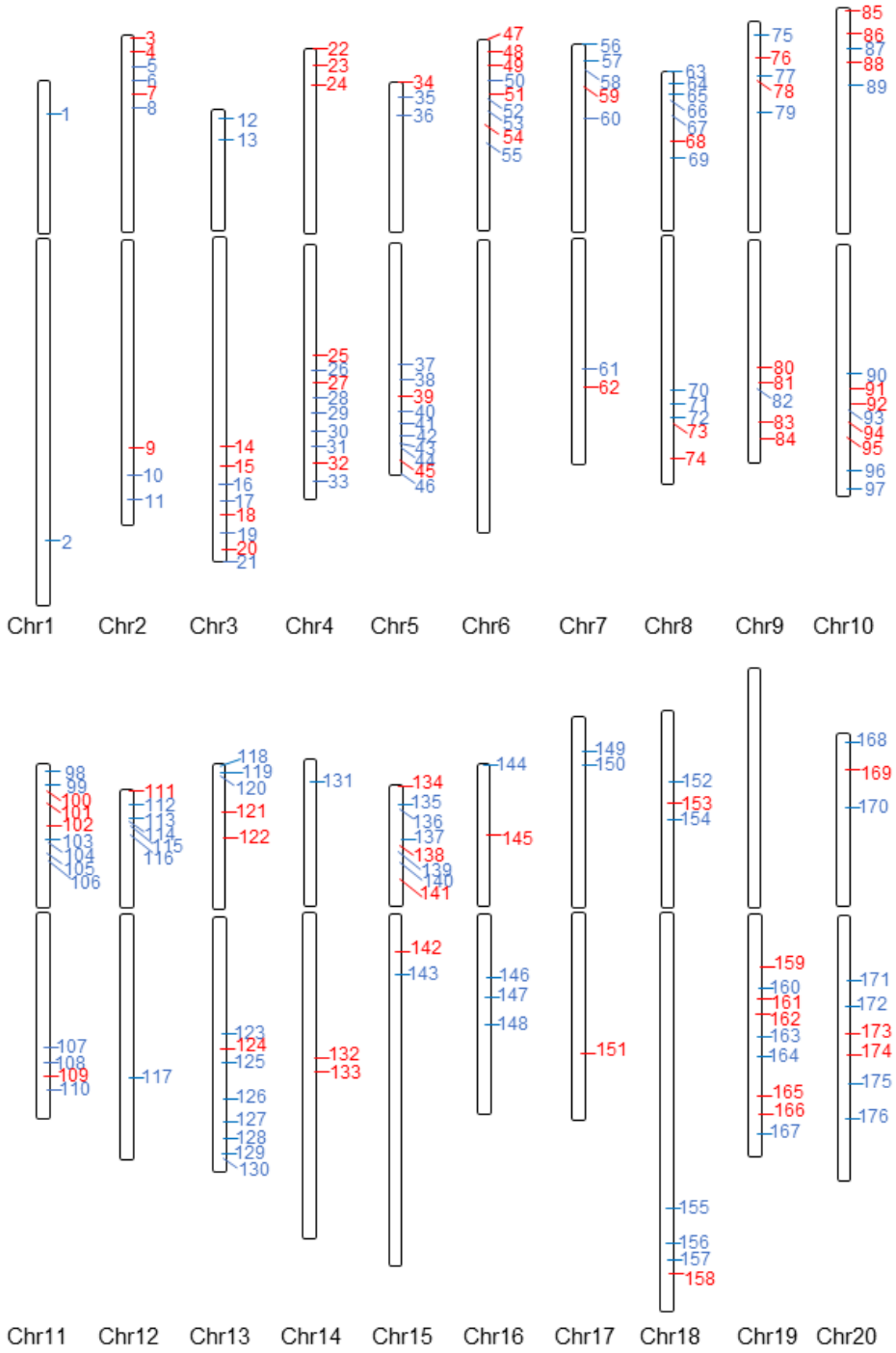

Figure 41. Location of genes encoding flooding-responsive proteins in soybean. The location of genes encoding flooding-responsive proteins was conducted using DAIZUbase (http://daizu.dna.affrc.go.jp/) based on the identified Protein ID. Red and blue colors indicate increased and decreased protein abundance, respectively, in flooded plant, compared to 2-day-old untreated soybean. The information of genes encoding flooding-responsive proteins was listed in Table 11.

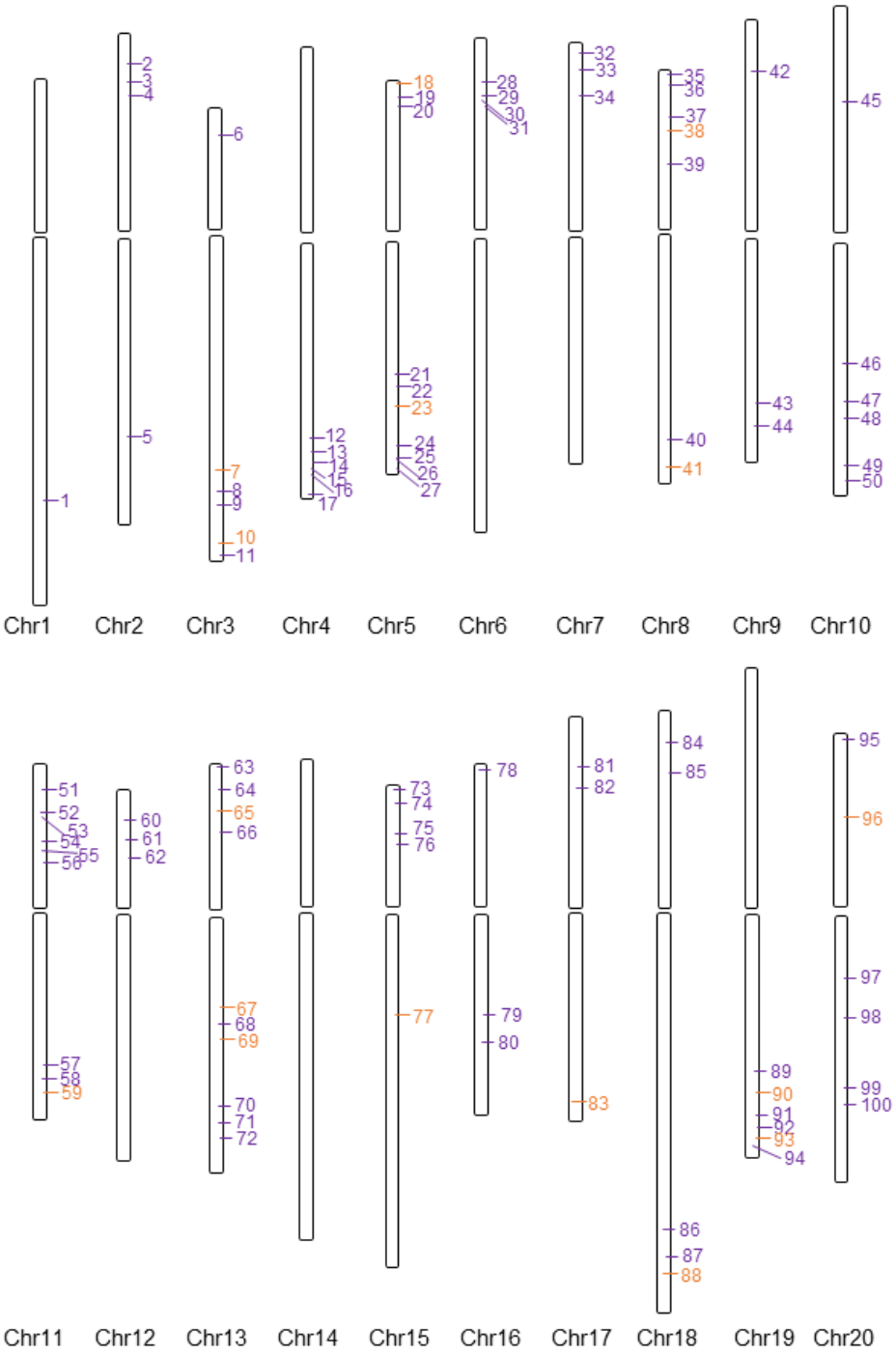

Figure 42. Location of genes encoding drought-responsive proteins in soybean. The location of genes encoding drought-responsive proteins was conducted using DAIZUbase (http://daizu.dna.affrc.go.jp/) based on the identified Protein ID. Orange and purple colors indicate increased and decreased protein abundance, respectively, in drought-stressed plant, compared to 2-day-old untreated soybean. The information of genes encoding drought-responsive proteins was listed in Table 12.

SUMMARY

Global climate changes influence the magnitude and frequency of hydrological fluctuations and cause unfavorable environment for plant growth and development. Soybean is the important crop with high abundant of protein, vegetable oil, and several phytochemicals. With the predominate values, soybean is cultivated with a long history, while it is sensitive to flooding and drought, which lead to deleterious effects on plant growth. Root growth was suppressed under flooding and drought, while the parameters of root elongation and root diameter differed between two conditions. To unveil the responsive mechanisms of soybean under flooding and drought, proteins were analyzed using the gel-free/label-free proteomic technique.

To obtain the sensitive organ towards flooding and drought at different developmental stages, the organ-specific and stage-dependent proteomic analyses were performed. Root tip, which is the first organ to sense stress conditions, was the most sensitive organ affected by flooding and drought in the early-stage soybean because more proteins were induced by both stresses compared to other organs. Fermentation and protein synthesis/degradation were major functional categories induced by flooding and drought in the root tip. Class II aminoacyl tRNA/biotin synthetases superfamily protein was increased under both stresses; however, biotin/lipoyl attachment domain containing protein was decreased and increased under flooding and drought, respectively. Moreover, β-amylase 5 was increased in the leaf of soybean seedling under both stresses. These results indicate that biotin and biotinylation might be involved in energy metabolism in soybean exposed to both stresses, while biotin metabolism such as biotinylation might be differently triggered in respect to flooding and drought.

To investigate the mechanisms in response to flooding and drought, which cause accumulation of misfolded or unfolded proteins, the ER proteomic analysis was performed. Ribosomal proteins were mainly decreased under both stresses, while oligosaccharyltransferases increased under flooding. As the protein-folding machinery, calnexin was decreased under both stresses, while PDI-like proteins or HSPs served as the major folding assistants for flooding or drought, respectively. The accumulation of glycoproteins was reduced; however, cytosolic calcium was increased under both

stresses. These results indicate that reduced accumulation of glycoproteins under both stresses might be due to dysfunction of protein folding. Furthermore, increased cytosolic calcium induced by both stresses might disturb the ER environment for proper folding.

To understand the mechanisms in response to calcium in the ER and cytosol of soybean under flooding and drought, the proteomic analysis was further conducted. With the application of chemicals, which inhibited the elevation of cytosolic calcium under both stresses, calnexin, PDI-like proteins, HSPs, and thioredoxin family proteins were abundant ER proteins. HCP-like superfamily protein was in response to calcium level and its gene expression was upregulated under both stresses. Besides, cellular metabolisms including glycolysis, fermentation, the tricarboxylic acid cycle, and amino acid metabolism were altered by calcium level under both stresses. Protein abundance and enzyme activity of pyruvate decarboxylase were increased or decreased under flooding or drought, respectively. In addition, pyruvate decarboxylase was increased in response to elevated cytosolic calcium. These results indicate that proteins in the ER are altered by the calcium level and pyruvate decarboxylase might be the key enzyme in response to calcium under both stresses.

Taken together, these findings suggest that biotin and biotinylation might participate in energy regulation under flooding and drought in the early-stage soybean. Calnexin together with PDI-like proteins or HSPs is responsive for proper folding of glycoproteins in the ER under flooding or drought. Moreover, calcium homeostasis is related to protein folding and ER-associated degradation, and calcium alters pyruvate decarboxylase in energy regulation of soybean under flooding and drought.

ACKNOWLEDGMENTS

I owe my specific thanks and gratitude to Prof. Hiroshi Matsumoto, in Graduate School of Life and Environmental Science at the University of Tsukuba, for his valuable corrections and suggestions for this manuscript.

I would like to express my deepest appreciation to my supervisor, Prof. Setsuko Komatsu, in Graduate School of Life and Environmental Science at the University of Tsukuba and in the National Institute of Crop Science at National Agriculture and Food Research Organization, for her patient guidance, criticisms, and suggestions through my research work.

I would like to express my gratitude to Prof. Toshiyuki Tanaka, in Graduate School of Life and Environmental Science at the University of Tsukuba, for his valuable comments for this manuscript. I also thank to Dr. Yukari Sunohara, in Graduate School of Life and Environmental Science at the University of Tsukuba, for her worthy suggestions to improve this manuscript.

I would like to convey my cordial thanks to Prof. Katsumi Sakata, in the Department of Life Sciences and Informatics at Maebashi Institute of Technology, for his help in bioinformatic data analysis in this manuscript.

I wish my special thanks to Dr. Yohei Nanjo for his great help and support for mass spectrometry analysis during my experiment in the National Institute of Crop Science. I would like to express my gratitude to Dr. Susumu Hiraga, Dr. Keito Nishizawa, and Dr. Akiko Hashiguchi for their valuable comments and advices in the seminar.

I appreciate Dr. Myeongwon Oh for her collaboration in this manuscript and thank to my colleagues Dr. Mudassar Nawaz Khan, Dr. Xiaojian Yin, and Dr. Ghazala Mustafa for their cheerful discussions.

I gratefully acknowledge the China Scholarship Council for supporting my Ph. D study in Japan and National Institute of Crop Science for providing me all the facilities to complete the research.

REFERENCES

Acevedo, R. M., Maiale, S. J., Pessino, S. C., Bottini, R., Ruiz, O. A., Sansberro, P. A. (2013) A succinate dehydrogenase flavoprotein subunit-like transcript is upregulated in *Ilex paraguariensis* leaves in response to water deficit and abscisic acid. Plant Physiology and Biochemistry 65, 48-54.

Agrawal, L., Gupta, S., Mishra, S. K., Pandey, G., Kumar, S., Chauhan, P. S., Chakrabarty, D., Nautiyal, C. S. (2016) Elucidation of complex nature of PEG induced drought-stress response in rice root using comparative proteomics approach. Frontiers in Plant Science 7, 1466

Ahsan, N., Lee, D. G., Lee, S. H., Kang, K. Y., Bahk, J. D., Choi, M. S., Lee, I. J., Renaut, J., Lee, B. H. (2007). A comparative proteomic analysis of tomato leaves in response to waterlogging stress. Physiologia Plantarum 131, 555-570.

Alam, I., Sharmin, S. A., Kim, K. H., Yang, J. K., Choi, M. S., Lee, B. H. (2010) Proteome analysis of soybean roots subjected to short-term drought stress. Plant and Soil 333, 491-505.

Ali, G. M., Komatsu, S. (2006) Proteomic analysis of rice leaf sheath during drought stress. Journal of Proteome Research 5, 396-403.

Alvarez, S., Marsh, E. L., Schroeder, S. G., Schachtman, D. P. (2008) Metabolomic and proteomic changes in the xylem sap of maize under drought. Plant Cell and Environment 31, 325-340.

Ambavaram, M. M., Basu, S., Krishnan, A., Ramegowda, V., Batlang, U., Rahman, L., Baisakh, N., Pereira, A. (2014). Coordinated regulation of photosynthesis in rice increases yield and tolerance to environmental stress. Nature Communications 5, 5302.

Anoop, V. M., Basu, U., McCammon, M. T., McAlister-Henn, L., Taylor, G. J. (2003) Modulation of citrate metabolism alters aluminum tolerance in yeast and transgenic canola overexpressing a mitochondrial citrate synthase. Plant Physiology 132, 2205-2217.

Araújo, W. L., Nunes-Nesi, A., Osorio, S., Usadel, B., Fuentes, D., Nagy, R., Balbo, I., Lehmann, M., Studart-Witkowski, C., Tohge, T., Martinoia, E. (2011) Antisense

inhibition of the iron-sulphur subunit of succinate dehydrogenase enhances photosynthesis and growth in tomato *via* an organic acid-mediated effect on stomatal aperture. Plant Cell 23, 600-627.

Armstrong, W. (1979) Aeration in higher plants. In: Woolhouse, H. W. W. (Ed.). Advances in Botanical Research, Academic Press, London, UK, pp. 225-332.

Asensi-Fabado, M. A., Munné-Bosch, S. (2010) Vitamins in plants: occurrence, biosynthesis and antioxidant function. Trends in Plant Science 15, 582-592.

Bacanamwo, M., Purcell, L. C. (1999) Soybean root morphological and anatomical traits associated with acclimation to flooding. Crop Science 39, 143-149.

Bailey-Serres, J., Lee, S. C., Brinton, E. (2012) Waterproofing crops: effective flooding survival strategies. Plant Physiology 160, 1698-1709.

Bailey-Serres, J., Voesenek, L. A. (2008) Flooding stress: acclimations and genetic diversity. Annual Review of Plant Biology 59, 313-339.

Bailey-Serres, J., Voesenek, L. A. (2010) Life in the balance: a signaling network controlling survival of flooding. Current Opinion in Plant Biology 13, 489-494.

Bakker, H., Lommen, A., Jordi, W., Stiekema, W., Bosch, D. (1999) An *Arabidopsis thaliana* cDNA complements the N-acetylglucosaminyltransferase I deficiency of CHO Lec1 cells. Biochemical and Biophysical Research Communications 261, 829-832.

Bao, C., Wang, J., Zhang, R., Zhang, B., Zhang, H., Zhou, Y., Huang S. (2012) *Arabidopsis* VILLIN2 and VILLIN3 act redundantly in sclerenchyma development *via* bundling of actin filaments. Plant Journal 71, 962-975.

Bergeron, J. J., Brenner, M. B., Thomas, D. Y., Williams, D. B. (1994) Calnexin: a membrane-bound chaperone of the endoplasmic reticulum. Trends in Biochemical Sciences 19, 124-128.

Bertolde, F. Z., Almeida, A. A., Pirovani, C. P. (2014) Analysis of gene expression and proteomic profiles of clonal genotypes from *Theobroma cacao* subjected to soil flooding. PLoS One 9, e108705.

Bian, Y., Deng, X., Yan, X., Zhou, J., Yuan, L., Yan, Y. (2017) Integrated proteomic analysis of *Brachypodium distachyon* roots and leaves reveals a synergistic network in the response to drought stress and recovery. Scientific Reports 7, 46183.

Blum, T., Briesemeister, S., Kohlbacher, O. (2009) MultiLoc2: integrating phylogeny and Gene Ontology terms improves subcellular protein localization prediction. BMC Bioinformatics 10, 274.

Bouchereau, A., Aziz, A., Larher, F., Martin-Tanguy, J. (1999) Polyamines and environmental challenges: recent development. Plant Science 140, 103-125.

Boyer, J. S. (1982) Plant productivity and environment. Science 218, 443-448.

Bradford, M. M. (1976) A rapid and sensitive method for the quantitation of microgram quantities of protein utilizing the principle of protein-dye binding. Analytical Biochemistry 72, 248-254.

Brosch, M., Yu, L., Hubbard, T., Choudhary, J. (2009) Accurate and sensitive peptide identification with mascot percolator. Journal of Proteome Research 8, 3176-3181.

Burgoyne, T., Patel, S., Eden, E. R. (2015) Calcium signaling at ER membrane contact sites. Biochimica et Biophysica Acta Molecular Cell Research 1853, 2012-2017.

Bush, D. S. (1995) Calcium regulation in plant cells and its role in signaling. Annual Review of Plant Biology 46, 95-122.

Byrne, M. E. (2009) A role for the ribosome in development. Trends in Plant Science 14, 512-519.

Cairns, J. R., Mahong, B., Baiya, S., Jeon, J. S. (2015) β-Glucosidases: Multitasking, moonlighting or simply misunderstood? Plant Science 241, 246-259.

Carafoli, E. (1991) The calcium pumping ATPase of the plasma membrane. Annual Review of Physiology 53, 531-547.

Causier, B., Ashworth, M., Guo, W., Davies, B. (2012a) The TOPLESS interactome: a framework for gene repression in *Arabidopsis*. Plant Physiology 158, 423-438.

Causier, B., Lloyd, J., Stevens, L., Davies, B. (2012b) TOPLESS co-repressor interactions and their evolutionary conservation in plants. Plant Signaling and Behavior 7, 325-328.

Chang, J., Clay, J. M., Chang, C. (2014) Association of cytochrome *b5* with ETR1 ethylene receptor signaling through RTE1 in *Arabidopsis*. Plant Journal 77, 558-567.

Chen, Q., Zhong, Y., Wu, Y., Liu, L., Wang, P., Liu, R., Cui, F., Li, Q., Yang, X., Fang, S., Xie, Q. (2016) HRD1-mediated ERAD tuning of ER-bound E2 is conserved

between plants and mammals. Nature Plants 2, 16094.

Chen, Y., Chen, X., Wang, H., Bao, Y., Zhang, W. (2014) Examination of the leaf proteome during flooding stress and the induction of programmed cell death in maize. Proteome Science 12, 33.

Cheng, W., Zhang, L., Jiao, C., Su, M., Yang, T., Zhou, L., Peng, R., Wang, R., Wang, C. (2013) Hydrogen sulfide alleviates hypoxia-induced root tip death in *Pisum sativum.* Plant Physiology and Biochemical 70, 278-286.

Choat, B., Jansen, S., Brodribb, T. J., Cochard, H., Delzon, S., Bhaskar, R., Bucci, S. J., Feild, T. S., Gleason, S. M., Hacke, U. G., Jacobsen, A. L. (2012) Global convergence in the vulnerability of forests to drought. Nature 491, 752-755.

Chung, W. S., Lee, S. H., Kim, J. C., Heo, W. D., Kim, M. C., Park, C. Y., Park, H. C., Lim, C. O., Kim, W. B., Harper, J. F., Cho, M. J. (2000) Identification of a calmodulin-regulated soybean Ca^{2+}-ATPase (SCA1) that is located in the plasma membrane. Plant Cell 12, 1393-1407.

Collins, N. C., Tardieu, F., Tuberosa, R. (2008) Quantitative trait loci and crop performance under abiotic stress: where do we stand? Plant Physiology 147, 469-486.

Collot, M., Kalff, M., Remacle, J. (1982) Relationship between endoplasmic reticulum and Golgi membranes; evidence for a heterogeneous localization of cytochrome *b5* in the Golgi membranes. European Journal of Cell Biology 29, 34-42.

Crozier, A., Jaganath, I. B., Clifford, M. N. (2009) Dietary phenolics: chemistry, bioavailability and effects on health. Natural Product Reports 26, 1001-1043.

Cui, G., Nan, B., Hu, J., Wang, Y., Jin, C., Xia, B. (2006) Identification and solution structures of a single domain biotin/lipoyl attachment protein from *Bacillus subtilis*. Journal of Biological Chemistry 281, 20598-20607.

Danon, A., Rotari, VI., Gordon, A., Mailhac, N., Gallois, P. (2004) Ultraviolet-C overexposure induces programmed cell death in *Arabidopsis*, which is mediated by caspase-like activities and which can be suppressed by caspase inhibitors, p35 and *Defender against Apoptotic Death*. Journal of Biological Chemistry 279, 779-787.

Das, A., Eldakak, M., Paudel, B., Kim, D. W., Hemmati, H., Basu, C., Rohila, J. S. (2016) Leaf proteome analysis reveals prospective drought and heat stress response

mechanisms in soybean. BioMed Research International 2016, 6021047.

Davies, W. J., Gowing, D. J. G. (1999) Plant responses to small perturbatioins in soil water status. In: Press, M. C., Scholes, J. D., Barker, M. G (Eds.). Physiological plant ecology. Blackwell Science, Oxford, UK, pp. 67-89.

de la Fuente, J. M., Ramírez-Rodríguez, V., Cabrera-Ponce, J. L., Herrera-Estrella, L. (1997) Aluminum tolerance in transgenic plants by alteration of citrate synthesis. Science 276, 1566-1568.

Degenhardt, R. F., Bonham Smith, P. C. (2008) *Arabidopsis* ribosomal proteins RPL23aA and RPL23aB are differentially targeted to the nucleolus and are disparately required for normal development. Plant Physiology 147, 128-142.

Delom, F., Emadali, A., Cocolakis, E., Lebrun, J. J., Nantel, A., Chevet, E. (2007) Calnexin-dependent regulation of tunicamycin-induced apoptosis in breast carcinoma MCF-7 cells. Cell Death and Differentiation 14, 586-596.

Deng, Y., Srivastava, R., Howell, S. H. (2013) Endoplasmic reticulum (ER) stress response and its physiological roles in plants. International Journal of Molecular Sciences 14, 8188-8212.

Depeint, F., Bruce, W. R., Shangari, N., Mehta, R., O'Brien, P. J. (2006) Mitochondrial function and toxicity: role of the B vitamin family on mitochondrial energy metabolism. Chemico-Biological Interactions 163, 94-112.

Deshmukh, R., Sonah, H., Patil, G., Chen, W., Prince, S., Mutava, R., Vuong, T., Valliyodan, B., Nguyen, H. T. (2014) Integrating omic approaches for abiotic stress tolerance in soybean. Frontiers in Plant Science 5, 244.

Du, F., Zhang, Y., Ren, H. (2011) The universal bundling activity of AtVLN4 in diffusely growing cells. Plant Signaling and Behavior 6, 1290-1293.

Du, H., Wu, N., Cui, F., You, L., Li, X., Xiong, L. (2014) A homolog of ETHYLENE OVERPRODUCER, OsETOL1, differentially modulates drought and submergence tolerance in rice. Plant Journal 78, 834-849.

Eigenbrod, F., Gonzalez, P., Dash, J., Steyl, I. (2015) Vulnerability of ecosystems to climate change moderated by habitat intactness. Global Change Biology 21, 275-86.

Ella, E. S., Dionisio-Sese, M. L., Ismail, A. M. (2010) Proper management improves

seedling survival and growth during early flooding in contrasting rice genotypes. Crop Science 50, 1997-2008.

Falcone Ferreyra, M. L., Pezza, A., Biarc, J., Burlingame, A. L., Casati, P. (2010) Plant L10 ribosomal proteins have different roles during development and translation under ultraviolet-B stress. Plant Physiology 153, 1878-1894.

Fayaz, S. M., Suvanish Kumar, V. S., Rajanikant, K. G. (2014) Finding needles in a haystack: application of network analysis and target enrichment studies for the identification of potential anti-diabetic phytochemicals. PLoS One 9, e112911.

Feldman, L. J. (1984) Regulation of root development. Annual Review of Plant Physiology 35, 223-242.

Fitchette, A. C., Dinh, O. T., Faye, L., Bardor, M. (2007) Plant proteomics and glycosylation. In plant proteomics: Methods and Protocols; Thiellement, H., Zivy, M., Damerval, C., Méchin, V. (Eds). Humana Press, Totowa, NJ, USA, pp 317-342.

Fragoso, S., Espíndola, L., Páez-Valencia, J., Gamboa, A., Camacho, Y., Martínez-Barajas, E., Coello, P. (2009) SnRK1 isoforms AKIN10 and AKIN11 are differentially regulated in *Arabidopsis* plants under phosphate starvation. Plant Physiology 149, 1906-1916.

Francklyn, C., Musier-Forsyth, K., Martinis, S. A. (1997) Aminoacyl-tRNA synthetases in biology and disease: new evidence for structural and functional diversity in an ancient family of enzymes. RNA 3, 954.

Franco, J. A., Banon, S., Vicente, M. J., Miralles, J., Martinez-Sanchez, J. J. (2011) Root development in horticultural plants grown under abiotic stress conditions-a review. Journal of Horticultural Science Biotechnique 86, 543-556.

Freedman, R. B., Hirst, T. R., Tuite, M. F. (1994) Protein disulphide isomerase: building bridges in protein folding. Trends in Biochemical Sciences 19, 331-336.

Fukao, T., Yeung, E., Bailey-Serres, J. (2011) The submergence tolerance regulator SUB1A mediates crosstalk between submergence and drought tolerance in rice. Plant Cell 23, 412-427.

Gallois, P., Makishima, T., Hecht, V., Despres, B., Laudié, M., Nishimoto, T., Cooke, R. (1997) An *Arabidopsis thaliana* cDNA complementing a hamster apoptosis suppressor mutant. Plant Journal 11, 1325-1331.

Gil-Quintana, E., Larrainzar, E., Seminario, A., Díaz-Leal, J. L., Alamillo, J. M., Pineda, M., Arrese-Igor, C., Wienkoop, S., González, E. M. (2013) Local inhibition of nitrogen fixation and nodule metabolism in drought-stressed soybean. Journal of Experimental Botany 64, 2171-2182.

Githiri, S. M., Watanabe, S., Harada, K., Takahashi, R. (2006) QTL analysis of flooding tolerance in soybean at an early vegetative growth stage. Plant Breeding 125, 613-618.

Gladish, D. K., Xu, J., Niki, T. (2006) Apoptosis-like programmed cell death occurs in procambium and ground meristem of pea (*Pisum sativum*) root tips exposed to sudden flooding. Annual of Botanty 97, 895-902.

Gleason, C., Huang, S., Thatcher, L. F., Foley, R. C., Anderson, C. R., Carroll, A. J., Millar, A. H., Singh, K. B. (2011) Mitochondrial complex II has a key role in mitochondrial-derived reactive oxygen species influence on plant stress gene regulation and defense. Proceedings of the National Academy of Sciences 108, 10768-10773.

Gomez, L., Chrispeels, M. J. (1994) Complementation of an *Arabidopsis thaliana* mutant that lacks complex asparagine-linked glycans with the human cDNA encoding *N*-acetylglucosaminyltransferase I. Proceedings of the National Academy of Sciences 91, 1829-1833.

Gounaris, A. D., Turkenkopf, I., Buckwald, S., Young, A. (1971) Pyruvate decarboxylase. I. Protein dissociation into subunits under conditions in which thiamine pyrophosphate is released. Journal of Biological Chemistry 246, 1302-1309.

Guo, Z., Tan, J., Zhuo, C., Wang, C., Xiang, B., Wang, Z. (2014) Abscisic acid, H_2O_2 and nitric oxide interactions mediated cold-induced *S*-adenosylmethionine synthetase in *Medicago sativa* subsp. *falcata* that confers cold tolerance through up-regulating polyamine oxidation. Plant Biotechnology Journal 12, 601-612.

Gupta, R., Brunak, S. (2002) Prediction of glycosylation across the human proteome and the correlation to protein function. Pacific Symposium on Biocomputing *7*, 310-322.

Harmon, A. C., Gribskov, M., Harper, J. F. (2000) CDPKs-a kinase for every Ca^{2+}

signal? Trends in Plant Science 5, 154-159.

Hashiguchi, A., Ahsan, N., Komatsu, S. (2010) Proteomics application of crops in the context of climatic changes. Food Research International 43, 1803-1813.

Hashiguchi, A., Sakata, K., Komatsu, S. (2009) Proteome analysis of early-stage soybean seedlings under flooding stress. Journal of Proteome Research 8, 2058-2069.

Hasinoff, B. B. (1990) Inhibition and inactivation of NADH-cytochrome *c* reductase activity of bovine heart submitochondrial particles by the iron (III)-adriamycin complex. Biochemical Journal 265, 865-870.

Hassel, B., Johannessen, C. U., Sonnewald, U., Fonnum, F. (1998) Quantification of the GABA shunt and the importance of the GABA shunt versus the 2-oxoglutarate dehydrogenase pathway in GABAergic neurons. Journal of Neurochemistry 71, 1511-1518.

Hattori, Y., Nagai, K., Furukawa, S., Song, X. J., Kawano, R., Sakakibara, H., Wu, J. Z., Matsumoto, T., Yoshimura, A., Kitano, H., Matsuoka, M., Mori, H., Ashikari, M. (2009) The ethylene response factors *SNORKEL1* and *SNORKEL2* allow rice to adapt to deep water. Nature 460, 1026-1030.

He, L., Li, B., Lu, X., Yuan, L., Yang, Y., Yuan, Y., Du, J., Guo, S. (2015) The effect of exogenous calcium on mitochondria, respiratory metabolism enzymes and ion transport in cucumber roots under hypoxia. Scientific Reports 5, 11391.

He, L., Lu, X., Tian, J., Yang, Y., Li, B., Li, J., Guo, S. (2012) Proteomic analysis of the effects of exogenous calcium on hypoxic-responsive proteins in cucumber roots. Proteome Science 10, 42.

Healy, S. J., Verfaillie, T., Jäger, R., Agostinis, P., Samali, A. (2012) Biology of the Endoplasmic Reticulum. In: Endoplasmic Reticulum Stress in Health and Disease; Agostinis, P. and Samali, A. (Eds). Springer Netherlands, Dordrecht, pp 3-22.

Heino, P., Palva, E. T. (2003) Signal transduction in plant cold acclimation. In: Plant Responses to Abiotic Stress; Hirt, H., Shinozaki, K., (Eds). Springer-Verlag, New York pp. 151-186.

Hepler, P. K. (2005) Calcium: a central regulator of plant growth and development. Plant Cell 17, 2142-2155.

Horton, P., Park, K. J., Obayashi, T., Fujita, N., Harada, H., Adams Collier, C. J., Nakai, K. (2007) WoLF PSORT: protein localization predictor. Nucleic Acids Research 35, W585-587.

Hossain, Z., Komatsu, S. (2014) Potentiality of soybean proteomics in untying the mechanism of flood and drought stress tolerance. Proteomes 2, 107-127.

Hossain, Z., Nouri, M. Z., Komatsu, S. (2012) Plant cell organelle proteomics in response to abiotic stress. Journal of Proteome Research 11, 37-48.

Howell, S. H. (2013) Endoplasmic reticulum stress responses in plants. Annual Review of Plant Biology 64, 477-499.

Huang, S., Jacoby, R. P., Millar, A. H., Taylor, N. L. (2014) Plant mitochondrial proteomics. In: Plant proteomics: Methods and Protocol; Jorrin Novo, J. V., Komatsu, S., Weckwerth, W., Wienkoop, S. (Eds). Springer, New York, pp 499-526.

Huang, S., Qu, X., Zhang, R. (2015) Plant villins: versatile actin regulatory proteins. Journal of Integrative Plant Biology 57, 40-49.

Huang, S., Robinson, R. C., Gao, L. Y., Matsumoto, T., Brunet, A., Blanchoin, L., Staiger, C. J. (2005) *Arabidopsis* VILLIN1 generates actin filament cables that are resistant to depolymerization. Plant Cell 17, 486-501.

Huda, K. M., Banu, M. S., Tuteja, R., Tuteja, N. (2013) Global calcium transducer P-type Ca^{2+}-ATPases open new avenues for agriculture by regulating stress signalling. Journal of Experimental Botany 64, 3099-3109.

Im, J. H., Cho, Y. H., Kim, G. D., Kang, G. H., Hong, J. W., Yoo, S. D. (2014) Inverse modulation of the energy sensor Snf1-related protein kinase 1 on hypoxia adaptation and salt stress tolerance in *Arabidopsis thaliana*. Plant Cell and Environment 37, 2303-2312.

Irsigler, A. S., Costa, M. D., Zhang, P., Reis, P. A., Dewey, R. E., Boston, R. S., Fontes, E. P. (2007) Expression profiling on soybean leaves reveals integration of ER-and osmotic-stress pathways. BMC Genomics 8, 431.

Ishihama, Y., Oda, Y., Tabata, T., Sato, T., Nagasu, T., Rappsilber, J., Mann, M. (2005) Exponentially modified protein abundance index (emPAI) for estimation of absolute protein amount in proteomics by the number of sequenced peptides per protein. Molecular and Cellular Proteomics 4, 1265-1272.

Ismond, K. P., Dolferus, R., de Pauw, M., Dennis, E. S., Good, A. G. (2003) Enhanced low oxygen survival in *Arabidopsis* through increased metabolic flux in the fermentative pathway. Plant Physiology 132, 1292-1302.

Jain, V., Singla, N. K., Jain, S., Gupta, K. (2010) Activities of enzymes of fermentation pathways in the leaves and roots of contrasting cultivars of sorghum (*Sorghum Bicolor* L.) during flooding. Physiology and Molecular Biology of Plants 16, 241-247.

Jha, U. C., Bohra, A., Jha, R. (2017) Breeding approaches and genomics technologies to increase crop yield under low-temperature stress. Plant Cell Report 36, 1-35.

Johnová, P., Skalák, J., Saiz-Fernández, I., Brzobohatý, B. (2016) Plant responses to ambient temperature fluctuations and water-limiting conditions: a proteome-wide perspective. Biochimica et Biophysica Acta Proteins and Proteomics, 1864, 916-931.

Kajiura, H., Okamoto, T., Misaki, R., Matsuura, Y., Fujiyama, K. (2012) *Arabidopsis* β1, 2-xylosyltransferase: substrate specificity and participation in the plant-specific *N*-glycosylation pathway. Journal of Bioscience and Bioengineering 113, 48-54.

Kamal, A. H. M., Komatsu, S. (2015) Involvement of reactive oxygen species and mitochondrial proteins in biophoton emission in roots of soybean plants under flooding stress. Journal of Proteome Research 14, 2219-2236.

Kamal, A. H. M., Komatsu, S. (2016) Jasmonic acid induced protein response to biophoton emissions and flooding stress in soybean. Journal of Proteomics 133, 33-47.

Kamal, A. H. M., Rashid, H., Sakata, K., Komatsu, S. (2015) Gel-free quantitative proteomic approach to identify cotyledon proteins in soybean under flooding stress. Journal of Proteomics 112, 1-13.

Kanehisa, M., Goto, S. (2000) KEGG: kyoto encyclopedia of genes and genomes. Nucleic Acids Research 28, 27-30.

Kang, J. S., Frank, J., Kang, C. H., Kajiura, H., Vikram, M., Ueda, A., Kim, S., Bahk, J. D., Triplett, B., Fujiyama, K., Lee, S. Y., von Schaewen, A., Koiwa, H. (2008) Salt tolerance of *Arabidopsis thaliana* requires maturation of *N*-glycosylated proteins in the Golgi apparatus. Proceedings of the National Academy of Sciences 105, 5933-

5938.

Kaplan, F., Guy, C. L. (2004) β-Amylase induction and the protective role of maltose during temperature shock. Plant Physiology 135, 1674-1684.

Kato, M., Minamida, K., Tojo, M., Kokuryu, T., Hamaguchi, H., Shimada, S. (2013) Association of *Pythium* and *Phytophthora* with pre-emergence seedling damping-off of soybean grown in a field converted from a paddy field in Japan. Plant Production Science 16, 95-104.

Kausar, R., Hossain, Z., Makino, T., Komatsu, S. (2012) Characterization of ascorbate peroxidase in soybean under flooding and drought stresses. Molecular Biology Reports 39, 10573-10579.

Khan, M. N., Komatsu, S. (2016) Proteomic analysis of soybean root including hypocotyl during recovery from drought stress. Journal of Proteomics 144, 39-50.

Khan, M. N., Sakata, K., Hiraga, S., Komatsu, S. (2014) Quantitative proteomics reveals that peroxidases play key roles in post-flooding recovery in soybean roots. Journal of Proteome Research 13, 5812-5828.

Khan, M. N., Sakata, K., Komatsu, S. (2015) Proteomic analysis of soybean hypocotyl during recovery after flooding stress. Journal of Proteomics 121, 15-27.

Khatoon, A., Rehman, S., Hiraga, S., Makino, T., Komatsu, S. (2012) Organ-specific proteomics analysis for identification of response mechanism in soybean seedlings under flooding stress. Journal of Proteomics 75, 5706-5723.

Khurana, P., Henty, J. L., Huang, S., Staiger, A. M., Blanchoin, L., Staiger, C. J. (2010) *Arabidopsis* VILLIN1 and VILLIN3 have overlapping and distinct activities in actin bundle formation and turnover. Plant Cell 22, 2727-2748.

Kieffer, M., Stern, Y., Cook, H., Clerici, E., Maulbetsch, C., Laux, T., Davies, B. (2006) Analysis of the transcription factor WUSCHEL and its functional homologue in *Antirrhinum* reveals a potential mechanism for their roles in meristem maintenance. Plant Cell 18, 560-573.

Kim, E. H., Kim, S. H., Chung, J. I., Chi, H. Y., Kim, J. A., Chung, I. M. (2006) Analysis of phenolic compounds and isoflavones in soybean seeds (*Glycine max* (L.) Merill) and sprouts grown under different conditions. European Food Research and Technology 222, 201-208.

Kim, E. H., Ro, H. M., Kim, S. L., Kim, H. S., Chung, I. M. (2012) Analysis of isoflavone, phenolic, soyasapogenol, and tocopherol compounds in soybean [*Glycine max* (L.) Merrill] germplasms of different seed weights and origins. Journal of Agricultural and Food Chemistry 60, 6045-6055.

Kim, K. Y., Park, S. W., Chung, Y. S., Chung, C. H., Kim, J. I., Lee, J. H. (2004) Molecular cloning of low-temperature-inducible ribosomal proteins from soybean. Journal of Experimental Botany 55, 1153-1155.

Knight, H., Trewavas, A. J., Knight, M. R. (1997) Calcium signalling in *Arabidopsis thaliana* responding to drought and salinity. Plant Journal 12, 1067-1078.

Komatsu, S., Deschamps, T., Hiraga, S., Kato, M., Chiba, M., Hashiguchi, A., Tougou, M., Shimamura, S., Yasue, H. (2011b) Characterization of a novel flooding stress-responsive alcohol dehydrogenase expressed in soybean roots. Plant Molecular Biology 77, 309-322.

Komatsu, S., Han, C., Nanjo, Y., Altaf-Un-Nahar, M., Wang, K., He, D., Yang, P. (2013a) Label-free quantitative proteomic analysis of abscisic acid effect in early-stage soybean under flooding. Journal of Proteome Research 12, 4769-4784.

Komatsu, S., Hiraga, S., Nouri, M. Z. (2014) Analysis of flooding-responsive proteins localized in the nucleus of soybean root tips. Molecular Biology Reports 41, 1127-1139.

Komatsu, S., Hiraga, S., Yanagawa, Y. (2012a) Proteomics techniques for the development of flood tolerant crops. Journal of Proteome Research 11, 68-78.

Komatsu, S., Hossain, Z. (2013) Organ-specific proteome analysis for identification of abiotic stress response mechanism in crop. Frontiers in Plant Science 4, 71.

Komatsu, S., Kobayashi, Y., Nishizawa, K., Nanjo, Y., Furukawa, K. (2010) Comparative proteomics analysis of differentially expressed proteins in soybean cell wall during flooding stress. Amino Acids 39, 1435-1449.

Komatsu, S., Kuji, R., Nanjo, Y., Hiraga, S., Furukawa, K. (2012b) Comprehensive analysis of endoplasmic reticulum-enriched fraction in root tips of soybean under flooding stress using proteomics techniques. Journal of Proteomics 77, 531-560.

Komatsu, S., Makino, T., Yasue, H. (2013b) Proteomic and biochemical analyses of the cotyledon and root of flooding-stressed soybean plants. PLoS One 8, e65301.

Komatsu, S., Tougou, M., Nanjo, Y. (2015) Proteomic techniques and management of flooding tolerance in soybean. Journal of Proteome Research, 14, 3768-3778.

Komatsu, S., Wada, T., Abaléa, Y., Nouri, M. Z., Nanjo, Y., Nakayama, N., Shimamura, S., Yamamoto, R., Nakamura, T., Furukawa, K. (2009a) Analysis of plasma membrane proteome in soybean and application to flooding stress response. Journal of Proteome Research 8, 4487-4499.

Komatsu, S., Yamamoto, A., Nakamura, T., Nouri, M. Z., Nanjo, Y., Nishizawa, K., Furukawa, K (2011a). Comprehensive analysis of mitochondria in roots and hypocotyls of soybean under flooding stress using proteomics and metabolomics techniques. Journal of Proteome Research 10, 3993-4004.

Komatsu, S., Yamamoto, R., Nanjo, Y., Mikami, Y., Yunokawa, H., Sakata, K. (2009b) A comprehensive analysis of the soybean genes and proteins expressed under flooding stress using transcriptome and proteome techniques. Journal of Proteome Research 8, 4766-4778.

Kong, F. J., Oyanagi, A., Komatsu, S. (2010) Cell wall proteome of wheat roots under flooding stress using gel-based and LC MS/MS-based proteomics approaches. Biochimica et Biophysica Acta 1804, 124-136.

Korte, L. L., Specht, J. E., Williams, J. H., Sorensen, R. C. (1983) Irrigation of soybean genotypes during reproductive ontogeny II. yield component responses. Crop Science 23, 528-533.

Kudla, J., Batistic, O., Hashimoto, K. (2010) Calcium signals: the lead currency of plant information processing. Plant Cell 22, 541-563.

Küppers, M. (1984) Carbon relations and competition between woody species in a Central European hedgerow. Oecologia 64, 344-354.

Kürsteiner, O., Dupuis, I., Kuhlemeier, C. (2003) The pyruvate decarboxylase1 gene of *Arabidopsis* is required during anoxia but not other environmental stresses. Plant Physiology 132, 968-978.

Laemmli, U. K. (1970) Cleavage of structural proteins during the assembly of the head of bacteriophage T4. Nature 227, 680-685.

Lakshmanan, M., Zhang, Z., Mohanty, B., Kwon, J. Y., Choi, H. Y., Nam, H. J., Kim, D. I., Lee, D. Y. (2013) Elucidating rice cell metabolism under flooding and drought

stresses using flux-based modeling and analysis. Plant Physiology 162, 2140-2150.

Lee, K. H., Piao, H. L., Kim, H. Y., Choi, S. M., Jiang, F., Hartung, W., Hwang, I., Kwak, J. M., Lee, I. J., Hwang, I. (2006) Activation of glucosidase *via* stress-induced polymerization rapidly increases active pools of abscisic acid. Cell 126, 1109-1120.

Li, J., Brader, G., Helenius, E., Kariola, T., Palva, E. T. (2012a) Biotin deficiency causes spontaneous cell death and activation of defense signaling. Plant Journal 70, 315-326.

Li, J., Wang, X., Zhang, Y., Jia, H., Bi, Y. (2011) cGMP regulates hydrogen peroxide accumulation in calcium-dependent salt resistance pathway in *Arabidopsis thaliana* roots. Planta 234, 709-722.

Li, M. W., Xin, D., Gao, Y., Li, K. P., Fan, K., Muñoz, N. B., Yung, W. S., Lam, H. M. (2017) Using genomic information to improve soybean adaptability to climate change. Journal of Experimental Botany 68, 1823-1834.

Li, Q., Li, P., Sun, L., Wang, Y., Ji, K., Sun, Y., Dai, S., Chen, P., Duan, C., Leng, P. (2012b) Expression analysis of β-glucosidase genes that regulate abscisic acid homeostasis during watermelon (*Citrullus lanatus*) development and under stress conditions. Journal of Plant Physiology 169, 78-85.

Li, X., Guo, C., Gu, J., Duan, W., Zhao, M., Ma, C., Du, X., Lu, W., Xiao, K. (2014) Overexpression of VP, a vacuolar H^+-pyrophosphatase gene in wheat (*Triticum aestivum* L.), improves tobacco plant growth under Pi and N deprivation, high salinity, and drought. Journal of Experimental Botany 65, 683-696.

Liao, C. T., Lin, C. H. (2001) Physiological adaptation of crop plants to flooding stress. Proceedings of the National Science Council, Republic of China. Part B, Life Sciences 25, 148-157.

Lilley, K. S., Dupree, P. (2006) Methods of quantitative proteomics and their application to plant organelle characterization. Journal of Experimental Botany 57, 1493-1499.

Linkemer, G., Board, J. E., Musgrave, M. E. (1998) Waterlogging effects on growth and yield components in late-planted soybean. Crop Science 38, 1576-1584.

Liu, L., Cui, F., Li, Q., Yin, B., Zhang, H., Lin, B., Wu, Y., Xia, R., Tang, S., Xie, Q. (2011) The endoplasmic reticulum-associated degradation is necessary for plant salt

tolerance. Cell Research 21, 957-969.

Liu, Q., Zhang, S., Liu, B. (2016) 14-3-3 proteins: macro-regulators with great potential for improving abiotic stress tolerance in plants. Biochemical and Biophysical Research Communications 477, 9-13.

Liu, Z., Karmarkar, V. (2008) Groucho/Tup1 family co-repressors in plant development. Trends in Plant Science 13, 137-144.

Long, J. A., Ohno, C., Smith, Z. R., Meyerowitz, E. M. (2006) TOPLESS regulates apical embryonic fate in *Arabidopsis*. Science 312, 1520-1523.

Luan, S., Kudla, J., Rodriguez-Concepcion, M., Yalovsky, S., Gruissem, W. (2002) Calmodulins and calcineurin B-like proteins: calcium sensors for specific signal response coupling in plants. Plant Cell 14, S389-S400.

Luna, E., van Hulten, M., Zhang, Y., Berkowitz, O., López, A., Pétriacq, P., Sellwood, M. A., Chen, B., Burrell, M., van De Meene, A., Pieterse, C. M. (2014) Plant perception of β-aminobutyric acid is mediated by an aspartyl-tRNA synthetase. Nature Chemical Biology 10, 450-456.

Maintz, J., Cavdar, M., Tamborski, J., Kwaaitaal, M., Huisman, R., Meesters, C., Kombrink, E., Panstruga, R. (2014) Comparative analysis of MAMP-induced calcium influx in *Arabidopsis* seedlings and protoplasts. Plant and Cell Physiology 55, 1813-1825.

Manavalan, L. P., Guttikonda, S. K., Tran, L. S. P., Nguyen, H. T. (2009) Physiological and molecular approaches to improve drought resistance in soybean. Plant and Cell Physiology 50, 1260-1276.

Martinis, S. A., Plateau, P., Cavarelli, J., Florentz, C. (1999a) Aminoacyl-tRNA synthetases: a family of expanding functions. EMBO Journal 18, 4591-4596.

Martinis, S. A., Plateau, P., Cavarelli, J., Florentz, C. (1999b) Aminoacyl-tRNA synthetases: a new image for a classical family. Biochimie 81, 683-700.

Maruyama, T., Kanaji, T., Nakade, S., Kanno, T., Mikoshiba, K. (1997) 2APB, 2-aminoethoxydiphenyl borate, a membrane-penetrable modulator of Ins(1,4,5)P_3-induced Ca^{2+} release. Journal of Biochemistry 122, 498-505.

Mathesius, U., Djordjevic, M. A., Oakes, M., Goffard, N., Haerizadeh, F., Weiller, G. F., Singh, M. B., Bhalla, P. L. (2011) Comparative proteomic profiles of the soybean

(*Glycine max*) root apex and differentiated root zone. Proteomics 11, 1707-1719.

Maurel, C., Boursiac, Y., Luu, D. T., Santoni, V., Shahzad, Z., Verdoucq L. (2015) Aquaporins in plants. Physiological Reviews 95, 1321-1358.

McKee, T. B., Doesken, N. J., Kleist, J. (1993) The relationship of drought frequency and duration to time scales. In Proceedings of the 8th Conference on Applied Climatology 17, 179-183.

Merewitz, E. B., Gianfagna, T., Huang, B. (2011) Protein accumulation in leaves and roots associated with improved drought tolerance in creeping bentgrass expressing an ipt gene for cytokinin synthesis. Journal of Experimental Botany 62, 5311-5333.

Messina, M., Messina, V. (2010) The role of soy in vegetarian diets. Nutrients 2, 855-888.

Mishra, A. K., Singh, V. P. (2010) A review of drought concepts. Journal of Hydrology 391, 202-216.

Mithöfer, A., Müller, B., Wanner, G., Eichacker, L. A. (2002) Identification of defence-related cell wall proteins in *Phytophthora sojae*-infected soybean roots by ESI-MS/MS. Molecular Plant Pathology 3, 163-166.

Mittler, R., Blumwald, E. (2010) Genetic engineering for modern agriculture: challenges and perspectives. Annual Review of Plant Biology 61, 443-462.

Mohammadi, P. P., Moieni, A., Hiraga, S., Komatsu, S. (2012) Organ-specific proteomic analysis of drought-stressed soybean seedlings. Journal of Proteomics 75, 1906-1923.

Moller, I. M. (2001) Plant mitochondria and oxidative stress: electron transport, NADPH turnover, and metabolism of reactive oxygen species. Annual Review of Plant Biology 52, 561-591.

Mucha, P. (2002) Aminoacyl-tRNA synthetases and aminoacylation of tRNA in the nucleus. Acta Biochimica Polonica-English Edition 49, 1-10.

Mustafa, G., Komatsu, S. (2014) Quantitative proteomics reveals the effect of protein glycosylation in soybean root under flooding stress. Frontiers in Plant Science 5, 627.

Mustafa, G., Komatsu, S. (2016) Insights into the response of soybean mitochondrial proteins to various sizes of aluminum oxide nanoparticles under flooding stress.

Journal of Proteome Research 15, 4464-4475.

Mustafa, G., Sakata, K., Hossain, Z., Komatsu, S. (2015a) Proteomic study on the effects of silver nanoparticles on soybean under flooding stress. Journal of Proteomics 122, 100-118.

Mustafa, G., Sakata, K., Komatsu, S. (2015b) Proteomic analysis of flooded soybean root exposed to aluminum oxide nanoparticles. Journal of Proteomics 128, 280-297.

Mustafa, G., Sakata, K., Komatsu, S. (2016) Proteomic analysis of soybean root exposed to varying sizes of silver nanoparticles under flooding stress. Journal of Proteomics 148, 113-125.

Mutava, R. N., Prince, S. J. K., Syed, N. H., Song, L., Valliyodan, B., Chen, W., Nguyen, H. T. (2015) Understanding abiotic stress tolerance mechanisms in soybean: a comparative evaluation of soybean response to drought and flooding stress. Plant Physiology and Biochemistry 86, 109-120.

Nägele, T., Mair, A., Sun, X., Fragner, L., Teige, M., Weckwerth, W. (2014) Solving the differential biochemical Jacobian from metabolomics covariance data. PloS One 9, e92299.

Nakamura, T., Yamamoto, R., Hiraga, S., Nakayama, N., Okazaki, K., Takahashi, H., Uchimiya, H., Komatsu, S. (2012) Evaluation of metabolite alteration under flooding stress in soybeans. Japan Agricultural Research Quarterly: JARQ 46, 237-248.

Nanjo, Y., Jang, H. Y., Kim, H. S., Hiraga, S., Woo, S. H., Komatsu, S. (2014) Analyses of flooding tolerance of soybean varieties at emergence and varietal differences in their proteomes. Phytochemistry 106, 25-36.

Nanjo, Y., Maruyama, K., Yasue, H., Yamaguchi-Shinozaki, K., Shinozaki, K., Komatsu, S. (2011) Transcriptional responses to flooding stress in roots including hypocotyl of soybean seedlings. Plant Molecular Biology 77, 129-144.

Nanjo, Y., Nakamura, T., Komatsu, S. (2013) Identification of indicator proteins associated with flooding injury in soybean seedlings using label-free quantitative proteomics. Journal of Proteome Research 12, 4785-4798.

Nanjo, Y., Skultety, L., Ashraf, Y., Komatsu, S. (2010) Comparative proteomic analysis of early-stage soybean seedlings responses to flooding by using gel and gel-free

techniques. Journal of Proteome Research 9, 3989-4002.

Nanjo, Y., Skultety, L., Uváčková, L., Klubicová, K., Hajduch, M., Komatsu, S. (2012) Mass spectrometry-based analysis of proteomic changes in the root tips of flooded soybean seedlings. Journal of Proteome Research 11, 372-385.

Ndimba, B. K., Chivasa, S., Simon, W. J., Slabas, A. R. (2005) Identification of *Arabidopsis* salt and osmotic stress responsive proteins using two-dimensional difference gel electrophoresis and mass spectrometry. Proteomics 5, 4185-4196.

Nouri, M. Z., Hiraga, S., Yanagawa, Y., Sunohara, Y., Matsumoto, H., Komatsu, S. (2012) Characterization of calnexin in soybean roots and hypocotyls under osmotic stress. Phytochemistry 74, 20-29.

Nouri, M. Z., Komatsu, S. (2010) Comparative analysis of soybean plasma membrane proteins under osmotic stress using gel-based and LC MS/MS-based proteomics approaches. Proteomics 10, 1930-1945.

Oh, M. W., Komatsu, S. (2015) Characterization of proteins in soybean roots under flooding and drought stresses. Journal of Proteomics 114, 161-181.

Oh, M. W., Komatsu, S., Nanjo, Y. (2014a) Gel-free proteomic analysis of soybean root proteins affected by calcium under flooding stress. Frontiers in Plant Science, 5, 559.

Oh, M. W., Nanjo, Y., Komatsu, S. (2014b) Analysis of soybean root proteins affected by gibberellic acid treatment under flooding stress. Protein and Peptide Letters 21, 911-947.

Oh, M. W., Nanjo, Y., Komatsu, S. (2014c) Identification of nuclear proteins in soybean under flooding stress using proteomic technique. Protein and Peptide Letters 21, 458-467.

Ohta, M., Takaiwa, F. (2014) Emerging features of ER resident J-proteins in plants. Plant Signaling and Behavior 9, e28194.

Oliveira, T. M., da Silva, F. R., Bonatto, D., Neves, D. M., Morillon, R., Maserti, B. E., Filho, M. A., Costa, M. G., Pirovani, C. P., Gesteira, A. S. (2015) Comparative study of the protein profiles of *Sunki mandarin* and *Rangpur lime* plants in response to water deficit. BMC Plant Biology 15, 69.

Olsen, J. V., de Godoy, L. M., Li, G., Macek, B., Mortensen, P., Pesch, R., Makarov, A.,

Lange, O., Horning, S., Mann, M. (2005) Parts per million mass accuracy on an Orbitrap mass spectrometer *via* lock mass injection into a C-trap. Molecular and Cellular Proteomics 4, 2010-2021.

Orzechowski, S. (2008) Starch metabolism in leaves. Acta Biochimica Polonica 55, 435-445.

Ou, W. J., Cameron, P. H., Thomas, D. Y., Bergeron, J. J. (1993) Association of folding intermediates of glycoproteins with calnexin during protein maturation. Nature 364, 771.

Ozga, J. A., Kaur, H., Savada, R. P., Reinecke, D. M. (2017) Hormonal regulation of reproductive growth under normal and heat-stress conditions in legume and other model crop species. Journal of Experimental Botany 68, 1885-1894.

Palmer, W. C. (1965) Meteorological drought. US Department of Commerce Research Paper 30, 45.

Pandey, A., Chakraborty, S., Datta, A., Chakraborty, N. (2008) Proteomics approach to identify dehydration responsive nuclear proteins from chickpea (*Cicer aritinum* L.). Molecular and Cellular Proteomics 7, 88-107.

Papp, S., Dziak, E., Michalak, M., Opas, M. (2003) Is all of the endoplasmic reticulum created equal? The effects of the heterogeneous distribution of endoplasmic reticulum Ca^{2+}-handling proteins. Journal of Cell Biology 160, 475-479.

Parre, E., Ghars, M. A., Leprince, A. S., Thiery, L., Lefebvre, D., Bordenave, M., Richard, L., Mazars, C., Abdelly, C., Savouré, A. (2007) Calcium signaling *via* phospholipase C is essential for proline accumulation upon ionic but not nonionic hyperosmotic stresses in *Arabidopsis*. Plant Physiology 144, 503-512.

Pattison, R. J., Amtmann, A. (2009) *N*-glycan production in the endoplasmic reticulum of plants. Trends in Plant Science 14, 92-99.

Peng, Z., Wang, M., Li, F., Lv, H., Li, C., Xia, G. (2009) A proteomic study of the response to salinity and drought stress in an introgression strain of bread wheat. Molecular and Cellular Proteomics 8, 2676-2686.

Peppiatt, C. M., Collins, T. J., Mackenzie, L., Conway, S. J., Holmes, A. B., Bootman, M. D., Berridge, M. J., Seo, J. T., Roderick, H. L. (2003) 2-Aminoethoxydiphenyl borate (2-APB) antagonises inositol 1,4,5-trisphosphate-induced calcium release,

inhibits calcium pumps and has a use-dependent and slowly reversible action on store-operated calcium entry channels. Cell Calcium 34, 97-108.

Perata, P., Armstrong, W., Voesenek, L. A. (2011) Plants and flooding stress. New Phytologist 190, 269-273.

Pérez, L., Aguilar, R., Méndez, A. P., de Jiménez, E. S. (1990) Phosphorylation of ribosomal proteins induced by auxins in maize embryonic tissues. Plant Physiology 94, 1270-1275.

Pezeshki, S. R. (2001) Wetland plant responses to soil flooding. Environmental and Experimental Botany 46, 299-312.

Pociecha, E., Kościelniak, J., Filek, W. (2008) Effects of root flooding and stage of development on the growth and photosynthesis of field bean (*Vicia faba* L. *minor*). Acta Physiologiae Plantarum 30, 529-535.

Polle, A., Chen, S. (2015) On the salty side of life: molecular, physiological and anatomical adaptation and acclimation of trees to extreme habitats. Plant Cell and Environment 38, 1794-1816.

Prakriya, M., Lewis, R. S. (2001) Potentiation and inhibition of Ca^{2+} release-activated Ca^{2+} channels by 2-aminoethyldiphenyl borate (2-APB) occurs independently of IP_3 receptors. Journal of Physiology 536, 3-19.

Probert, M. E., Keating, B. A. (2000) What soil constraints should be included in crop and forest models? Agriculture, Ecosystems and Environment 82, 273-281.

Qi, X. H., Xu, X. W., Lin, X. J., Zhang, W. J., Chen, X. H. (2012) Identification of differentially expressed genes in cucumber (*Cucumis sativus* L.) root under waterlogging stress by digital gene expression profile. Genomics 99, 160-168.

Qin, S. Y., Hu, D., Matsumoto, K., Takeda, K., Matsumoto, N., Yamaguchi, Y., Yamamoto, K. (2012) Malectin forms a complex with ribophorin I for enhanced association with misfolded glycoproteins. Journal of Biological Chemistry 287, 38080-38089.

Quimio, C. A., Torrizo, L. B., Setter, T. L., Ellis, M., Grover, A., Abrigo, E. M., Oliva, N. P., Ella, E. S., Carpena, A. L., Ito, O., Peacock, W. J. (2000) Enhancement of submergence tolerance in transgenic rice overproducing pyruvate decarboxylase. Journal of Plant Physiology 156, 516-521.

Ranjan, A., Pandey, N., Lakhwani, D., Dubey, N. K., Pathre, U. V., Sawant, S. V. (2012) Comparative transcriptomic analysis of roots of contrasting *Gossypium herbaceum* genotypes revealing adaptation to drought. BMC Genomics 13, 680.

Roberts, M. R., Salinas, J., Collinge, D. B. (2002) 14-3-3 proteins and the response to abiotic and biotic stress. Plant Molecular Biology 50, 1031-1039.

Rodriguez-Melendez, R., Zempleni, J. (2003) Regulation of gene expression by biotin (review). Journal of Nutritional Biochemistry 14, 680-690.

Rolland, F., Baena-Gonzalez, E., Sheen, J. Sugar sensing and signaling in plants: conserved and novel mechanisms. (2006) Annual Review of Plant Biology 57, 675-709.

Rosenfeld, M. G., Marcantonio, E. E., Hakimi, J., Ort, V. M., Atkinson, P. H., Sabatini, D., Kreibich, G. (1984) Biosynthesis and processing of ribophorins in the endoplasmic reticulum. Journal of Cell Biology 99, 1076-1082.

Ruiz-May, E., Kim, S., Brandizzi, F., Rose, J. K. (2012) The secreted plant *N*-glycoproteome and associated secretory pathways. Frontiers in Plant Science 3, 117.

Russell, D. A., Wong, D. M., Sachs, M. M. (1990) The anaerobic response of soybean. Plant Physiology 92, 401-407.

Sacks, M. M., Silk, W. K., Burman, P. (1997) Effect of water stress on cortical cell division rates within the apical meristem of primary roots of maize. Plant Physiology 114, 519-527.

Sadiq, I., Fanucchi, F., Paparelli, E., Alpi, E., Bachi, A., Alpi, A., Perata, P. (2011) Proteomic identification of differentially expressed proteins in the anoxic rice coleoptile. Journal of Plant Physiology 168, 2234-2243.

Sairam, R. K., Dharmar, K., Chinnusamy, V., Meena, R. C. (2009) Waterlogging-induced increase in sugar mobilization, fermentation, and related gene expression in the roots of mung bean (*Vigna radiata*). Journal of Plant Physiology 166, 602-616.

Salavati, A., Khatoon, A., Nanjo, Y., Komatsu, S. (2012) Analysis of proteomic changes in roots of soybean seedlings during recovery after flooding. Journal of Proteomics 75, 878-893.

Sarwat, M., Naqvi, A. R. (2013) Heterologous expression of rice calnexin (*OsCNX*)

confers drought tolerance in *Nicotiana tabacum*. Molecular Biology Reports 40, 5451-5464.

Schmutz, J., Cannon, S. B., Schlueter, J., Ma, J., Mitros, T., Nelson, W., Hyten, D. L., Song, Q., Thelen, J. J., Cheng, J., Xu, D., Hellsten, U., May, G. D., Yu, Y., Sakurai, T., Umezawa, T., Bhattacharyya, T. U., Sandhu, D., Valliyodan, B., Lindquist, E., Peto, M., Grant, D., Shu, S., Goodstein, D., Barry, K., Futrell-Griggs, M., Abemathy, B., Du, J., Tian, Z., Zhu, L., Gill, N., Joshi, T., Libault, M., Sethuraman, A., Zhang, X. C., Shinozaki, K., Nguyen, H. T., Wing, R. A., Cregan, P., Specht, J., Grimwood, J., Rokhsar, D., Shoemaker, R. C., Jackson, S. A. (2010) Genome sequence of the palaeopolyploid soybean. Nature 463, 178-183.

Schulze, E. D. (1986) Carbon dioxide and water vapor exchange in response to drought in the atmosphere and in the soil. Annual Review of Plant Physiology 37, 247-274.

Seki, M., Narusaka, M., Ishida, J., Nanjo, T., Fujita, M., Oono, Y., Kamiya, A., Nakajima, M., Enju, A., Sakurai, T., Satou, M. (2002) Monitoring the expression profiles of 7000 *Arabidopsis* genes under drought, cold and high-salinity stresses using a full-length cDNA microarray. Plant Journal 31, 279-292.

Serraj, R., Shelp, B. J., Sinclair, T. R. (1998) Accumulation of γ-aminobutyric acid in nodulated soybean in response to drought stress. Physiologia Plantarum 102, 79-86.

Shao, H. B., Song, W. Y., Chu, L. Y. (2008) Advances of calcium signals involved in plant anti-drought. Comptes Rendus Biologies 331, 587-596.

Sharp, R. E., Poroyko, V., Hejlek, L. G., Spollen, W. G., Springer, G. K., Bohnert, H. J., Nguyen, H. T. (2004) Root growth maintenance during water deficits: physiology to functional genomics. Journal of Experimental Botany 55, 2343-2351.

Shi, H., Ye, T., Zhong, B., Liu, X., Chan, Z. (2014) Comparative proteomic and metabolomic analyses reveal mechanisms of improved cold stress tolerance in bermudagrass (*Cynodon dactylon* (L.) Pers.) by exogenous calcium. Journal of Integrative Plant Biology 56, 1064-1079.

Shinozaki, K., Yamaguchi-Shinozaki, K. (2007) Gene networks involved in drought stress response and tolerance. Journal of Experimental Botany 58, 221-227.

Silverman-Gavrila, L. B., Lew, R. R. (2001) Regulation of the tip-high Ca^{2+} gradient in growing hyphae of the fungus *Neurospora crassa*. European Journal of Cell

Biology 80, 379-390.

Silvertown, J., Dodd, M. E., Gowing, D. J., Mountford, J. O. (1999) Hydrologically defined niches reveal a basis for species richness in plant communities. Nature 400, 61-63.

Singhania, R. R., Patel, A. K., Sukumaran, R. K., Larroche, C., Pandey, A. (2013) Role and significance of beta-glucosidases in the hydrolysis of cellulose for bioethanol production. Bioresource Technology 127, 500-507.

Sitia, R., Braakman, I. (2003) Quality control in the endoplasmic reticulum protein factory. Nature 426, 891-894.

Smith, A. M., Zeeman, S. C., Smith, S. M. (2005) Starch degradation. Annual Review of Plant Biology 56, 73-98.

Stael, S., Rocha, A. G., Robinson, A. J., Kmiecik, P., Vothknecht, U. C., Teige M. (2011) *Arabidopsis* calcium-binding mitochondrial carrier proteins as potential facilitators of mitochondrial ATP-import and plastid SAM-import. FEBS Letters 585, 3935-3940.

Studart-Guimarães, C., Fait, A., Nunes-Nesi, A., Carrari, F., Usadel, B., Fernie, A. R. (2007) Reduced expression of succinyl-coenzyme A ligase can be compensated for by up-regulation of the γ-aminobutyrate shunt in illuminated tomato leaves. Plant Physiology 145, 626-639.

Sturn, A., Quackenbush, J., Trajanoski, Z. (2002) Genesis: cluster analysis of microarray data. Bioinformatics 18, 207-208.

Subbaiah, C. C., Bush, D. S., Sachs, M. M. (1994) Elevation of cytosolic calcium precedes anoxic gene expression in maize suspension-cultured cells. Plant Cell 6, 1747-1762.

Sugiyama, A., Ueda, Y., Takase, H., Yazaki, K. (2015) Do soybeans select specific species of *Bradyrhizobium* during growth? Communicative and Integrative Biology 8, e992734.

Sze, H., Li, X., Palmgren, M. G. (1999) Energization of plant cell membranes by H^+-pumping ATPases. Regulation and biosynthesis. Plant Cell 11, 677-690.

Szopa, J. (2002) Transgenic 14-3-3 isoforms in plants: the metabolite profiling of repressed 14-3-3 protein synthesis in transgenic potato plants. Biochemical Society

Transactions 30, 405-410.

Tanaka, N., Mitsui, S., Nobori, H., Yanagi, K., Komatsu, S. (2005) Expression and function of proteins during development of the basal region in rice seedlings. Molecular and Cellular Proteomics 4, 796-808.

Tanz, S. K., Castleden, I., Hooper, C. M., Vacher, M., Small, I., Millar, H. A. (2013) SUBA3: a database for integrating experimentation and prediction to define the SUBcellular location of proteins in *Arabidopsis*. Nucleic Acids Research 41, D1185-1191.

Thomson, L. J., Xing, T., Hall, J. L., Williams, L. E. (1993) Investigation of the calcium-transporting ATPases at the endoplasmic reticulum and plasma membrane of red beet (*Beta vulgaris*). Plant Physiology 102, 553-564.

Tissot, G., Job, D., Douce, R., Alban, C. (1996) Protein biotinylation in higher plants: characterization of biotin holocarboxylase synthetase activity from pea (*Pisum sativum*) leaves. Biochemical Journal 314, 391-395.

Toorchi, M., Yukawa, K., Nouri, M. Z., Komatsu, S. (2009) Proteomics approach for identifying osmotic-stress-related proteins in soybean roots. Peptides 30, 2108-2117.

Tougou, M., Hashiguchi, A., Yukawa, K., Nanjo, Y., Hiraga, S., Nakamura, T., Nishizawa, K., Komatsu, S. (2012) Response to flooding stress in soybean seedlings with the alcohol dehydrogenase transgene. Plant Biotechnology 29, 301-305.

Tu, B. P., Weissman, J. S. (2004) Oxidative protein folding in eukaryotes: mechanisms and consequences. Journal of Cell Biology 164, 341-346.

Tyug, T. S., Prasad, K. N., Ismail, A. (2010) Antioxidant capacity, phenolics and isoflavones in soybean by-products. Food Chemistry 123, 583-589.

Umeda, M., Uchimiya, H. (1994) Differential transcript levels of genes associated with glycolysis and alcohol fermentation in rice plants (*Oryza sativa* L.) under submergence stress. Plant Physiology 106, 1015-1022.

Upadhyaya, H., Panda, S. K., Dutta, B. K. (2011) $CaCl_2$ improves post-drought recovery potential in *Camellia sinensis* (L) O. Kuntze. Plant Cell Reports 30, 495-503.

Usadel, B., Nagel, A., Thimm, O., Redestig, H., Blaesing, O. E., Palacios-Rofas, N., Selbig, J., Hannemann, J., Piques, M. C., Steinhauser, D., Scheible, W. R., Gibon, Y., Morcuende, R., Weicht, D., Meyer, S., Stitt, M. (2005) Extension of the visualization tool MapMan to allow statistical analysis of arrays, display of corresponding genes, and comparison with known responses. Plant Physiology 138, 1195-1204.

Usadel, B., Poree, F., Nagel, A., Lohse, M., Czedik-Eysenberg, A., Stitt, M. (2009) A guide to using MapMan to visualize and compare Omics data in plants: a case study in the crop species, Maize. Plant Cell and Environment 32, 1211-1229.

Valente, M. A., Faria, J. A., Soares-Ramos, J. R., Reis, P. A., Pinheiro, G. L., Piovesan, N. D., Morais, A. T., Menezes, C. C., Cano, M. A., Fietto, L. G., Loureiro, M. E., Aragão, F. J., Fontes, E. P. (2009) The ER luminal binding protein (BiP) mediates an increase in drought tolerance in soybean and delays drought-induced leaf senescence in soybean and tobacco. Journal of Experimental Botany 60, 533-546.

vanToai, T. T., St Martin, S. K., Chase, K., Boru, G., Schnipke, V., Schmitthenner, A. F., Lark, K.G. (2001) Identification of a QTL associated with tolerance of soybean to soil waterlogging. Crop Science 41, 1247-1252.

Vitale, A., Boston, R. S. (2008) Endoplasmic reticulum quality control and the unfolded protein response: insights from plants. Traffic 9, 1581-1588.

Vizcaíno, J. A., Côté, R. G., Csordas, A., Dianes, J. A., Fabregat, A., Foster, J. M., Griss, J., Alpi, E., Birim, M., Contell, J., O'Kelly, G., Schoenegger, A., Ovelleiro, D., Pérez-Riverol, Y., Reisinger, F., Ríos, D., Wang, R., Hermjakob, H. (2013) The PRoteomics IDEntifications (PRIDE) database and associated tools: Status in 2013. Nucleic Acids Research 41, D1063-D1069.

Voesenek, L. A., Colmer, T. D., Pierik, R., Millenaar, F. F., Peeters, A. J. (2006) How plants cope with complete submergence. New phytologist 170, 213-226.

Voit, E. O. (2000) Computational analysis of biochemical systems. Cambridge, UK: Cambridge University Press.

Wang, F., Chen, Z. H., Liu, X., Colmer, T. D., Zhou, M., Shabala, S. (2016) Tissue-specific root ion profiling reveals essential roles for the CAX and ACA calcium transport systems for hypoxia response in *Arabidopsis*. Journal of Experimental

Botany 67, 3747-3762.

Wang, G., Cai, G., Kong, F., Deng, Y., Ma, N., Meng, Q. (2014b) Overexpression of tomato chloroplast-targeted DnaJ protein enhances tolerance to drought stress and resistance to *Pseudomonas solanacearum* in transgenic tobacco. Plant Physiology and Biochemistry 82, 95-104.

Wang, H. J., Murphy, P. A. (1994) Isoflavone content in commercial soybean foods. Journal of Agricultural and Food Chemistry 42, 1666-1673.

Wang, J., Lan, P., Gao, H., Zheng, L., Li, W., Schmidt, W. (2013) Expression changes of ribosomal proteins in phosphate- and iron-deficient *Arabidopsis* roots predict stress-specific alterations in ribosome composition. BMC Genomics 14, 783.

Wang, K., Liu, Y., Dong, K., Dong, J., Kang, J., Yang, Q., Zhou, H., Sun, Y. (2011) The effect of NaCl on proline metabolism in *Saussurea amara* seedlings. African Journal of Biotechnology 10, 2886-2893.

Wang, L., Liu, X., Liang, M., Tan, F., Liang, W., Chen, Y., Lin, Y., Huang, L., Xing, J., Chen, W. (2014a) Proteomic analysis of salt-responsive proteins in the leaves of mangrove *Kandelia candel* during short-term stress. PLoS One 9, e83141.

Wang, W., Vinocur, B., Altman, A. (2003) Plant responses to drought, salinity and extreme temperatures: towards genetic engineering for stress tolerance. Planta 218, 1-14.

Wang, W., Vinocur, B., Shoseyov, O., Altman, A. (2004) Role of plant heat-shock proteins and molecular chaperones in the abiotic stress response. Trends in Plant Science 9, 244-252.

Wang, X., Komatsu, S. (2016) Plant subcellular proteomics: Application for exploring optimal cell function in soybean. Journal of Proteomics 143, 45-56.

Wang, Y., Li, K., Li, X. (2009) Auxin redistribution modulates plastic development of root system architecture under salt stress in *Arabidopsis thaliana.* Journal of Plant Physiology 166, 1637-1645.

Watkinson, J. I., Hendricks, L., Sioson, A. A., Heath, L. S., Bohnert, H. J., Grene, R. (2008) Tuber development phenotypes in adapted and acclimated, drought-stressed *Solanum tuberosum ssp. andigena* have distinct expression profiles of genes associated with carbon metabolism. Plant Physiology and Biochemistry 46, 34-45.

Weis, B. L., Kovacevic, J., Missbach, S., Schleiff, E. (2015) Plant-specific features of ribosome biogenesis. Trends in Plant Science 20, 729-740.

Williams, D. B. (2006) Beyond lectins: the calnexin/calreticulin chaperone system of the endoplasmic reticulum. Journal of Cell Science 19, 615-623.

Wilson, D. N., Doudna Cate, J. H. (2012) The structure and function of the eukaryotic ribosome. Cold Spring Harbor Perspectives in Biology 4.

Wu, T., Yuan, T., Tsai, S. N., Wang, C., Sun, S. M., Lam, H. M., Ngai, S. M. (2009) Mass spectrometry analysis of the variants of histone H3 and H4 of soybean and their post-translational modifications. BMC Plant Biology 9, 98.

Wuebker, E. F., Mullen, R. E., Koehler, K. (2001) Flooding and temperature effects on soybean germination. Crop Science 41, 1857-1861.

Xie, H., Yang, D. H., Yao, H., Bai, G. E., Zhang, Y. H., Xiao, B. G. (2016) iTRAQ-based quantitative proteomic analysis reveals proteomic changes in leaves of cultivated tobacco (*Nicotiana tabacum*) in response to drought stress. Biochemical and Biophysical Research Communications 469, 768-775.

Xu, C., Li, X., Zhang, L. (2013) The effect of calcium chloride on growth, photosynthesis, and antioxidant responses of *Zoysia japonica* under drought conditions. PLoS One 8, e68214.

Xu, H., Heath, M. C. (1998) Role of calcium in signal transduction during the hypersensitive response caused by basidiospore-derived infection of the cowpea rust fungus. Plant Cell 10, 585-598.

Xu, W., Shi, W., Jia, L., Liang, J., Zhang, J. (2012) *TFT6* and *TFT7*, two different members of tomato 14-3-3 gene family, play distinct roles in plant adaption to low phosphorus stress. Plant Cell and Environment 35, 1393-1406.

Yamaguchi, M., Valliyodan, B., Zhang, J., Lenoble, M. E., Yu, O., Rogers, E. E., Nguyen, H. T., Sharp, R. E. (2010) Regulation of growth response to water stress in the soybean primary root. I. Proteomic analysis reveals region-specific regulation of phenylpropanoid metabolism and control of free iron in the elongation zone. Plant Cell and Environment 33, 223-243.

Yamaguchi-Shinozaki, K., Shinozaki, K. (2006) Transcriptional regulatory networks in cellular responses and tolerance to dehydration and cold stresses. Annual Review of

Plant Biology 57, 781-803.

Yan, J., He, C., Wang, J., Mao, Z., Holaday, S. A., Allen, R. D., Zhang, H. (2004) Overexpression of the *Arabidopsis* 14-3-3 protein GF14λ in cotton leads to a "stay-green" phenotype and improves stress tolerance under moderate drought conditions. Plant and Cell Physiology 45, 1007-1014.

Yanagawa, Y., Komatsu, S. (2012) Ubiquitin/proteasome-mediated proteolysis is involved in the response to flooding stress in soybean roots, independent of oxygen limitation. Plant Science 185, 250-258.

Yao, Y. X., Dong, Q. L., Zhai, H., You, C. X., Hao, Y. J. (2011) The functions of an apple cytosolic malate dehydrogenase gene in growth and tolerance to cold and salt stresses. Plant Physiology and Biochemistry 49, 257-264.

Yasmeen, F., Raja, N. I., Mustafa, G., Sakata, K., Komatsu, S. (2016) Quantitative proteomic analysis of post-flooding recovery in soybean root exposed to aluminum oxide nanoparticles. Journal of Proteomics 143, 136-150.

Yin, G., Sun, H., Xin, X., Qin, G., Liang, Z., Jing, X. (2009) Mitochondrial damage in the soybean seed axis during imbibition at chilling temperatures. Plant and Cell Physiology 50, 1305-1318.

Yin, X., Komatsu, S. (2015) Quantitative proteomics of nuclear phosphoproteins in the root tip of soybean during the initial stages of flooding stress. Journal of Proteomics 119, 183-195.

Yin, X., Komatsu, S. (2016) Nuclear proteomics reveals the role of protein synthesis and chromatin structure in root tip of soybean during the initial stage of flooding stress. Journal of Proteome Research 15, 2283-2298.

Yin, X., Nishimura, M., Hajika, M., Komatsu, S. (2016) Quantitative proteomics reveals the flooding-tolerance mechanism in mutant and abscisic acid-treated soybean. Journal of Proteome Research 15, 2008-2025.

Yin, X., Sakata, K., Komatsu, S. (2014b) Phosphoproteomics reveals the effect of ethylene in soybean root under flooding stress. Journal of Proteome Research 13, 5618-5634.

Yin, X., Sakata, K., Nanjo, Y., Komatsu, S. (2014a) Analysis of initial changes in the proteins of soybean root tip under flooding stress using gel-free and gel-based

proteomic techniques. Journal of Proteomics 106, 1-16.

Zhang, H., Qu, X., Bao, C., Khurana, P., Wang, Q., Xie, Y., Zheng, Y., Chen, N., Blanchoin, L., Staiger, C. J., Huang, S. (2010) *Arabidopsis* VILLIN5, an actin filament bundling and severing protein, is necessary for normal pollen tube growth. Plant Cell 22, 2749-2767.

Zhang, J., Zhang, Y., Du, Y., Chen, S., Tang, H. (2011b) Dynamic metabonomic responses of tobacco (*Nicotiana tabacum*) plants to salt stress. Journal of Proteome Research 10, 1904-1914.

Zhang, Y., Wen, Z., Washburn, M. P., Florens, L. (2009) Effect of dynamic exclusion duration on spectral count based quantitative proteomics. Analytical Chemistry 81, 6317-6326.

Zhang, Y., Xiao, Y., Du, F., Cao, L., Dong, H., Ren, H. (2011a) *Arabidopsis* VILLIN4 is involved in root hair growth through regulating actin organization in a Ca^{2+}-dependent manner. New Phytologist 190, 667-682.

Zhu, J. K. (2002) Salt and drought stress signal transduction in plants. Annual Review of Plant Biology 53, 247-273.

Zhu, S. Y., Yu, X. C., Wang, X. J., Zhao, R., Li, Y., Fan, R. C., Shang, Y., Du, S. Y., Wang, X. F., Wu, F. Q., Xu, Y. H., Zhang, X. Y., Zhang, D. P. (2007) Two calcium-dependent protein kinases, CPK4 and CPK11, regulate abscisic acid signal transduction in *Arabidopsis*. Plant Cell 19, 3019-3036.

Zhu, X. G., Long, S. P., Ort, D.R. (2010) Improving photosynthetic efficiency for greater yield. Annual Review of Plant Biology 61, 235-261.

Zhu, X., Feng, Y., Liang, G., Liu, N., Zhu, J. K. (2013) Aequorin-based luminescence imaging reveals stimulus- and tissue-specific Ca^{2+} dynamics in *Arabidopsis* plants. Molecular Plant 6, 444-455.